8-J

FINAL REPORT

DEVELOPMENT OF IMPROVED BLOWOUT PREVENTION PROCEDURES FOR DEEP WATER DRILLING OPERATIONS

Contract No. 14-08-0001-17225, Mod. 5

Sponsored by

United States Deprtment of the Interior
Minerals Management Service
Reston, VA 22091

Principal Investigators:

A. T. Bourgoyne, Campanile Professor and Chairman
Petroleum Engineering Department

William R. Holden, Union Oil Company Professor
Petroleum Engineering Department

J. P. Langlinais, Assistant Professor
Petroleum Engineering Department

May, 1983

ABSTRACT

A number of new blowout control problems are associated with extending the search for hydrocarbons beyond the continental shelf to the deeper water depths of the continental slope using floating drilling vessels. These problems become much more severe as the water depth increases, because of the increased length of the marine riser and subsea flowlines and the increased susceptibility of shallow formations to fracture. This research project was concerned with the development of improved blowout prevention procedures, for use with existing well control equipment, which are better suited to deep water drilling operations.

A research well facility centered around a 6000 ft. well was constructed to allow deep water blowout prevention procedures to be experimentally studied. The research well was constructed to model the flow geometry present for a floating drilling vessel operating in 3000 feet of water. Specific blowout prevention procedures studied included: well shut-in procedures, procedures for handling upward gas migration in a shut-in well, pump start-up procedures, and procedures for more safely circulating formation gas to the surface. In addition, an improved mathematical model of the well control process was developed which will allow more accurate prediction of well behavior for various operating conditions.

CONTENTS

CHAPTER 1

INTRODUCTION

Some of the most costly events that have ever occurred in the history of the oil industry have been caused by a loss of well control, commonly called a "blowout". Serious losses to life, property, and the environment have been directly related to "blowouts", yet little emphasis has ever been placed on well control when embarking on new frontiers of exploration. It has taken events such as those which occurred at Spindletop and the Santa Barbara Channel to remind the oil industry of the importance of well control procedures. In a continuing search for hydrocarbon deposits or accumulations and with the increasing demand for fossil fuels imposed by the nations of the world, the oil industry is about to embark onto yet another new frontier, i.e., the slopes of the outer continental shelf and the deep marine sedimentary basins of the world. If blowout prevention theory and practice is to advance along with the technology now being developed for drilling in deeper waters, certain aspects of drilling, and situations which could develop, must be studied and analyzed.

Special blowout prevention equipment and procedures are often required for the control of high pressure formation fluids encountered while drilling for oil and gas. When a permeable formation at depth is penetrated by the drill bit, the pressure of its contained fluids (water, oil and/or gas) must always be offset or balanced by the hydrostatic pressure of the drilling fluid (mud) in the bore hole. Otherwise a threatened blowout or so-called well "kick" will occur. With an influx of formation fluid into the bore hole, the drilling mud is displaced or kicked up the hole, causing an increased rate of mud return flow at the surface. If this condition is not recognized immediately and proper control procedures initiated, the entire annulus can be voided of mud to be followed by the uncontrolled discharge (blowout) of formation fluids to the atmosphere. Since formation pressures in advance of the drill bit cannot always be predicted, well kicks of them-

selves can be a routine drilling experience. The infrequent development of a kick into a disastrous blowout is usually the cause of some human error or perhaps an equipment failure.

In the late 1940's, the industry's search for new accumulations of petroleum had led to the shallow marine environments of the outer continental shelf. Jack-up and submersible drilling rigs were designed to drill in this type of environment. These rigs were supported by the sea bottom with the BOP equipment located on the surface. They had their drilling decks fixed in respect to the sea floor. This enabled a conductor pipe to be driven into the sea floor to provide support for a BOP stack. Both jack-ups and submersibles contained their own BOP equipment, choke and kill mainfold, standpipe manifold, and piping and valve arrangement, which differed slightly from rig to rig. However, the same blowout prevention equipment, piping arrangements, and techniques used to circulate out a kick on the land rigs were applied to the jack-ups and submersibles. As time progressed drilling activity expanded into deeper water depths. Eventually, water depth was the limiting factor for both the jack-up and the submersible rigs. Most of these rigs could not drill in water depths much beyond 300 ft.

By the early 1960's, semisubmersible rigs and drillships were developed that could drill from a floating position. With the advent of floating vessels, the BOP stack could no longer be fixed to the conductor pipe at a surface location. The continuous motion of the floating vessels in the deeper waters required that the blowout preventers be installed on the ocean floor. In addition, emergency conditions, usually adverse weather, might force a rig to suspend operations or move off location. With the BOP stack and wellhead on the ocean floor the marine riser could be removed with little danger of damage to the well.

In 1974, Shell Oil Company drilled the first well in 2,000 feet of water.[1] Since 1974, some 70 wells have been drilled from floating platforms and drillships in water depths greaters than 2000 feet (Fig. 1). Likewise the record water depth for exploratory drilling increased steadily (Fig. 2), the current record being held by the drillship Discoverer Seven Seas for a well drilled off the coast of Newfoundland in 4876 feet of water.[2-3] This year, this same vessel is scheduled to drill in the Mediterranean Sea offshore of Marseilles in 5600 feet of

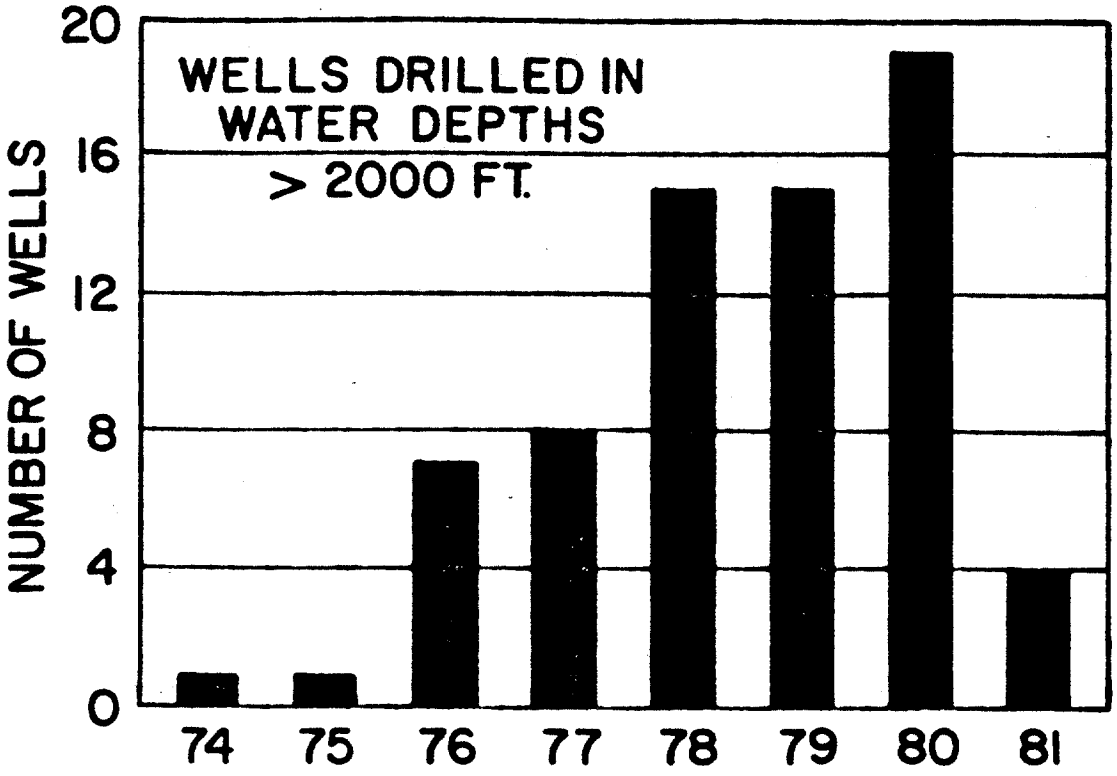

Fig. 1 - Annual number of wells drilled in water depths greater than 2000 feet.

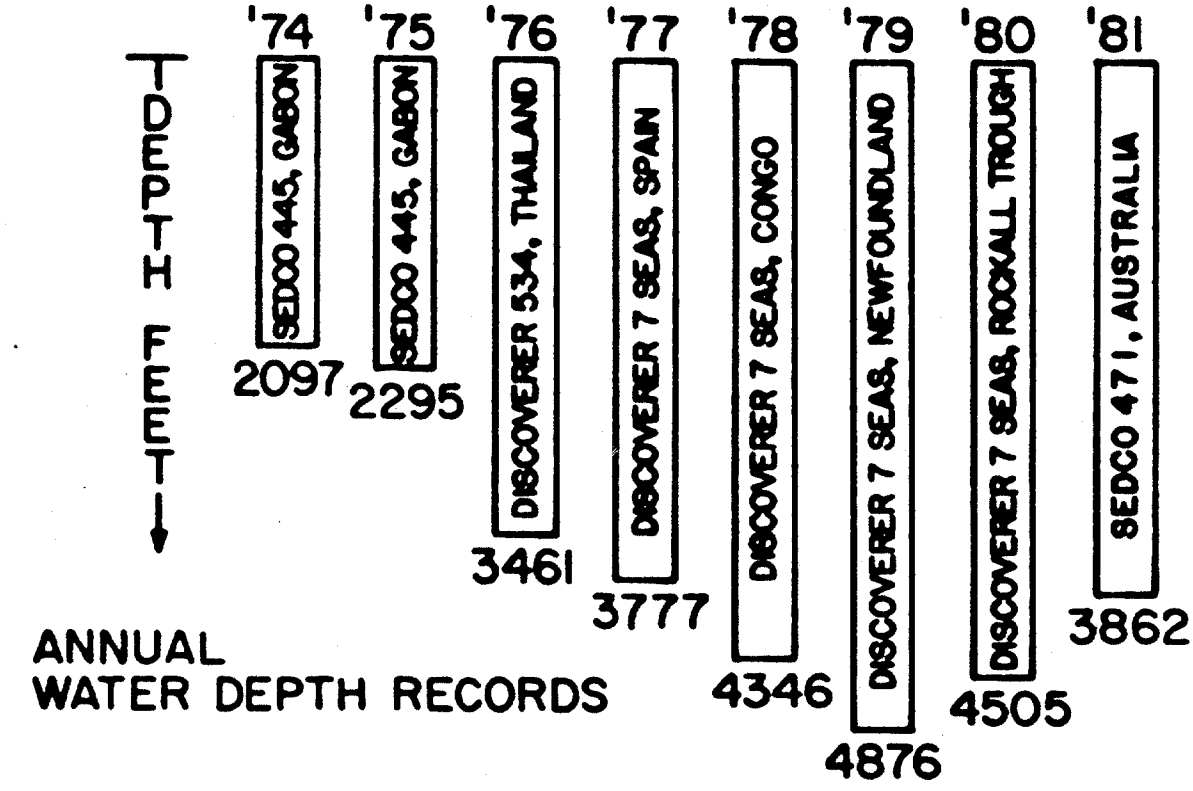

Fig. 2 - Annual Water Depth Record for wells drilled using a marine riser.

water. In 1985-86, two wells are planned for the Wilmington Canyon area of the U. S. East Coast in 5500 feet of water. In a global sense, at least, drilling in deep water is becoming more commonplace.

Like many other aspects of drilling operations, the problem of blowout prevention increases in complexity for floating drilling vessels operating in deep water. Several special well control problems stem from a greatly reduced fracture resistance of the marine sediments and from the use of long subsea flow lines extending vertically from the blowout preventer (BOP) stack at the sea floor to the choke manifold and other well-control equipment located at the surface. Shown in Figure 3 is the approximate effect of water depth on fracture resistance, expressed in terms of the maximum mud density which can be sustained during normal drilling operations without hydrofracture. Note that the maximum mud density which can be used with casing penetrating 3500 feet into the sediments decreases from about 13.9 ppg on land to about 10.7 ppg in 1500 feet of water, and to about 9.8 ppg in 13,000 feet of water. Next, the well head and BOP stack must be located on the sea floor and must be connected to the surface well-control equipment by means of long, vertical flow lines. Designed for high-pressure service, these subsea flow lines have small internal diameters, usually 2 to 3½ inches. The need for greatly increased lengths of these small diameter flowlines in the deep water drilling environment can greatly increase the complexity of blowout prevention procedures.

In recent years, there has been considerable concern expressed by many offshore drilling personnel attending well control training seminars at LSU about the need for modified procedures which address the special blowout prevention problems associated with the deep water environment. This research project was undertaken largely in response to these concerns. Thus, the objective of the research was the development of improved blowout prevention procedures designed specifically for deep water drilling operations. A review was made of the applicable existing equipment and procedures. Based on this review, a research well facility was designed and constructed to allow deep water blowout prevention procedures to be experimentally studied. Specific procedures studied included:

1. Well shut in procedures,
2. Procedures for handling upward gas migration in a shut-in well,
3. Pump start-up procedures, and
4. Kick pump out procedures.

In addition, an improved mathematical model of the well control process was developed which will allow a more accurate prediction of well behavior for various operating conditions.

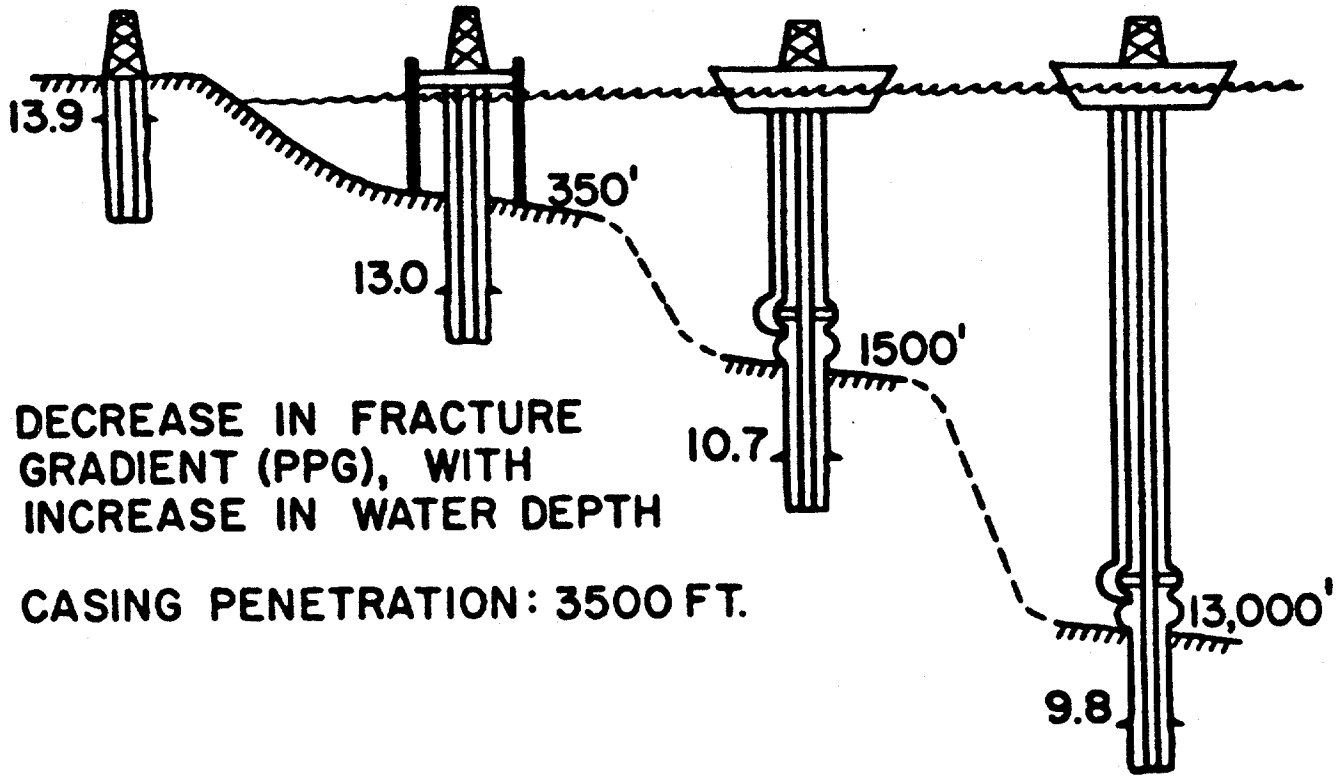

Fig. 3 - Approximate effect of water depth on fracture gradient.

CHAPTER 2

REVIEW OF EXISTING EQUIPMENT AND PROCEDURES

The primary objectives of the first phase of the study were to identify the floating drilling vessels capable of drilling in 2,000 feet of water or deeper, and to inventory the well control equipment contained on these drilling vessels. In addition, the current well control procedures employed by various operators during well control operations were examined.

2.1 DEEP WATER RIG AVAILABILITY

Every second year a "Directory of Marine Drilling Rigs" is produced by Gulf Publishing Company.[4] This directory includes all available marine drilling rigs, i.e., barges, submersibles, jack-ups, semisubmersibles, and drillships. It was through the use of this directory, that the rig owners were contacted.

Based on the "Directory of Marine Drilling Rigs[4]", one could infer that there is an abundant supply of marine rigs available. Four hundred and sixty-three rigs are listed along with their specifications and descriptions. However, reviewing specifications for these rigs indicates a rapid reduction in rig availability with increasing water depth. Drilling barges, submersible and jack-up rigs are all limited by water depth. Most submersible rigs and drilling barges are restricted to a maximum water depth somewhat less than 100 feet. The maximum water depth of jack-up rigs is about 300 feet of water. This leaves us with just two types of rigs capable of drilling in water depths of 300 feet or deeper, semisubmersibles and drillships.

Most semisubmersibles were constructed to operate on the outer continental shelf. This is generally considered to be in water depths approaching 600 to 800 feet. Only a small percentage of the semisubmersibles are equipped to drill in deeper waters. There are only 67 semisubmersible rigs equipped to drill in 1,000 feet of water. Only 11 semisubmersibles are capable of drilling water depths greater than 2,000 feet. Table 1 lists these vessels.[4]

There are even fewer drillships available to the industry. Of the 75 drillships, only 17 are equipped to drill in water depths greater than 2,000 feet. Table 2 is a listing of these drillships.[4]

Figure 4 illustrates the availability of floating drilling vessels as a function of water depth. In all there are only 28 drilling vessels worldwide capable of drilling in 2,000 feet of water or deeper.

2.2 SURVEY SAMPLE

Of the 28 drilling vessels equipped to drill in deep waters, 7 are owned and operated by foreign companies and 21 are owned by American companies. Fifteen are owned by only 4 American companies. This study was limited to the 21 American owned vessels. Further investigation indicated that only 9 of these vessels have actually drilled in water depths exceeding 2,000.

Through 1980, when this portion of the study was completed, only 66 wells were drilled in water depths of 2,000 feet or deeper.[3] Table 3 lists these wells by year giving the location and drilling vessel used to drill each well. Table 4 shows the number of wells that each vessel has drilled in 2,000 feet of water or deeper. The Discoverer Seven Seas, the Sedco 472, and the Sedco 445 have drilled over half of the deep water wells. The Discoverer Seven Seas hold the water depth record for the well drilled by Texaco Canada off the shore of Newfoundland in 4,876 feet of water.[2]

2.3 SURVEY RESULTS

The owners of the 9 American owned drilling vessels which had drilling experience in water depth in excess of 2000 feet were contacted for information concerning their rigs. All 9 of the rig owners contacted responded by supplying brochures containing the equipment carried on each of their rigs. Some of this literature was more descriptive than others, but all contained information on the subsea blowout prevention equipment used. Besides these 9 drilling vessels, equipment information on the "Pelerin" a foreign owned vessel, appeared in one of the trade journals.[5] Using the equipment description for these 10 drilling vessels,the equipment manufacturers were contacted to submit information concerning their subsea equipment. All of these equipment manufacturers

Table 1 - Semisubmersibles Capable of Drilling in Water Depths of 2,000 Feet or Deeper[4]

Rig Owner	Rig Name	MaximumDepth
Fearnley Drilling & Expl.	Fernstate	3,000
Keydrill Company	Aleutian Key	2,000
Marine Drilling S. A.	Sedco 709	6,000
Penrod Drilling Company	Penrod 74	2,000
Sedco Inc.	Sedco 703	2,000
Western Oceanic/Exxon	Alaskan Star	2,000
Zapata Corp.	Zapata Concord	2,000
Zapata Corp.	Zapata Lexington	2,000
Zapata Corp.	Zapata Saratoga	2,000
Zapata Corp.	Zapata Ugland	2,000
Zapata Corp.	Zapata Yorktown	2,000

Table 2 - Drillships Capable of Drilling in Water Depths of 2,000 feet or Deeper[4]

Rig Owner	Rig Name	Maximum Depth
Amoshore Drilling Company	Discoverer 511	2,000
Global Marine Inc.	Glomar Atlantic	2,000
Global Marine Inc.	Glomar Challanger	20,000
Global Marine Inc.	Glomar Pacific	2,000
Helmer Stanbo & Co.	Pelerin	3,300
Marine Drilling & Coring Co.	Candrill I	5,000
Neddrill (Nederland) B.V.	Nedrill	6,000
ODECO/Ben Line Offshore	Ben Ocean Lancer	3,000
The Offshore Company	Discoverer II	2,000
The Offshore Company	Discoverer 534	3,000
The Offshore Company	Discoverer Seven Seas	4,500
Offshore Europe N.V.	Petrel	3,000
Overseas Drilling Ltd.	Sedco/BP 471	4,500
Pacnorse Drilling Corp.	Pacnorse I	3,000
Saipern	Saipern Due	2,000
Sedco Inc.	Sedco 445	3,500
Sedco Inc.	Sedco 472	4,500

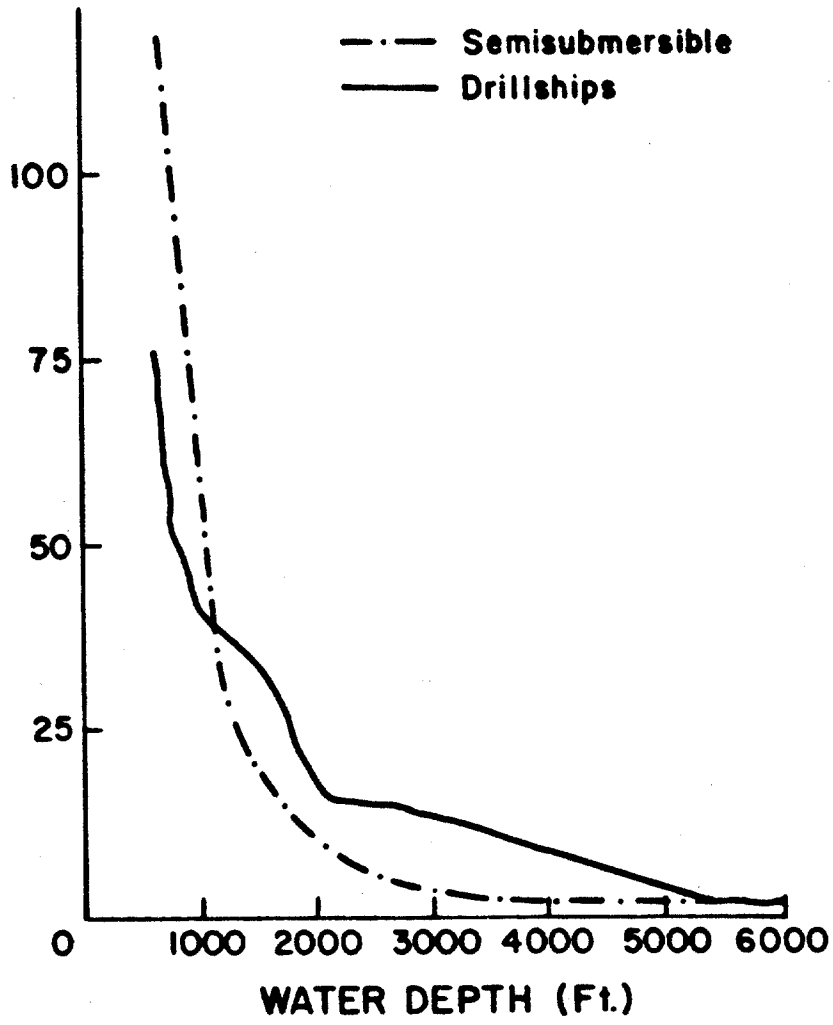

Figure 4 - Drilling Vessels Available for Drilling in Deep Waters[4]

Table 3 - Listing of Wells Drilled in 2000 Feet of Water or Deeper[3]

Operator	Well Location	Rig Name	Water Depth (in feet)
	1980		
BNOC	Rockall Trough, 163/6-1	Discoverer Seven Seas	4505
Esso Australia	Australia, Vinck-1	Sedco 472	4504
Esso Australia	Australia, N.W. Shelf	Sedco 472	4500
Esso Australia	Exmouth Plateau	Sedco 472	4473
Esso Australia	Exmouth Plateau	Sedco 472	3881
Phillips Petroleum	Exmouth Plateau	Sedco/BP 471	3864
Esso Australia	Australia, Sirius-1	Sedco 472	3851
Hispanoil	Mauratania, Ras al Baidu	A-1 Discoverer Seven Seas	3672
Woodside Pet.	Exmouth Plateau	Sedco 471	2933
AGIP	Aquila, Italy	Discoverer Seven Seas	2713
Chevron Spain	Montanazo D-3, Spain	Pacnorse I	2650
Woodside Pet.	Exmouth Plateau	Sedco 445	2640
Esso Australia	West Australia	Sedco 472	2526
Esso Australia	Exmouth Plateau	Sedco 472	2430
Esso Australia	Zeepaard, Australia	Sedco 472	2426
Woodside Pet.	West Australia	Sedco 445	2400
Phillips Petroleum	Miss. Canyon, OCSG-4135 #1	Zapata Concord	2150
Woodside Pet.	Exmouth Plateau	Sedco 445	2079
Shell Expro.	West Shellands 206/2-1	Petrel	2004
	1979		
Texaco Canada	Newfoundland, Texaco Shell et at Blue H-28	Discoverer Seven Seas	1876
Enlepsa	Spain, Cabriel B-2	Discoverer Seven Seas	4589
Getty Oil	Spain, Grumete C 1X	Discoverer Seven Seas	4441
Esso Australia Ltd.	Australia, Zeewolf-1	Sedco 472	3920
Phillips Petroleum	Australia Exmouth Plateau Mercury IX	Sedco 471	3746
Esso Resources Ltd.	Canada, EVG C-60	Sedco 709	3636
Esso Australia Ltd.	Australia, Resolution-1	Sedco 472	3565
Esso Resources Ltd.	Canada EHB Gjoa G-37	Sedco 709	3276
Phillips Petroleum	Austrlia, Exmouth Plateau Jupiter No. 1	Sedco 471	3070

Table 3 (continued) - Listing of Wells Drilled in 2000 Feet of Water or Deeper[3]

Operator	Well Location	Rig Name	Water Depth (in feet)
	1979 continued		
Esso Australia Ltd.	Australia, Searborough-1	Sedco 472	2992
Phillips Petroleum	Ghann, So. Dix Cover IX	Discoverer Seven Seas	2927
Esso Australia Ltd.	Australia, Investigator-1	Sedco 472	2758
Chevron	Baltimore Canyon, Cost B-3	Ben Ocean Lancer	2687
Chevron	Gambia	Pelerin	2295
	1978		
Getty Oil	Pointe Noire, Congo	Discoverer Seven Seas	4346
Esso Expl. Guyane S.A.R.L.	French Guiana, FG 2-1	Sedco 472	4100
Esso Expl. Surinam Inc.	Surinam, A 2-1	Sedco 472	3806
Hispanoil/Eniepsa	Gulf of Valencia	Discoverer Seven Seas	3755
Chevron	Montanazo C-1	Ben Ocean Lancer	3209
AGIP	Adriatic, Rovesli 1	Discoverer Seven Seas	3133
Total	Kenya, Simba 1	Pelorin	3019
Total/Kenya SNEA	Kenya	Pelorin	3018
CFP	Algeria, Haabibas	Pelorin	3001
Phillips	Ghana, South 1-X	Discoverer Seven Seas	2947
Chevron Standard	Nova Scolia, Acadia K-62	Ben Ocean Lancer	2841
Shell Tooranata	West Const. of Ireland 35/29-1	Sedco 709	2638
Chevron Overseas	Spain, Montanazo D-2	Ben Ocean Lancer	2467
Hipco of New Zealand	So. Island, New Zealand	Penrod 74	2300
Chevron Overseas	Spain, Montanazo C-1	Ben Ocean Lancer	2209
	1977		
Enlepsa	Spain, Ibiza Marino AN-1	Discoverer Seven Seas	3777
Total Algeria	Algeria-Habibas 1	Pelerin	3038
Esso Egypt	Red Sea, RSO T'95-1	Discoverer 534	2737
Esso Egypt	Red Sea, RSO Z'95	Discoverer 534	2506
Hipco of New Zealand	So. Irland, New Zealand	Penrod 74	2250
Hipco of New Zealand	So. Irland, New Zealand	Penrod 74	2247
Hipco of New Zealand	So. Irland, New Zealand	Penrod 74	2100
Wepco	Egypt Qaseir Well	Discoverer Seven Seas	2060

Table 3 (continued) - Listing of Wells Drilled in 2000 Feet or Water or Deeper[3]

Operator	Well Location	Rig Name	Water Depth (in feet)
	1976		
Esso Exploration	Thailand, W9-E1	Discoverer 534	3461
Esso Exploration	Thailand, W9-C1	Discoverer 534	2959
Esso Exploration	Red Sea, RSO T'95-1	Discoverer 534	2737
Esso Exploration	Thailand, W9-D1	Discoverer 534	2652
Esso Exploration	Thailand, W9-B1	Discoverer 534	2632
Union Oil of Thailand	West Thailand	Sedco 445	2039
Union Oil of Thailand	West Thailand	Sedco 445	2028
Union Oil of Thailand	West Thailand	Sedco 445	2017
	1975		
Shell	Gabon	Sedco 445	2292
	1974		
Shell	Gabon	Sedco 445	2097

Table 4 - Number of Wells Drilled in 2,000 Feet of Water or Deeper per Drilling Vessel[3] through 1980.

Rig Name	Number of Wells Drilled
Sedco 472	14
Discoverer Seven Seas	13
Sedco 445	8
Discoverer 534	7
Ben Ocean Lancer	5
Pelerin*	5
Sedco/PB 471	4
Penrod 74	4
Sedco 709	3
Pacnorse*	1
Zapata Concord	1
Petrel*	1
	66

* Foreign Owned Vessel

responded by sending equipment catalogs. These equipment catalogs contained information on dimensions, weights, and pressure ratings for the various components, which will be described in a later section.

Under the laws established for drilling in U.S. federal waters, drilling rig personnel must be trained in well control procedures from an approved U.S.G.S. training course.[6] At the time of this study, eleven courses designed for floating drilling operations are conducted within individual oil companies and have been approved by the U.S. Minerals Management Service (MMS). The training manuals for these 11 operator courses were requested from the MMS. Because the volume of the materials requested was too great to send by mail, only five manuals were obtained. The MMS assured that these manuals are typical course manuals and should provide a representative sample of existing blowout prevention procedures.

2.4 TYPICAL PIPING DIAGRAMS

In addition to the equipment information gathered on the 10 drilling vessels that have already drilled in 2,000 feet of water or deeper, piping diagrams of the well control equipment used on the Alaskan Star and the Zapata Concord were obtained. These rigs happened to be drilling in the Gulf of Mexico at the time of this study, and were available for a personal inspection. Both of these rigs are capable of drilling in deep waters, and the Zapata Concord has already drilled a well for Phillips Petroleum in the Mississippi Canyon in a water depth of 2,150 feet.[3] The operators of the Alaskan Star and the Zapata Concord were contacted and arrangements were made to tour these rigs. The equipment contained on these vessels and all the piping and valve arrangements were visually inspected. Rig personnel provided schematic diagrams of the choke and kill manifold, standpipe manifold, and flow diagrams. While the actual placement of these manifolds varied according to the rig layout, the flow path and valve arrangements were the same. All the piping and valves on the rigs were permanently attached to the rig structure.

Figures 5-9 are flow diagrams of the piping and valve arrangements of the high pressure mud return system used on the Zapata Concord. Figures 10-11 show the piping and valve arrangement used on the Alaskan

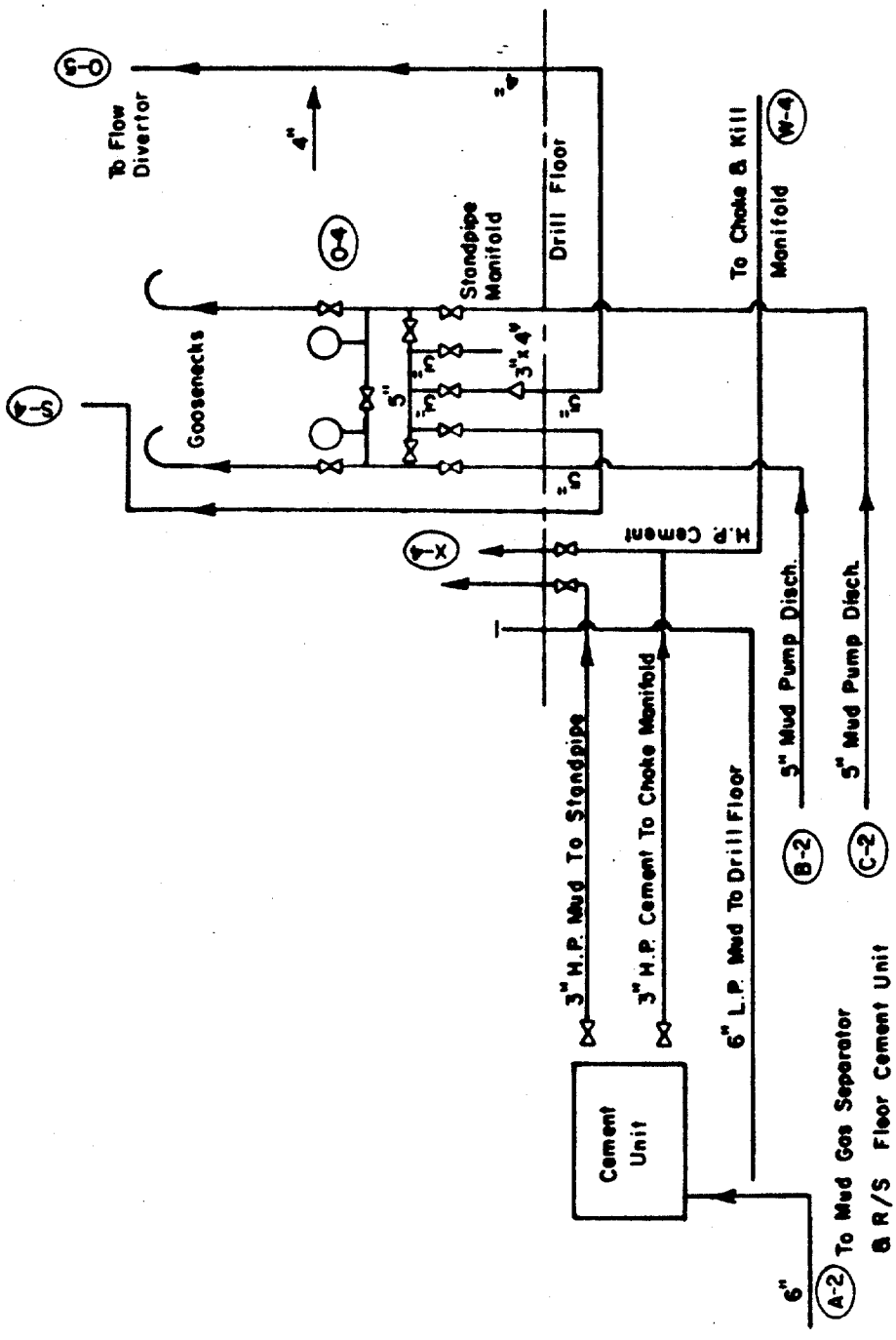

FIGURE 5. STANDPIPE & CEMENT UNIT ON ZAPATA CONCORD

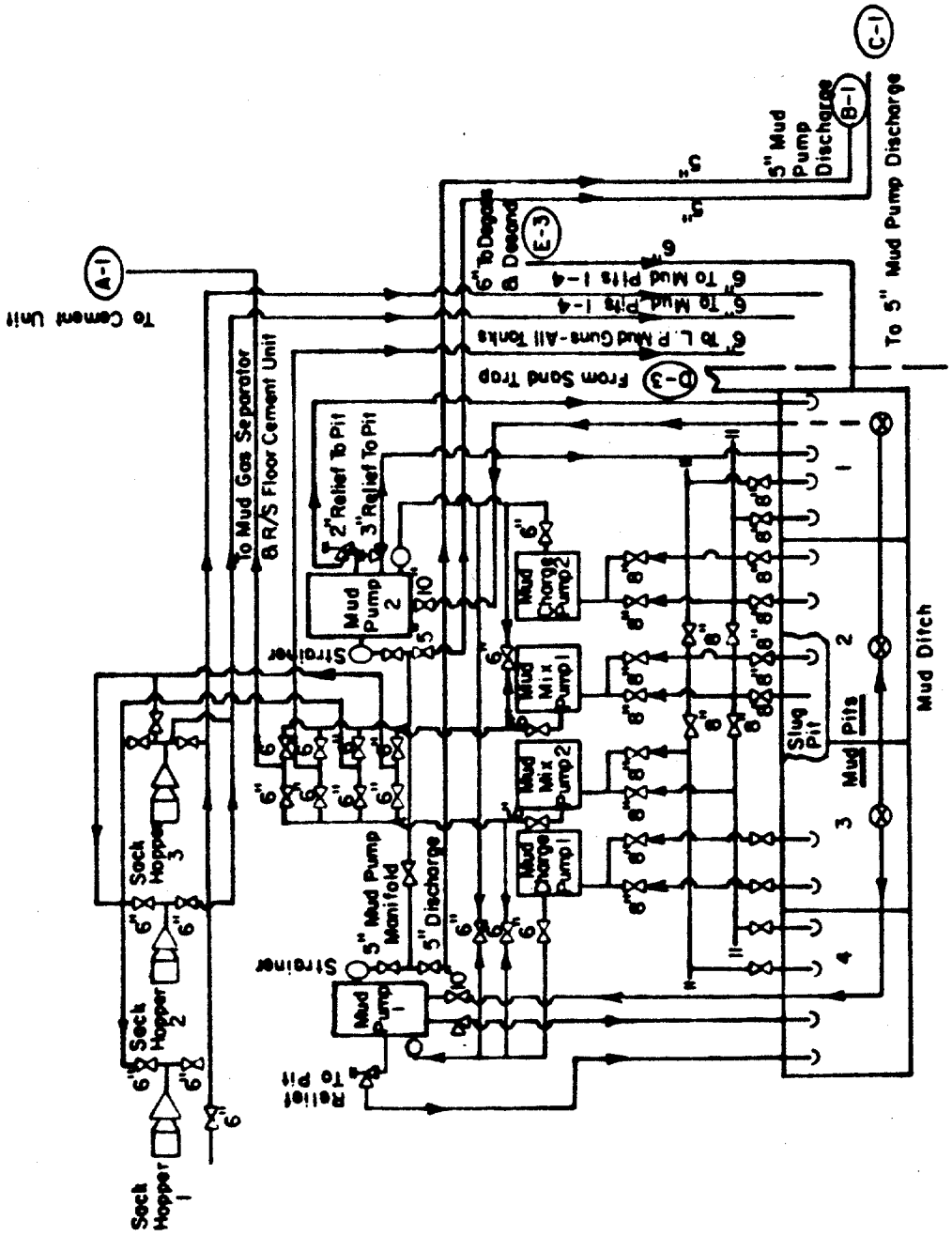

FIGURE 6. MUD PUMP PIPING ON ZAPATA CONCORD

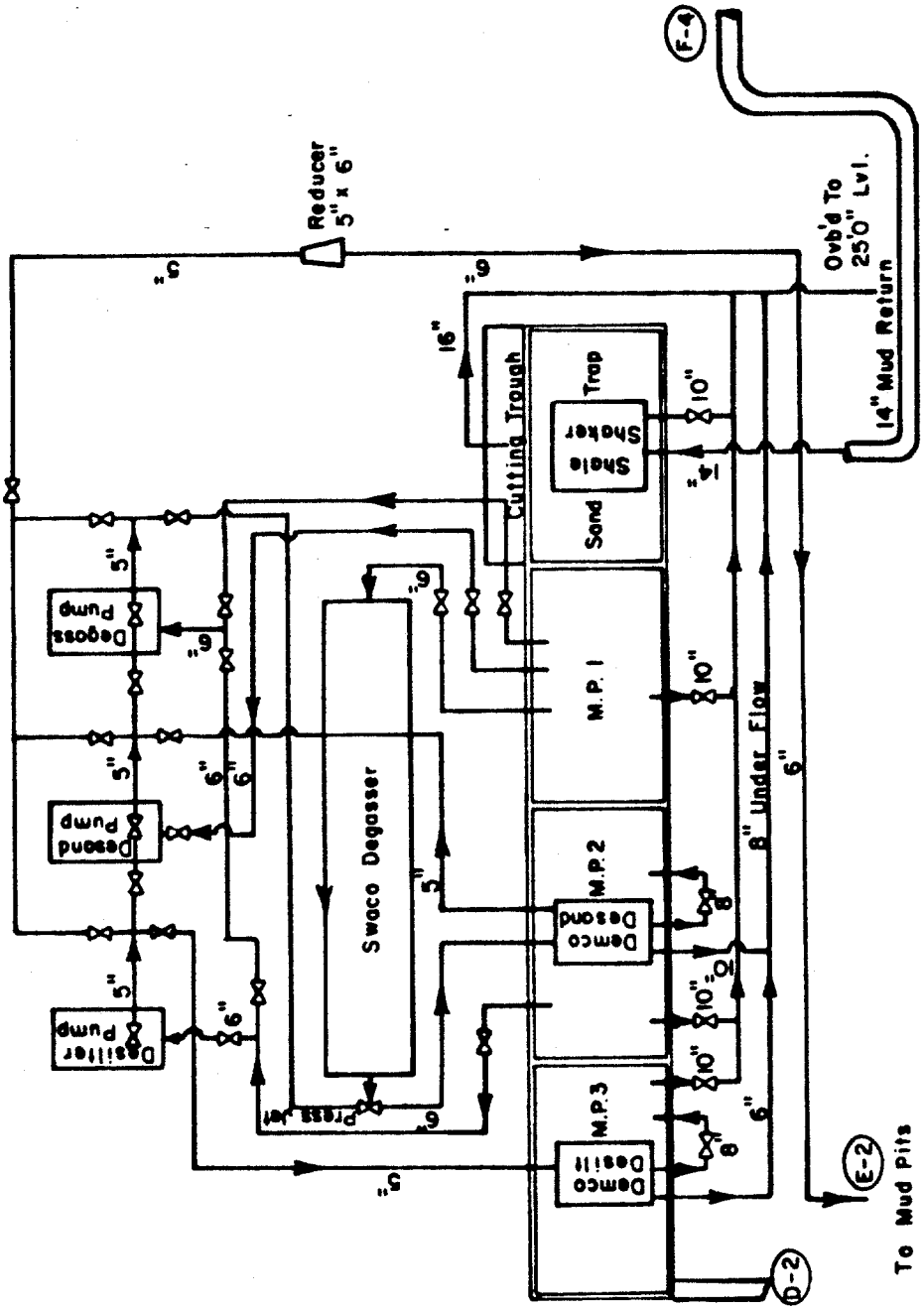

FIGURE 7. SHALE SHAKER & SAND TRAPS ON ZAPATA CONCORD

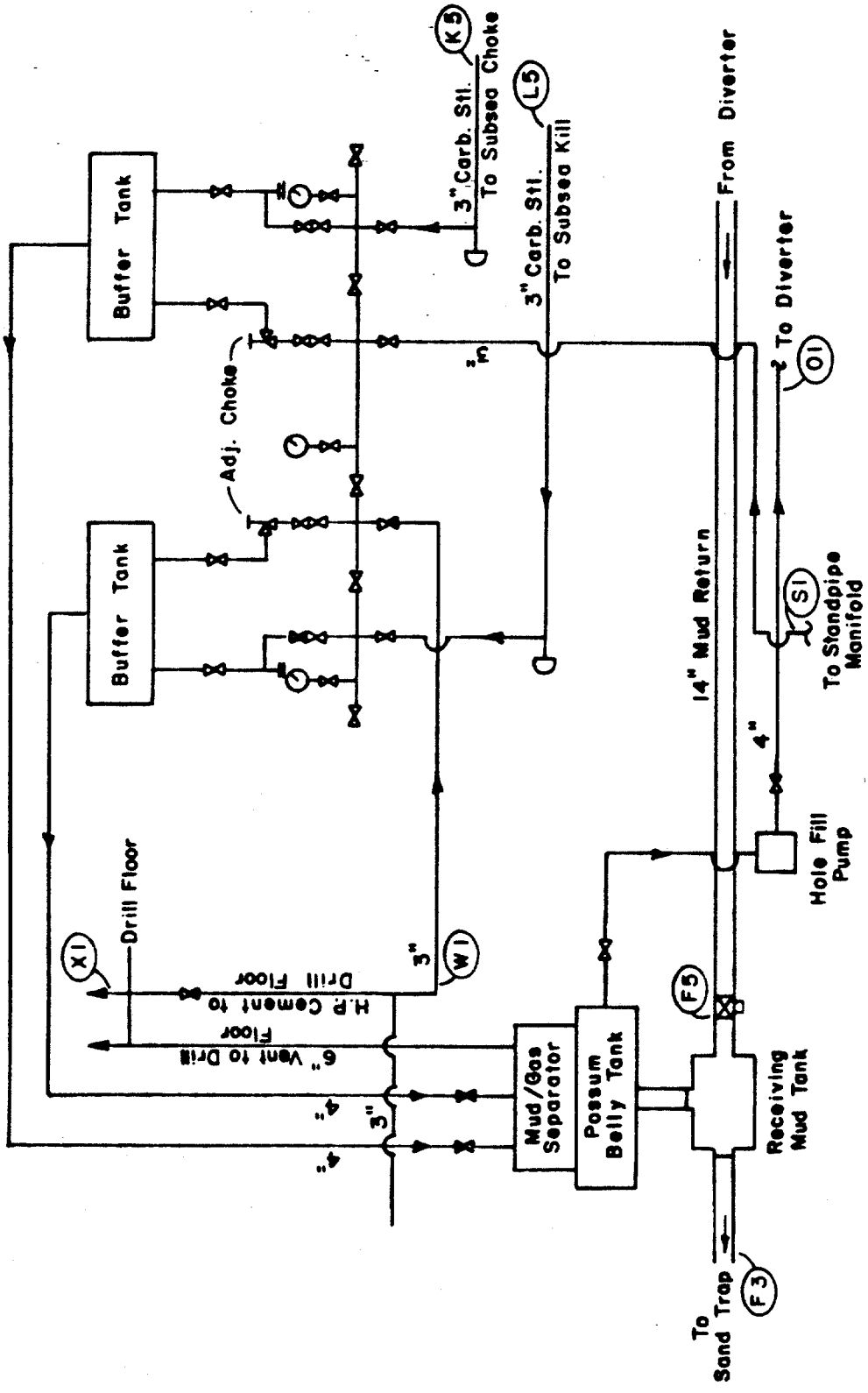

FIGURE 8. CHOKE MANIFOLD & MUD/GAS SEPARATOR ON ZAPATA CONCORD

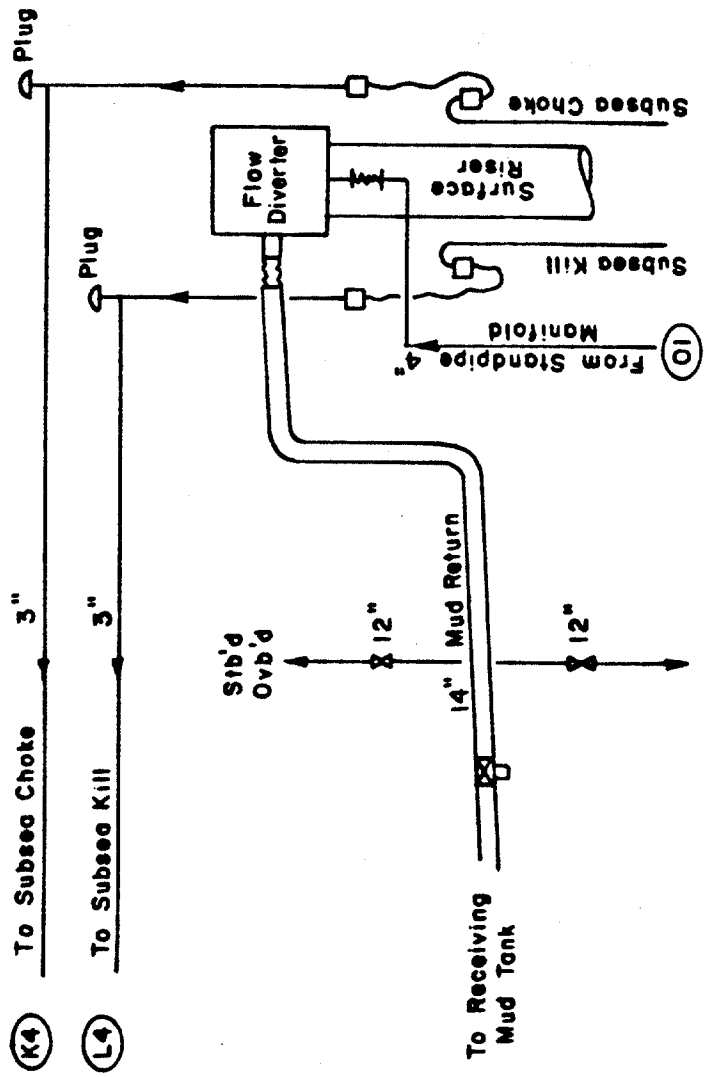

FIGURE 9. DIVERTER SYSTEM & TRIP TANK ON ZAPATA CONCORD

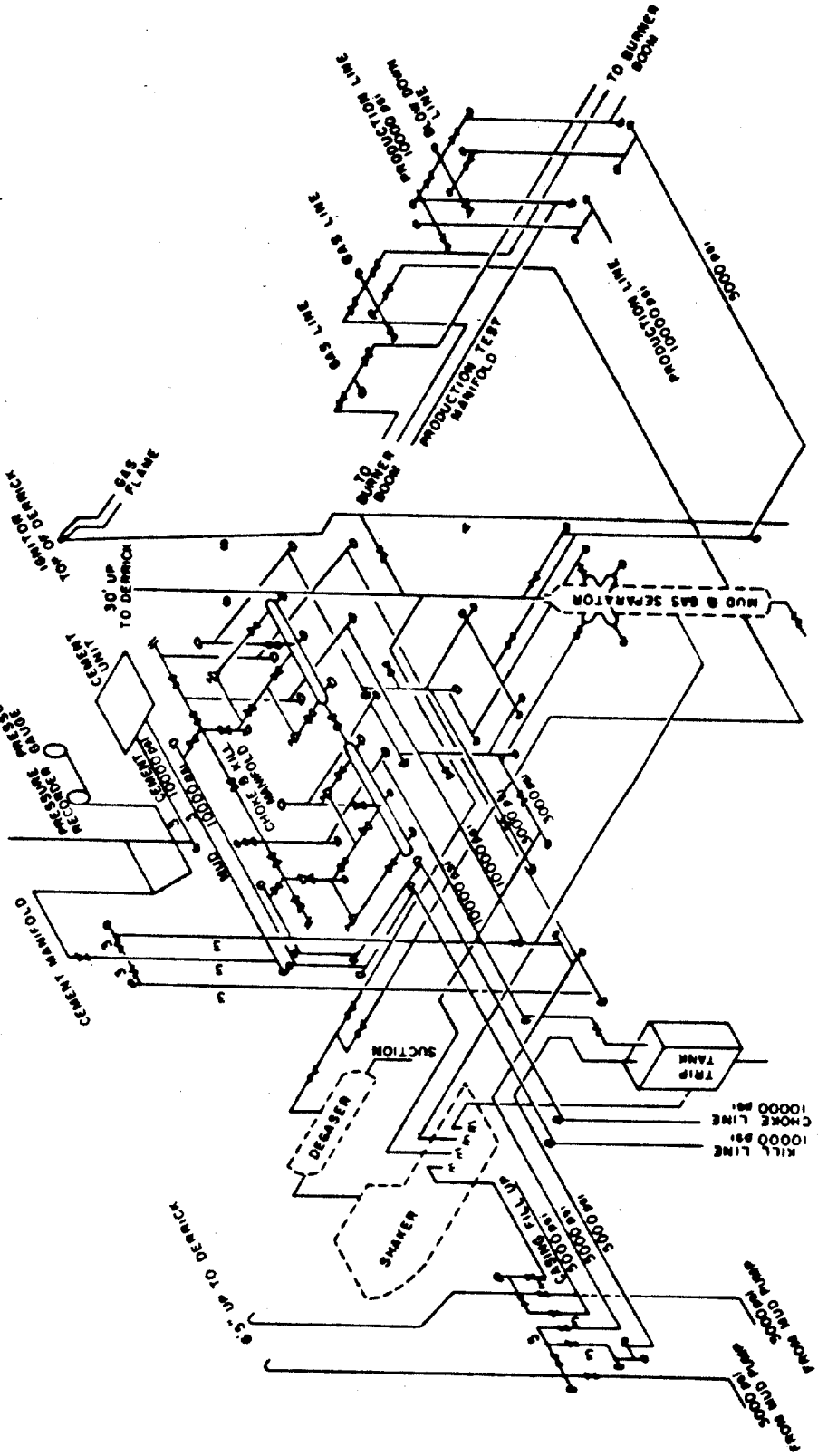

Figure 10 - Alaskan Star Piping Arrangement

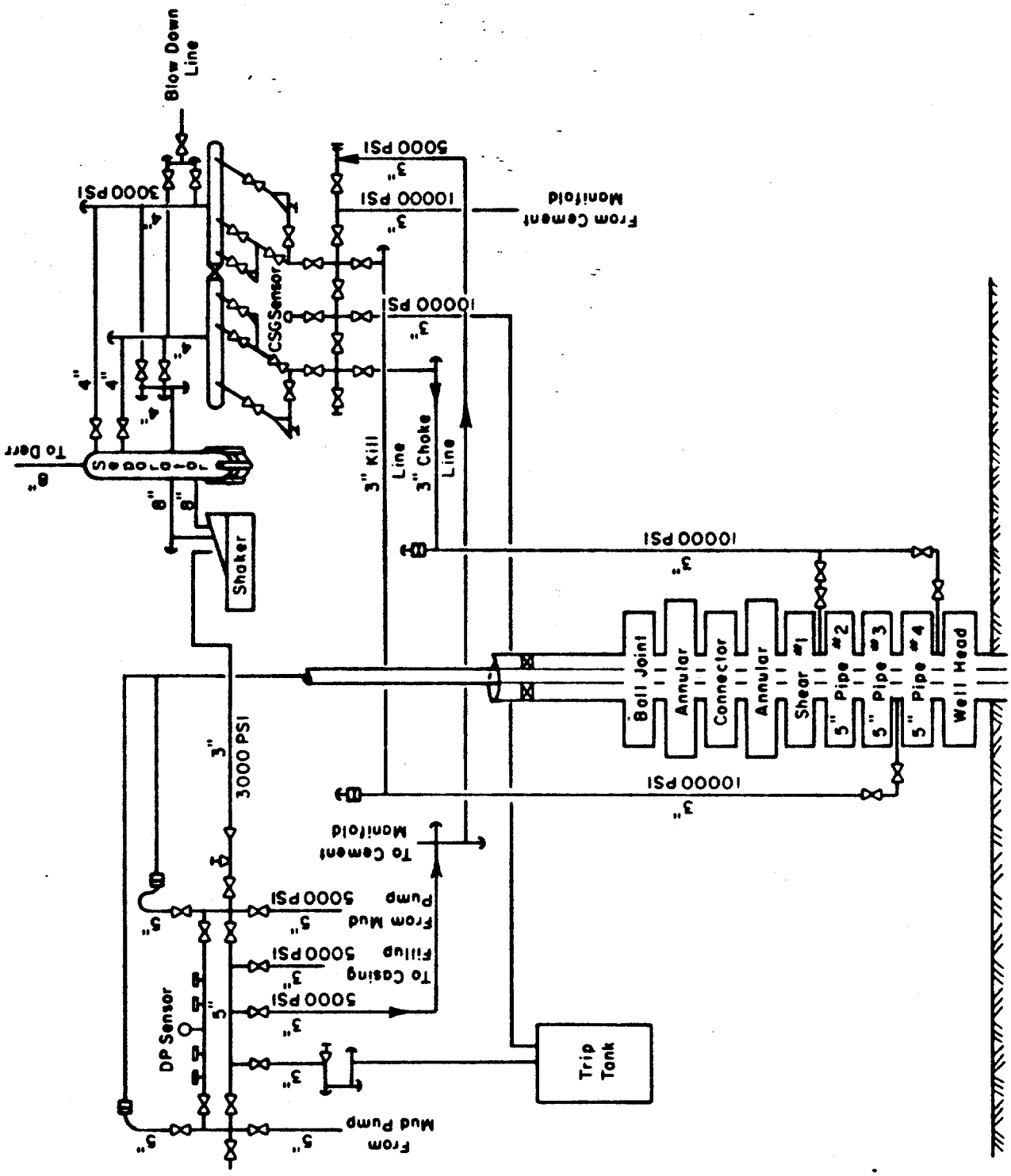

FIGURE 11. ALASKAN STAR WELL CONTROL PIPING SUMMARY

Star. Both of these flow paths are similar in that flow may be directed from the choke and kill lines through a manifold to either the shale shaker, the mud/gas separator, the flare or vent lines, or to the standpipe manifold. Flow may also be directed from the mud pumps or cement pumps through the choke and kill manifold down either the choke or kill line or both, and into the wellbore annuli. The manifolds on the various components, i.e., choke and kill, standpipe, or cement manifolds, provide almost any flow path desired in a well control operation. These flow paths are felt to be typical of floating drilling vessels using a subsea BOP stack assembly.

Figure 12 is a typical piping diagram for a diverter system. Low pressure flow may be directed to either a port or a starboard vent line, a trip tank, or the shale shaker, depending on the situation encountered.

2.5 SUBSEA BLOWOUT PREVENTION EQUIPMENT

The well control equipment used on floating drilling vessels is available from only a limited number of suppliers. The equipment used for well control, such as blowout prevention equipment, riser systems, and diverter systems were custom designed for the drilling industry. Consequently, only the major oil field suppliers entered the market for well control equipment. Existing floating drilling vessels have unique piping and valve arrangements dictated by the general layout of the rig itself. However, the well control equipment used on these rigs can only be obtained from this limited number of suppliers.

The well control system consists of the following components (1) The Blowout Preventer Stack, (2) The Control System, (3) The Marine Riser, (4) The Diverter System, and (5) The Choke and Kill Manifolds. The following sections will discuss the types of equipment found to be used on floating drilling vessels, and any government regulations or API recommended practices that are applicable.

2.5.1 The Blowout Preventer Stack

The subsea Blowout Preventer (BOP) stack as discussed herein will consist of (1) a guidebase, (2) a subsea wellhead assembly, (3) various combinations of ram-type and annular-type blowout preventers, and (4) a

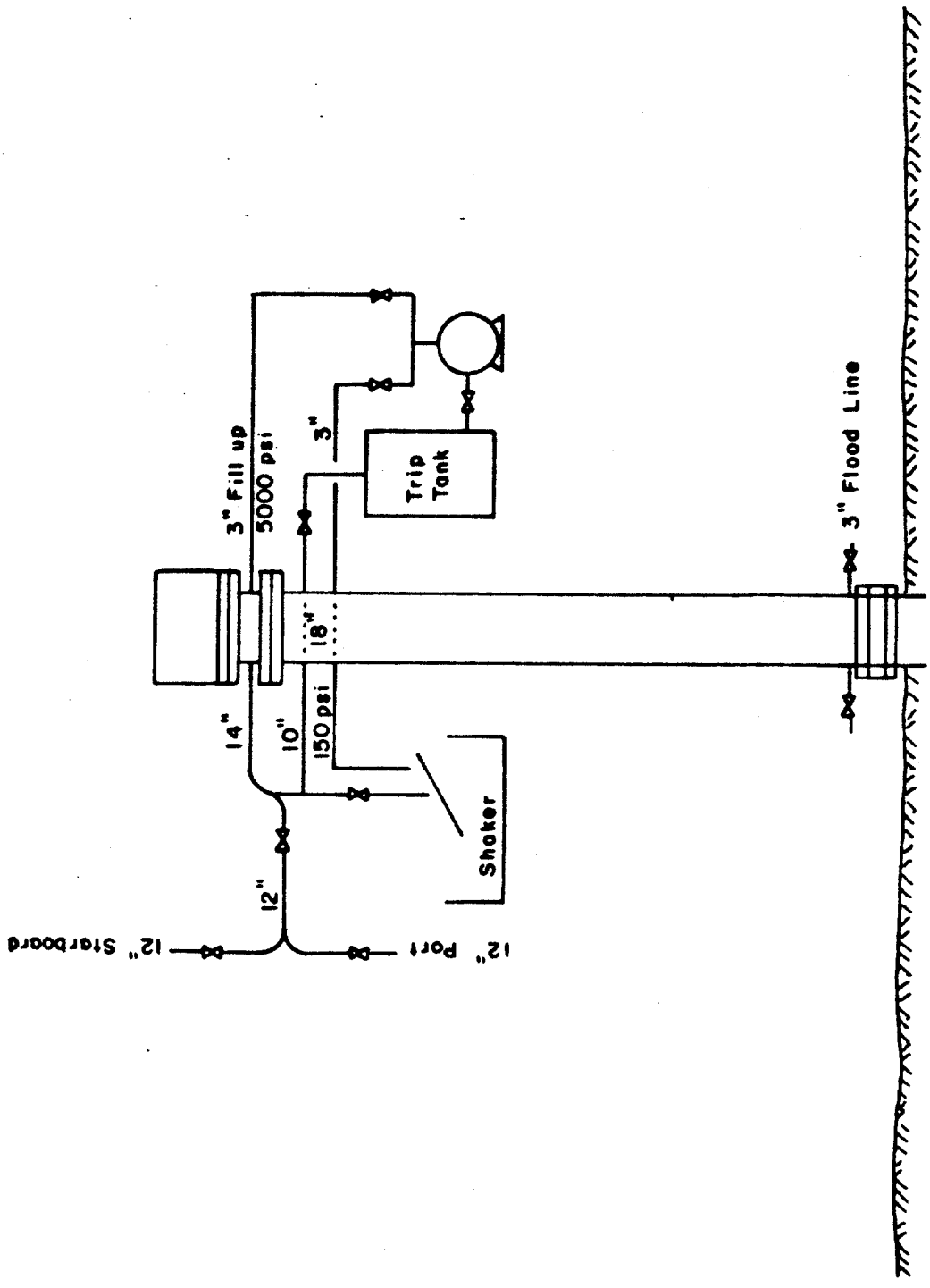

FIGURE 12. TYPICAL FLOW DIVERTER SYSTEM

lower marine riser connector. Fifty-eight (58) of the sixty-six (66) wells drilled in deep water, were drilled by rigs employing a guideline-less drilling system.[3] Drilling without guidelines utilizes a temporary guidebase attached directly to the sea floor, to which a permanent guidebase can be aligned.

The temporary guidebase consists of a large diameter re-entry funnel with a flat bottomed based mounted on top of a caisson. The funnel is cone-shaped to provide easy re-entry of tools into the borehole and to guide the stack into the wellhead. It provides for landing of subsequent casing strings and the wellhead assembly. Four sonar reflectors are positioned around the periphery of the base on extension arms. Figure 13 illustrates a temporary guidebase.[7]

The permanent guidebase, Figure 14, consists of a large diameter funnel with gimbal pads on the underside.[7] The gimbal pads are designed to land on the funnel of the temporary guidebase and allow the permanent guidebase to set level. At the base of the permanent guidebase is a profile for accepting the conductor housing. A diverter assembly can be installed to divert returns and cutting out through the discharge lines away from the base template. Vetco Offshore Group and National Supply Company are the major suppliers of guidebases.

The subsea wellhead is the starting point for most blowout-preventer assemblies. It is a vital link between the casing and the preventer equipment. The surface casing is nearly always welded to the wellhead housing. Subsequent casing strings are then run using the well-housing for support. Figure 15 illustrates a subsea wellhead system.[8] The wellhead housing also provides a pressure seal and hold-down arrangement between the surface casing and BOP stack. There are many suppliers for subsea wellhead assemblies, such as B.J. Hughes, Cameron Iron Works, National Supply Co., Regan Offshore, and Vetco Offshore.

Blowout preventers for a floating drilling rig serve the same purpose as conventional land drilling. They provide a means of pressure control when an undesired flow develops, and they provide for circulating and conditioning the drilling fluid during a flow condition. The blowout preventer stack must also permit:

1. Sustained circulation under pressure for prolonged periods of time;

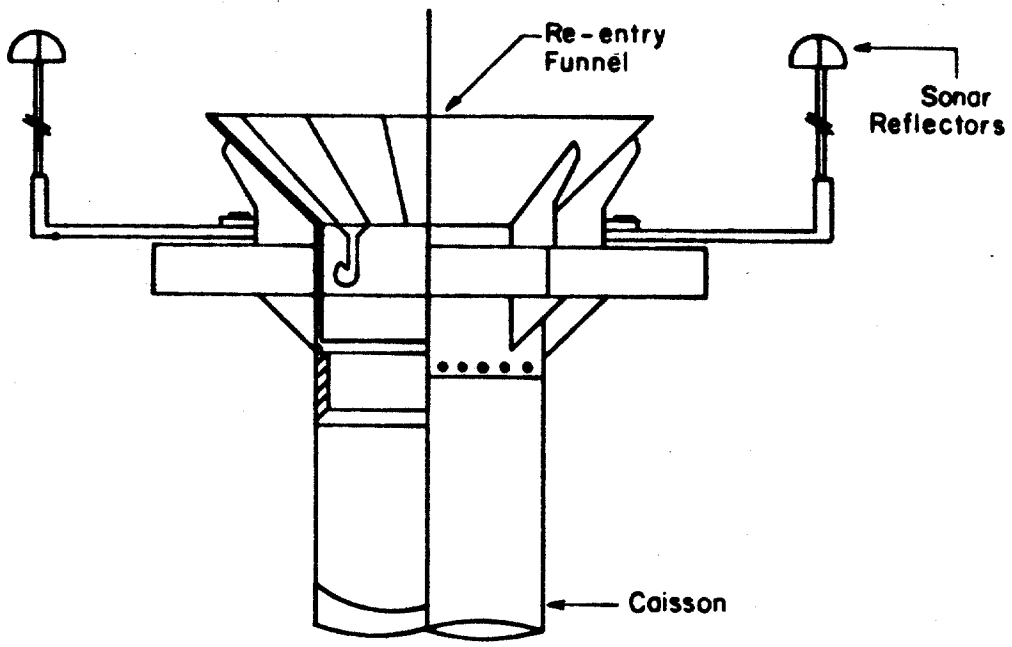

FIGURE 13. TEMPORARY GUIDEBASE[7]

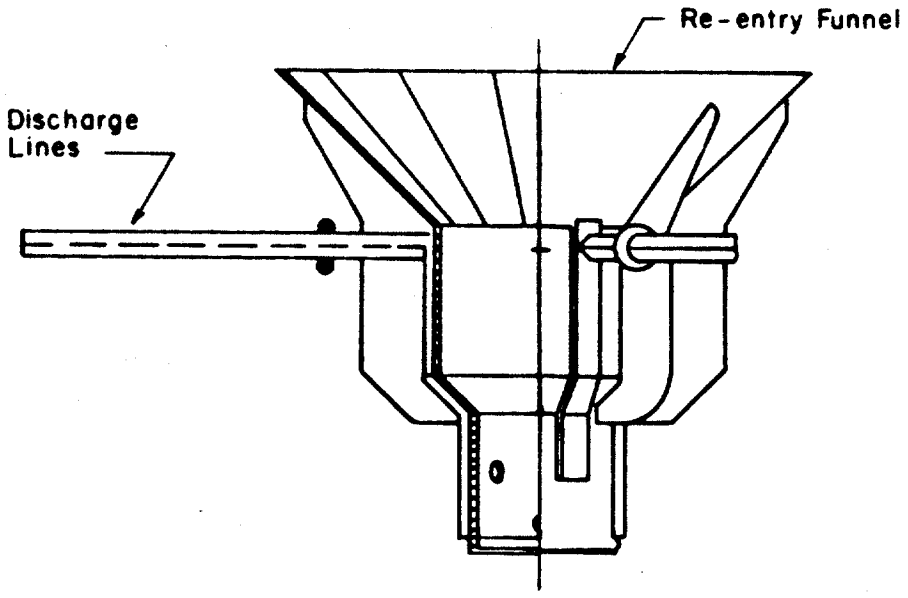

FIGURE 14. PERMANENT GUIDEBASE[7]

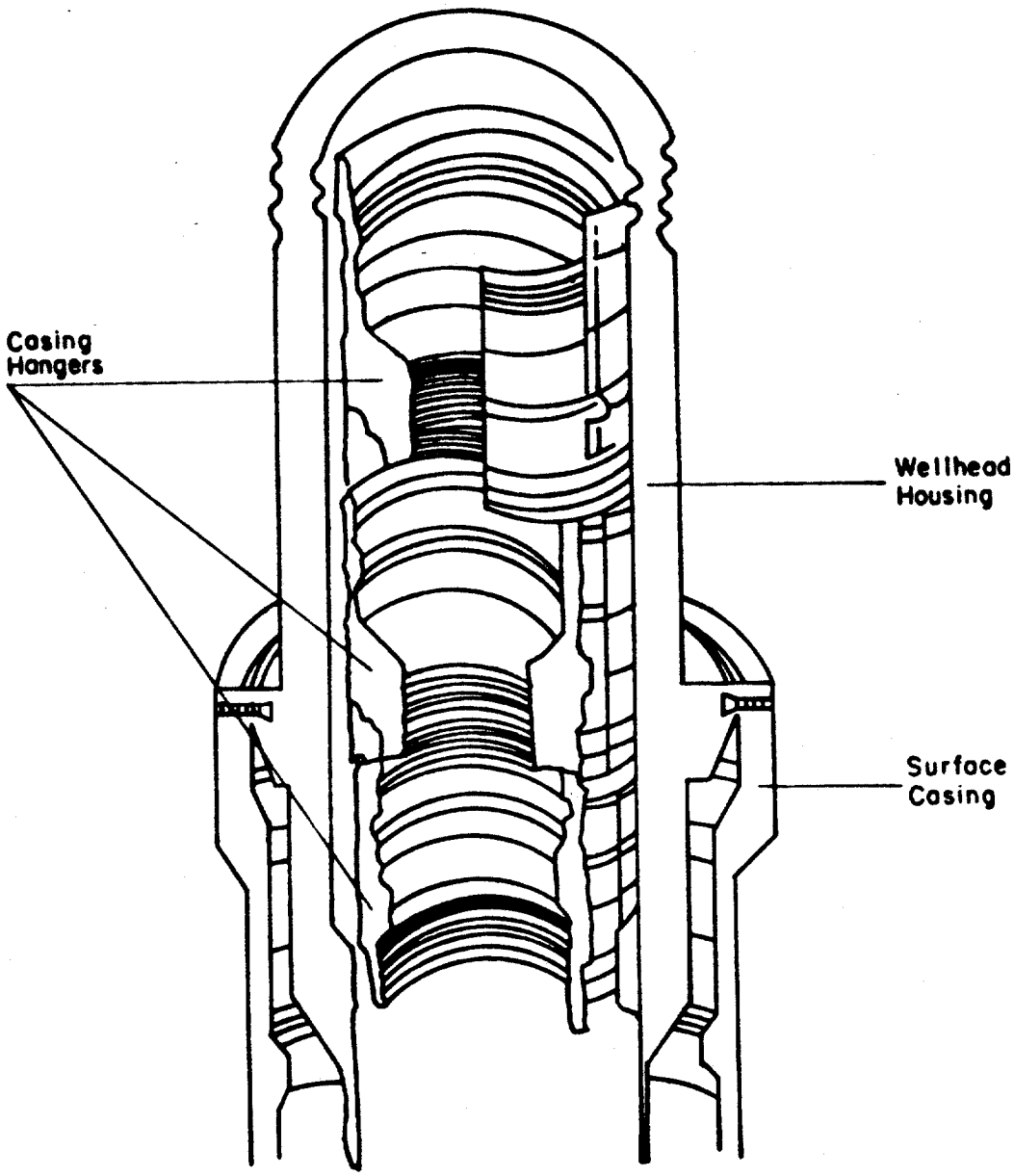

FIGURE 15. WELLHEAD SYSTEM[8]

2. Such actions as hanging off the drill pipe, closing in the well, and moving the drill vessel off location;
3. The reestablishment of the drill vessel on location and the monitoring and reestablishment of circulation down the drill pipe; and
4. Alternate methods of well control in case of failure of any part of the BOP stack.

Any assembly of blowout prevention equipment must be rated by the lowest pressure-rated item in the hookup, whether it is the casing, casing-head, preventers, or the other fittings exposed to pressure. The BOP equipment used on the rigs surveyed were rated at 10,000 psi, and were either 18-3/4 inches or 16-3/4 inches in size. Table 5 is a listing of the rigs surveyed giving the size and pressure ratings of the BOP equipment on each.

A typical subsea BOP stack contains four ram-type preventers and two annular-type preventers. The arrangement of these preventers is determined by the oil company to which the rig is contracted, but the most commonly used arrangements are shown in Figure 16. These two arrangements are those recommended by the API in Recommended Practice No. 53.[9] The arrangements of subsea blowout preventer stacks are similar to the typical surface installations with certain differences. The differences are:

1. Choke and kill lines normally are connected to ram preventer body outlets.
2. Spools may be used to space preventers for shearing tubulars, hanging off drill pipe, or stripping operations.
3. Choke and kill lines are manifolded for dual purpose usage.
4. Blind/shear rams are normally used in place of blind rams.
5. Ram preventers are usually equipped with an integral or remotely operated locking system.

Ram-type BOPs for subsea service differ only slightly from those used on land. The primary difference is the addition of a remote ram-locking device. As one might expect, the same companies that supply the surface BOPs also supply the subsea BOPs. Cameron Iron Works, Hydril Company, and NL Rig Equipment are the largest suppliers of this type of equipment. Tables 6 and 7 contain a listing by manufacturers of the various dimensions and weight for ram-type blowout preventers.[10-12]

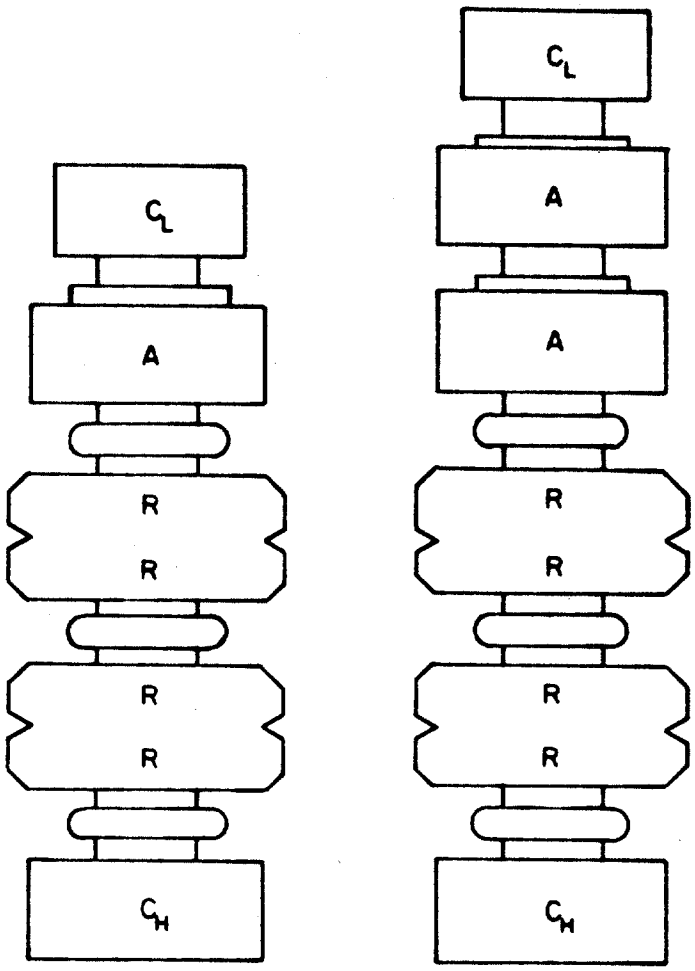

A - annular-type blowout preventer

R - ram-type preventer

C_H - remotely operated high pressure connector used to attach wellhead or preventers to each other

C_L - remotely operated low pressure connector used to attach marine riser to the blowout preventer stack

FIGURE 16. MOST COMMONLY USED PREVENTER ARRANGEMENTS[9] (API RP53)

Table 5 - Size and Pressure Ratings of BOP Equipment on Rigs Surveyed

Rig Name	Size(in.)	Pressure Rating(psi)	Choke & Kill ID (inches)	Number of Subsea Lines
Ben Ocean Lancer	16-3/4	10,000	3.5	2
Discoverer Seven Seas	16-3/4	10,000	3.152	2
Discoverer 534	16-3/4	10,000	2.738	2
Pelerin	16-3/4	10,000		
Penrod 74	18-3/4	10,000		
Dedco 445	16-3/4	10,000	2.5	2
Sedco/BP 471	16-3/4	10,000	3.0	2
Sedco 472	16-3/4	10,000	3.0	2
Sedco 709	16-3/4	10,000	3.0	2
Zapata Concord	18-3/4	10,000	2.4	2

Table 6 - Listing of Dimension and Working Pressures by Manufacturers for Single Ram-type Preventers

	CAMERON IRON WORKS[10]			NL RIG EQUIPMENT[11]			HYDRIL[12]	
Size	16-3/4	16-3/4	18-3/4	16-3/4	16-3/4	18-3/4	16-3/4	18-3/4
Pressure	5,000	10,000	10,000	5,000	10,000	10,000	10,000	10,000
Over-all length (inches)	129.25	139	156.375	118.375	127.25	129.375	132.5	138.25
Over-all height flanged (in)	43.062	49.688	--	43.5	55.875	60.25	44.875	54.25
Over-all height hub (in)	34.938	41.938	43.234	37.75	49.5	51.934	37.625	43.125
Over-all width (inches)	35.75	39.5	42.5	46.5	55.125	56.875	57.375	59.625
Centerline lower outlet to lower flange (inches)	14.812	19.375	--	15.375	21.313	23.5	13.75	18.875
Centerline lower outlet to lower hub (inches)	10.75	15.5	13.875	12.5	--	19.375	10.125	13.313
Top of upper ram to top flange (inches)	16.906	20.219	--	19	23.934	26.406	17.688	22.125
Top of upper ram to top hub (inches)	12.844	16.344	15.344	16.125	20.75	22.25	14.063	16.563
Ram height (inches)	9.25	9.25	12	5.5	8	8	9.5	10
Centerline of preventer to outlet flange (inches)	--	--	--	28.313	33.375	34.25	29.5	33.375
Weight (pounds)	13,750	23,300	28,900	9,475	19,870	20,400	21,000	28,500

Table 7 - Listing of Dimension and Working Pressures by Manufacturer for Double Ram-type Preventers

	CAMERON IRON WORKS[10]			NL RIG EQUIPMENT[11]			HYDRIL[12]	
Size	16-3/4	16-3/4	18-3/4	16-3/4	16-3/4	18-3/4	16-3/4	18-3/4
Pressure	5,000	10,000	10,000	5,000	10,000	10,000	10,000	10,000
Over-all length (inches)	129.25	139	156.375	118.375	127.25	129.375	132.5	138.25
Over-all height flanged(in)	68.875	77.75	--	61.375	74.125	78.063	73	85.75
Over-all height Hub (in)	60.75	70.0	73.812	55.625	65.75	69.75	65.75	74.625
Over-all width (inches)	35.75	39.5	42.5	46.5	55.125	56.875	57.375	59.625
Centerline lower outlet to lower flange (inches)	14.812	19.375	--	15.375	20.813	22.781	13.75	18.875
Centerline lower outlet to lower hub (inches)	10.75	15.5	13.875	12.5	17.625	18.625	10.125	13.313
Top of upper ram to top flange (inches)	16.906	20.219	--	19	23.934	26.406	17.687	22.125
Top of upper ram to top hub (inches)	12.844	16.344	15.344	16.125	20.75	21.25	14.063	19.563
Ram height (inches)	9.25	9.25	12	5.5	8	8	9.5	10
Centerline upper outlet to lower flange (inches)	40.625	47.438	--	33.25	40.25	42.25	41.875	50.375
Centerline upper outlet to lower hub (inches)	36.562	43.562	44.875	30.375	36.875	37.875	38.25	44.813
Top of lower ram to bottom of upper ram (inches)	16.562	18.812	19.125	12.375	11.25	11.25	23.625	21.5
Centerline of preventer to outlet flange (inches)	--	--	--	28.313	33.375	34.25	29.5	33.375
Weight (pounds)	26,940	43,500	56,950	16,200	30,400	35,060	43,000	52,000

Eight of the rigs surveyed were equipped with Cameron ram "type U" preventers. The other two rigs did not indicate the manufacturer of their ram preventers. The ram-type preventers must be fitted with rams that fit the size pipe in the hole and can not be used except on round shapes. It is absolutely vital that the pipe rams in a blowout preventer stack fit the pipe that is in use. If more than one size of pipe is in use M.M.S. OCS Order No. 2[6] requires that a second ram-type preventer be in the stack in order to have both sizes of rams available for instant use. In subsea applications, ram-locking is accomplished hydraulically. Many of the rigs surveyed also had acoustic backups for closing the BOP's. When rams have been locked in the closed position, loss of hydraulic pressure does not affect operation.

The annular-type preventer employs a ring of reinforced synthetic rubber as a packing unit that surrounds the wellbore to effect a shut-off. Annular preventers can effect pressure shut-off on any object of any shape or diameter that might be in the hole. Thus an annular BOP can be closed on the drill string the moment a kick is detected, irrespective of the position of a tool joint relative to the BOP stack. Once the annular BOP is closed on the drill string, the operator can raise or lower the pipe until the tool joint is clear of the stack, after which the proper ram-type preventer may be closed. The annular BOP can be used for continuous stripping. Since tool joints will pass through the closed annular BOP without damage to the packer, continuous stripping either into or out of the hole is possible. Stripping into the hole is often necessary when a kick occurs, since it is necessary to get the pipe back down to the bottom of the hole for total circulation. Continuous stripping represents a substantial savings of rig time as compared to the "hand over hand" stripping that is necessary when stripping through closed rams. Of the rigs surveyed, five were equipped with Shaffer annular preventers while three rigs contained Hydril preventers.

A low-pressure connector on the top of the BOP stack connects the marine riser to the BOP stack. The lower marine riser assembly rotates to align and connect the hydraulic lines as well as choke and kill line subs. The BOP stack remains stationary as the lower riser assembly is rotated until the locking pin engages the slot in the receiver plate on the BOP stack. When the pin is engaged, the retractable connectors in

the lower marine riser stab plate are aligned with the receptacle openings of the BOP receiver plate. Hydraulic pressure applied to the receptacle connectors extend the connectors into the receptacle openings. Cameron Iron Works is one company which provides for this type of connector.

Figure 17 is the blowout preventer stack assembly used on the Zapata Concord at the time of this study. This stack is a 10,000 psi, 18 1/4 inch BOP assembly composed of two Cameron type U double ram preventers, and two NL Rig spherical preventers. The number 1 pipe ram is a shear/blind ram. The number 2 and 4 rams are 5 inch pipe rams, and the number 3 ram is a 3 1/2 inch pipe ram. Note that the second spherical preventer is actually attached to the lower marine riser package. This is a typical subsea blowout preventer stack arrangement for the deep-water floaters.

2.5.2 The Control System

The control system is a means to operate and control the equipment on the BOP stack from the surface location by electrically, hydraulically, or acoustically opening and closing the various preventers. The control system must also handle the choke and kill line valves as well as provide a means to connect and disconnect the BOP stack. The control system plays an important role in any well control operation. The rapid closure of the preventers is essential, not only to minimize entry of fluid into the wellbore, but also to lessen the damage to the rams and packing units due to mud abrasion. The control system is composed of surface equipment, subsea hose reels, and subsea remotely controlled pods. The surface equipment includes accumulator banks, power supplies, and various control panels. The subsea hose reels provide storage for the hydraulic hoses and/or electric cables which provide communication between the surface equipment and subsea control pods. The subsea control pods receive signals from the surface control panels and perform the actual opening and closing of the BOP stack preventers and valves.

The surface components include accumulators of sufficient capacity to close all the units in the BOP assembly at least once with a reasonable reserve of fluid and pressure. In addition to the surface accumulators, subsea accumulators are placed on the BOP stack. Because of

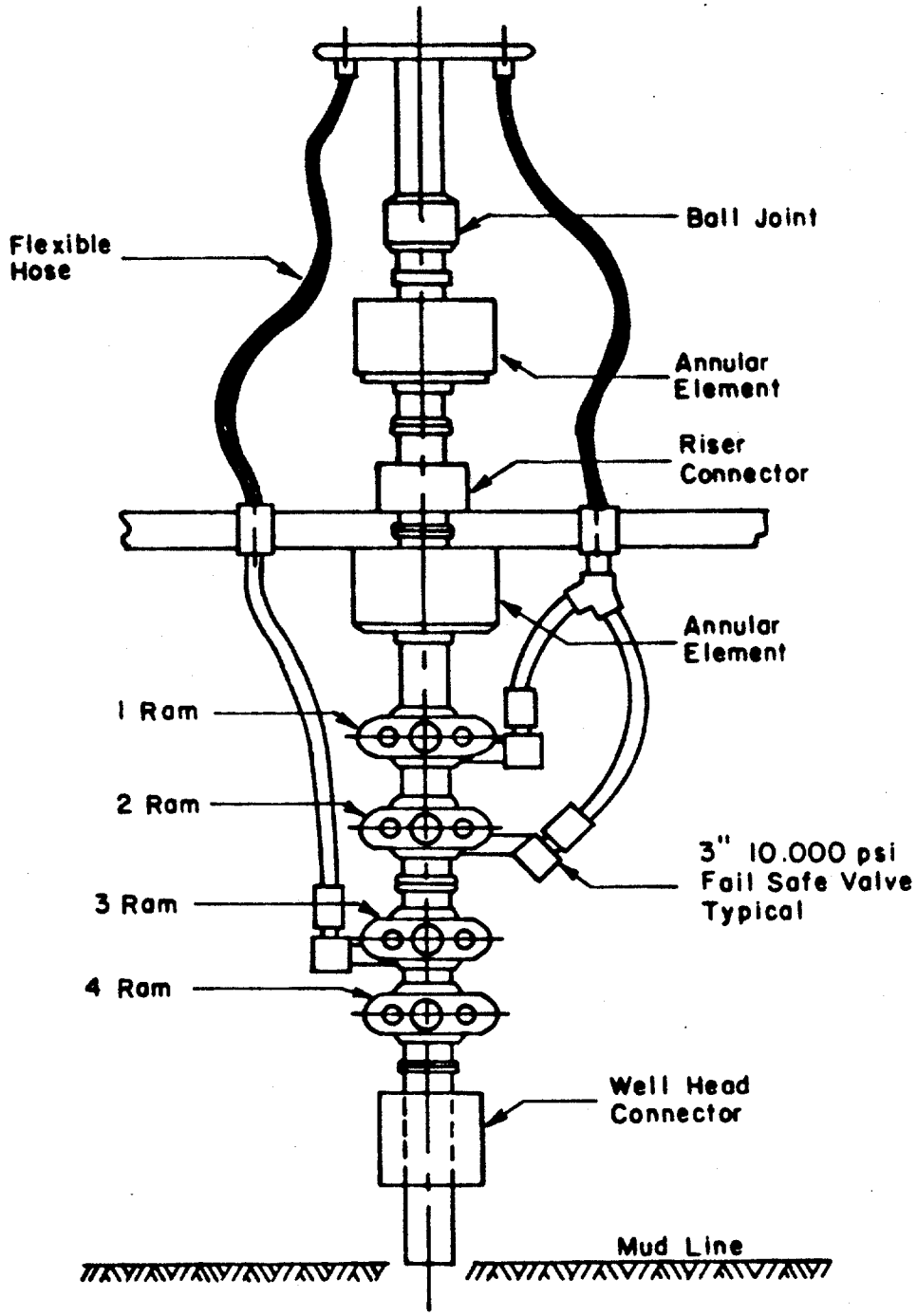

FIGURE 17. ZAPATA CONCORD'S BLOWOUT PREVENTER STACK ASSEMBLY

their proximity to the control pods, the subsea accumulators provide high pressure and high flow rates for faster operation of the stack functions.

Two systems have been developed for remote control of the stack equipment.[13] The first is a completely hydraulic control system. The control hoses are stored on powered reels on the floating rig and are attached to a separate wireline cable as they are lowered to the subsea BOP stack. The opening and closing of the preventers and valves on the BOP stack are accomplished by sending hydraulic signals from the surface control panel down through the hydraulic hose lines to the subsea control pods. Hydraulic pressure is then directed to the appropriate preventer or valve on the BOP stack.

In the second system the surface control panel transmits electrical commands to the subsea BOP control pod through an electrical cable. The subsea electrical components receive these commands and convert them into hydraulic signals for operation of the BOP stack components. This type of system is called an electro-hydraulic system and boasts of a quicker surface to BOP stack response time. Both the totally hydraulic and the electro-hydraulic control systems are equipped with two pods and control cables to have 100 percent standby capacity in case of failure of one pod. Each pod is completely independent of the other.

In addition to the hydraulic and electro-hydraulic systems that are employed in the control system, an acoustic system is also available in which a transducer is mounted on the hull of the drillship or floating rig. This transducer sends signals to a receiving tranducer located on the subsea stack. The subsea unit then actuates the appropriate solenoid valves, which control the stack preventers and valves. The subsea unit can then transmit signals back to the surface unit confirming that the desired action is completed. This system is now being employed strictly as a backup to the previously described control systems.

Of the rigs surveyed, most are equipped with the electro-hydraulic control system. The remaining rigs are equipped with the totally hydraulic system. The majority of the rigs surveyed do have an acoustic backup system.

API Recommended Practice No. 53[9] suggests as a minimum requirement, closing units for subsea installations should be equipped with accumu-

lator bottles with sufficient volumetric capacity to provide the usable fluid volume* (with pumps inoperative) to open and close the ram preventers and one annular preventer and retain a 50 percent reserve.

The accumulator pumps and closing manifold should be located at a safe distance from the well. An alternate control panel should be located on the rig floor or at another location convenient to the driller. Alternate means of producing hydraulic pressure should be provided in case the main system fails. The usual hydraulic-power-arrangement is to provide electrically driven pumps, with standby air-powered pumps, plus stored compressed air.

API Recommended Practice No. 53[9] suggest that a flow meter be included in the surface control system in which the volume of fluid going to a particular function will indicate if that function is operating properly.

API Recommended Practice No. 53[9] also suggests the combination of air and electric pumps should be capable of charging the entire accumulator system from precharge to the maximum rated charge pressure in fifteen minutes or less. The pumps should be installed so that when the accumulator pressure drops to 90 percent of the preset level, a pressure switch is triggered and the pumps are automatically turned on.

2.5.3 Marine Riser Systems

A marine riser system is used to provide a return flow path from the wellbore to the floating drilling vessel and to guide the drill string and tools to the wellhead on the ocean floor. Components of this system include remotely operated connectors, flexible (ball) joints, riser sections, telescopic joints, and tensioners. The marine riser system should have adequate strength to withstand:

1. Dynamic loads while running and pulling the blowout preventer stack;
2. Lateral forces from current and acceptable vessel displacement;

---

*Usable fluid volume is defined as the volume of fluid recoverable from an accumulator between the accumulator operating pressure and 200 psi above the precharge pressure.

3. Cyclic forces from waves and vessel movement;
4. Axial loads from the riser weight, drilling fluid weight, and any free standing pipe within the riser;
5. Axial tension from the riser tensioning system at the surface or from buoyancy modules attached to the exterior of the riser.

Internal pressure rating of the marine riser system, i.e., pipe, connectors, and flexible joint, should be at least equal to the rated working pressure of the diverter system plus the maximum difference in hydrostatic pressures of the drilling fluid and sea water at the ocean floor.

A remotely operated connector (hydraulically actuated) connects the riser pipe to the blowout preventer stack and can also be used as an emergency disconnect from the preventer stack should conditions warrant. Connector internal diameter should be at least equal to the riser system. On most of the rigs, an annular preventer is included in the lower riser package, thus, the hydraulic connector should have a pressure rating conforming to the annular preventers in the stack.

A flexible joint (ball joint) is used in the marine riser system to minimize bending movements, stress concentrations, and problems of misaligned engagement. The angular freedom of a flexible joint is normally 10 degrees from vertical. The flexible joint is always installed at the bottom of the riser system immediately above the annular preventer.

Riser pipe size is determined by the bore of the blowout preventer stack and wellhead, with allowance for clearance in running drilling assemblies, casing, and hangers. For a 16-3/4 inch BOP stack, an 18-5/8 inch O.D. riser pipe is used. An 18-3/4 inch BOP stack employs a 21 inch O.D. riser, usually with 1/2 inch wall thickness. Riser pipe joints are normally made to standard lengths of 50 feet. Pup joints 5, 10, 15, and 25 feet long are employed to obtain assemblies shorter than even increments of the 50 foot lengths.

Marine riser connectors are designed to minimize installation time of the riser system. The riser connectors must be able to support the weight of the BOP stack as it is lowered and landed on the wellhead. The integral marine riser, the standard arrangement at this time, has

the choke and kill lines installed on the riser joints so that they are simultaneously stabbed and made up when the riser connector is made up. This eliminates the handling, rigging, and running time that was necessary with older types of systems. The choke and kill lines can be tested while being run to ensure that they are pressure tight using the integral riser system. The choke and kill lines on the marine riser terminate at the telescopic joint just below the vessel hull. Flexible lines extend from the telescopic joint to the drilling vessel where connections are made to lines leading to the choke and kill manifold. The choke and kill lines on the rigs surveyed are pressure rated at 10,000 psi. The choke and kill lines vary in diameter from 24 in. I.D. to 3.5 in. I.D. (Table 5).

The telescopic, or slip joint is used at the top of the marine riser and functions as follows:

1. It compensates for vertical movement (heave) of the vessel while drilling.
2. It provides a means of connecting a bell nipple or diverter assembly to the riser.
3. It provides fittings for choke and kill line hoses to the drilling vessel.
4. It provides attachment for the riser tensioner system.

A telescopic joint (Figure 18) is comprised of an outer barrel attached to the marine riser assembly and an inner barrel attached to the drilling vessel. The bell-nipple or diverter assembly is attached to the inner barrel which in turn is suspended from the rotary beams of the rig. The outer barrel is connected to the top joint of the marine riser and has connections for attachment of the riser-tensioning lines. The stroke length of the inner barrel inside the outer barrel is usually on the order of 40 to 50 feet.

The outer barrel of the telescopic joint is connected to the riser pipe and remains fixed with respect to the ocean floor. It is suspended from the floating vessel by means of the tensioning system. It provides connections for the kill and choke lines.

The inner barrel is attached to and moves with the drilling vessel. It has an internal diameter that makes it compatible with other parts of the riser system. The top of the inner barrel is attached to the bell-

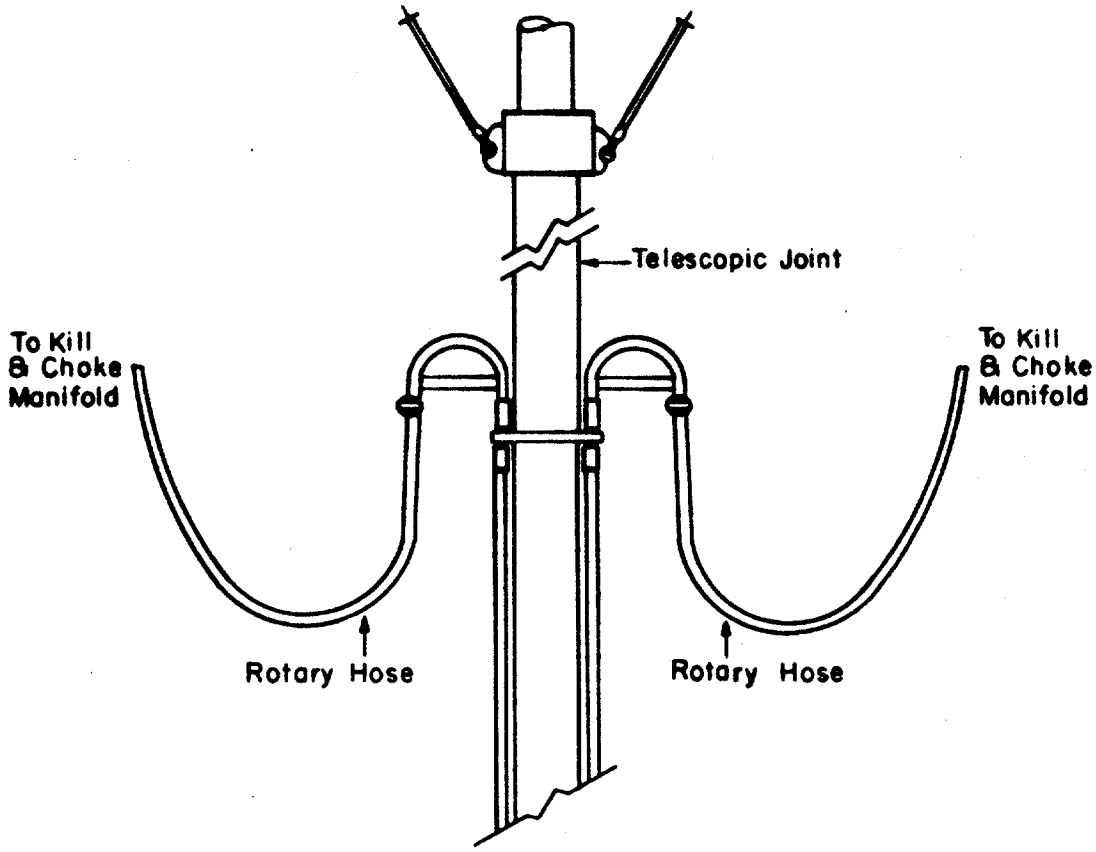

FIGURE 18. TELESCOPIC JOINT SHOWING FLEXIBLE CONNECTIONS AT THE TOP OF THE MARINE RISER FOR CHOKE AND KILL LINES

nipple, or diverter system, and to the mud-return circulating system of the rig.

The major suppliers of marine riser systems are Cameron Iron Works, National Supply Company, Regan Offshore, and Vetco Offshore.

2.5.4 The Diverter System

A diverter system is a means of controlling well flows encountered at relatively shallow depths by directing the flow away from the rig. A diverter system gives a degree of protection prior to setting the casing string on which the blowout preventer stack is installed. It is designed to pack-off around the kelly or drill string and direct flow safely away from the drill vessel. Valves in the system direct the well flow through piping on the vessel so that gas is vented downwing (Figure 19). Prior to setting surface casing, the well cannot be safely shut-in because of the danger of creating a hydrofracture from beneath the conductor casing to the surface. In an extreme case, hydrofracture outside the casing can lead to the formation of a large crater.

When a diverter system is used, the marine riser is attached to the drive pipe or conductor casing, and the diverter system is connected to the inner barrel of the telescopic joint and secured to the rig substructure. Vent lines from the diverter usually have large diameters (10 inches or more) and are designed to divert well fluids with a minimum of back pressure on the well. They are directed to opposite extremities of the vessel. All valves in the diverter line are full opening and are usually designed to automatically open whenever the diverter is closed. High pressure on the diverter is not practical because the telescopic joint pack-off seal is not useful for pressure exceeding 50 to 100 psi and because excessive pressure on the diverter could cause formation rupture and cratering around the conductor casing and create a very hazardous condition for the floating rig.

Most of the functions of the diverter system are hydraulically operated from the diverter control panel. Once the diverter is closed on the drill string, the flow line on the shale shaker is automatically closed and the port or starboard line valve is opened depending on wind direction.

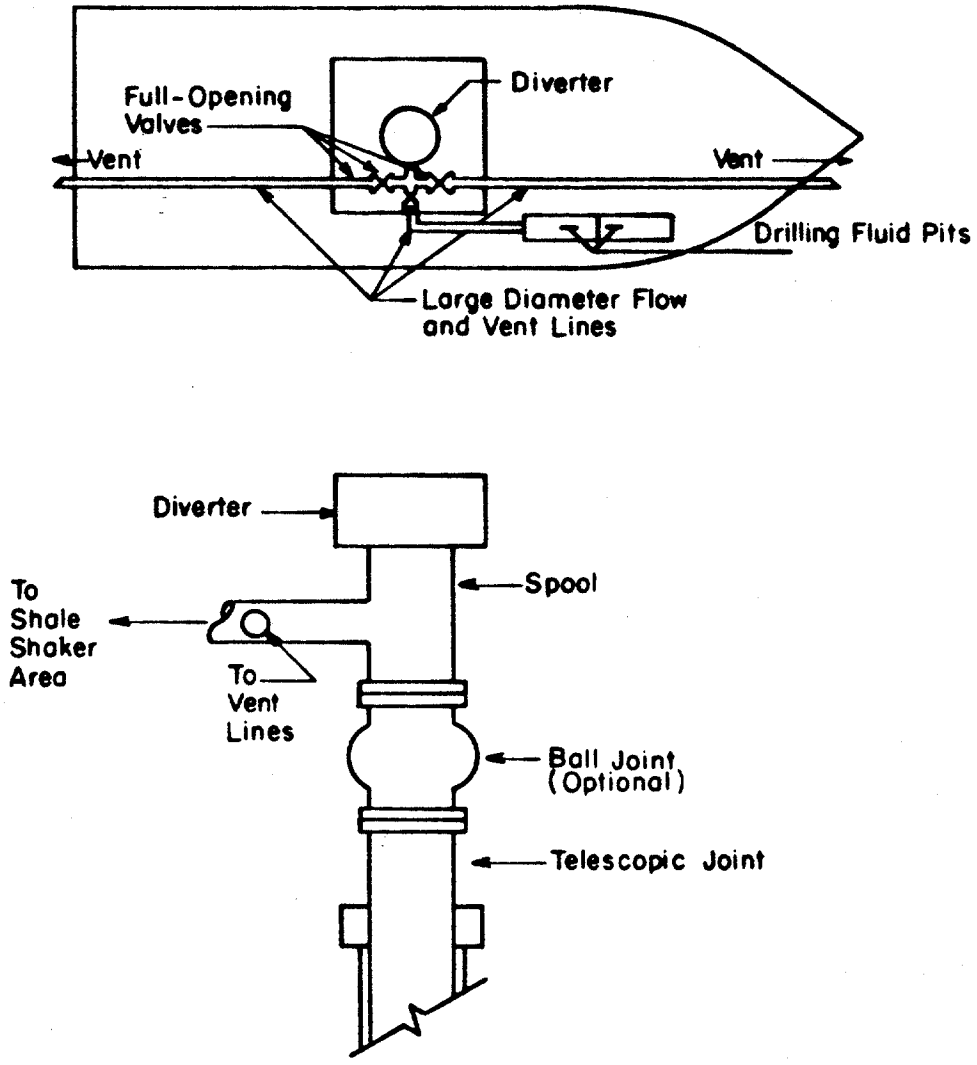

FIGURE 19. TYPICAL DIVERTER SYSTEM FOR SUBSEA INSTALLATION

Both Regan Offshore and Vetco Offshore offer diverter systems which can be run through 37-1/4 inch or 49-1/2 inch rotary tables and land in a housing built into the rotary table beams.

2.5.5 The Choke and Kill Manifolds

If the hydrostatic head of the drilling fluid is insufficient to control subsurface pressure, formation fluids will flow into the well. To maintain well control, back pressure is applied by routing mud returns through adjustable chokes until the well flow condition is corrected. The chokes are connected to the blowout preventer stack through an arrangement of valves, fittings, and lines which provide alternative return flow routes or permit the flow to be halted entirely. This equipment assemblage is designated the "choke manifold". Figure 20 illustrates a typical choke and kill manifold assembly for a subsea installation with facilities adequate for 10,000 psi rated working pressure.[9] On subsea installations, choke and kill lines are manifolded to permit pumping through either line. Other features are remotely controlled adjustable chokes, duplicate adjustable or manual choke systems to permit control through either the choke or kill line, double valves immediately upstream of each choke, accurate pressure gauges, and tie-ins to both drilling fluid and high pressure pump systems.

The API Recommended Practice No. 53[9] for the planning and installation of choke manifolds for subsea installations include:

1. The assembly, connections, full-opening valves, fittings, piping, etc., subject to well or pump pressure should be flanged, clamped, or welded and have a rated working pressure at least equal to the rated working pressure of the blowout preventers.
2. All components should be selected in accordance with applicable API Specifications, taking into consideration pressures, volumes, temperatures, and conditions under which they may be operated.
3. The assembly should be 3 inch nominal diameter or larger, have a minimum number of turns, and be securely anchored. Turns in the assembly should be targeted.
4. The choke control station, whether at the manifold or remote from the rig floor, should be as convenient as possible and should include all monitors necessary to furnish an overview of the well

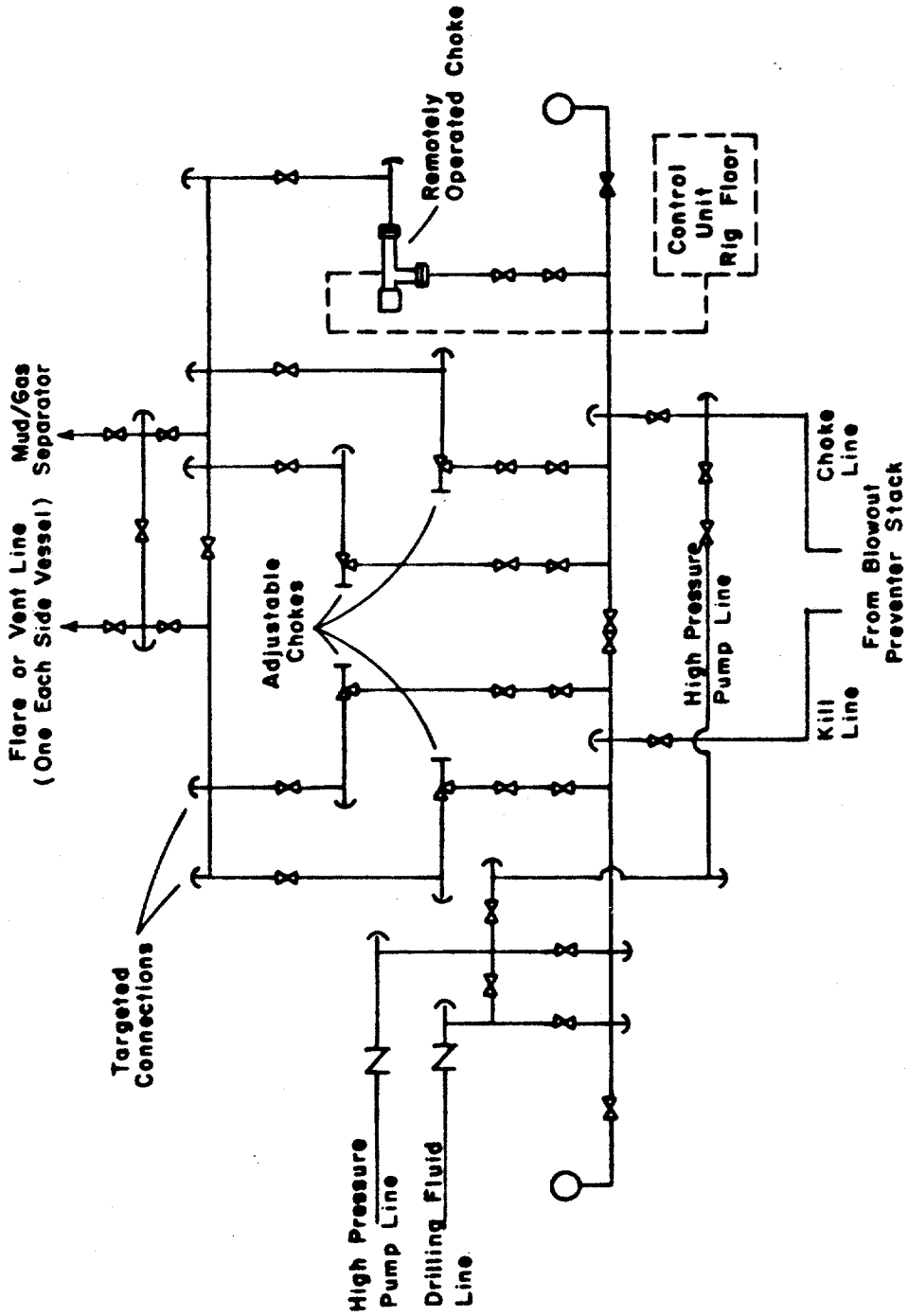

FIGURE 20. TYPICAL CHOKE MANIFOLD ASSEMBLY FOR SUBSEA INSTALLATION[9]

control situation. The ability to monitor and control from the same location such items as standpipe pressure, casing pressure, pump strokes, etc., greatly increases well control efficiency.

5. Rig air systems should be checked to assure their adequacy to provide the necessary pressure and volume requirements for controls and chokes. A redundant automatic choke control system should be provided in the event that air becomes unavailable.
6. Initial testing of the entire choke and manifold assembly to the rated working pressure of the preventers should be performed when the blowout preventer stack is on the test stump, and thereafter whenever the blowout preventers are tested.
7. Lines downstream of the choke manifold are normally not required to contain rated manifold working pressure, but should be tested during the initial installation.
8. Lines downstream of the choke manifold should be securely anchored, be of sufficient size to minimize friction, and permit flow direction either to a mud/gas separator, ventlines, or to production facilities or emergency storage. Two vent lines diametrically opposite one another are required to compensate for variations in wind direction.

Choke and kill manifolds are permanently installed at the time of rig construction. However all of the rigs surveyed utilized the recommended configuration of the API.

2.6 CURRENT BLOWOUT PREVENTION PROCEDURES

The primary method of controlling formation pressures is accomplished by monitoring the weight of the circulating fluid in the hole. In the event that this does not prove adequate, the hole will be protected by actuating the blowout preventer equipment. This will prevent further intrusion of the formation fluids into the hole. In this static state, the proper mud weight can then be calculated. By opening the choke line, the formation fluids can then be circulated out of the borehole by pumping mud down the drill string, up the well annulus, up the choke line and out of the well through an adjustable choke at the surface. Numerous methods for circulating out a "kick" from the borehole have been developed. Basically they all have the same general

principle of keeping the bottom hole pressure constant at a value slightly above the formation pressure while pumping the kick fluids from the well and the new, higher density mud into the well. The desired bottom hole pressure must be achieved by proper operations of the adjustable choke.

2.6.1 Government Regulations

It is critical that the drilling personnel aboard a rig can recognize the indications that a kick is occurring, determine that formation fluids have entered the borehole, and if so can safely and swiftly circulate the formation fluids from the wellbore. The U.S. Government is requiring drilling personnel to attend classroom lectures and hands-on demonstrations to qualify to drill on offshore locations. Under M.M.S. OCS Order No. 2[6], paragraph 7.3, all drillers, toolpushers, and operator's representatives should receive training in well-control operations. In order to maintain qualifications, drillers, toolpushers, and operator's representatives should successfully complete a refresher course annually and repeat the basic well-control course every 4 years. The refresher course should be completed within 60 days of the students anniversary date. Records should be maintained at the drill site for the affected personnel, indicating the specific training and refresher courses successfully completed, the dates of completion, and the names and dates of the courses.

2.6.2 Approved Well Control Training

Both the basic training course and the refresher course must be approved by the M.M.S. The Minerals Management Service has issued "Outer Continental Shelf Standard Training and Qualifications of Personnel in Well-Control Equipment and Techniques for Drilling on Offshore Locations"[15] (GSS-OCS-T1). This publication presents guidelines for course curricula. This includes course curricula for the rotary helper, the derrickman, the driller, the toolpusher, and operator's representative. Topics such as the blowout-prevention equipment, warning signs of kicks, drilling fluids, properly shutting in a well for well control purposes, well control operations, and relevant government regulations are outlined. The American Petroleum Institute

has published similar training and qualifications guidelines in their Recommended Practice API RPT-3.[16]

An M.M.S. representative will visit the training site to discuss with course lecturers their curricula and qualifications. He will review the course manuals and outline to see if they comply with the "Outer Continental Shelf Standard Training and Qualifications of Personnel in Well-Control Equipment and Techniques for Drilling on Offshore Location".[15] He may elect to participate in an actual course before recommending that the course receive M.M.S. approval. To date, 38 schools have been approved by the M.M.S. for basic training courses in Blowout Prevention for Subsea Stacks for the driller, toolpusher, and operator's representative (Table 8.) All but one of these schools also have been approved by M.M.S. for a refresher training course in Blowout Prevention for Subsea Stacks.

2.6.3 Well Shut-in Procedures

Of the 38 approved basic training courses, 11 are conducted by oil company personnel for in-house training of their workers. These courses were of special interest in this study, since in all cases, it is the operator's prerogative to elect the method of well control he will utilize during the drilling of a well. The M.M.S. was contacted to provide the well control manuals for these 11 courses. However, due to the large volume of material requested, only five of these training manuals were received. The M.M.S. stated that these manuals would provide a representative sample of the course curricula and procedures recommended by these courses. The manuals received were from the courses approved for Exxon Corporation, Cities Service Company, Gulf Research and Development, Shell Oil Company, and Texaco, Inc.

The shut-in procedures outlined in these manuals differed slightly from operator to operator. Most operators in the study sample favor a soft shut-in procedure, with the idea of minimizing any shock pressure loadings associated with the rapid deceleration of fluid being ejected from the well. This is accomplished during drilling operations using the following shut-in procedure:

1. Stop the rotary.
2. Pick up kelly to previously calculated space out elevation.
3. Shut down the mud pumps.

Table 8 - M.M.S. Approved Basic Courses In Blowout Prevention with Subsea Stacks for Drillers, Toolpushers, and Operator Representatives.

1. Chevron U.S.A. Inc.		OR	SUR, SS
2. Conoco Inc.		OR	SUR, SS
3. Delta Drilling Company	DR, TP,	OR	SUR, SS
4. Dresser Industries	DR, TP,	OR	SUR, SS
5. EXXON	DR, TP,	OR	SUR, SS
6. IMCO SERVICES	DR, TP,	OR	SUR, SS
7. Louisiana State University	DR, TP,	OR	SUR, SS
8. Milchem Incorporated	DR, TP,	OR	SUR, SS
9. Shell Oil Company	DR, TP,	OR	SUR, SS
10. Texaco	DR, TP,	OR	SUR, SS
11. University of Southwestern Louisiana	DR, TP,	OR	SUR, SS
12. Ventura College	DR, TP,	OR	SUR, SS
13. Petroleum Training and Technical Services	DR, TP,	OR	SUR, SS
14. Murchison Drilling Schools	DR, TP,	OR	SUR, SS
15. Ocean Drilling and Exploration Co.	DR, TP,	OR	SUR, SS
16. Diamond M. Company	DR, TP,	OR	SUR, SS
17. Cities Service Company		OR	SUR, SS
18. Shell Oil Company (White Castle)	DR, TP,	OR	SUR, SS
19. University of Oklahoma	DR, TP,	OR	SUR, SS
20. NL Petroleum Services	DR, TP,	OR	SUR, SS
21. University of Texas at Austin (PETEX)	DR, TP,	OR	SUR, SS
22. Gulf Research and Development	DR, TP,	OR	SUR, SS
23. Rike Service Inc.	DR, TP,	OR	SUR, SS
24. Prentice and Records Enterprises, Inc.	DR, TP,	OR	SUR, SS
25. AMOCO Production Company		OR	SUR, SS
26. Loffland Brothers Company	DR, TP,	OR	SUR, SS
27. Atlantic Pacific Marine Corp.	DR, TP,	OR	SUR, SS
28. Basic Research and Training, Inc.	DR, TP,	OR	SUR, SS
29. Well Control School, Inc.	DR, TP,	OR	SUR, SS
30. Alaska Skill Center	DR, TP,	OR	SUR, SS
31. Keydril Company	DR, TP,	OR	SUR, SS
32. Arco Oil & Gas Company	TP,	OR	SUR, SS
33. Marlin Drilling Company, Inc.	DR, TP,	OR	SUR, SS
34. Oklahoma Petroleum Training Corp.	DR, TP,	OR	SUR, SS
35. Union Oil Company of California	DR, TP,	OR	SUR, SS
36. Cape Cod Community College	DR, TP,	OR	SUR, SS
37. Western Oceanic, Inc.	DR, TP,	OR	SUR, SS
38. Dixilyn-Field Drilling Company	DR, TP,	OR	SUR, SS

4. Check for flow.
5. If flowing, notify superintendent and toolpusher.
6. Open the subsea choke valve on BOP control panel.
7. Close the annular preventer.
8. Close the adjustable choke.
9. Record the drill pipe and casing pressures.
10. Record the pit gain.
11. Adjust the closing pressure on the annular BOP.
12. Initiate hang-off procedure.
13. Re-evaluate the shut-in pressures.
14. Initiate kill procedures.

Notice that with this procedure, fluid deceleration is achieved in step 8, by closing the adjustable choke.

Other operators prefer a more rapid shut-in, with the idea of minimizing the influx of formation fluids as much as possible. For gas kicks, the choke pressure observed when the gas reaches the surface will be lower for a smaller kick size. This is accomplished during drilling operations using the following procedure:

1. When a primary warning sign of a kick has been observed, immediately raise the kelly to the point previously designated during the spacing out procedure.
2. Stop the mud pumps.
3. Close the annular preventer.
4. Notify the company personnel.
5. Close the upper set of pipe rams.
6. Reduce the hydraulic pressure on the annular preventer.
7. Lower the drill pipe until the pipe is hung-off on the rams.
8. Read and record the shut-in drill pipe pressure, shut-in casing pressure, and the pit gain.

2.6.4 Procedures for Handling Upward Gas Migration

After a well has been shut-in due to the presence of a kick, there may be a considerable lapse of time before circulation of the kick fluids from the well can be initiated. Delays may be caused by problems achieving the desired kill mud density or mechanical problems with equipment or high pressure flow conduits. It is widely recognized

that migration of gaseous kick fluids during a prolonged shut-in period can cause excessive and unnecessarily high wellbore pressures. The manuals in the survey sample were in agreement that this problem is best solved by periodically bleeding mud through a choke at the surface to maintain the bottom hole pressure nearly constant. Changes in bottom hole pressure are best ascertained by observing changes in the surface drill pipe pressure (drill pipe pressure method). When this cannot be done, a casing pressure/pit gain schedule can be computed and followed (volumetric method). None of the manuals addressed any special problems of using these methods with the well geometry present for deep water floating drilling operations.

2.6.5 Pump Start-up Procedure

Starting the pump, like well closure, is a critical part of the overall well control procedure. Many underground blowouts are thought to occur during pump start-up. Problems occur at this time because in modern well control procedures, operation of the adjustable choke is based primarily on drill pipe pressure observations made while the pump is running at a constant speed, called the kill speed.

Unfortunately, before the pump speed is brought to and stabilized at this kill speed, the transient well conditions are more difficult to describe and control.

The basic intent during pump start-up, as in all phases of well control operations is to keep the bottom hole pressure at a value equal to or slightly above the formation pressure. Usually, the bottom hole pressure is allowed to increase during pump start-up by an amount equal to the frictional pressure loss in the well annulus at the selected kill speed. A small pressure increase is desirable because it provides some margin for error on the part of the choke operator. Annular frictional pressure loss is a good means of providing this safety margin because the portion of the frictional pressure loss in the annulus which occurs below the casing seat does not add to the pressure at the casing seat. The control of bottom hole pressure during pump start-up must be accomplished using the well pressure information routinely available at the surface.

The present-day well control method used to initiate the circulation of formation fluids from the wellbore is to start pumping while simultaneously opening the choke so that the casing pressure is maintained constant at, or slightly above, its previous shut-in value. Because of the high frictional pressure drop in the long underwater flowlines associated with floating drilling operations, this procedure can produce an excessive annular back-pressure. This in turn could lead to formation fracture and a subsequent underground blowout. In addition, the subsea flowlines are sometimes filled with water to prevent plugging of the flowlines when they are not in use. This complicates the annular pressure behavior during start-up because of the density difference between the water initially in the flowline and the drilling fluid which will ultimately displace this water. Most of the well control manuals examined did not fully address the special deep water well control problems associated with the excessively high frictional pressure losses in the long subsea flowlines. Those that did, recommended the routine measurement of choke line friction by noting pump pressure when circulating the well through the marine riser and through the choke line. Choke line friction is determined as the difference between these two values. When starting the pump during well control operations, it is recommended that casing pressure be allowed to decrease by an amount equal to choke line friction as the pump comes up to the desired kill speed.

Additional potential solutions to this problem that have been suggested in personal communications with various individuals in drilling operations include:

1. Measurement of choke line frictional pressure losses at the kill speed by pumping down the choke line and up the marine riser.
2. Measurement of choke line frictional pressure losses at the kill speed by pumping down the kill line and up the choke line.
3. Measurement of choke line frictional pressure losses by pumping down the drill string and taking the return flow up the choke line, but through a partially closed choke. The kill line is used as a monitor line and choke line friction is determined as the difference between the monitor line pressure and the choke pressure.

4. Use of a drill pipe pressure/pump speed schedule designed to keep a near constant bottom hole pressure during pump start-up.
5. Use of a casing pressure/pump speed schedule designed to keep a near constant bottom hole pressure during pump start-up.
6. Use of a subsea wellhead pressure monitor during pump start-up.
7. Use of the kill line as a monitor line during pump start-up.
8. Use of multiple choke lines.
9. Use of a remote operated subsea choke.

2.6.6 Pump Out Procedures

When a gas kick is circulated from a well in deep water, an operational problem could exist when the gas bubble reaches the subsea preventer stack located on the ocean floor. There follows a very rapid elongation of the bubble as it exits the large casing and proceeds upward through the small diameter choke line which parallels the larger marine riser pipe. There is a question whether a choke operator would have adequate time to respond properly to the rapidly changing pressure conditions associated with this phenomenon. This potential problem was not addressed in any of the well control manuals studied. However, potential solutions that have been suggested in personal communications with various individuals in drilling operations include:

1. Use of a greatly reduced pump speed just prior to gas reaching the seafloor.
2. Use of multiple choke lines.
3. Use of larger diameter choke lines.
4. Development and use of a subsea choke.

2.7 SUMMARY

After completing the review of existing blowout prevention equipment and procedures for use in deep-water floating drilling operations, it was felt that considerable experimental work was needed to clarify several potential problem areas. The advance from the relatively modest water depths of the continental shelf to the deep water of the continental slope has just begun, and is being conducted with only minor changes in equipment and procedures developed in much shallower water.

Special procedures and training for deep-water well control operations are being actively discussed, but this area has not yet developed to the point of being included in detail in well control manuals. The current MMS training requirements address only surface and subsea BOP stack arrangements, regardless of water depth.

CHAPTER 3

RESEARCH WELL FACILITY

After completing the review of existing blowout prevention equipment and procedures used on floating drilling vessels, a research well facility was designed which closely models the special flow geometry present for deep water well control operations. The design of the model well facility was aided by computer simulations of a large number of well-control operations for a variety of deep-water drilling situations and a variety of well geometries. A current "state of the art" well-control model used in these simulations assumes: (1) that any formation gas which enters the well remains as a continuous slug and occupies the entire cross-sectional area of the annulus during all of the well-control operations, (2) that the gas flows at the same velocity as the drilling fluid during the well-control operations, and (3) that the well-control operator maintains a constant bottom-hole pressure. Although these assumptions are not entirely true, the results obtained are considered sufficiently valid to be used in design considerations of the experimental facility.

One of the deep water drilling situations used in the computer simulations was a well drilled in 1978 in 4342 feet of water off the Congo with the drill-ship Discoverer Seven Seas. Shown in Fig. 21 is a schematic drawing of this well and additional well data are given in Table 9. The well was drilled to a depth of 16,000 feet with no reported kicks. The situation assumed in Fig. 21 for the purpose of the computer simulations represents shut-in conditions which would have resulted from a 0.5 ppg kick while drilling with a 9.2 ppg mud at a depth of 11,540 feet.

Shown in Figure 22 is the results of the computer simulations for the Congo Well example. Consideration of this figure shows several important aspects of the well-control process which the experimental facility must model. An initial shut-in choke pressure of 440 psig results in a well-bore pressure at the casing seat very near the

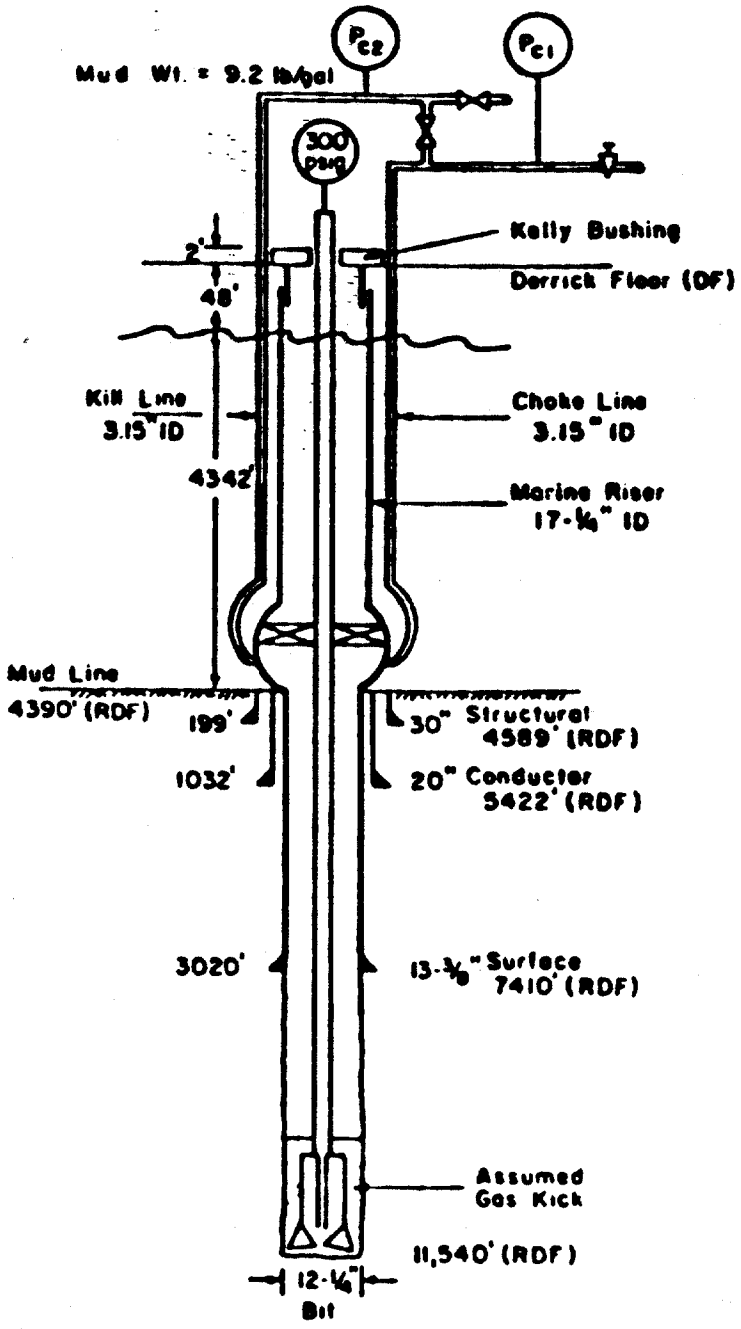

Figure 21 - Schematic Diagram for Congo Well Example

Table 9 - Data for Congo Well Example.

WELL DATA

1.	Casing:	13 3/8 in., J-55, 61 lb/ft
2.	Drill Pipe:	5 in., 19.5 lb/ft
3.	Drill Collars:	540 ft, 8 x 3 in.
4.	Drill Bit:	12 1/4 in., 12-13-13/32 in. jets
5.	Mud:	9.2 ppg. μ_p = 16cp, τ_y = 10lb/100 sq ft.

PUMP DATA

1.	Type:	Single Acting Triplex
2.	Liner Size:	6 1/2 in.
3.	Stroke:	11 in.
4.	Efficiency:	96%

CIRCULATION DATA

		Drill-pipe Pressures, Psig		
Conditions	SPM	Thru Riser	Thru Choke Line	Choke Line Friction, psi
Norm. Drilling	110	2400		
Reduced Rate 1	50	600	880	280

KICK DATA (Simulated)

1.	Shut-in Drill-pipe Press.:	300 psig
2.	Shut-in Choke Press:	440 psig
3.	Pit Volume Gain:	30 bbl

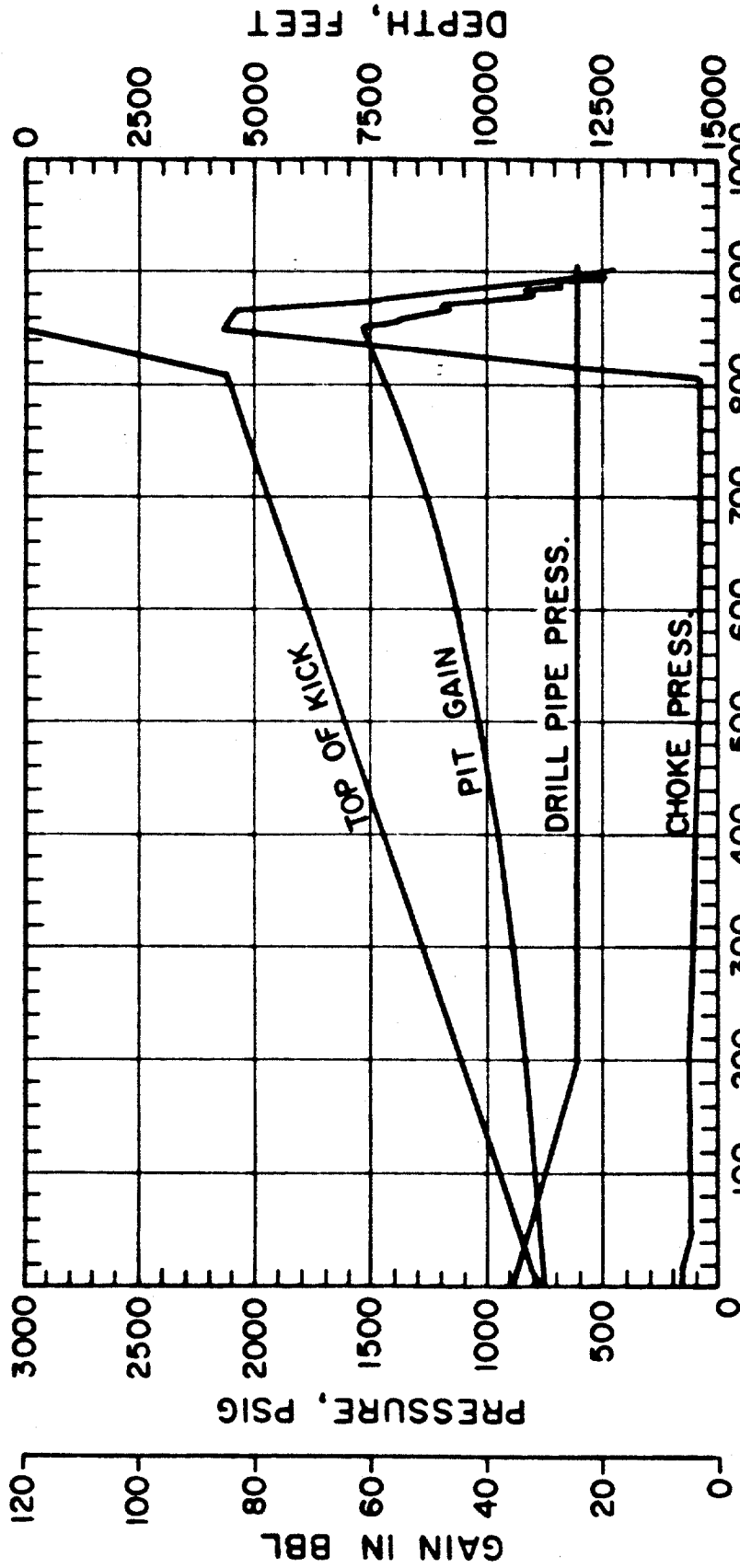

FIGURE 22. PREDICTED WELL BEHAVIOR FOR CONGO EXAMPLE

fracture pressure. The circulating frictional pressure loss in the choke line is 280 psi for a pump speed of 50 spm and, upon pump start-up, the choke pressure falls from 440 psig to 160 psig. There follows a long and relatively uneventful period as the kick is circulated from the bottom of the well to the seafloor. However, once the gas reaches the seafloor and enters the choke line, the choke pressure must rapidly increase from less than 100 psig to more than 2100 psig. A short time later, a rapid decrease in choke pressure is required as mud displaces gas from the choke line. The average mud velocity in the choke line, which is felt to be a measure of how rapidly the pressures must change, is 562 ft/min in this example.

Numerous examples, such as the one shown in Figure 22, were studied using data from different rigs and a wide variety of assumed well conditions. Other examples were studied using data from proposed wells in the Ocean Margin Drilling Program[17] which have been planned for water depths of up to 13,000 feet. Computed choke-pressure profiles are shown in Figure 23 for the proposed modified Glomar Explorer drillship on a location offshore from New Jersey in 7875 ft of water. Note that the results are similar to those previously discussed.

It was felt that the experimental well facility should model the significant phases of the previously discussed example and in addition allow the experimental study of the special well-control procedures identified in the review of existing and recommended well control procedures. The desired features of the experimental well facility included:

1. Realistic values for circulating frictional pressure loss in the choke line.
2. Realistic values for changes in choke pressure when a gas kick is circulated through the choke line.
3. Realistic values of circulating drill pipe pressures.
4. The availability of two subsea flow lines, one of which could be closed at the simulated sea floor to prevent collection of gas in the line when it was not in use.
5. Reasonable kick circulation time.
6. Reasonable initial cost and operating cost.
7. Reasonable nitrogen injection pressure at realistic gas influx rates.

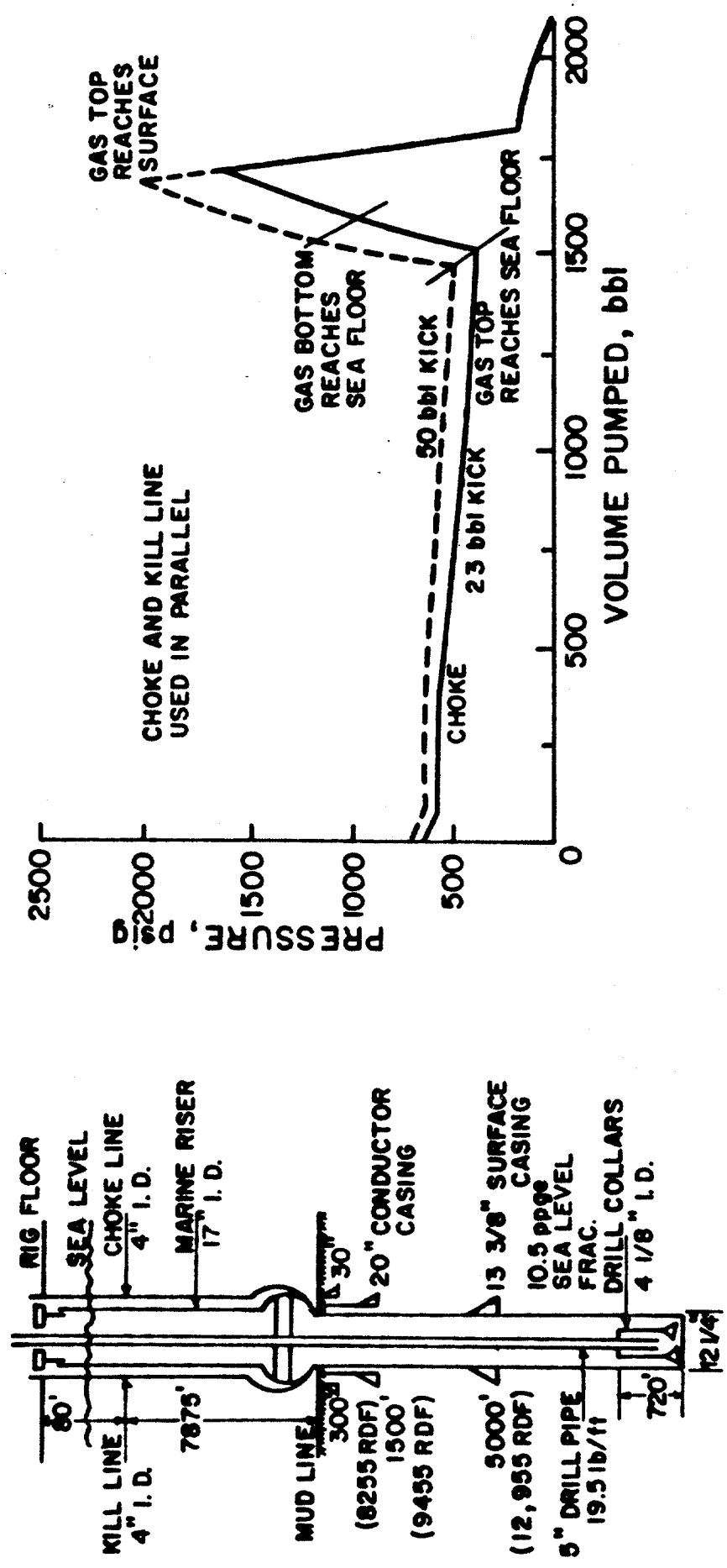

FIGURE 23 . PREDICTED WELL BEHAVIOR FOR GLOMAR EXPLORER DRILLSHIP ON PROPOSED OFFSHORE NEW JERSEY LOCATION

All of these factors interact considerably, making an optimal design difficult to determine. The basic approach used was to simulate the model well behavior on a computer for a large number of possible well designs and then select a final design which appeared to achieve the best balance of the above design criteria.

The final well design selected is shown in Figures 24 and 25 and a photograph of the well and surface installation which is on the LSU Campus is shown in Figure 26. A simulated water depth of 3000 feet was selected and the simulated subsea choke and kill lines (2.375 in. tubing) were run inside 10.75 in. casing to this depth. The effect of the BOP stack located on the sea floor is modeled in the well using a packer and triple parallel flow tube designed by Baker. A subsea kill line valve at 3000 feet is modeled by using a surface-controlled subsurface safety valve designed by Hydril. This control allows experiments to be conducted using only the choke line, the kill line being isolated from the system as is often the case in well-control operations on floating drilling vessels. The drill string is simulated using 6000 feet of 2.875 in. tubing. Nitrogen gas is injected into the bottom of the well at 6,100 feet through 1.315 in. tubing placed in the drill string. A pressure sensor is located at the bottom of the nitrogen injection line to allow continuous surface monitoring of bottom hole pressure during simulated well-control operations. The pressure signal is transmitted to the surface through 0.125 in. capillary tubing which is strapped to the 1.315 in. tubing. A check value, located at the bottom of the nitrogen injection line, allows the line to be isolated from the system after introducing the gas kick in the well.

A graphic history of predicted experimental well behavior during pump-out of a typical kick is shown in Figure 27. At a circulating rate of 2 bbl/min, a choke line friction of 340 psi was predicted. When the gas reached the seafloor, the choke pressure must increase rapidly from about 200 psig to about 1700 psig. A short time later, a rapid decline in choke pressure is required. The average velocity of mud in the choke line is 517 ft/min. Pumping time for a complete kick simulation is about one hour and circulating drill pipe pressure is about 1700 psig. Realistic kick simulations can be accomplished with reasonable gas volumes and pump horsepower requirements.

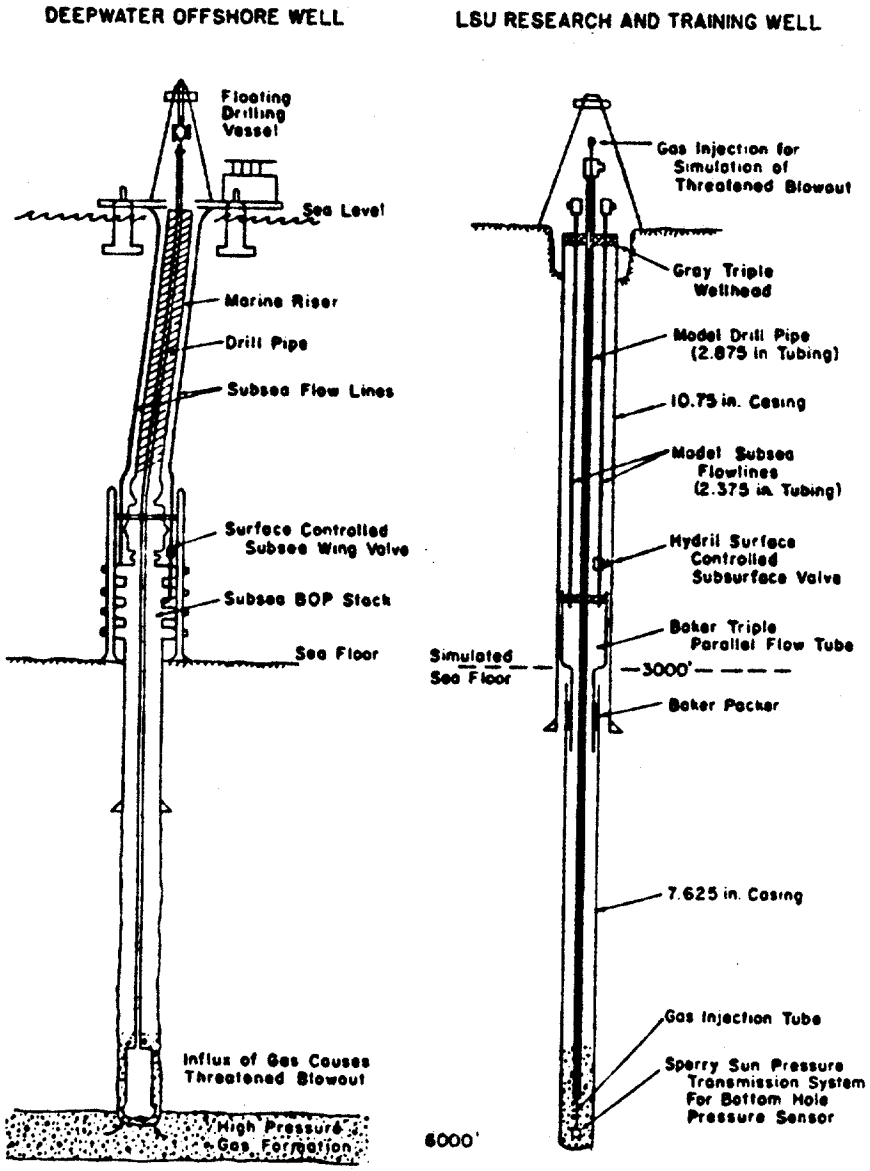

Figure 24 - Well Design Selected to Model Well-Control Operations on a Deepwater Offshore Well.

Figure 26 - New well-control facility for modeling well-control operations on floating drilling vessels

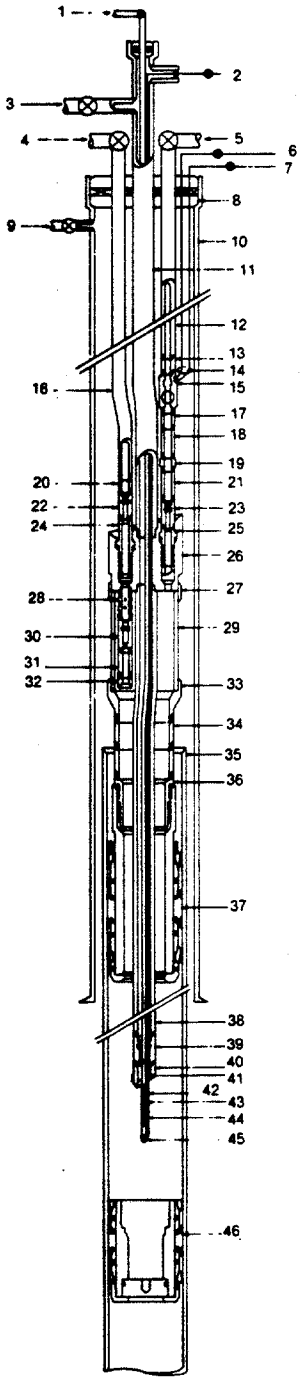

LEGEND

1. Nitrogen injection tubing
2. Bottom-hole pressure monitor line
3. Drill string
4. Choke line
5. Kill line
6. Control line
7. Balance line
8. Gray tool wellhead and triple string tubing hanger
9. Casing valve
10. Casing 10¾" OD 40.5 lbs/ft
11. Tubing 2⁷/₈" OD 6,5 lbs/ft EUE 8rd
12. Tubing 2³/₈" OD 4.7 lbs/ft EUE 8rd
13. Flow coupling size: 2³/₈" EUE 8rd x 6' long
14. Hydril dual control line bundle
15. Hydril tubing mounted surface controlled subsurface safety valve Size: 2³/₈" Min: ID 1.875"
16. Tubing 2³/₈" OD 4.7 lbs/ft EUE 8rd
17. Flow coupling Size: 2³/₈" EUE 8rd x 6' long
18. Tubing 2³/₈" OD 4.7 lbs/ft EUE 8rd (one joint)
19. Baker guide collar size: 4.9 x 2³/₈"
20. Pup joint 2³/₈" OD 4.7 lbs/ft EUE 8rd x Pin 4' long
21. Tubing 2³/₈" OD 4.7 lbs/ft EUE 8rd (one joint)
22. Baker model "F" seating nipple size 1.31 with 2³/₈ EUE 8rd box x Pin min. ID 1.81"
23. Baker model "F" seating nipple Size: 1.81 with 2³/₈" 4.7 lbs/ft EUE 8rd Pup joint 2' long
24. Baker "J-Lock" seal nipple Size: 40-26 min. ID 1.968" with 2³/₈" EUE 8rd box x blank and chamfered bottom
25. Baker "J-Lock" seal nipple Size: 21-19 min. ID 1.323" with 2³/₈" EUE 8rd box by half muleshoe bottom
26. Baker triple string parallel flow tube head Size: 9¹/₈ x 2⁷/₈ x 2.688 x 1.968
27. Baker casing coupling Size: 8⁵/₈" OD—36 lbs/ft with national buttress box x box 25' long
28. Baker perforated spacer tube Size: 2³/₈" NU IO RD pin x Pin 10' long min. ID 1.995"
29. Baker casing nipple Size: 8⁵/₈" OD—36 lbs/ft national buttress pin x Pin 25' long
30. Baker model "R" seating nipple Size: 1.81" with 2³/₈ NU 10 RD box x Pin with special clearance OD min. ID (thru NOGO) 1.760"
31. Baker spacer tube Size: 2³/₈ NU 10 RD box x Pin with special clearance connections min. ID 1.995"
32. Baker wireline entry guide Size: 2³/₈" NU 10 RD with special clearance OD min. ID 1.995"
33. Baker casing crossover sub Size: 8⁵/₈" OD 36 lbs/ft national buttress box by 6⁵/₈" OD 24 lbs/ft hydril "FJ" pin
34. Baker casing nipple Size: 6⁵/₈" OD 24 lbs/ft by 40' long with hydril "FJ" box by pin connections
35. Liner 7⁵/₈" OD 26.4 lbs/ft
36. Baker model "K-22" anchor tubing seal nipple Size: 80FA52 min. ID 4.400"
37. Baker[6] model "FA-1" production packer Size: 91FA52 min. ID 4.400' set at 3,034'
38. Tubing 2⁷/₈" OD 6.5 lbs/ft EUE 8rd
39. Baker model "F" seating nipple Size 2.31
40. Baker wireline entry guide Size: 2⁷/₈"
41. Nitrogen injection tubing Size: 1.315"-1.72 lbs/ft integral joint
42. Pressure monitor line to surface
43. Check valve
44. Ported sub
45. Sperry-Sun bottom-hole pressure sensor
46. Baker model "N-1" bridge plug (set at 6200 ft.)

Figure 25 - Schematic of new research well

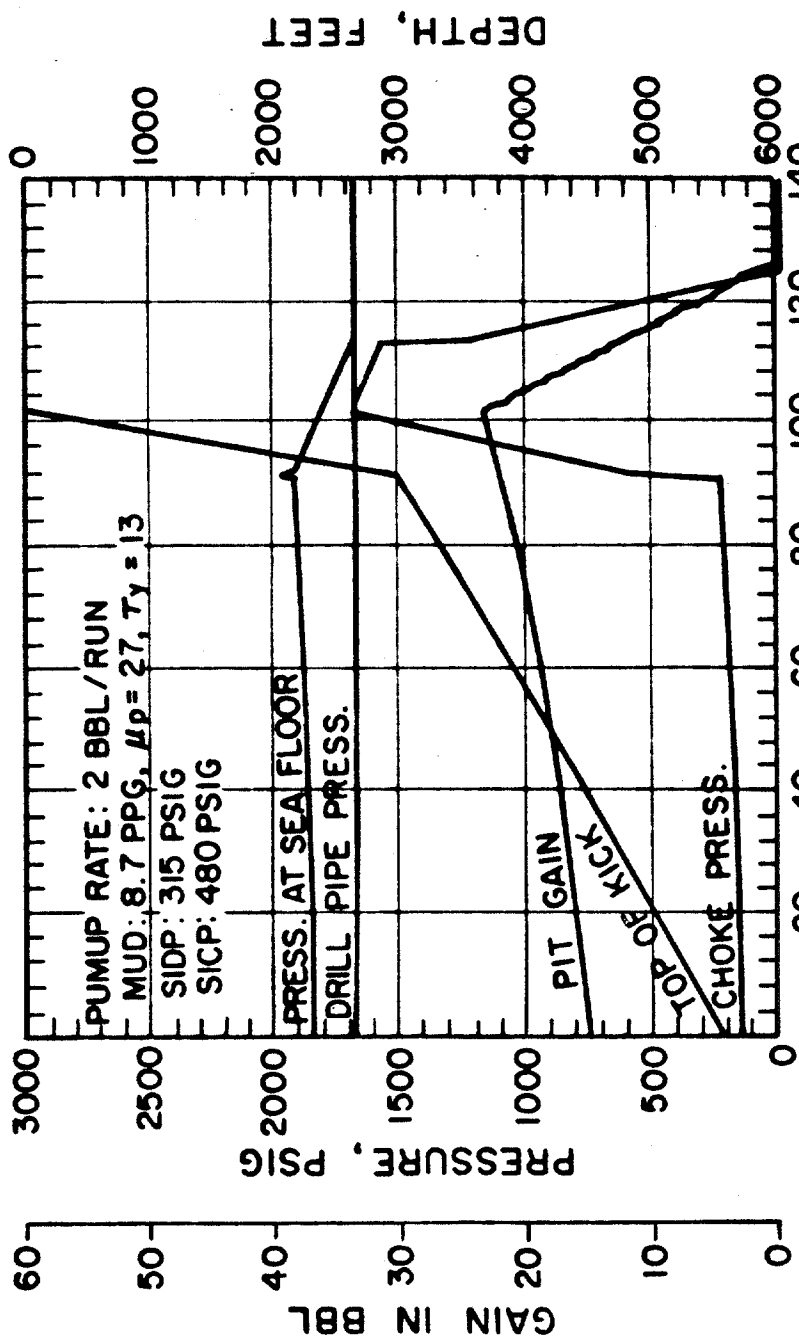

FIGURE 27. PREDICTED BEHAVIOR OF EXPERIMENTAL WELL

A schematic of the associated surface equipment for the experimental well facility is shown in Figure 28. The main components of this equipment include: (1) a choke manifold containing several 15,000 psi adjustable drilling chokes of varying design, (2) a 250 hp triplex mud pump, (3) two mud tanks having a total capacity of 540 bbl, (4) two 15 bbl metering tanks, (5) a mud gas separator, (6) three mud degassers of varying designs, (7) a mud mixing system, (8) an experimental flow loop for an annular preventer, and (9) an instrumentation and control house. A photograph taken inside the instrumentation and control house is shown in Figure 29.

Once construction of the well facility was completed, an experimental program was conducted to evaluate alternative procedures for:

1. Well shut-in
2. Handling upward gas migration
3. Pump start-up
4. Kick pump-out

In addition, basic research on two phase gas/mud flow in the well and surface equipment was conducted to allow an improved understanding of the flow mechanics of the deepwater well control process. The new data was then used to develop more accurate well control computer simulation procedures.

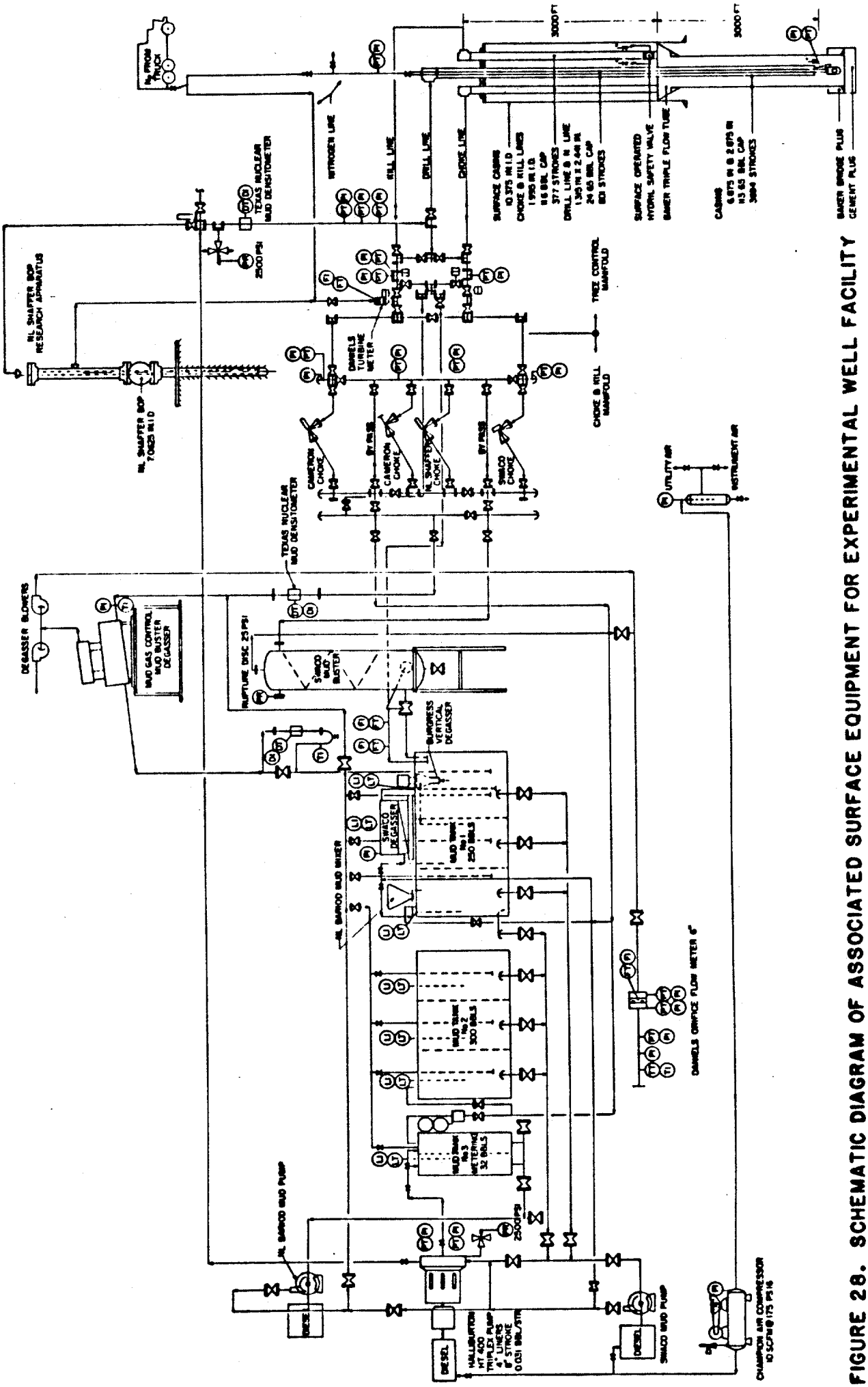

FIGURE 28. SCHEMATIC DIAGRAM OF ASSOCIATED SURFACE EQUIPMENT FOR EXPERIMENTAL WELL FACILITY

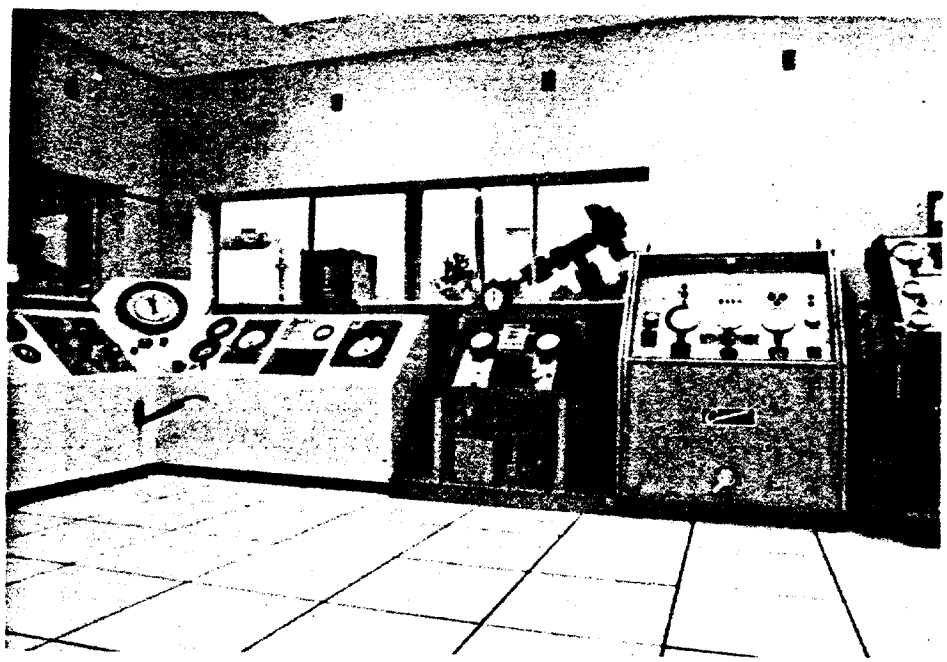

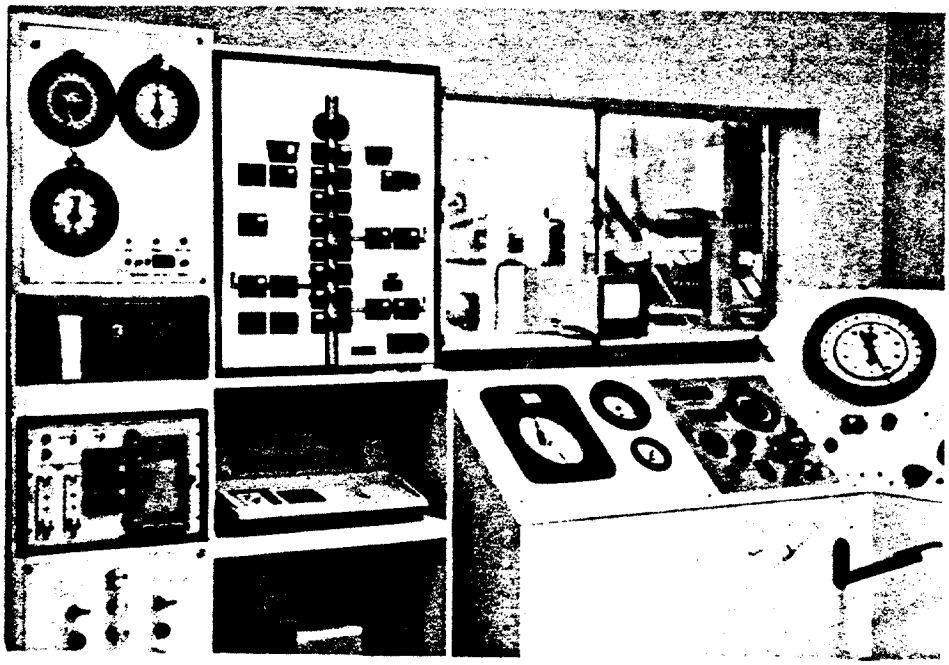

Figure 29 - Instrumentation Panels in Control Room

CHAPTER 4

SHUT-IN PROCEDURES

A very important phase of any well control operation is the early detection of a kick and subsequent shut-in of the well to minimize the volume of formation fluid which enters the well. Ths shut-in procedure used varies slightly from one operator to the next, but there are two basic philosophies within the industry. Both philosophies are based on intuitive explanations of the transient behavior of the well during shut-in.

The "hard shut-in" procedure is followed by many operators in an attempt to minimize the kick volume and is accomplished by simply closing the blowout preventer immediately after shutting the rig pump down and verifying that the well is flowing. The blowout preventer is the ultimate closing mechanism in this procedure.

An alternate procedure, the "soft shut-in," is used by some operators in an attempt to avoid the surge pressures that they believe are created by the sudden closure of a valve or blowout preventer. The soft shut-in procedure calls for a less abrupt termination of flow to reduce the magnitude of the surges produced. When a kick is taken, the HCR valve and the remote adjustable choke are placed in the open position and then the blowout preventer is closed. After the blowout preventer has been closed, then the choke is slowly closed to achieve a gradual shut-in of the well.

The surge pressure produced by the closure of the blowout preventer could, conceivably, cause failure in surface equipment exposed to this pressure or a down-hole failure such as a fracture at the casing seat. The presence of surge pressures is particularly undesirable in subsea operations since the additional hydrostatic pressure induced by a long vertical choke line and riser from the seafloor to drilling vessel causes a reduction in the mud weight which can be tolerated at any depth within the well. The surges are analogous to the surges created by the water hammer phenomenon characteristic of transient pipeline flow.

One obvious disadvantage of the soft shut-in is the longer time period required to achieve shut-in. This extra time allows more formation fluid to enter the well resulting in a larger initial kick volume. In the case of a gas kick, the ultimate casing pressure encountered in kick circulation is a direct function of the initial volume of the kick as shown in Figure 30. Thus, the ultimate casing pressure during kick circulation is higher when the soft shut-in procedure is used, possibly high enough to cause fracture of the casing seat or surface equipment failure.

It appears that each method of shut-in has its own advantages and disadvantages which could be considered in choosing an optimum shut-in procedure. The hard shut-in, while assuring the minimum influx of formation fluid, can conceivably produce pressure surges which might damage surface equipment or subsurface strata. On the other hand, the soft shut-in theoretically reduces the magnitude of the pressure surges due to shut-in. However, it allows a larger kick volume to enter the well, which could produce higher casing pressures during subsequent well control operations.

There is much disagreement within the industry as to which method of well closure is most appropriate. This disagreement is due, in part, to the fact that the surge pressure (water hammer) phenomenon is not well understood, as applied to the well bore. The soft shut-in procedure is based on an intuitive explanation of the transient behavior of the well system during shut-in. Proponents of the soft shut-in argue that the closure of the blowout preventer constitutes a rapid termination of flow, while the choke can be closed at any desired rate. Proponents of the hard shut-in have various reasons for supporting this method. Some feel that the surges produced, if any, are not of a magnitude which would constitute a threat to the operation, or that although surges may be produced at the surface they are not propagated down-hole and so only the surface equipment needs to resist the surges. Still others argue that a conventional hard shut-in which uses an annular blowout preventer is, in effect, a soft shut-in due to the time (typically about 20 - 30 seconds) that is required for the preventer to be hydraulically activated by the accumulator and effect a complete closure.

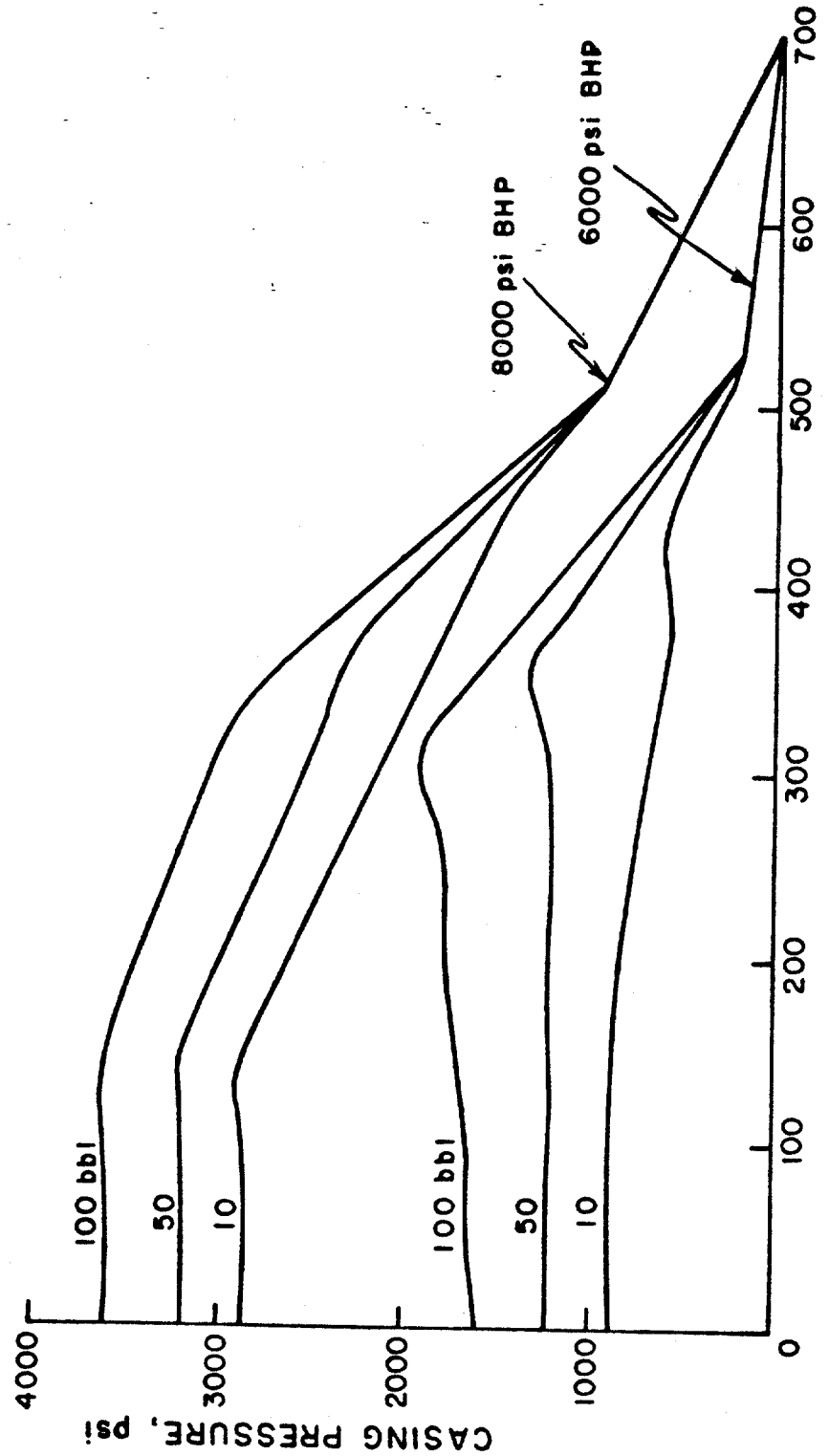

Figure 30. Effect of Initial Volume of Gas Kick on Ultimate Casing Pressure. (After McKenzie[18])

As was mentioned previously, the arguments frequently heard supporting either method of well closure are based primarily on intuition. The author is unaware of any published research, either experimental or theoretical, on the transient behavior of the well system during shut-in. Considering the importance of the initial shut-in phase in any well control procedure used, it seems that an investigation of shut-in procedures is long overdue.

In order to evaluate present and alternative procedures for well shut-in, an accurate mathematical model of the well system and its behavior during shut-in is needed. The first phase of this study was a literature study of the available techniques for the development of such a model. The next phase of the study was experimental work needed to adequately model the drilling equipment used in well shut-in procedures. Specifically, this involved an examination of the pressure losses occuring during flow through a spherical-type, annular blowout preventer and also through drilling chokes at various degrees of closure. Three types of fluids were examined to determine the effects of viscosity and four pipe sizes were used to examine the effects of annular geometry on the closing characteristics of the blowout preventer.

The characteristics of an annular blowout preventer prescribes the downstream boundary condition of a well system during a hard shut-in. The characteristics of drilling chokes prescribes the boundary condition for a soft shut-in. These closing characteristics were ultimately incorporated into a mathematical model of the well system.

4.1 FUNDAMENTALS OF WATER HAMMER

Water hammer refers to the pressure surge which occurs in a pipe carrying a flowing liquid when a valve is abruptly closed. This is the phenomenon which causes water pipes to rattle when a kitchen faucet is shut off quickly. It occurs in large industrial pipe lines and, depending on the magnitude of the pressure surges, can present rather difficult design problems. In recent years, much attention has been given to the postulated double-ended line rupture problem in feedwater lines in nuclear power plants. Damaging surge pressure (water hammer) can result from the rapid closure of conventional check-valves in such a line. The magnitude of this surge pressure is a function of the change in velocity

of the flowing fluid. Valves designed to stop the flow of fluids very quickly, for instance, subsurface safety valves installed in oil and gas wells, must be able to withstand the water hammer effects that such a closure will induce.

Analytical studies in the area of water hammer during the last century are quite extensive. Many of the ideas and equations developed in these works are quite helpful in analyzing the behavior of a well during shut-in operations.

4.1.1 The Mechanism of Water Hammer

Many published references concerning water hammer[9-25] provide a brief description of the sequence of events which produces the water hammer effect when a valve in a pipe line is abruptly closed. Basically, the phenomenon is a series of cyclic loadings in which the kinetic energy of the system is converted into potential energy and then reconverted to kinetic energy through four mechanical processes, illustrated in Figures 31-34, which assumes instantaneous closure of the valve at the downstream end of a frictionless system. This idealized case of water hammer provides the clearest explanation of the basic mechanisms involved.

The liquid in the pipe of Figure 31a is orginally flowing under steady state conditions with velocity $V = V_o$. The valve at the downstream end of the system is closed instantaneously at time $t = 0$. The liquid in most of the pipe continues to flow at velocity, V_o. However, the liquid nearest the valve is compressed and the wall of the pipe is stretched. The kinetic energy of the liquid in this section is converted to potential energy as the velocity of the liquid drops to zero and the hydraulic head (pressure) within the liquid increases by a value Δh. Each section in turn undergoes the same energy conversion process as the pressure wave moves toward the origin at the velocity of propagation, a, (Figure 31a). At time $t = L/a$ the pressure wave has reached the upstream end of the system as shown in Figure 31b. The entire liquid column is now at rest, but is under an excess pressure, Δh.

In Figure 32a the liquid in the pipe has begun to flow backwards at velocity $V = -V_o$ due to the pressure difference between the pipe and the reservoir. The pressure in the system drops to the normal, static value

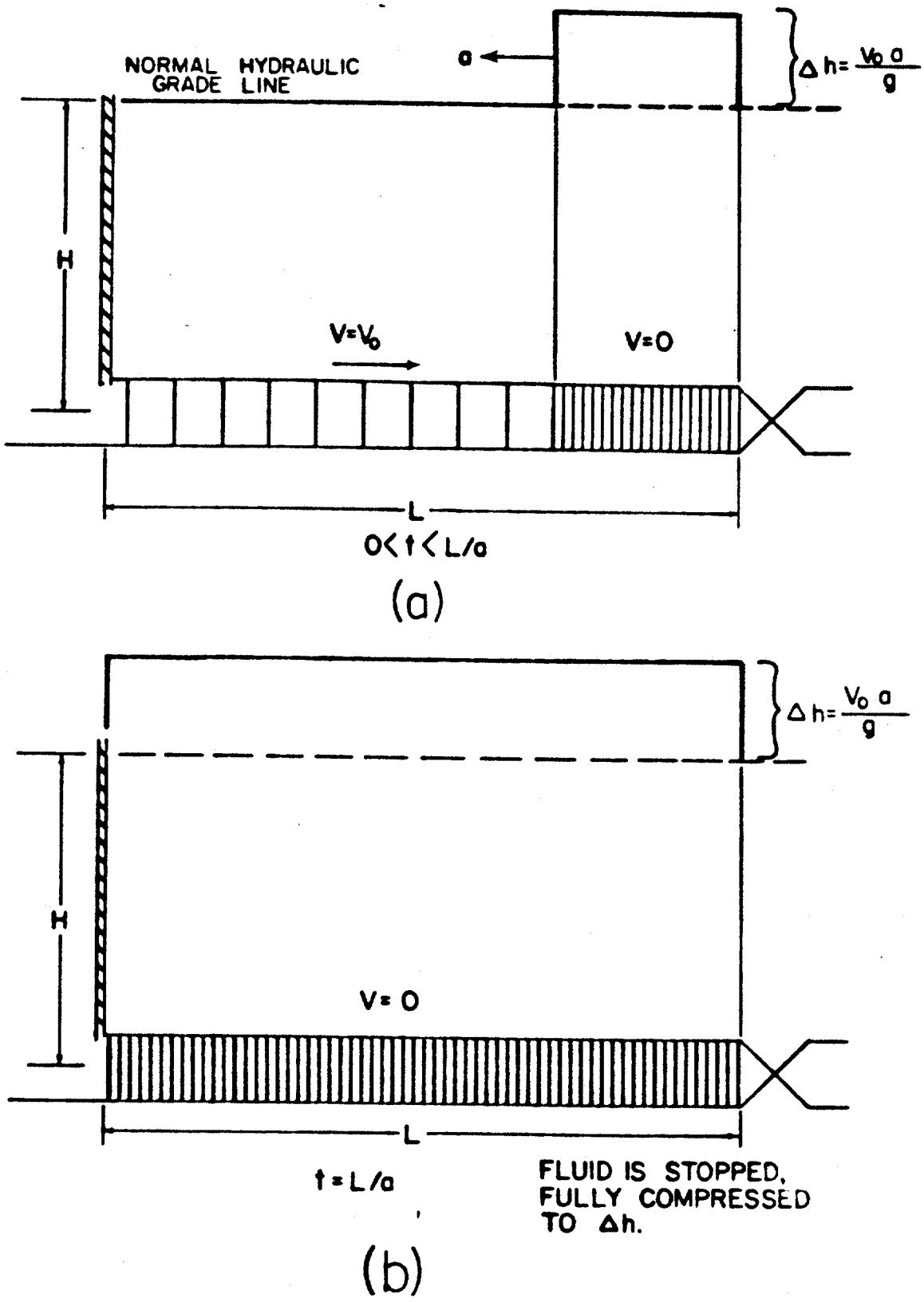

Figure 31. Transient Response of Frictionless Pipe at Time L/a After Instaneous Valve Closure.

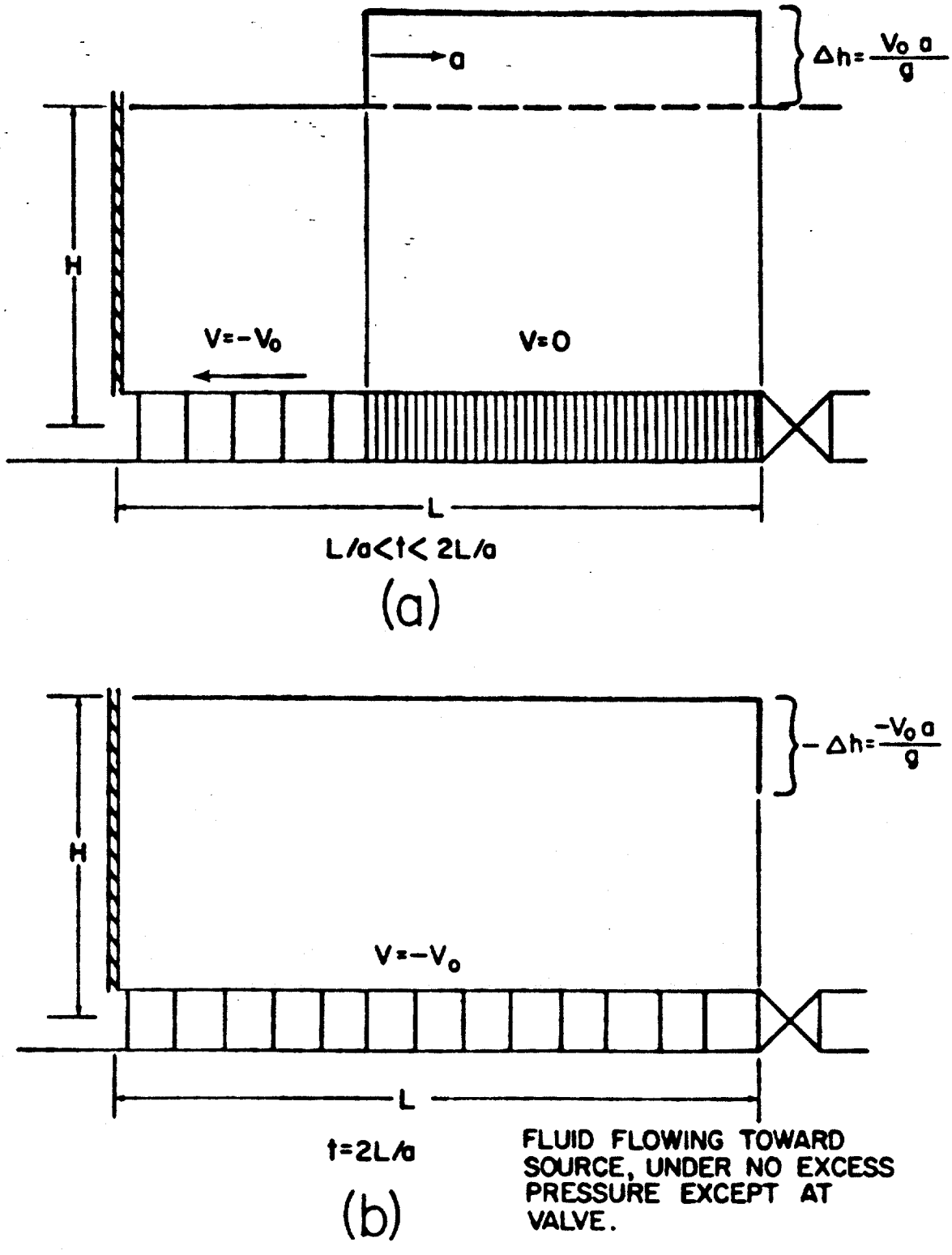

Figure 32. Transient Response of Frictionless Pipe at Time 2L/a After Instantaneous Valve Closure.

as the rarefactive wave travels toward the valve at velocity, a. Successive laminae of water expand and the pipe walls relax, beginning at the reservoir. Figure 32b shows the system at time t = 2L/a. The unloading wave has now reached the valve and the pressure throughout the pipe is the normal static pressure. However, since the valve is closed, the flow at velocity V = $-V_o$ cannot be maintained.

The fluid near the valve expands beyond its normal volume as it continues to flow away from the valve, inducing a pressure drop at the valve which is as far below the static pressure as the initial pressure rise was above it. This negative pressure drop now travels as a wave toward the source as successive layers of liquid expand and are brought to a halt (Figure 33a). At time t = 3L/a, in Figure 33b, all the liquid in the pipeline is at rest but the pressure level in the pipe is below the pressure in the reservoir by $-\Delta h$ feet of hydraulic head.

As seen from Figure 34a, the pressure differential between the pipe and the reservoir induces flow of liquid in the positive sense at a velocity V = V_o. The pressure returns to the normal static level again as the unloading wave travels with velocity, a, toward the valve. At time t = 4L/a, (Figure 34b), the velocity of the liquid is V = V_o everywhere in the pipe and the pressure is also at the normal level throughout the pipe. The conditions in the pipe are now the same as at the moment of closure. The entire cycle will continue until friction, which has been neglected up to this point, reduces the pressure vibrations to zero and the fluid in the pipe comes to rest. The same type of analysis used for the case of instantaneous closure can also be used to examine cases of water hammer due to the closure of a valve in a finite element of time. For less than instantaneous closure, the closure is treated as a series of instantaneous partial closures and the effects of each partial closure are superimposed to obtain the net effect of the total closure. Joukovsky[20] was one of the first to recognize this method of analysis.

4.1.2 Velocity of Propagation and the Magnitude of the Water Hammer

As previously shown, the pressure surge created as the result of valve closure is propagated as a wave through the system. In 1898, Joukovsky[20] developed an accurate equation for calculating the velocity

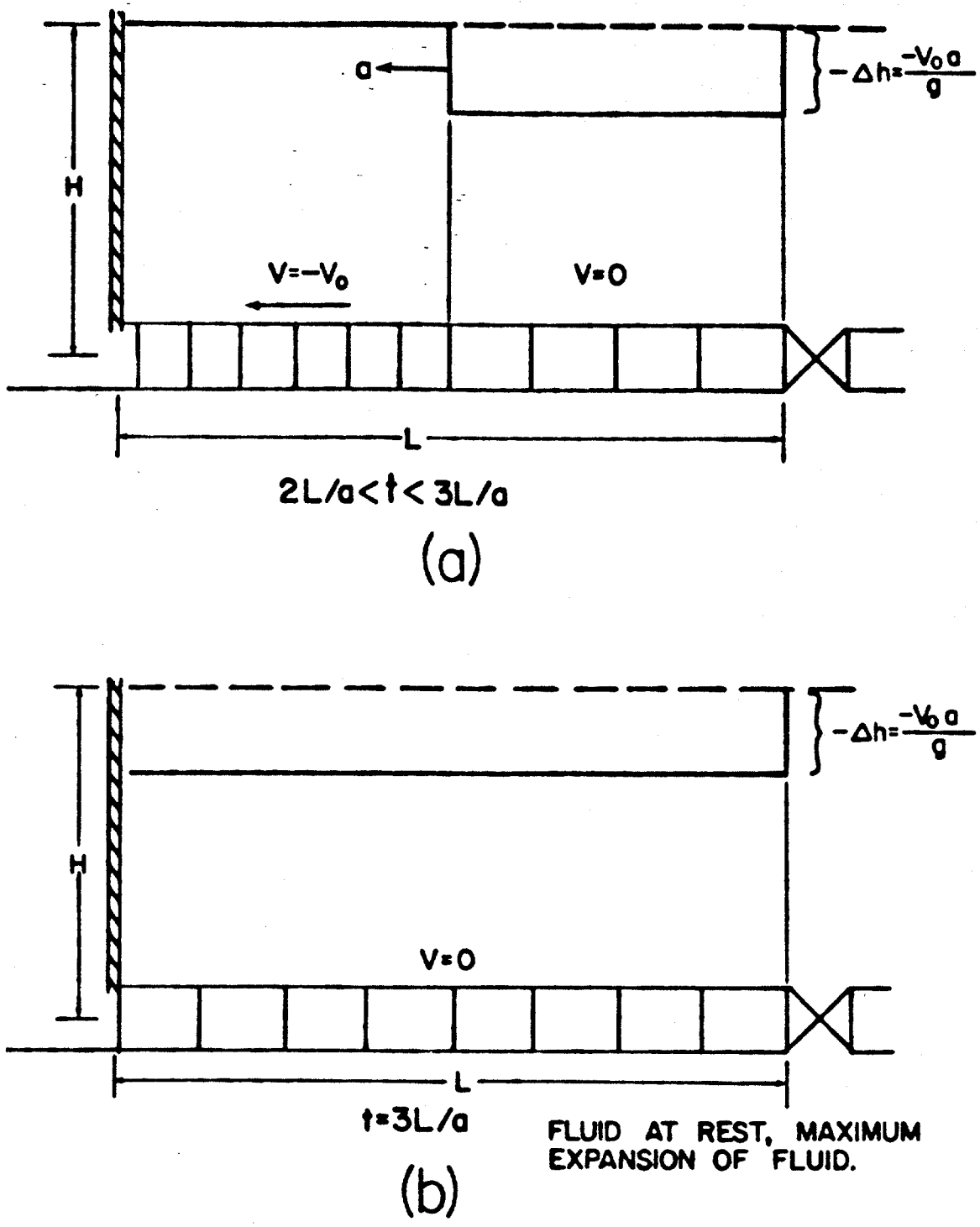

Figure 33. Transient Response of Frictionless Pipe at Time 3L/a After Instantaneous Valve Closure.

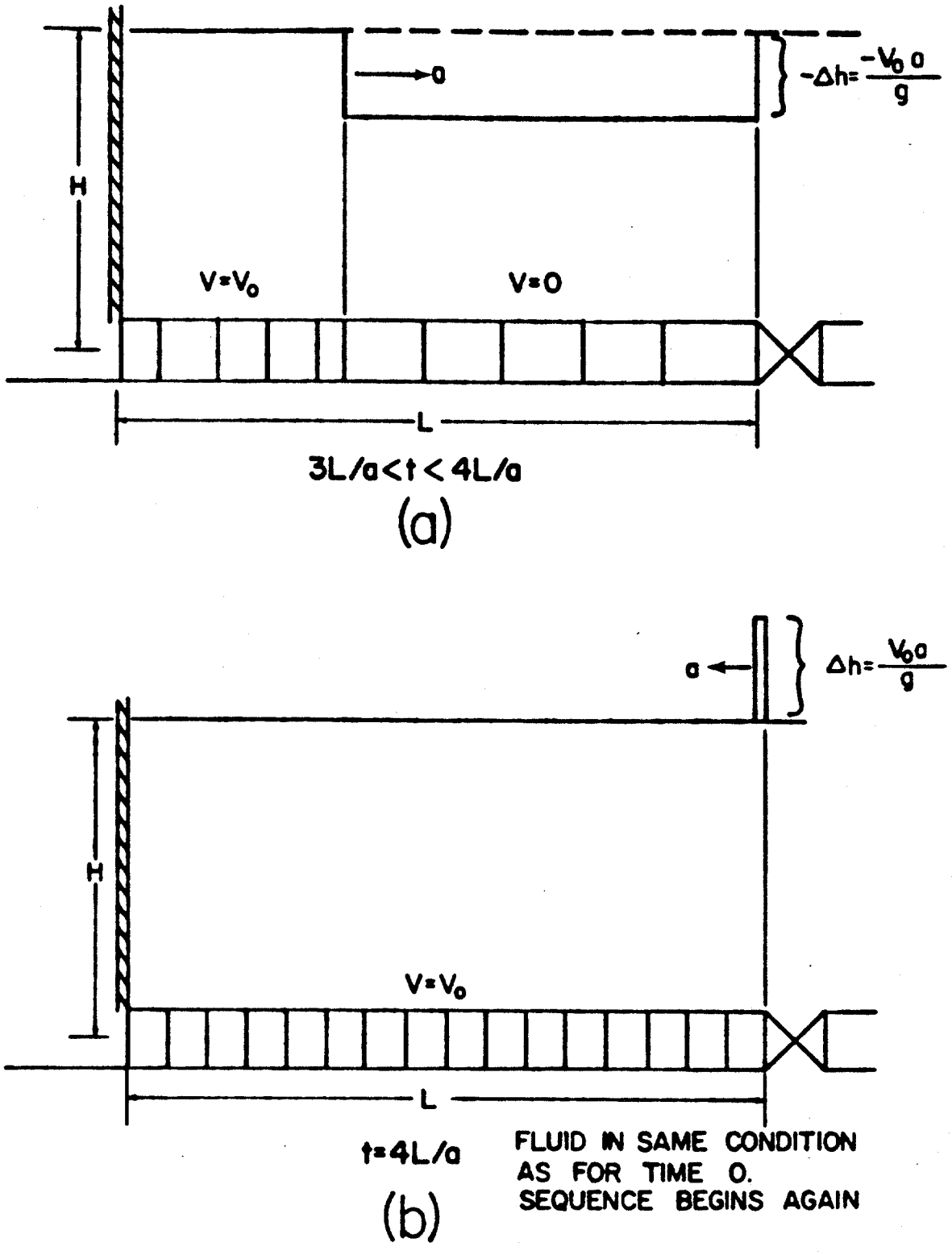

Figure 34. Transient Response of Frictionless Pipe at Time 4L/a After Instantaneous Valve Closure.

of propagation, a, which he later verified experimentally using long runs of various diameter pipes. The same basic formula was also derived independently by Allievi[26] in 1902. The equation for the velocity of propagation in thin walled pipe, written in common field units, is:

$$a = \frac{24.886}{\sqrt{c\rho(1+\frac{1}{CE}\frac{d}{t})}} \qquad (4.1)$$

where a = velocity of propagation, ft/sec
c = fluid compressibility, psi^{-1}
E = Young's modulus of elasticity of pipe material, psi
ρ = fluid density, lbm/gal
$\frac{d}{t}$ = the ratio of pipe diameter to pipe thickness

The above equation agrees with that previously developed for the velocity of sound in an elastic pipe filled with a compressible liquid.[20] This would be expected since both water hammer and sound are special cases of pressure waves being propagated through a medium.

Joukousky[20] also pointed out that the velocity of propagation is independent of pressure intensity and the length of the system. Rather, the velocity of propagation is a function of only the compressibility of the fluid and the elasticity of the conduit.

More recent authors[21,25] include a dimensionless constant, C_1, in the previous equation for the velocity of propagation:

$$a = \frac{24.886}{\sqrt{c\rho(1+\frac{C_1}{CE}\frac{d}{t})}} \qquad (4.2a)$$

The coefficient, C_1, is calculated using the equations given by Streeter and Wylie[25] or by Watters[29] to accomodate various assumptions made in developing the continuity equation for the system. The stress distribution is different in thick-walled vessels than in thin-walled vessels. Therefore, the value of C_1 is partly determined by the relative thickness of the pipe walls, (d/t). The force balance on the pipe is also affected by the restraining forces which oppose pipe movement, so C_1 is also controlled by the type of anchoring system used and by the presence or absence of expansion joints. Streeter and Wylie also give

values for C_1 for the special cases of circular tunnels and lined tunnels, which might be used in analyzing cased and uncased boreholes.

When free air occurs in a substantial portion of a pipeline, either as small bubbles or in larger discrete lumps, the wave speed in the pipe is decreased. As a consequence, the pressure extremes and the wave propagation patterns are altered.

The wave speed of the air-liquid mixture is computed as previously done for a homogeneous liquid, but with the use of an average density for the mixture. This approach implicitly assumes the mixture is evenly distributed throughout a significant portion of the pipe. The elasticity of the liquid air mixture is dramatically affected by a small amount of entrained air so the elasticity of both substances must be included.

Application of the momentum equation and conservation of mass leads to the following equation for wave speed from Tullis, Streeter and Wylie[30].

$$a = \frac{24.886}{\sqrt{C_\ell \rho_{avg}\left(1 + \frac{C_1}{C_\ell}\frac{d}{t}\frac{E}{} + (1-H_\ell)\frac{C_g}{C_\ell}\right)}} \qquad (4.2b)$$

where H_ℓ is the liquid fraction or holdup and the subscripts g, ℓ, and avg., refer to gas, liquid, and average, respectively.

Joukovsky was apparently the first to develop an analytical expression for the maximum pressure rise caused by instantaneous valve closure in a simple pipe system. The rigorous mathematical development of his equation is quite complicated. However, in 1933, Moody[27] proposed a simplified development of the same equation for water hammer in a single, uniform pipe.

Joukovsky's experimental work, originally commissioned to determine the maximum safe velocity for use in the new Moscow water works, verified his equation. The equation , in common field units, is given by:

$$\Delta p_c = \frac{V_o\ a\ \rho}{619} \qquad (4.3)$$

Where Δp_c = pressure rise due to valve closure, psi

V_o = velocity of fluid prior to valve closure, ft/sec

a = velocity of propagation, ft/sec

ρ = density of flowing fluid, lbm/gal

In terms of feet of hydraulic head we have:

$$h = \frac{\Delta p_a}{0.052\rho} = \frac{V_o\ a}{32.17} \tag{4.4}$$

Where h = hydraulic head increase due to valve closure, ft

Equations (4.3) and (4.4) are also applicable to the partial closure of a valve, resulting in a change in the velocity of the fluid and producing a pressure rise. For partial closure we have:

$$\Delta p_i = \frac{\Delta V_i\ a\ \rho}{619} \tag{4.5}$$

or

$$\Delta h_i = \frac{\Delta V_i\ a}{32.17} \tag{4.6}$$

As previously mentioned, the non-instantaneous closure of a valve can be represented as a series of instantaneous partial closures. The pressure rise due to each partial closure is then calculated using Equation (4.5) or (4.6) and the total pressure rise is calculated using superposition. In using this method of analysis, the effects of rarefactive waves reflected from the reservoir end of the pipe must be included in the calculation of the total pressure change. The extent that reflected waves affect the total pressure rise produced by valve closure is determined by the time of closure, t_c, for the valve.

4.3 EFFECT OF SPEED OF VALVE CLOSURE ON THE WATER HAMMER

Valve closure in the real world can never be instantaneous, but is achieved over a finite length of time called time of closure t_c. In water hammer analysis there are two cases of closure time which are usually considered. "Rapid closure" refers to closure for which $t_c<2L/a$ while "slow closure" refers to closure where $t_c>2L/a$. This critical time $t_c=2L/a$, is the time required for a pressure wave to travel from the valve to the source of flow and then return to the valve as a rarefactive wave.

Joukovsky concluded from his work that if the valve were closed completely in a time interval less than 2L/a, then at least part of the pipe would experience a pressure increase the same as that for instantaneous closure, as given by Equation (4.3). Consider, for example, the comparison of the maximum pressure peaks along the pipe for instantaneous closure and rapid closure shown in Figure 35. Friction is included in the normal grade line for the pipe, but it is assumed that it has no effect on the magnitude of the pressure surge caused by water hammer. For instantaneous closure, the maximum pressure peak extends along the entire system from the valve to the reservoir. However, for the case of rapid closure, the maximum pressure peak extends from the valve to a distance, x. Upstream of this point, the pressure surge decreases uniformly from the maximum valve at x to zero at the reservoir.

Streeter[23] gives Equation (4.7) below for calculating the length of pipe, x, which is exposed to the full pressure increase, as shown in Figure 35.

$$x = L - \frac{a\ t_c}{2} \tag{4.7}$$

Where x = length of pipe exposed to full pressure peak, ft
L = total length of pipe, ft
a = velocity of propagation, ft/sec
t_c = time of closure, sec

The time of duration of the maximum pressure surge is also affected by the speed of closure. For any point, x', in the region of full pressure rise of Figure 35, the maximum pressure surge lasts only for a time equal to the difference between the closing time of the valve and the time for the pressure wave to travel from x' to the reservoir and be reflected back to x'. Equation (4.8) below can be used to calculate the time of duration.

$$t_d = \frac{2\ (L - x')}{a} - t_c \tag{4.8}$$

where t_d = time of duration of maximum pressure peak at x', sec

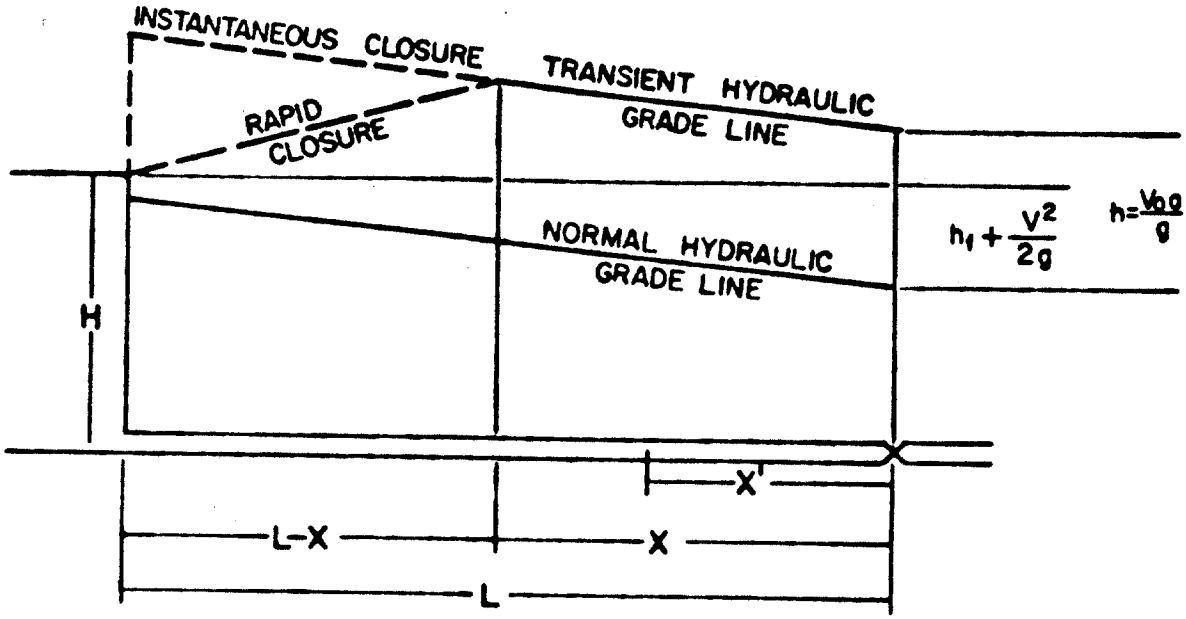

Figure 35. Maximum Pressure Peak Profile for Instantaneous Closure and Rapid Closure.

t_c = time of closure, sec
L = total length of pipe, ft
x' = distance from valve to point of interest, ft
a = velocity of propagation, ft/sec

For the special case where the time of closure, t_c, is 2L/c, Equation (4.7) gives x = 0. This means that the pressure peak attains the maximum possible value only at the valve, and that the pressure peak falls only at the valve, and that the pressure peak falls uniformly from this valve at x = 0 to zero at the reservoir. Also, Equation (4.8) gives the time of duration of the maximum pressure peak at the valve, t_d = 0. The pressure at the valve begins to fall as soon as the maximum peak is reached.

To summarize the effects of rapid closure, where $0 < t_c < 2L/c$, two points should be made. First, the maximum pressure peak for part of the pipe is equal to the maximum peak for instantaneous closure. The length of pipe which is exposed to the maximum pressure peak depends on the total length of the system and on the time required to close the valve. Secondly, the time of duration of this pressure peak is not as long as for instantaneous closure and is also a function of the time of closure.

The effect of closure of the valve in times greater than 2L/a is to reduce the magnitude of the maximum pressure peak produced in the system. This is due to the fact that for $t_c > 2L/c$, the pressure waves produced by the initial action of the valve have time to reach the source and be reflected as rarefactive waves back to the valve before closure has been completed.[19] Assuming that the closure of the valve is linear, these rarefactive waves prevent the pressure from increasing further due to subsequent valve movement. The maximum pressure peak occurs at the valve and is somewhat less than the maximum pressure peak for the case of instanstaneous closure. The pressure rise along the pipe decreases uniformly from the value at the valve to zero at the reservoir.

4.1.4 Effect of Branching Pipes and Changing Pipe Geometries on the Water Hammer

Complexities in the pipe network, such as a change in the pipe diameter, have significant effects on the water hammer propagation

through a given system. Branching pipes and their effects on water hammer were studied by Joukousky.[20] Choke and kill lines would be examples of branch pipes. He examined both open-ended and close-ended branch pipes. He found that the pressure intensity within a branching pipe was doubled as the pressure wave reflects undiminished from the dead-end of the pipe. This behavior is also explained by Parmakian.[21] Joukousky goes on to conclude that the pressure in the main pipe, while not doubled, is increased by the reflected pressure wave in the branch pipe.

The case of an open-ended or discharging branch pipe shows quite a different effect on the water hammer pressure wave. As the pressure wave reaches the discharge of the branch pipe it is reflected as it would be from a reservoir at atmospheric pressure. A rarefactive wave is reflected and the pressure rise in the branch pipe is diminished rather than doubled. The overall effect of a discharging branch pipe is to lower the intensity of the pressure wave in the main pipe.

Various authors[21-22,28] have treated also the problem of changes in cross-sectional area. However Parmakian[21] gives the simplest explanation of the effects of changes in pipe geometry or material on the water hammer. When the pressure wave encounters a change in pipe diameter from d_1 to d_2, the velocity of the wave is changed from a_1 to a_2 as predicted by Equation (4.1). Likewise the intensity of the pressure rise is also altered in the new section of pipe in accordance with Equation (4.3). The pressure wave is also partly reflected back toward the valve. According to Equation (4.1) the velocity of propagation is a function not only of pipe diameter, d, but also wall thickness, t, and shear modulus, E. Thus, similar behavior to that explained above should be expected for changes in pipe wall thickness and/or pipe material.

4.2. METHODS OF ANALYSIS FOR WATER HAMMER

Streeter[25] presents a review of the various methods which have been used to analyze water hammer. Each method is based on an equation of motion and some particular form of the continuity equation, and is limited by the restrictive assumptions inherent in its development. Two of these methods which are more commonly used include the arithmetic integration method and the method of characteristics.

4.2.1 Arithmetic Integration Method

The Arithmetic Integration Method[21-25] of analysis was discussed briefly in a previous section. Its primary application is in the analysis of water hammer in cases of gradual valve closure.

The closure of a valve is represented as a series of instantaneous partial closures. The water hammer due to each of these partial closures is computed using Equation (4.5) and total water hammer at any time, t, is taken to be the sum of all direct and reflected pressure waves up to that time.

Streeter[25], treats the valve as an orifice with variable frictional area A_f, giving the equation below:

$$V \cdot A = C_d \cdot A_f \sqrt{2 \cdot g \cdot h} \tag{4.9}$$

where V = velocity of fluid, ft/sec
A = cross-sectional area of pipe, ft^2
C_d = valve coefficient
A_f = effective area of orifice or valve, ft
h = pressure head loss across the valve, ft

Just prior to closure, Equation (4.9) becomes:

$$V_o \cdot A = C_d \cdot A_{fo} \sqrt{2 \cdot g \cdot h_o} \tag{4.10}$$

The velocity at any time is a function of the frictional area of the value. In dimensionless terms, Streeter's equation is written:

$$\frac{V}{V_o} = \frac{A_f}{A_{fo}} \sqrt{\frac{h}{h_o}} \tag{4.11a}$$

or

$$\frac{V}{V_o} = \tau \sqrt{\frac{h}{h_o}} \tag{4.11b}$$

where τ = dimensionless valve area, A_f/A_{fo}

If the closure of the valve is represented as a series of partial clo-

sures we have, after one partial closure:

$$\frac{V - \Delta V_{t1}}{V_o} = \tau_{t1} \cdot \sqrt{\frac{h + h_{t1}}{h_o}} \tag{4.12}$$

Equation (4.6) can be written in dimensionless terms as:

$$\frac{\Delta h}{h_o} = \frac{a\ v_o}{g\ h_o} \cdot \frac{\Delta V}{V_o} \tag{4.13}$$

Equations (4.12) and (4.13) can be solved simultaneously for the conditions at the valve at t_1 to obtain $\Delta h/h_o$ and $\Delta V/V_o$. Then the values of h and V are updated and Equations (4.12) and (4.13) are solved again for $\Delta h/h_o$ and $\Delta V/V_o$.

The calculations involved in the arithmetic integration method of water hammer analysis can be quite lengthy and tedious. The process becomes more complicated for slow closure of a valve or for analysis of points in the system other than at the valve. Also, the equations used in the analysis assume a frictionless, horizontal system, although corrections can be made to account for frictional losses in the system.

2.2.2 Method of Characteristics

The Method of Characteristics[24,25] is felt to be the most practical method of analysis for water hammer. The assumptions made in developing this method are minimal, making it applicable to a large range of problems. The two partial differential equations of motion and continuity are converted to four total differential equations which can be solved using finite difference techniques on a digital computer.

Parmakien[21] presents a development of the differential equations governing water hammer. However, his development assumes that both frictional losses and velocity head are negligible. The continuity equation presented by Parmakien is:

$$\frac{a^2}{g} = \frac{\delta V}{\delta x} + \frac{\delta h}{\delta t} = 0 \tag{4.14}$$

where a = velocity of propagation, ft/sec
V = velocity, ft/sec
h = hydraulic head, ft
t = time, sec
x = distance from reservoir, ft
g = acceleration of gravity, ft/sec^2

The equation of dynamic equilibrium, (motion) is written:

$$\frac{1}{g}\frac{\delta V}{\delta t} + \frac{\delta h}{\delta x} = 0 \qquad (4.15)$$

In Streeter's[24,25] development of the continuity and motion equations, frictional losses and velocity head are included. These terms, which were previously neglected in order to allow solution of the differential equations, can be included in the method of characteristics and, thus, provide improved accuracy in the results obtained. The equation of continuity, including friction and velocity head, is:

$$L_1 = \frac{a^2}{g} \cdot \frac{\delta V}{\delta x} + V\frac{\delta h}{\delta x} + \frac{\delta h}{\delta t} + V \sin\theta = 0 \qquad (4.16)$$

where a = velocity of propagation, ft/sec
g = acceleration of gravity, ft/sec^2
V = velocity, ft/sec
h = hydraulic head, ft
x = distance from reservoir, ft
t = time, sec
θ = angle of inclination of pipe, degrees

The equation of motion, L_2 including friction and velocity head, is given by:

$$L_2 = g\frac{\delta h}{\delta x} + V\frac{\delta V}{\delta x} + \frac{\delta V}{\delta t} + \frac{f\ V\ V}{2D} = 0 \qquad (4.17)$$

where g = acceleration of gravity, ft/sec^2
V = velocity, ft/sec
h = hydraulic head, ft
x = distance from reservoir, ft

t = time, sec

f = Moody friction factor

D = pipe diameter, ft

As stated previously, the method of characteristics converts the two partial differential equations, L_1 and L_2, into four total differential equations. This is accomplished by combining L_1 and L_2 using an unknown multiplier λ to give:

$$L = L_1 + \lambda L_2 \tag{4.18}$$

Streeter showed that if $\lambda = \pm a/g$, then the following equations resulted:

$$\frac{dh}{dt} + \frac{a}{g}\frac{dV}{dt} + V \cdot \sin\theta + \frac{a \cdot f \cdot V\,V}{2 \cdot g \cdot D} = 0 \tag{4.19}$$

for

$$\frac{dx}{dt} = V + a \tag{4.20}$$

and

$$\frac{dh}{dt} - \frac{a}{g}\frac{dV}{dt} + V \cdot \sin\theta - \frac{a \cdot f \cdot V\,V}{2 \cdot g \cdot D} = 0 \tag{4.21}$$

for

$$\frac{dx}{dt} = V - a \tag{4.22}$$

Equations (4.19) and (4.21) are total differential equations in V and h in terms of the independent variables x and t. The solution is carried out on an x-t plot as shown in Fig. 36. Equation (4.19) defines h and V along the C+ characteristic, Equation (4.20), and Equation (4.21) defines h and V along the C- characteristic, (Equation 4.22). Usually the characteristic equations are simplified by dropping the term V which is negligible compared to a. This produces the straight lines for the characteristic curves in Figure 36.

Equations (4.19) and (4.21) are expressed in finite different form, and integrated along their respective characteristics. Then, by knowing h and V, at two points, x_{i-1} and x_{i+1}, at the present time level, t_j,

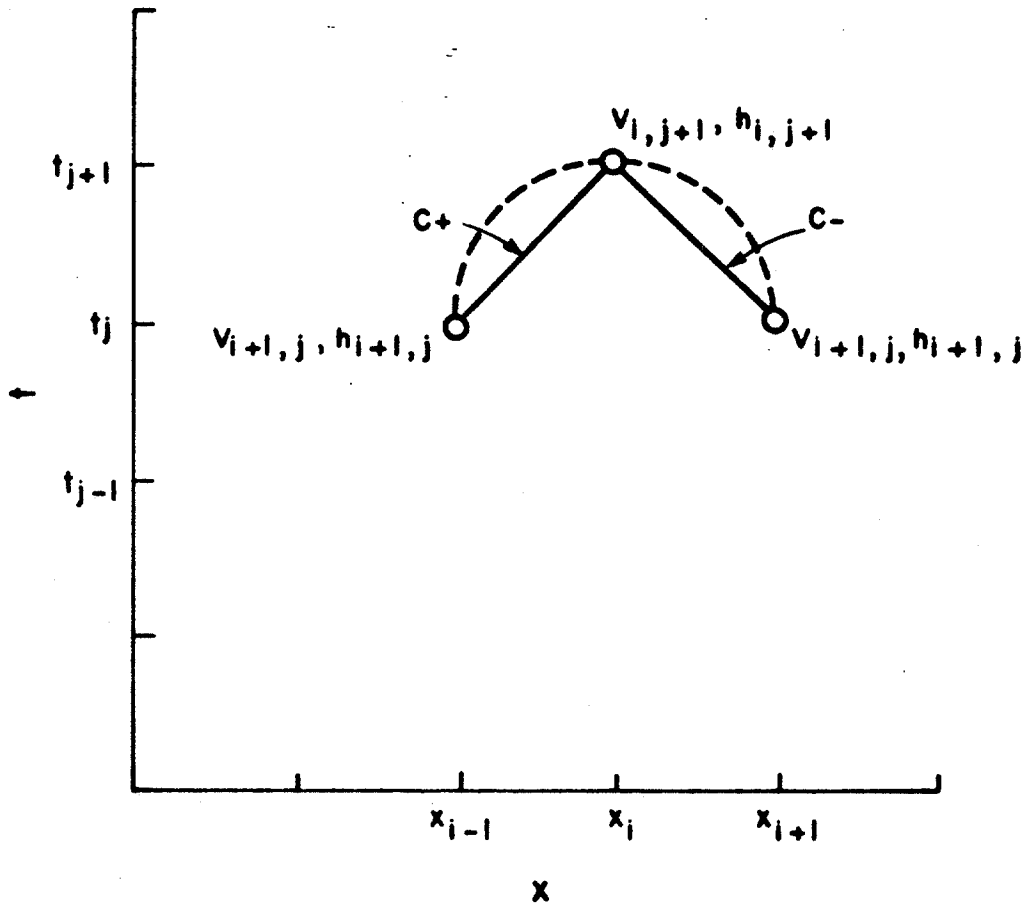

FIGURE 36. x–t GRID FOR METHOD OF CHARACTERISTICS

the two equations can be solved simultaneously to give h and V at the point, x_i, at the next time level t_{j+1} (see Figure 36). Obviously, this process can only be carried out over a limited range unless the boundary conditions of the system are known.

The application of method of characteristics to pressure surge analysis was recently addressed in detail by Watters.[29] Numerous complex examples are solved using numerical analysis techniques and a high speed digital computer. The work of this author formed the basis of the techniques eventually adopted in this study for the surge pressure analysis of a well during the shut-in period.

In summary, the method of characteristics of water hammer analysis seems to be the most up to date method of analysis. It includes the effects of friction and the effects of the pipes being non-horizontal. It also accomodates a variety of boundary conditions and complex pipe networks. All of these considerations are important in regard to the analysis of the transient behavior of a wellbore during shut-in.

4.3 Boundary Conditions

As stated previously, in using the method of characteristics, the computations can only be carried out over a limited portion of the pipe unless the conditions at the ends of the system are known. The equations which are used to determine the pressure and velocity at a given point, x_i, at time level t_{j+1}, are expressed in terms of the pressures and velocities at the points to either side of that point, x_{i-1} and x_{i+1}, at the previous time level, t_j. Therefore, at each end of the system, only Equation (4.19) or (4.21) holds. Therefore, other equations must be used to define the conditions at each boundary as a function of time in order to be able to solve for both unknowns h and V.

Streeter[23, 24] and Watters[29] describe methods of handling various boundary conditions which are applicable to pipe flow. Among these are:

1. Reservoir at upstream end
2. Valve at downstream end
3. Minor losses (due to sudden expansions of pipe)
4. Junctions of pipe segments
5. Restrictions, (orifices), in pipeline
6. Surge chambers

Some of the conditions listed above are directly applicable in the analysis of a well during shut-in. For instance, the choke manifold is tied into the well head and can be treated in the same manner as the junction of two pipes. The closure of the blowout preventer in the hard shut-in procedure can be thought of as the rapid closure of a valve. The most direct approach is to treat the preventer or choke as having an effective area which varies as a known function of time. The dimensionless orifice equation, (4.11a), and Equation (4.21) can then be solved simultaneously to give the velocity, V, and hydraulic head, h.

The pressure drop across a valve or choke through which is flowing a slightly compressible fluid can be approximately represented in

$$\Delta p = \frac{\rho q^2}{12032} \frac{1}{A_f{}^2} \tag{4.23}$$

where

A_f = frictional area coefficient, in ^{2}

ρ = density, lb/gal

q = flow rates gal/min

In addition to frictional area coefficient, there are other commonly used expressions for describing flow through a choke. These alternative equations involve the use of either a valve coefficient, C_v, or the use of an actual choke port area, A_o, corrected by an appropriate discharge coefficient, C_d. The effective frictional area is related to these other parameters as follows:

$$A_f = \frac{C_v}{38} \tag{4.24}$$

$$A_f = \frac{C_d{}^2 A_o{}^2}{[1 - (\frac{Ao}{A_1})^2]} \tag{4.25}$$

These expressions allow the results obtained in this study to be easily expressed using any of these equivalent terms.

4.4 EXPERIMENTAL STUDY OF BOP FLOW CHARACTERISTICS

An experimental study was undertaken to determine the flow characteristics of an annular blowout preventer during closure. This study was needed to define the boundary conditions for the pressure surge analysis.

4.4.1 Experimental Procedures

The test stump for the spherical blowout preventer used in this study is described in Figure 37. A Shaffer 7-1/16 in. 3000 psi spherical blowout preventer is mounted on a 9-1/2 ft joint of 7.921 in. I.D. casing sunken partially below ground level. The casing joint is fitted with a bottom plate of hardened steel to prevent erosion due to the washing action of flow across the bottom of the system, and to provide a closed flow system.

The top flange on the bell nipple above the blowout preventer is fitted with a threaded box for hanging various sizes of pipe in the hole. Since this analysis considered pressure drops in the annulus across the blowout preventer, the use of actual drill pipe and drill collars were not necessary. Instead four sizes of relatively light weight pipe were used to simulate various annular geometries, each pipe size having an outer diameter equal to that of commonly used tubing, drill pipe, or drill collars. The pipe sizes examined were 2-3/8, 3-1/2, 4-1/2, and 5-1/2 in. outer diameters.

Each joint of pipe is fitted with a tool joint pin to accomodate hanging the pipe from the top flange of the bell nipple. Each joint has centralizers welded to its lower body to keep the pipe centered and stationary in the assembly. The bottom of each joint is also open-ended to minimize the pressure losses upstream of the annulus.

Just above the blowout preventer the 4.0 in. return line is flanged to the bell nipple to allow for minimal back pressure on the preventer. The pressure sensing equipment, which was used to monitor annular pressure directly upstream of the preventer, is tied into the system by a manifold of 1/2 in. schedule 80 pipe and high pressure gate valves just below the blowout preventer.

The 7-1/16 in. 3000 psi Shaffer spherical blowout preventer is shown in Figure 38. This particular design of annular blowout preventer

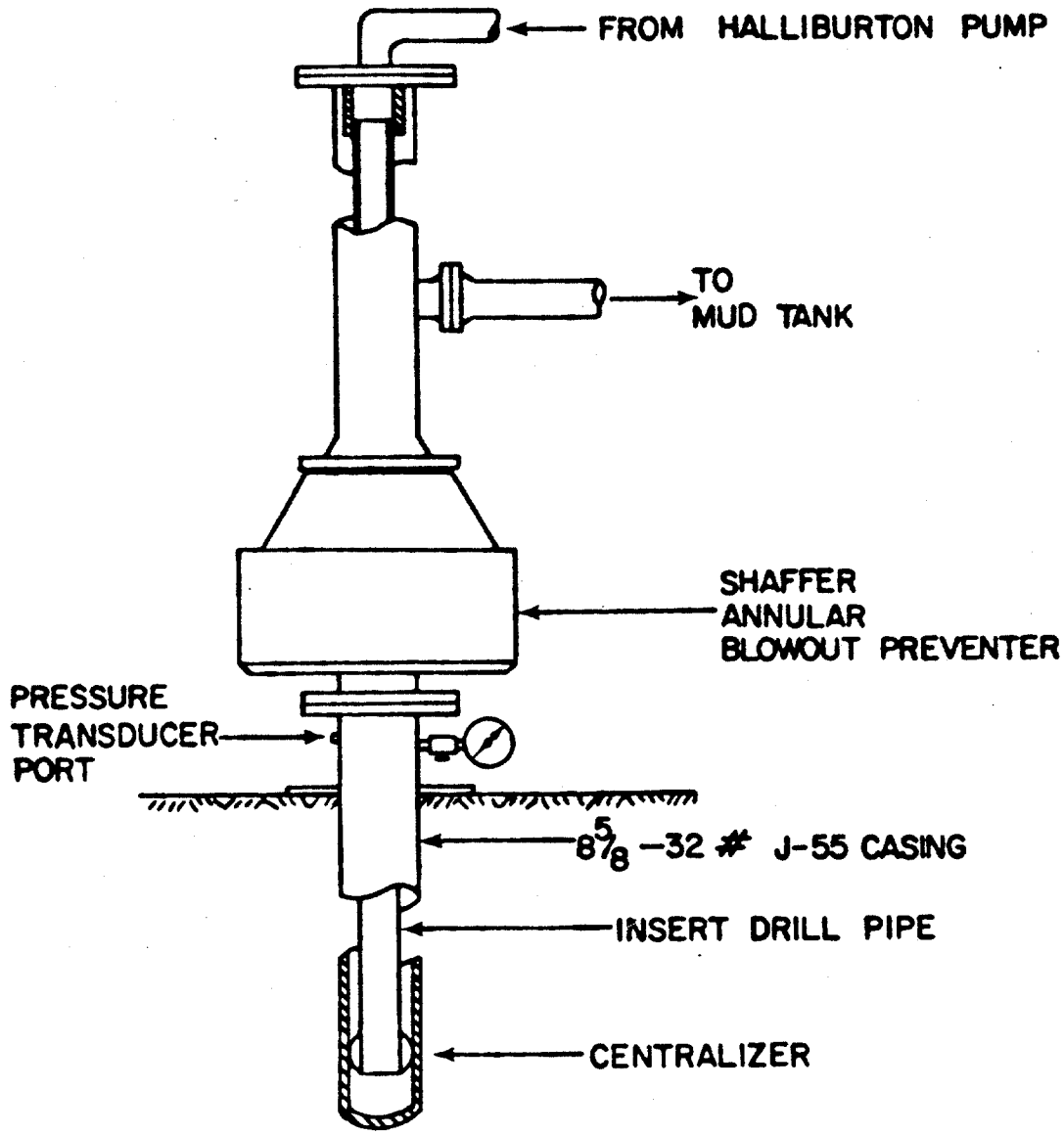

Figure 37. - Spherical Blowout Preventer Test Stump

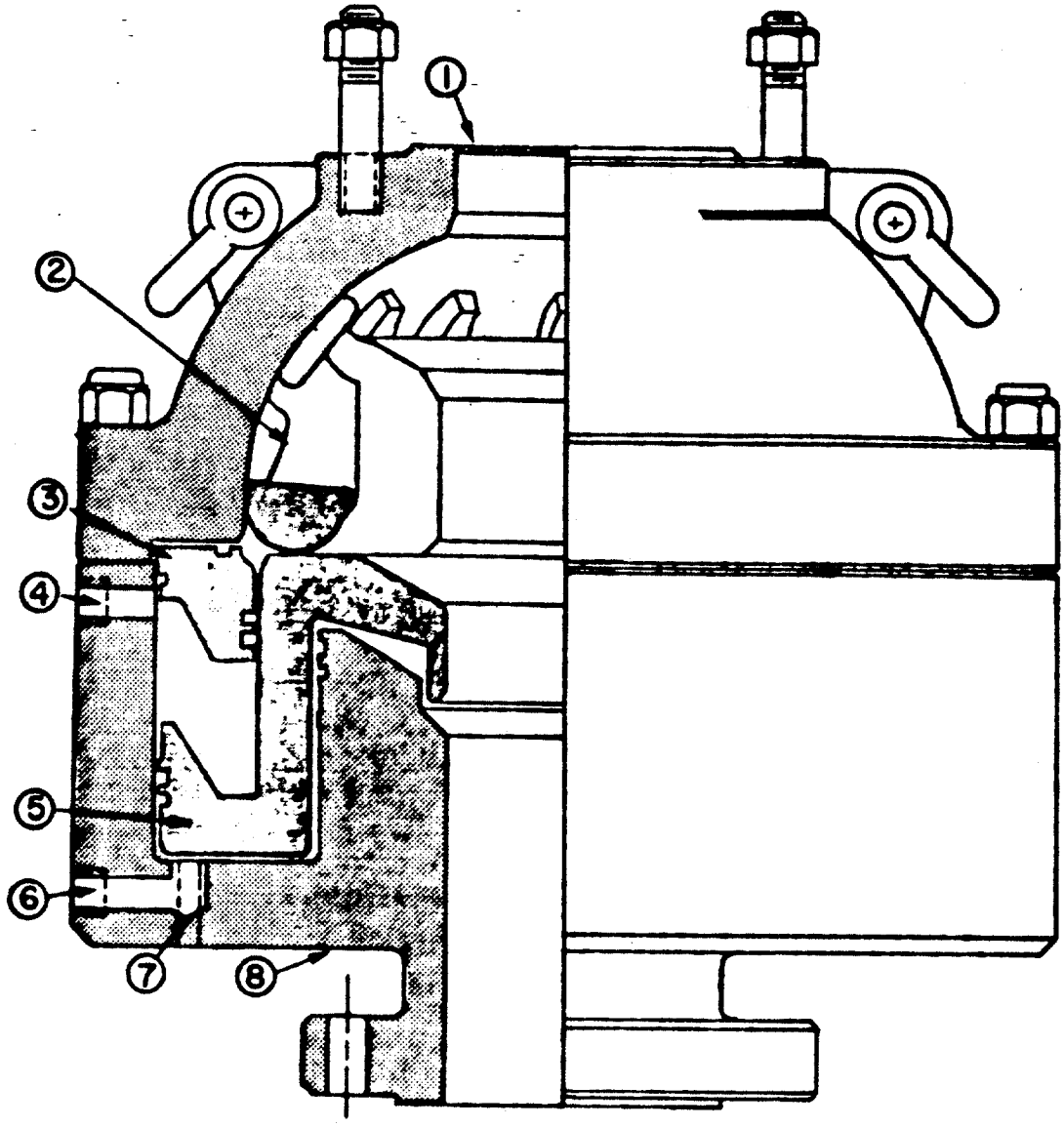

Figure 38. - Cutaway View of 7-1/16 in. Shaffer Spherical Blowout Preventer

derives its name from the shape of the inside of its upper housing, a design feature which plays an integral part in the closing mechanism of the preventer.

The main components of the blowout preventer are the upper and lower housings, the piston, the adapter ring, and the sealing element. The sealing element consists primarily of rubber with spherical steel inserts molded into the rubber to reinforce the rubber and to provide a low friction, metal-to-metal sliding contact between the sealing element and the spherical upper housing of the preventer. The element is designed to allow closure around any size or shape of pipe as well as on an open hole.

Figure 38 shows the preventer in the full open position, with the sealing element fully relaxed. To close the preventer, fluid is pumped in the closing chamber, forcing the piston upward as fluid is expelled from the opening chamber above the piston. The piston, in turn, drives the spherical sealing element upward as it contacts the spherical-shaped, inside surface of the preventer's upper housing. A feature of the spherical design is the assist in closing the element that is obtained by well pressure exerted below the element. To open the preventer, fluid is pumped into the opening chamber displacing the piston downward and allowing the sealing element to relax and return to the full open position. It should be noted that the sales literature for the preventer specifies that in stripping operations, opening energy is provided by the tool joint forcing its way into the element. This fact, along with the design feature of well pressure assist, on closing, suggests that even with opening pressure applied to the piston, the well pressure may be adequate to maintain the sealing element in the fully closed position. In order to open the blowout preventer under a well pressure capable of maintaining element closure, either the pressure must be bled down to a level which would allow the element to relax, or movement of the pipe in the hole can provide the energy to open the element.

Hydraulic fluid to the opening and closing chambers is supplied through 1 in. high pressure lines tied into a hydraulic accumulator, according to the recommendations of the blowout preventer manufacturer. However, each line was also equipped with a high-pressure needle valve

to regulate the flow of hydraulic fluid into each of the two chambers. Valves in the control lines are not recommended for field use because inadvertent closure of a valve would put the blowout preventer out of service. A fitting is also provided on the closing chamber to allow the hook-up of a pressure gage for monitoring hydraulic pressure in the chamber.

The valve to the opening chamber is left fully open at all times to conform more accurately to actual field conditions. The needle valve on the closing control line is opened or closed as needed to regulate the flow of hydraulic fluid into the closing chamber when adjusting the position of the piston. With the piston in the desired position, the closing line valve is shut to prevent additional hydraulic fluid from flowing into the closing chamber and moving the piston.

The degree to which the blowout preventer is closed at any time is monitored by means of a 1/4 in. steel follower rod. The rod extends through a packed-off port bored through the lower housing of the blowout preventer specifically for this purpose. The rod, in contact with the steel piston, follows the piston's movement as the blowout preventer is closed or opened.

An external lever and weight mechanism was developed to apply a constant upward force to the end of the follower rod, keeping the rod in contact with the preventer piston at all times. This was necessary because the hydraulic pressure within the closing chamber imposes a force on the opposite end of the rod and tends to pump the rod out the port in the lower housing and thereby lose contact with the piston.

Since the rod remains in contact with the piston, rod movement is measured to determine the degree of closure of the preventer. A dial indicator, fastened to the rod as shown in Figure 39, is used to measure the rod travel, in inches, from the full open position.

The total rod travel from full open to full closed is from 3 to 4 inches depending on the pipe size in the hole. The dial indicator used in this study has a range of 2.000 in. with an increment of 0.001 in. It was therefore necessary to use an extender block of known dimensions to accomodate the full travel of the rod. The dial indicator is positioned on the rod to read near full scale (2.0 in.) with the preventer in the closed position. Then the full open position is read with the

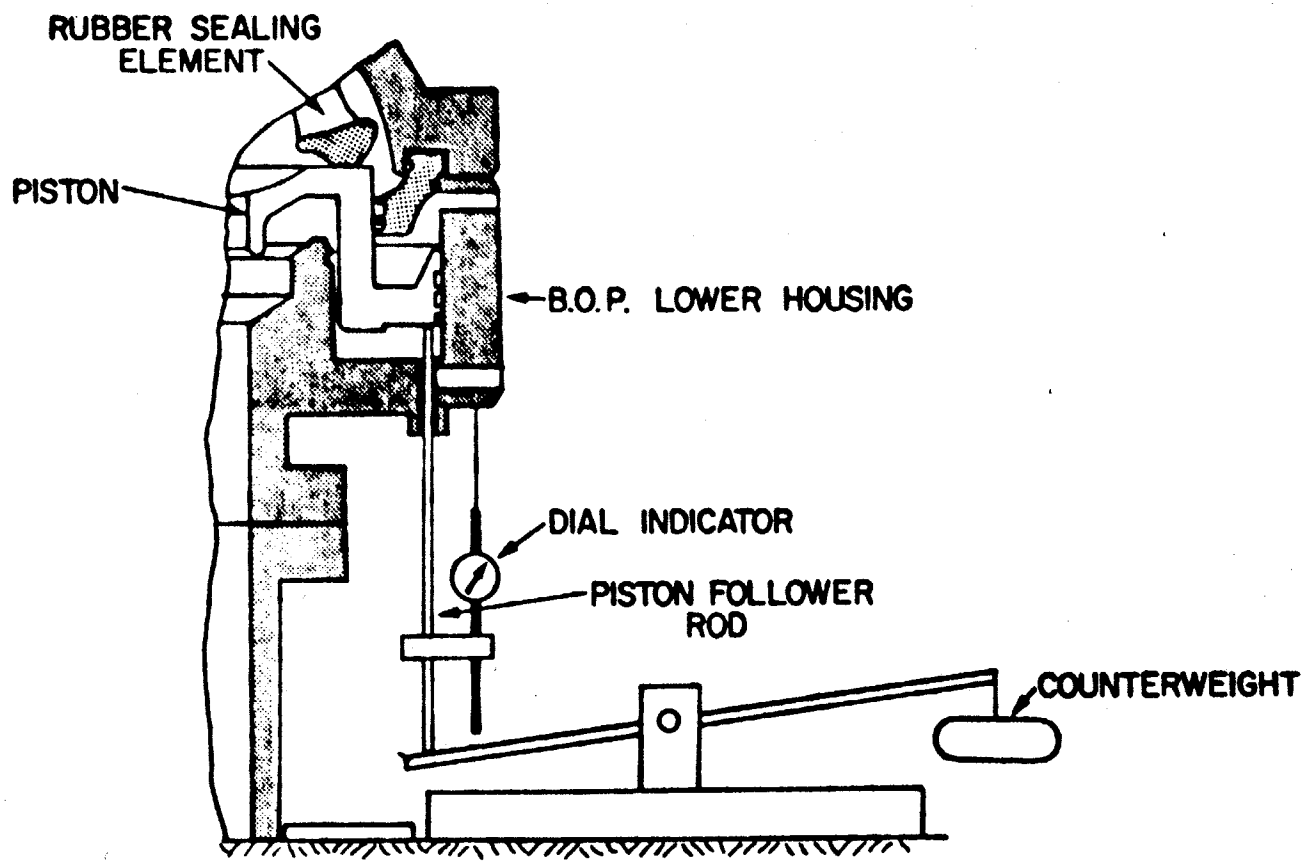

Figure 39. - Piston Position Indicator Assembly Used with Spherical Blowout Preventer

extender block inserted between the tip of the indicator rod and the lower housing of the blowout preventer surface. From the reading at full open and the thickness of the extender block, a full open reference mark is established for determining total rod travel using the equations below:

With extender block inserted:

Travel = Present dial reading - full open dial reading, inches.

Without extender block (dial indicator tip in contact with blowout preventer):

Travel = Present Dial Reading + (L - Full Open Dial Reading), inches.

where L = thickness of extender block, inches.

As flow rate and pressure data were collected, the closing chamber pressure was monitored also in the control house in an effort to detect possible piston movement. It was found that at high differential pressures across the preventer, the closing pressure tends to rise, as the piston tends to back up slightly toward a more open position. This was an important observation in that with each set of pressure drop - flow rate data it was assumed that the piston remained in a fixed, pre-set position.

A data monitoring console, specially designed and built by Halliburton Services for the L.S.U. Blowout Prevention Facility, is used to monitor pressure drops and flow rates across the blowout preventer. The unit combines various components having specific measuring or display capabilities into a semi-portable instrument console.

Annular pressures directly below the preventer are transmitted through a precharged gage protector and hydraulic line to a set of two pressure transducers. Teledyne-Taber model 2204 pressure transducers with pressure ranges of 0 - 500 psi and 0 - 2000 psi are arranged in parallel in order to avoid the use of valves which would induce loss of the hydraulic precharge of the system, requiring recalibration.

The flow sensing components of the system generates signals from two sources: (1) a shaft encoder mounted on the T-10 triplex pump and (2) a Fisher Porter magnetic flow meter mounted on the return line from the choke manifold. The flow selector switch on the front display console allows the user to monitor flow rate based on either source of the flow signal.

Pressure drop measurements were made for steady-state flow through the blowout preventer at various partial closures. Mud properties are checked before and after the pressure and flow rate data are taken in order to detect significant changes in the mud properties which might affect the quality of the data. The properties which are monitored are:

1. Density
2. Temperature
3. Six Fann Viscometer Readings
4. 10 sec. gel strength, and 10 min. gel strength

In determining the pressure drop across the annular preventer as a function of flow rate, the piston positions were set using closing pressure only. In the event that the desired piston position was passed, opening pressure was not used to reverse the piston movement. Rather, the blowout preventer was fully opened and then closing pressure used to obtain the appropriate setting. The rubber element seems to behave differently under closing pressure than under opening pressure. Therefore, the most obvious reason for using closing pressure only in adjusting piston position is that this procedure more accurately describes the physical experience of the blowout preventer during closure in an actual well control situation.

The well, or annular, pressure was monitored as the closing pressure was applied to the blowout preventer, as a guide in choosing an appropriate piston position. In general, an increase in well pressure of 200 - 300 psi between one piston position and the next was used to provide useful results. However, the first piston position used was chosen at the initial pressure response in order to identify the minimum piston movement which gave a measureable affect on the flow rate - pressure drop response of the preventer.

Well pressure was recorded for an increasing sequence of flow rates in order to obtain more consistent data. Also, to provide a larger range of flow rates and pressures, the pump was shifted manually from second gear for low flow rates to third gear for high flow rates.

As the piston position approaches the full closed position, the rubber element has a tendency to close itself with the assist obtained from well pressure. Under these conditions, if the well pressure approaches 2500 psi, the pressure at which the pump's pop-off valve was

set, then the pump was quickly throttled down and the Swaco Super Choke was opened to bleed off this excess pressure to avoid activating the pop-off valve.

The procedure was continued for various piston positions until the pressures and flow rates encountered indicate automatic closure of the blowout preventer. Closure of the blowout preventer can be induced by the well pressure assisting the hydraulic pressure and is apparent from a rapid and steady decrease in pump rate with a corresponding rise in well pressure. The piston position at which the element ultimately seals to all flow was determined by applying well pressure to the system by throttling the pump slightly. Then the closing line valve was opened slightly, to very slowly move the piston upward. When no flow through the blowout preventer could be heard, the preventer was assumed to be fully closed to flow and the piston position (dial indicator reading) was noted.

4.4.2 Experimental Results

Graphical displays of the pressure drop - flow rate characteristics of the preventer were developed from experimental data to show the effects of:

1. Power piston travel, or degree of preventer closure,
2. Type and viscosity of flowing fluid,
3. Annular geometry, i.e., O.D. of pipe in preventer.

In order to study the effects of fluid viscosity on the blowout preventer pressure drop - flow rate characteristics, 3 fluids were examined for each pipe size. The fluid properties are shown in Table 10. The desired viscosity was obtained by adding bentonite clay to the mud in the tanks. Annular geometry effects were studied by using four pipe sizes of various diameters. The dimensions of the pipes are shown in Table 11.

Valve coefficients, used in the valve industry to characterize pressure losses through valves and fittings, were determined for the blowout preventer at each degree of closure (piston position). Curves of valves coefficients were developed to define the pressure drop - flow rate characteristics of the blowout preventer as a function of piston position.

Mud No.	Temp., °F	Density, lb/gal	Fann Viscometer Readings 600 rpm	300 rpm	200 rpm	100 rpm	6 rpm	3 rpm	10-sec gel, lb/100ft^2	10-min gel, lb/100ft^2	Plastic Viscosity, cp	Yield Point lb,100ft^2
1	70	8.33	2.0	1.0	.67	.33	-	-	0.0	0.0	1.0	0.0
2	86	8.59	20.0	17.0	14.0	6.0	1.0	0.5	0.0	2.0	3.0	14.0
	110+	8.57	21.0	15.0	12.0	8.0	2.0	1.5	1.5	14.0	6.0	9.0
3	-	-	-	-	-	-	-	-	-	-	-	-
4	78	8.61	21.0	13.0	10.0	8.0	3.5	2.0	1.0	1.0	8.0	5.0
	85	8.60	22.0	15.0	12.0	9.0	5.0	3.0	3.0	-	7.0	8.0
5	98	8.59	30.0	20.0	16.0	12.0	4.0	3.5	2.0	13.0	10.0	10.0
	109	8.59	38.0	27.0	21.0	14.5	5.0	4.0	3.0	24.0	11.0	16.0
6	94	8.63	125.0	88.0	73.0	55.0	30.0	29.0	43.0	75.0	37.0	51.0
	110+	-	161.0	118.0	102.0	80.0	48.0	47.0	69.0	90.0	43.0	75.0
7	90	8.64	143.0	98.0	79.0	57.0	27.0	25.0	34.0	64.0	45.0	53.0
	110+	-	148.0	110.0	95.0	75.0	47.0	46.0	50.0	90.0	38.0	72.0
8	94	8.60	155.0	109.0	92.0	69.0	37.0	36.0	47.0	74.0	46.0	63.0
	110+	8.62	166.0	120.0	103.0	79.0	48.0	47.0	58.0	90.0	46.0	74.0
9	100	8.67	225.0	160.0	136.0	104.0	57.0	56.0	70.0	105.0	65.0	95.0
	110+	8.65	245.0	176.0	152.0	119.0	69.0	69.0	88.0	110.0	69.0	107.0

Table 10 Summary of Fluid Properties

I.D., Inches	O.D., Inches
1.833	2 3/8
3.083	3 1/2
3.833	4 1/2
4.667	5 1/2

Table 11 Pipe Dimensions

The correlation between the piston position and the volume of hydraulic fluid pumped into the closing chamber of the blowout preventer was also determined. This relation was developed to allow the characteristics of the blowout preventer to be interfaced with the performance of the hydraulic accumulator in the ultimate analysis of shut-in procedures using a mathematical model.

Figures 40 through 51 show the experimental results for the various annuar geometries and drilling fluids. Each figure shows pressure drop across the blowout preventer as a function of flow rate for various positions of the piston in the blowout preventer. The piston movement can be used as a gage of the degree of closure for the blowout preventer.

The most obvious observation which can be made from the data presented here is that, regardless of fluid type or pipe size in the hole, the flow is essentially unrestricted until a fairly high degree of closure is attained. For instance, in Figure 40, the pressure drop across the blowout preventer is negligible until the piston has traveled approximately 2.5 in. In contrast, movement of the piston from 2.593 to 2.803 in., only 21 hundreds of an inch, produces a very large increase in pressure drop. For the conditions in Figure 40, the blowout preventer was fully closed with a total piston travel of 2.96 in. The piston must travel 85% of its total traverse before any significant restriction of the flow is realized. The actual shut-in can be attributed to the final 15% of total piston travel.

Rapid closure of a valve in a pipeline produces a water hammer pressure surge approaching that of instantaneous closure. More gradual closure, where the closure time, t_c, is greater than the time for a pressure wave to be reflected from the upstream end of the system, produces a less intense pressure rise. The above results seem to support the theory that a hard shut-in could produce surge pressures comparable to rapid valve closure. Even if the total time to close the blowout preventer is long enough to constitute a slow closure, the behavior of the blowout preventer could reduce the effective closing time and produce a rapid closure with a correspondingly higher pressure surge.

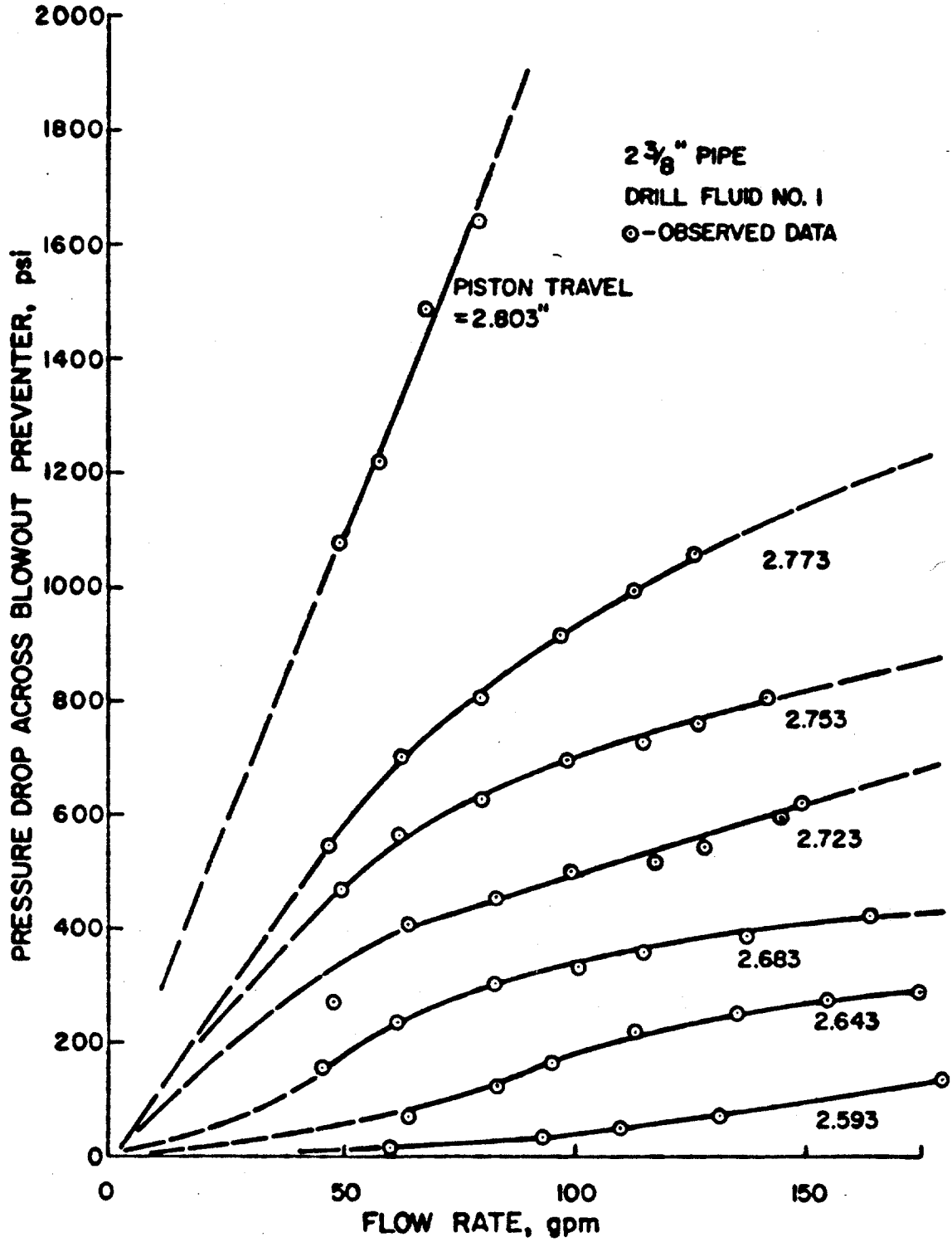

Figure 40 - Pressure Drop Through Spherical Preventer for Fluid 1 and Pipe Size 1

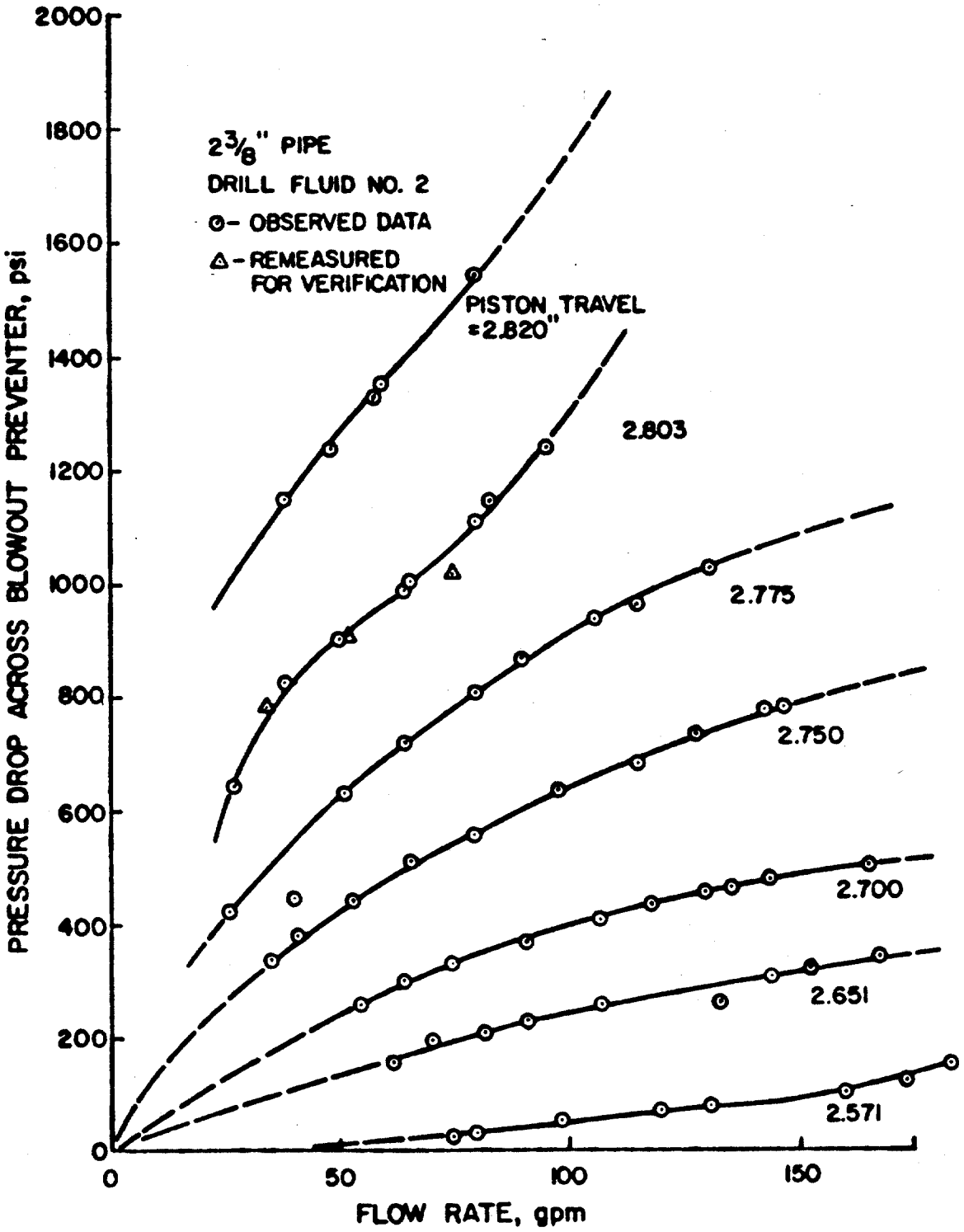

Figure 41 - Pressure Drop Througe Spherical Preventer for Fluid 2 and Pipe Size 1

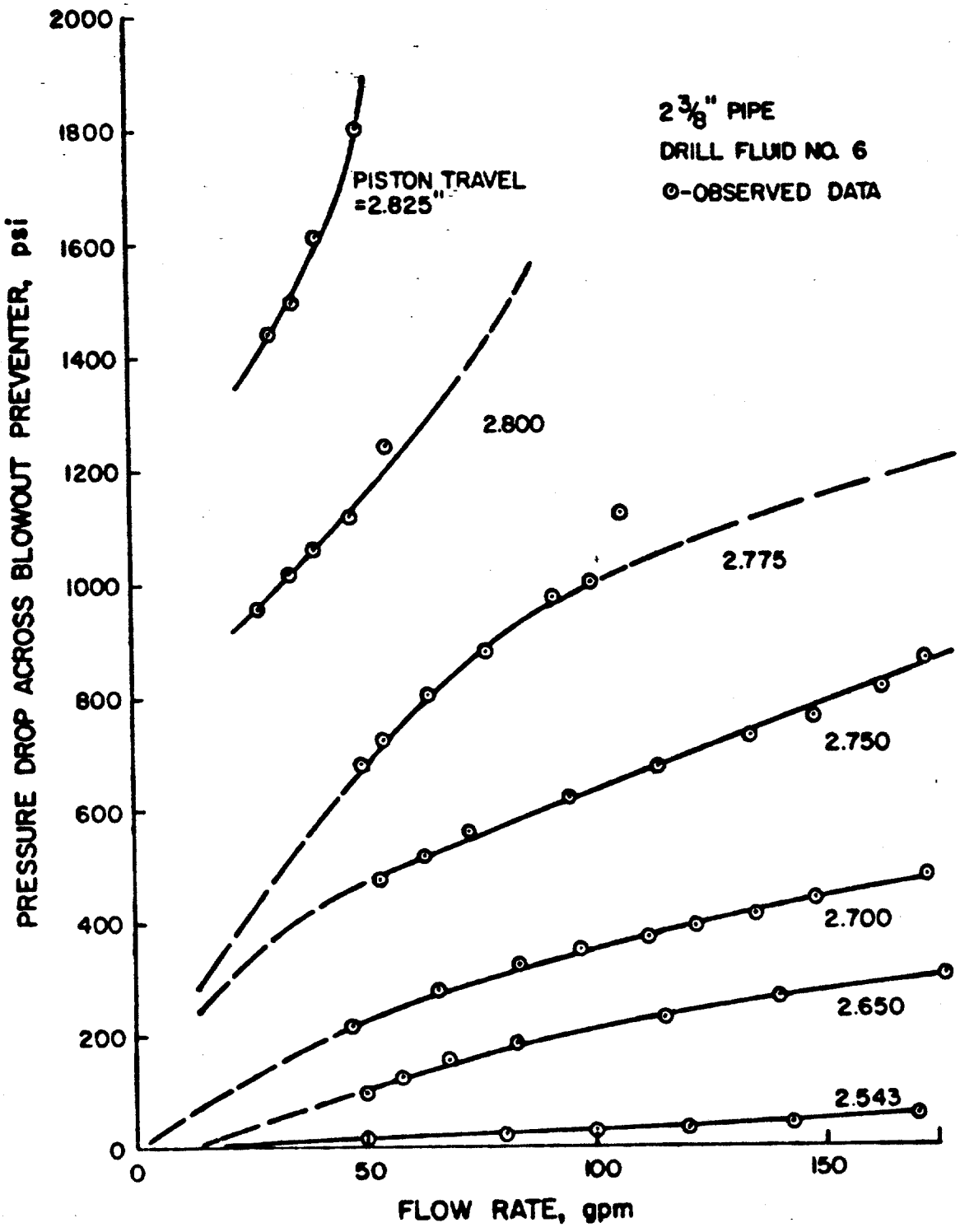

Figure 42 - Pressure Drop Through Spherical Preventer for Fluid 6 and Pipe Size 1

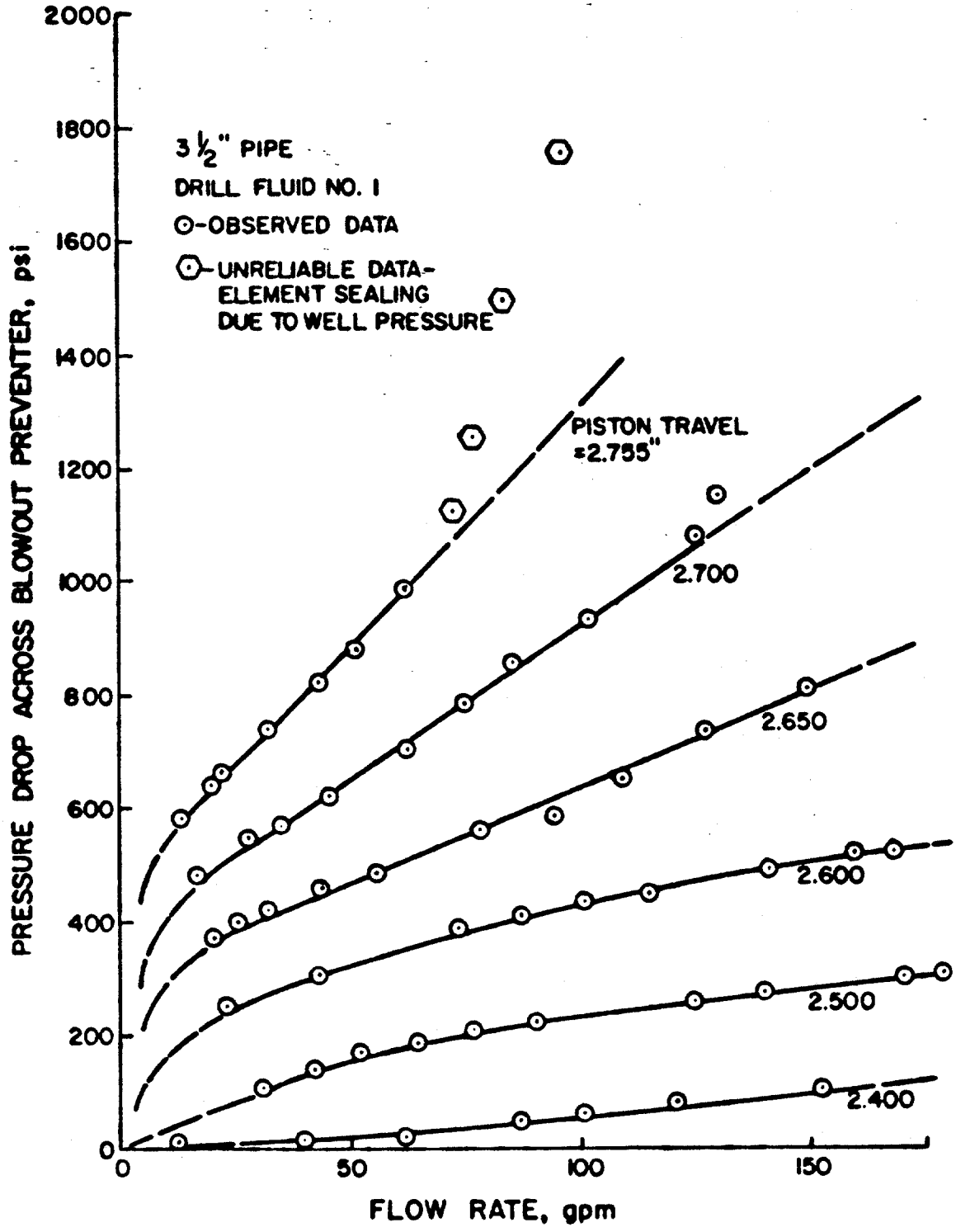

Figure 43 - Pressure Drop Through Spherical Preventer for Fluid 1 and Pipe Size 2

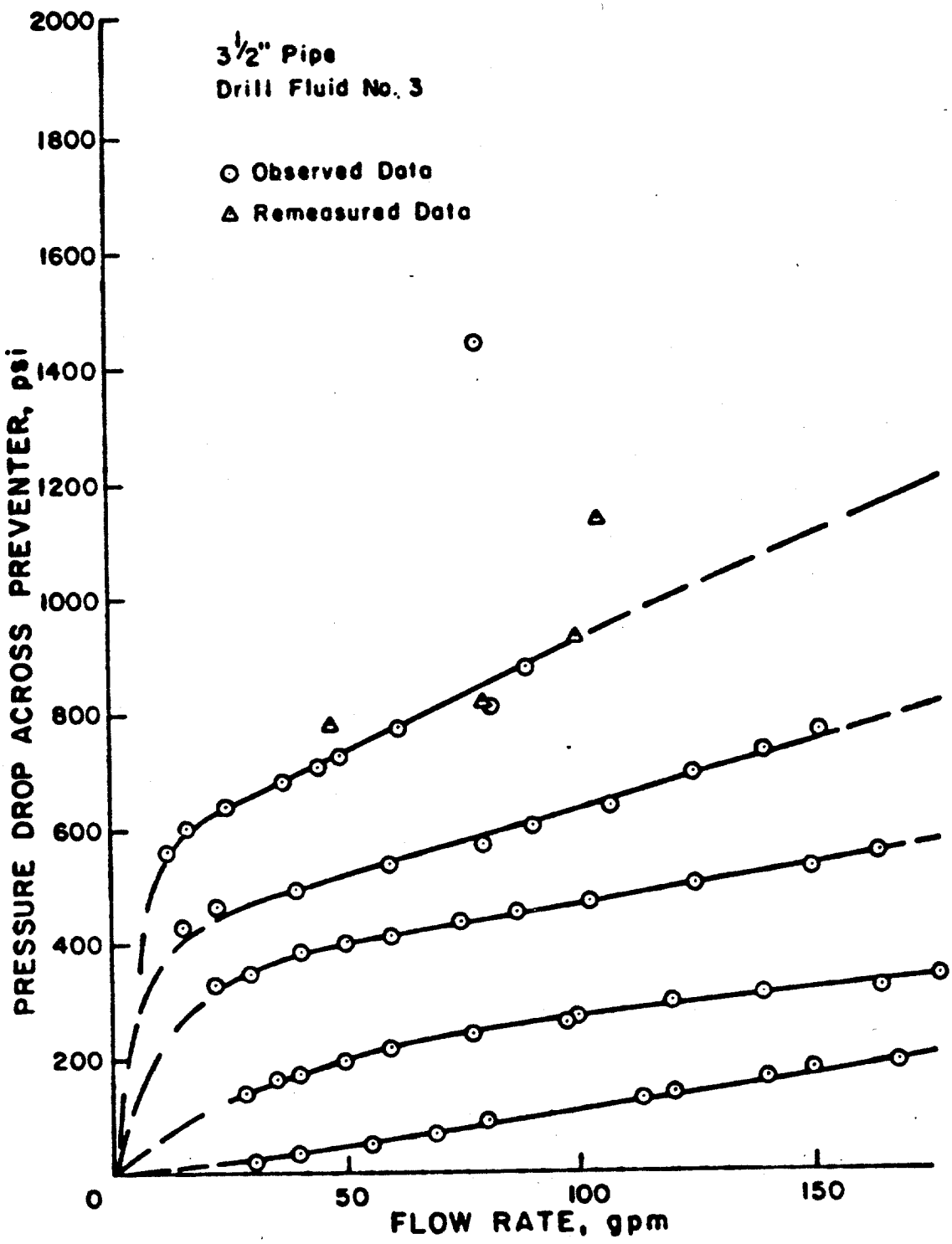

Figure 44 - Pressure Drop Through Spherical Preventer for Fluid 3 and Pipe Size 2

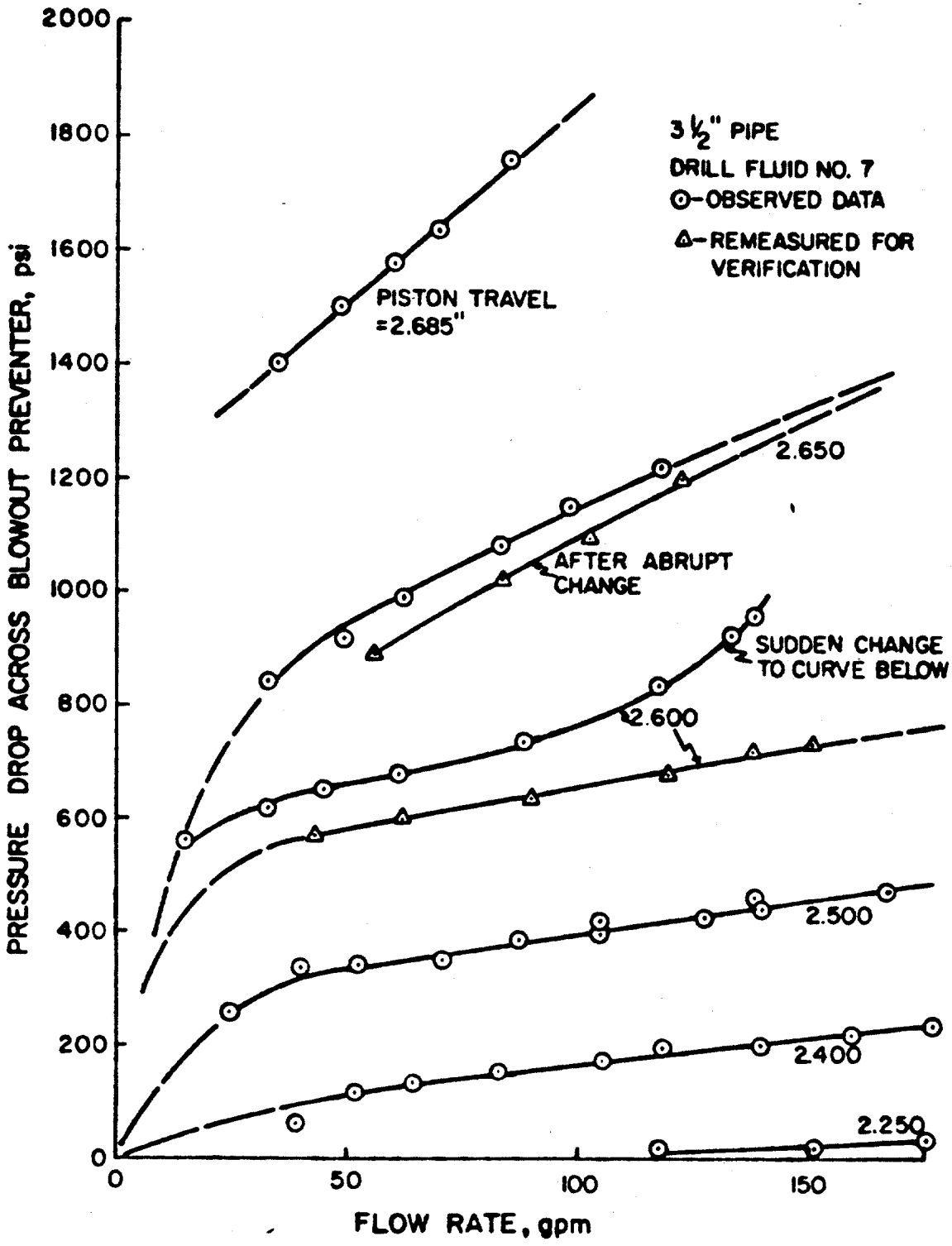

Figure 45 - Pressure Drop Through Spherical Preventer for Fluid 7 and Pipe Size 2

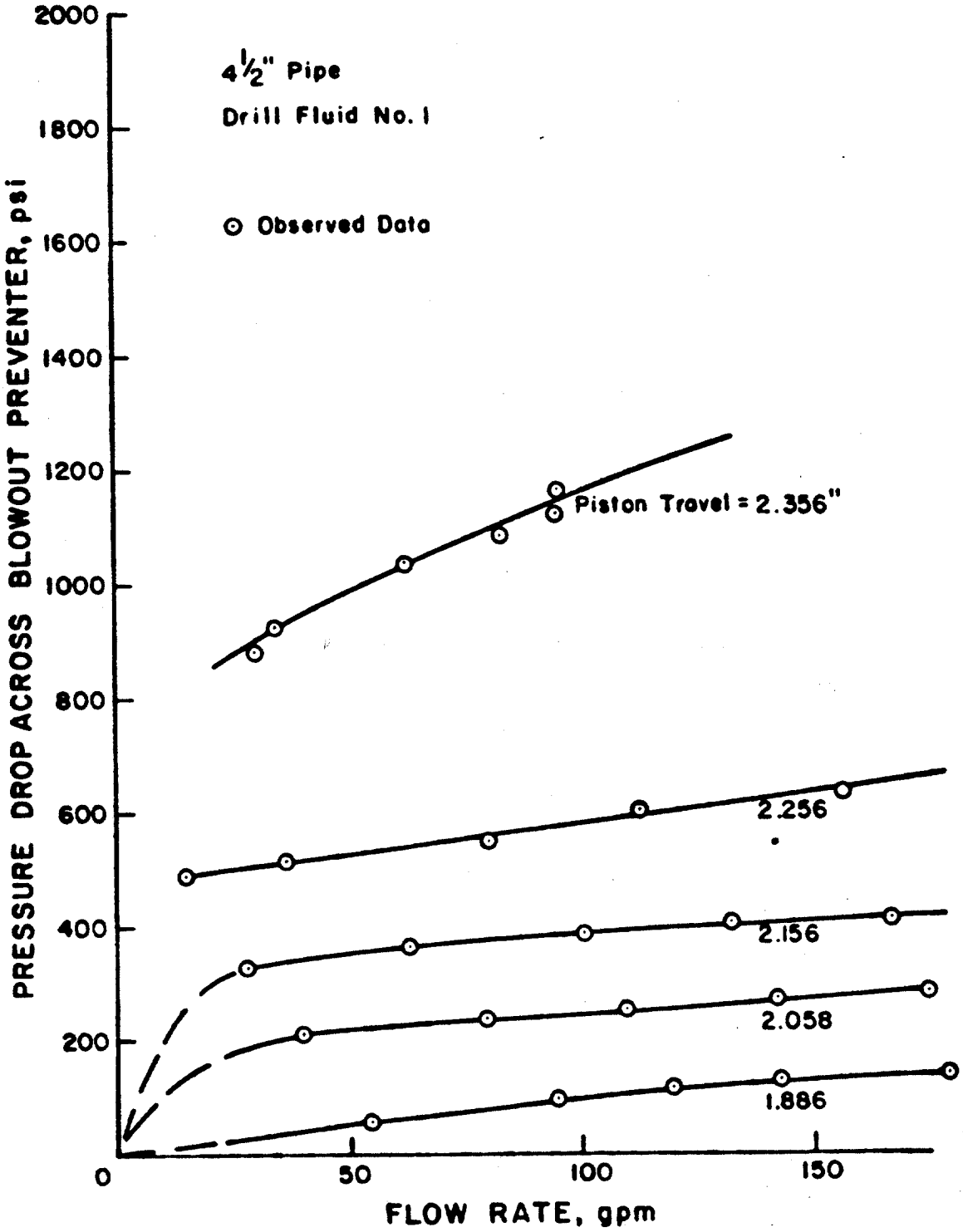

Figure 46 - Pressure Drop Through Spherical Preventer for Fluid 1 and Pipe Size 3

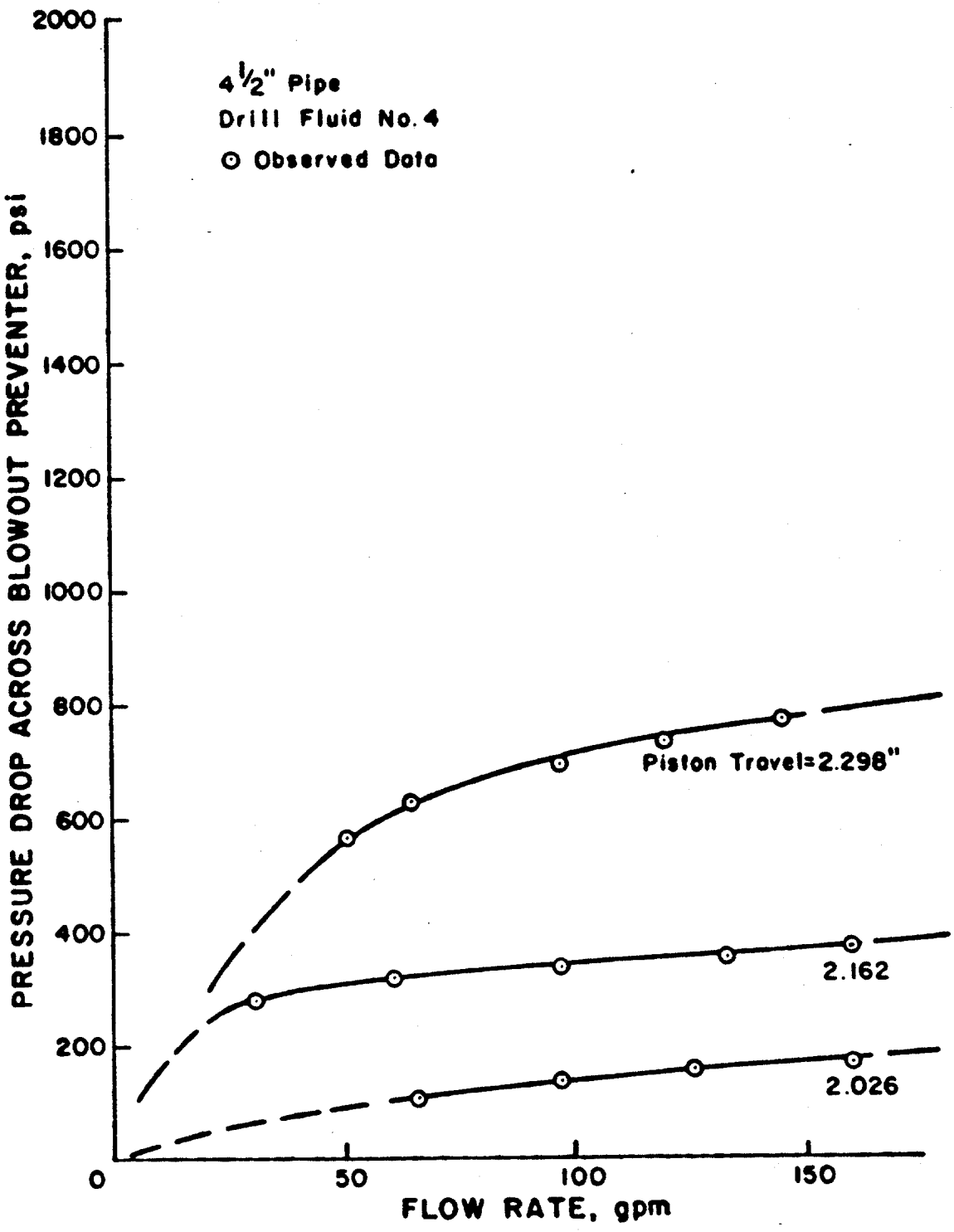

Figure 47 - Pressure Drop Through Spherical Preventer for Fluid 4 and Pipe Size 3

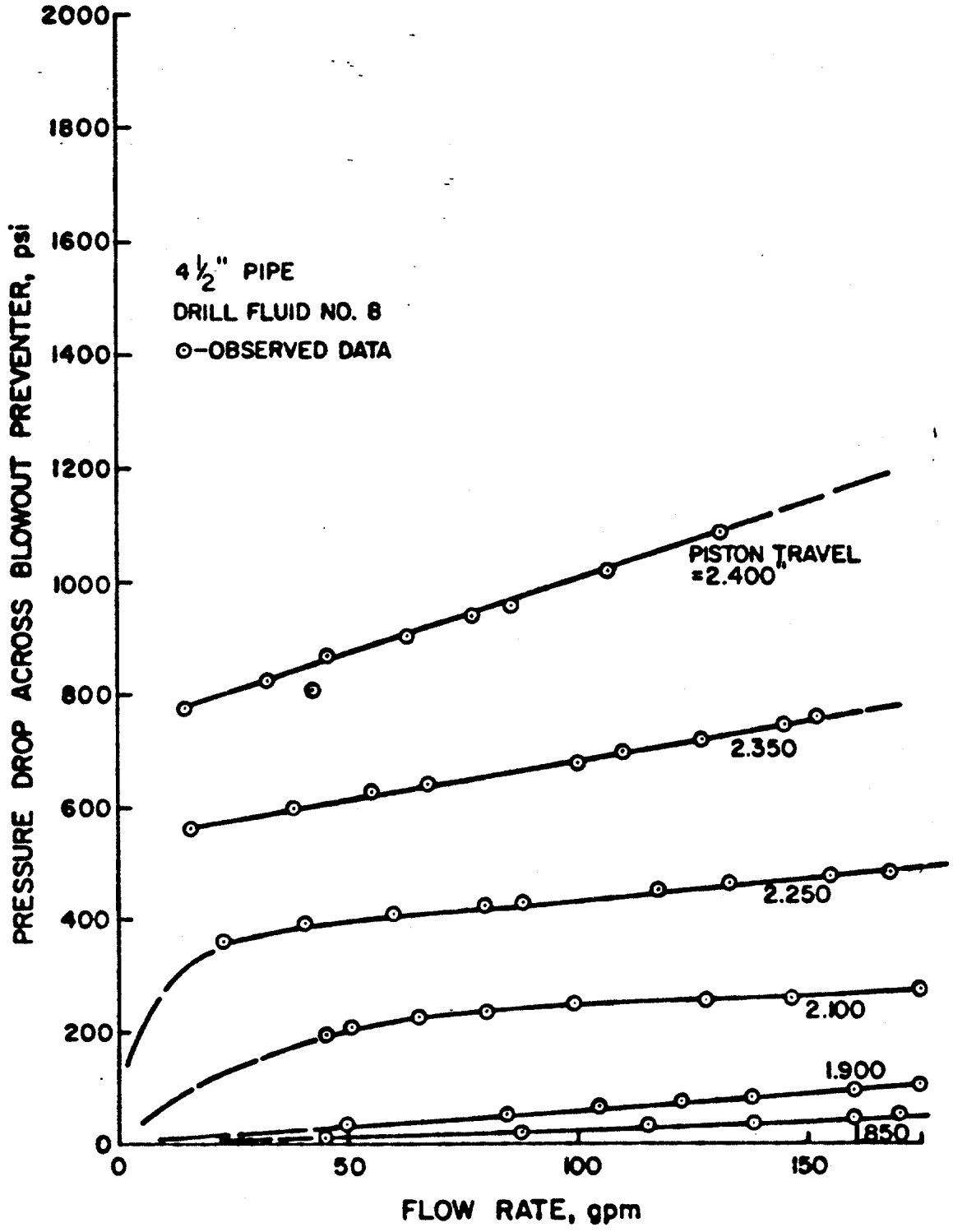

Figure 48 - Pressure Drop Through Spherical Preventer for Fluid 8 and Pipe Size 3

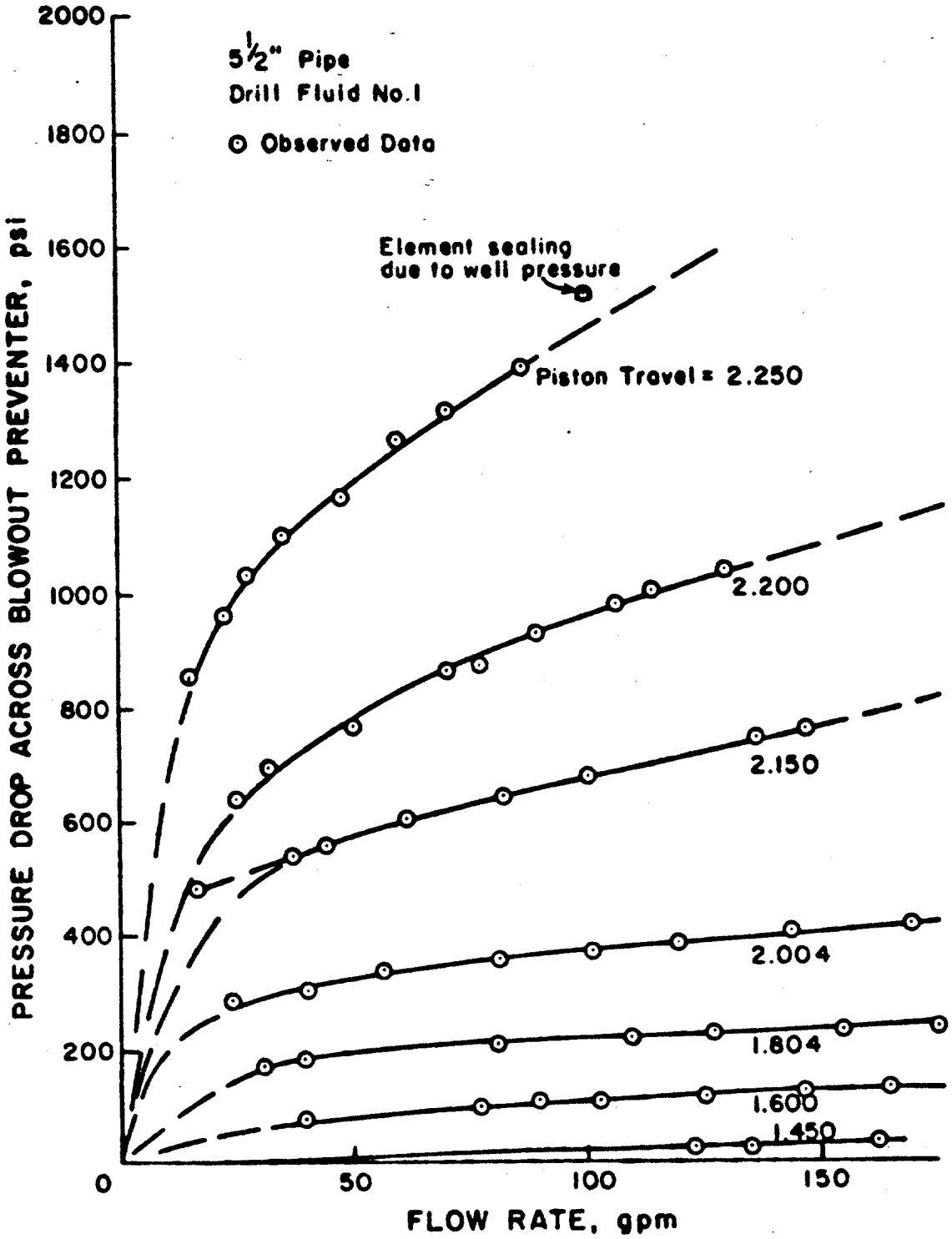

Figure 49 - Pressure Drop Through Spherical Preventer for Fluid 1 and Pipe Size 4

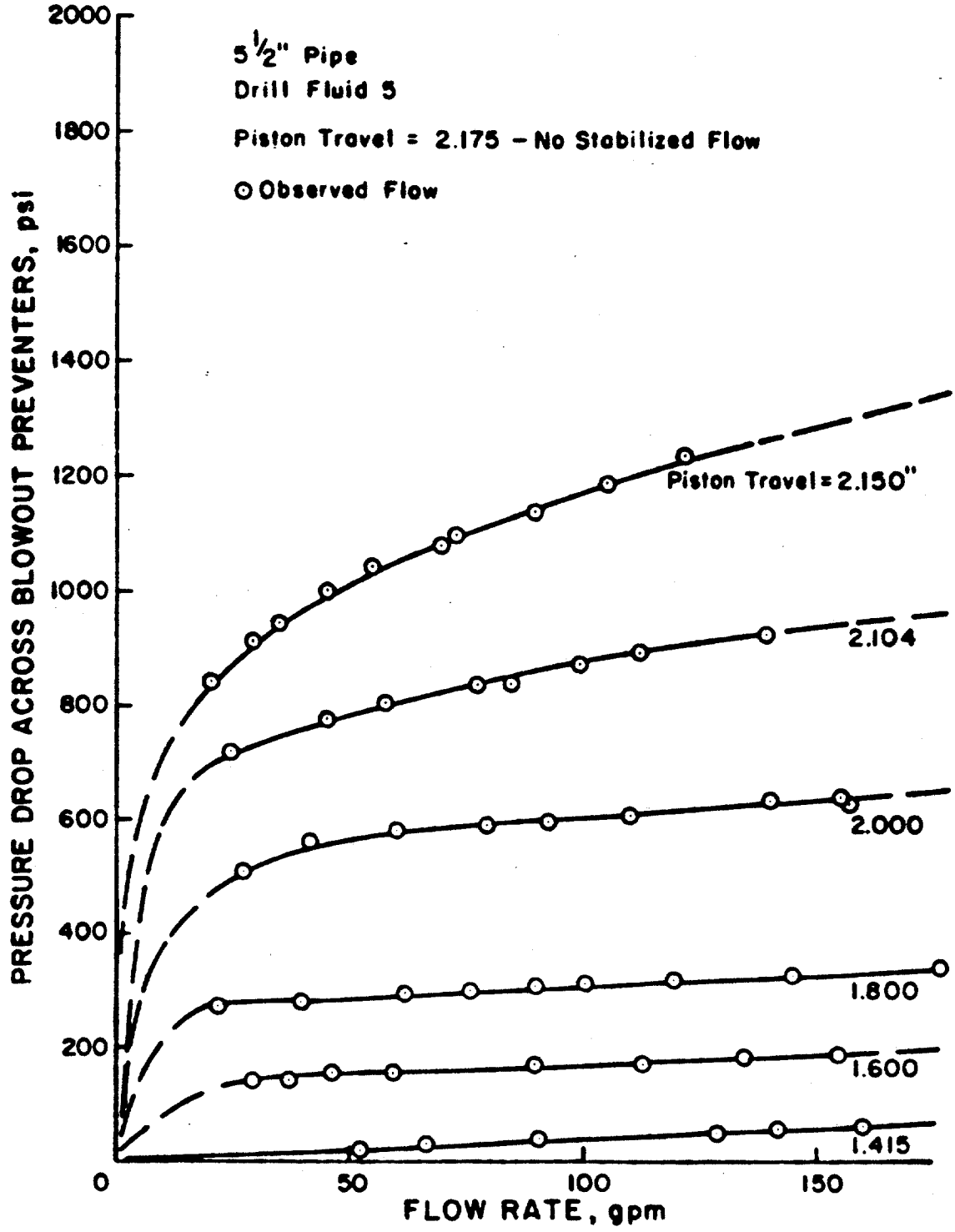

Figure 50 - Pressure Drop Through Spherical Preventer for Fluid 5 and Pipe Size 4

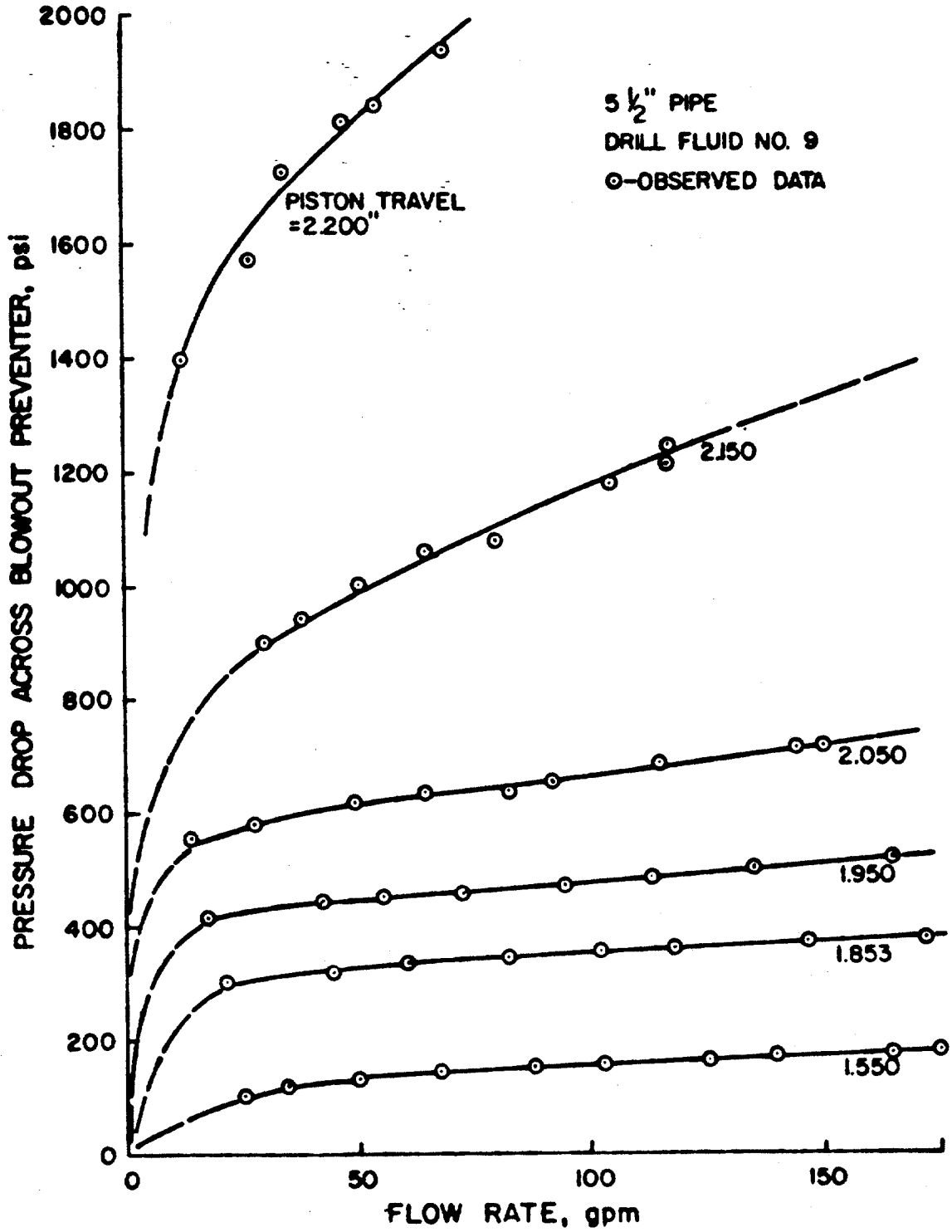

Figure 51 - Pressure Drop Through Spherical Preventer for Fluid 9 and Pipe Size 4

The varying behavior of the rubber sealing elements seems to be a dominant factor in the characteristics of the blowout preventer during closure. The rubber element is deformed as it is forced upward and inward by the piston. The piston position is therefore used to gage the degree of closure of the blowout preventer. However, the data of Figures 44 and 45 show slightly varying results for measurements made at the same piston positions. For instance, in Figure 45, the upper curve at a piston position of 2.600 was obtained and then the data was remeasured without moving the piston. There is a significant difference between the two curves. Slight differences are also shown by the total travel required to achieve full closure of the preventer. The configuration of the rubber element, and thus the area open to flow, seems to change each time the element is exercised. Therefore, even though the exact piston position can be reproduced, the exact flow restriction may not be duplicated, and thus, some degree of irreproducibility can be expected owing to the deformation characteristics of the rubber element.

The slope of the pressure drop versus flow rate curves also seems to be influenced by the behavior of the rubber sealing element. The curves are uncharacteristically flat for certain ranges of piston position between the initial pressure response and the full closed position. Figure 40 illustrates this point rather well. Assuming laminar flow in a closed conduit, if the flow rate is doubled, then the pressure drop through the conduit should also be doubled. Turbulent flow would produce an even larger increase in the pressure drop through the conduit. In the case of an orifice, the pressure drop increase due to an increase in flow rate is much the same as for turbulent flow in a conduit. However, referring to Figure 40, for piston positions from approximately 2.70 to 2.77 in., the increase in pressure drop does not correspond to the increase in flow rate as expected. For a piston position of 2.723 in., the pressure drop increases from 340 psi at 50 gpm to 495 psi at 100 gpm, an increase of only 45%. However, for a piston position of 2.803, the pressure drop increases from 1080 psi at 50 gpm to 2100 psi at 100 gpm (from extrapolation), which is close to the expected behavior for laminar flow. It still, however, is not as large of an increase as would be expected for flow through an orifice.

The response of the rubber element to increases in pressures and flow rates may account for the unexpected behavior above. With the blowout preventer piston stationary, as the flow rate is increased the rubber element seems to deform or "breathe", assuming a different configuration or area open to flow. The pressure drop across the preventer is increased less than for a rigid flow restriction. As the piston approaches the full closed position, the rubber seems to lose its ability to relieve itself or "breathe". This may be due to the higher pressure encountered under these conditions compressing the rubber. Whatever the reason, the slope of the pressure drop - flow rate curves increases as the blowout preventer element approaches full closure, and increases in flow rate seem to induce more reasonable increases in pressure drop across the blowout preventer.

The valve industry often uses a valve coefficient, C_v, to characterize the pressure drop across a valve for any flow rate. The parameter is used in this study to characterize flow rate and pressure drop through the 7-1/16 in. spherical blowout preventer. Values of C_v were calculated for various positions of the piston and various flow rates. Figures 52 through 63 show C_v plotted as a function of piston position for various flow rates from 25 gpm to 175 gpm.

In dealing with valves, the valve coefficient is often assumed to be constant, regardless of the flow rate or pressure across the valve. It was found from the results of this investigation that, for a constant piston position, the value of C_v is not constant. Instead of a single curve representing C_v as a function of piston position, the results show a family of curves, each representing C_v as a function of piston position for a different flow rate.

Although Figures 52 through 63 each represent different annular geometries and/or fluid properties, the same general trends are apparent in the curves of C_v. For the blowout preventer in the full open position, the pressure drop across the preventer is negligible and the value of C_v approaches infinity. The value of C_v remains very high until the piston reaches the point where the initial restriction to flow is felt. Then, as the piston moves upward, C_v decreases until, at full closed, C_v is equal to 0. The exact path followed cannot be determined but would likely be somewhere in an envelope encompassing the steady state data points shown in Figures 52-63. These curves can provide an approxima-

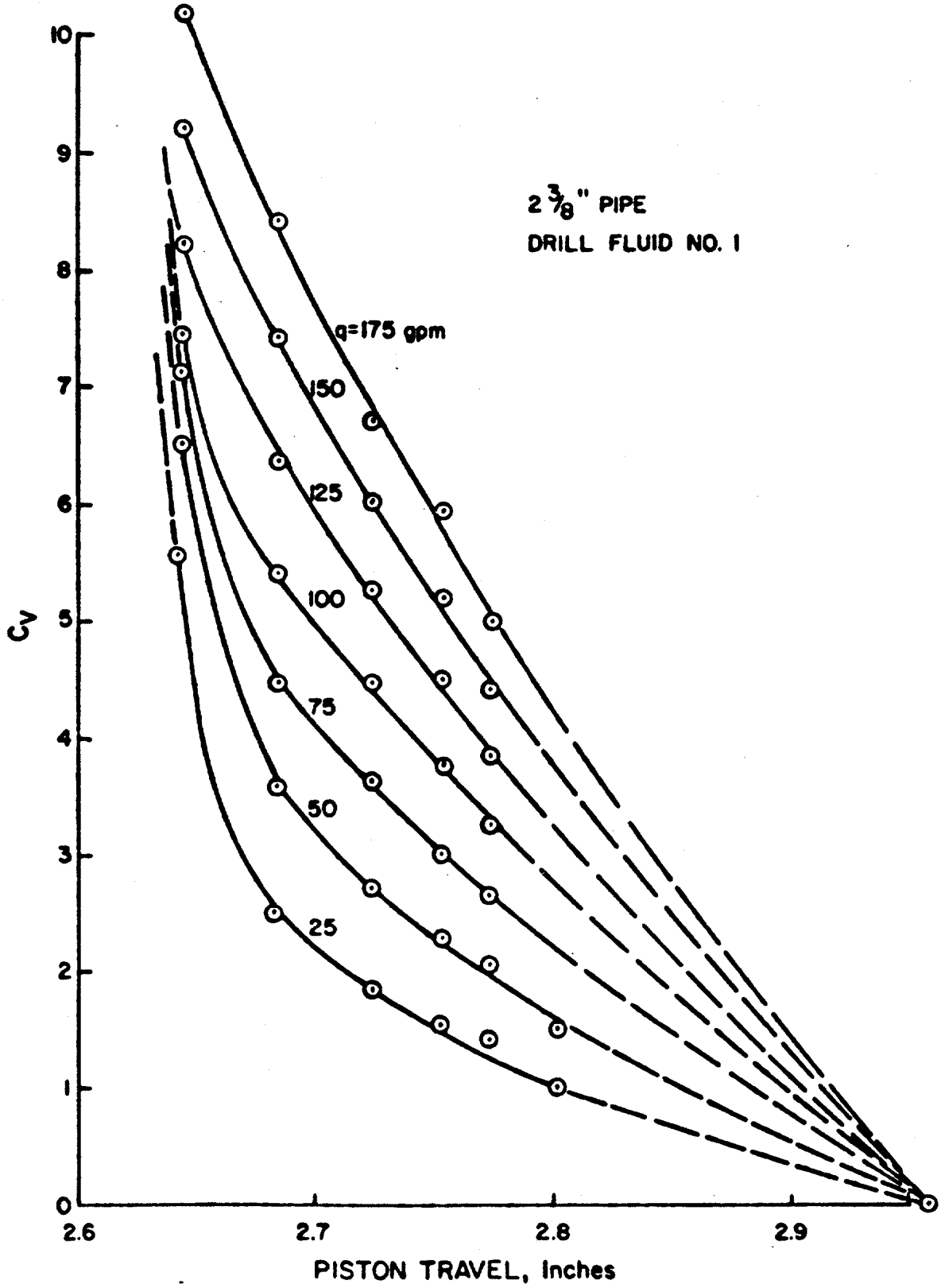

Figure 52 - Valve Coefficient for Spherical Preventer with Fluid 1 and Pipe Size 1

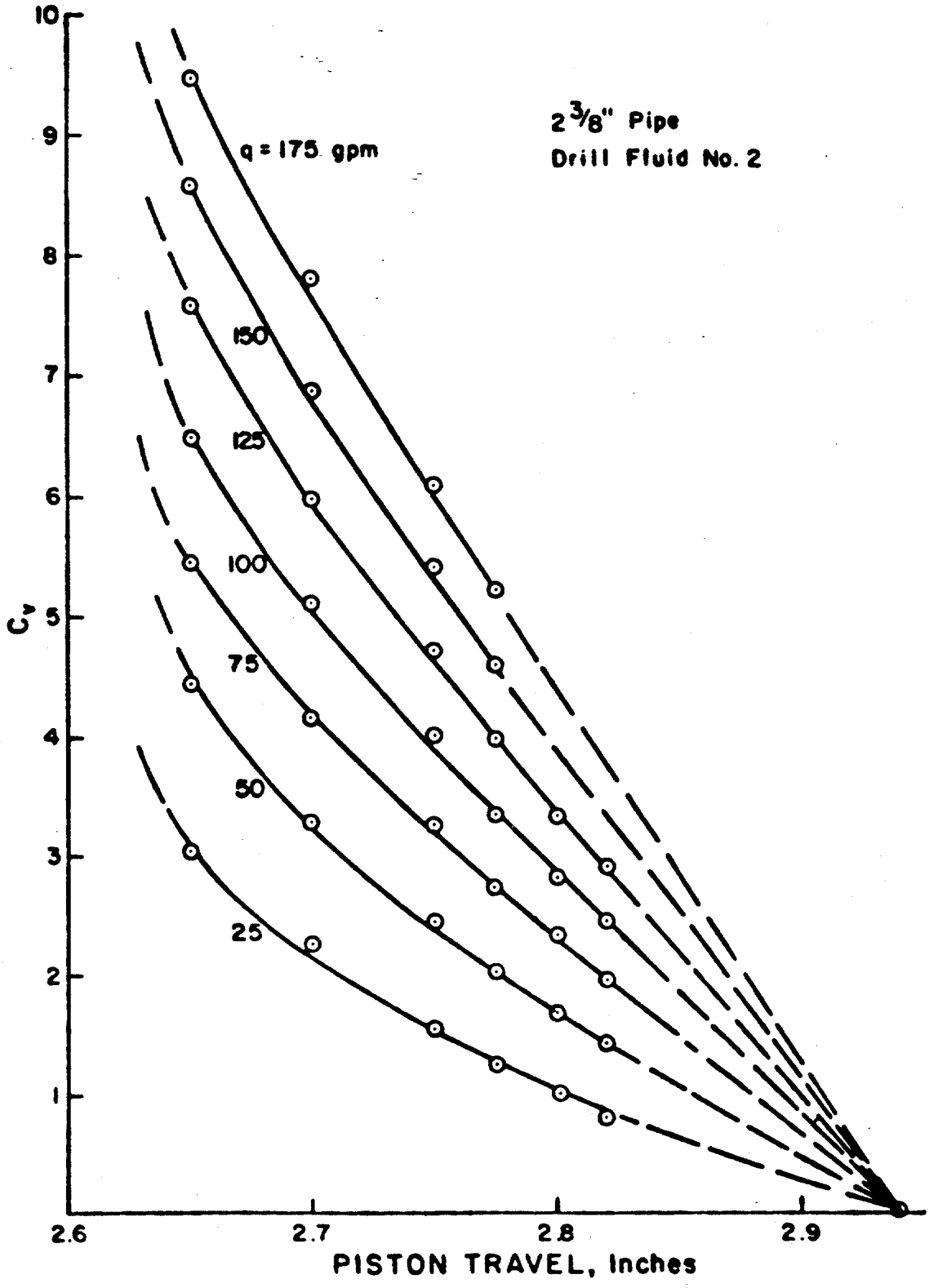

Figure 53 - Valve Coefficient For Spherical Preventer with Fluid 2 and Pipe Size 1

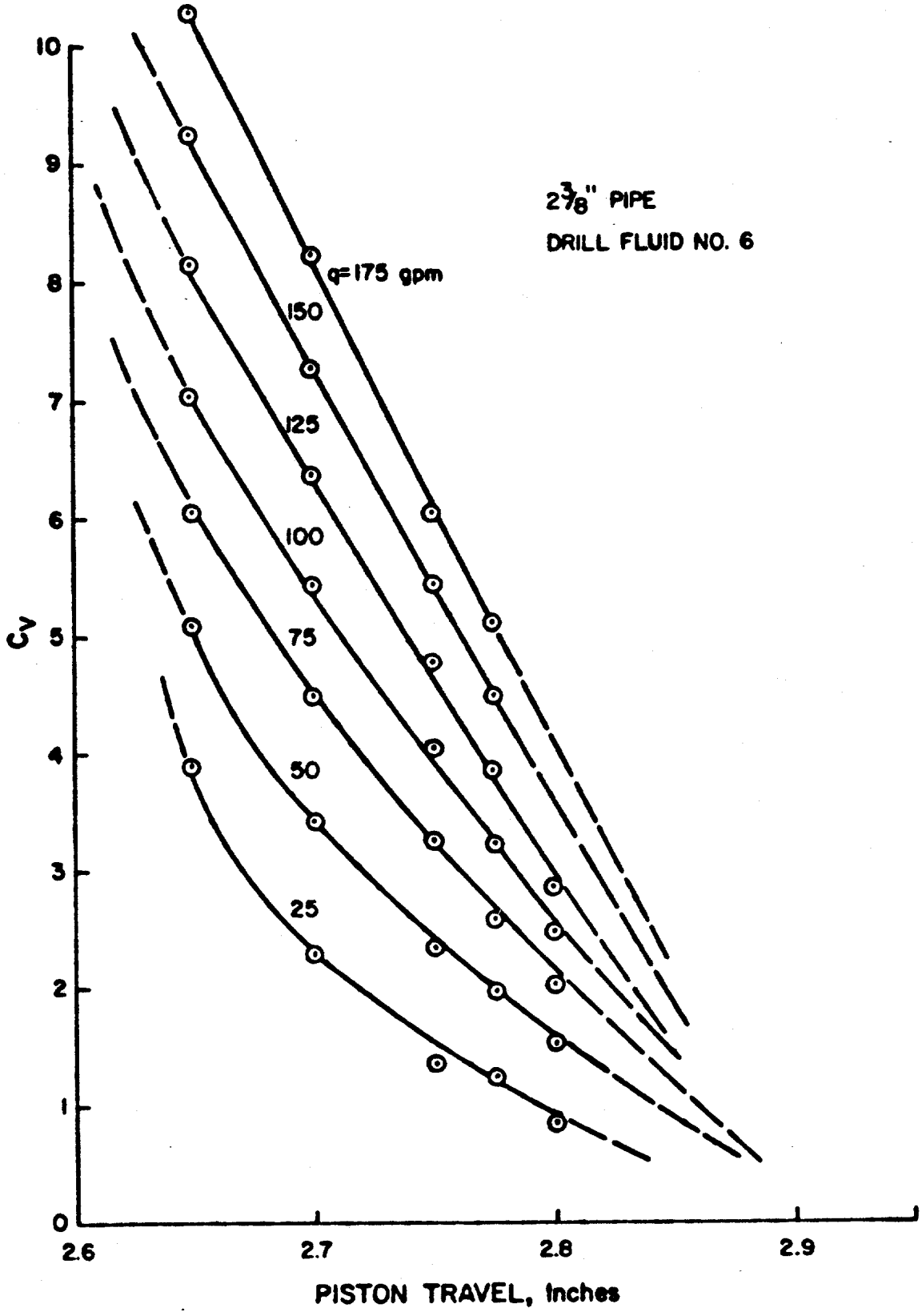

Figure 54 - Valve Coefficient For Spherical Preventer with Fluid 6 and Pipe Size 1

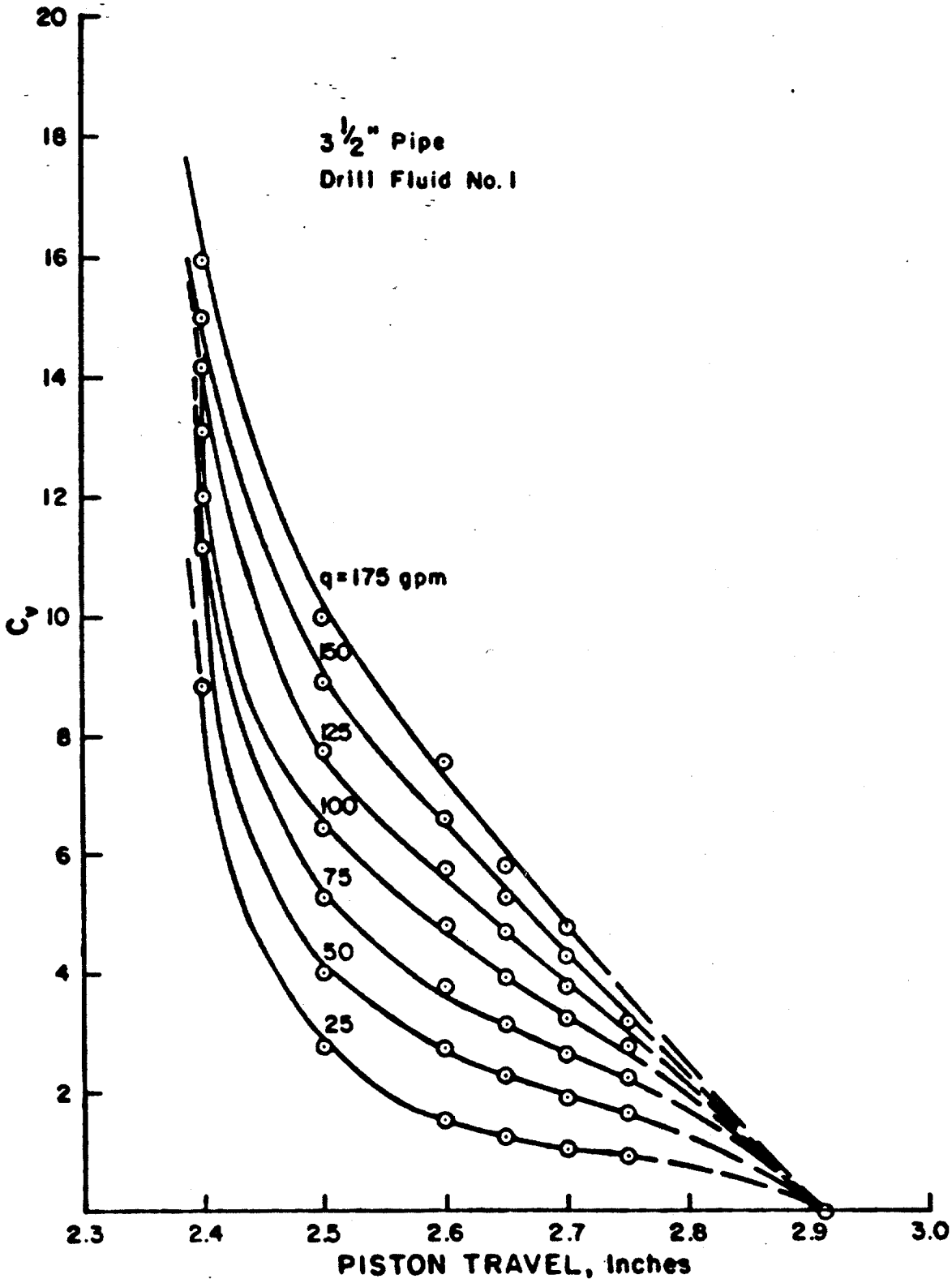

Figure 55 - Valve Coefficient For Spherical Preventer with Fluid 1 and Pipe Size 2

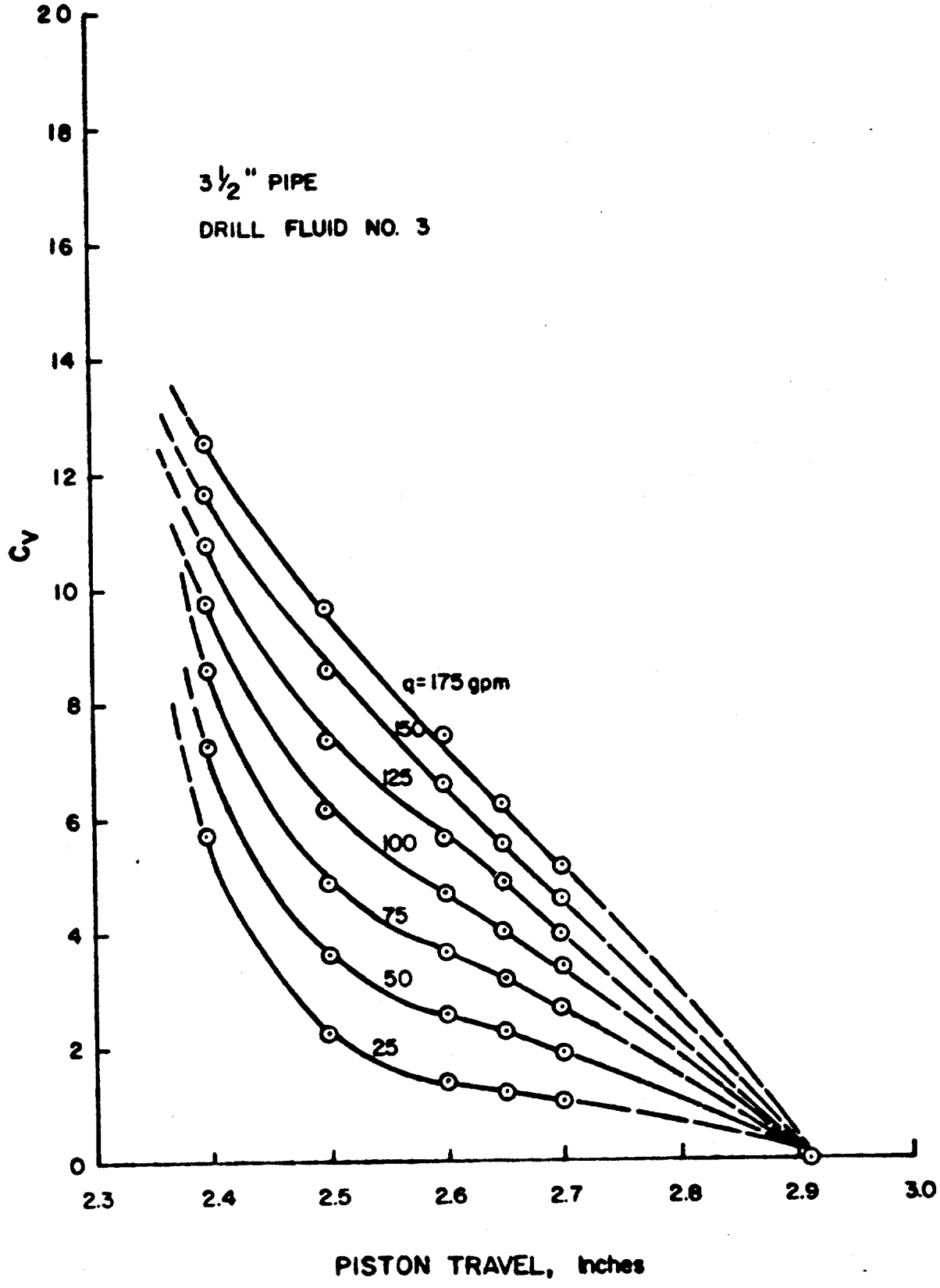

Figure 56 - Valve Coefficient For Spherical Preventer with Fluid 3 and Pipe Size 2

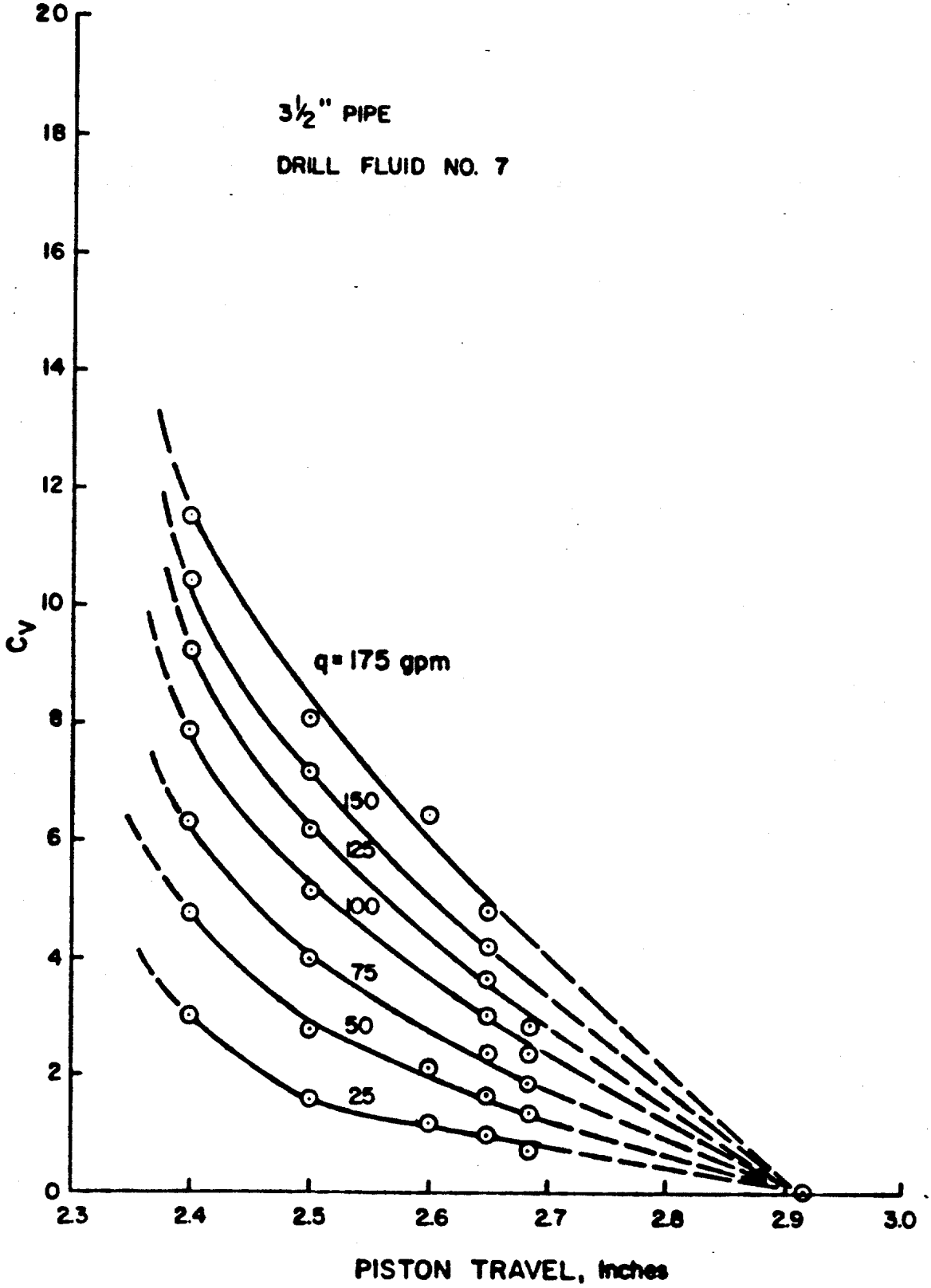

Figure 57 - Valve Coefficient For Spherical Preventer with Fluid 7 and Pipe Size 2

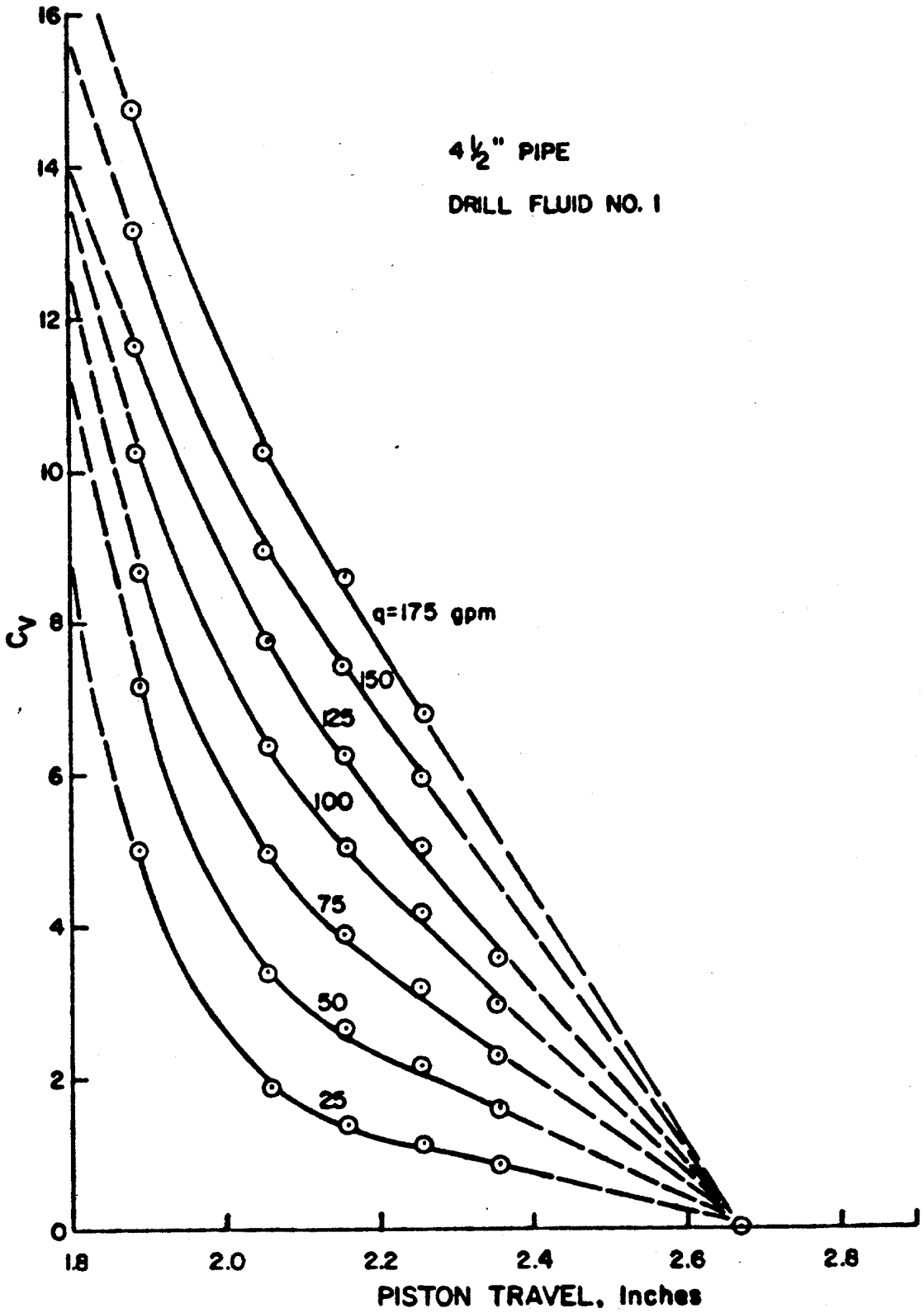

Figure 58 - Valve Coefficient For Spherical Preventer with Fluid 1 and Pipe Size 3

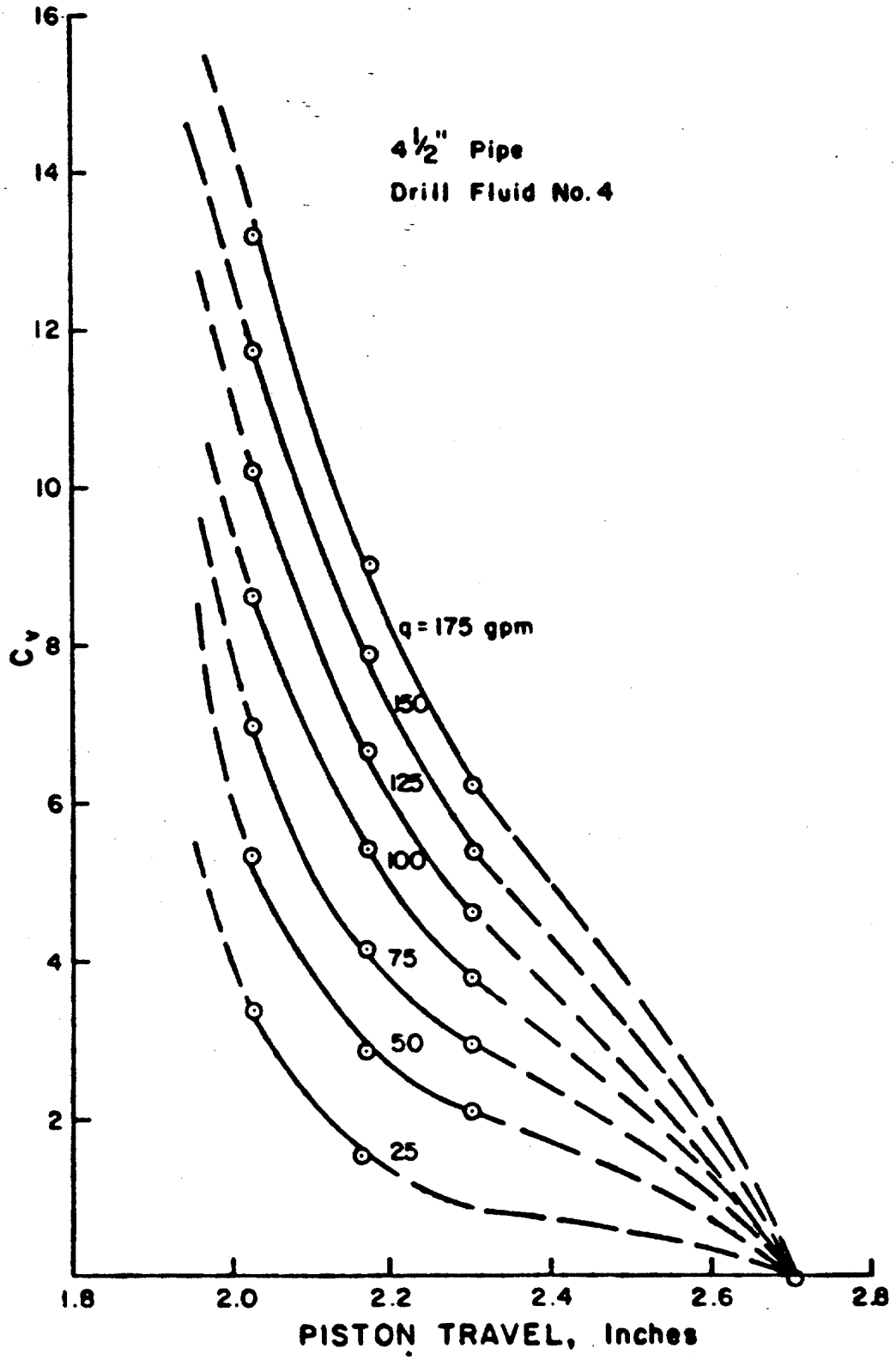

Figure 59 - Valve Coefficient For Spherical Preventer with Fluid 4 and Pipe Size 3

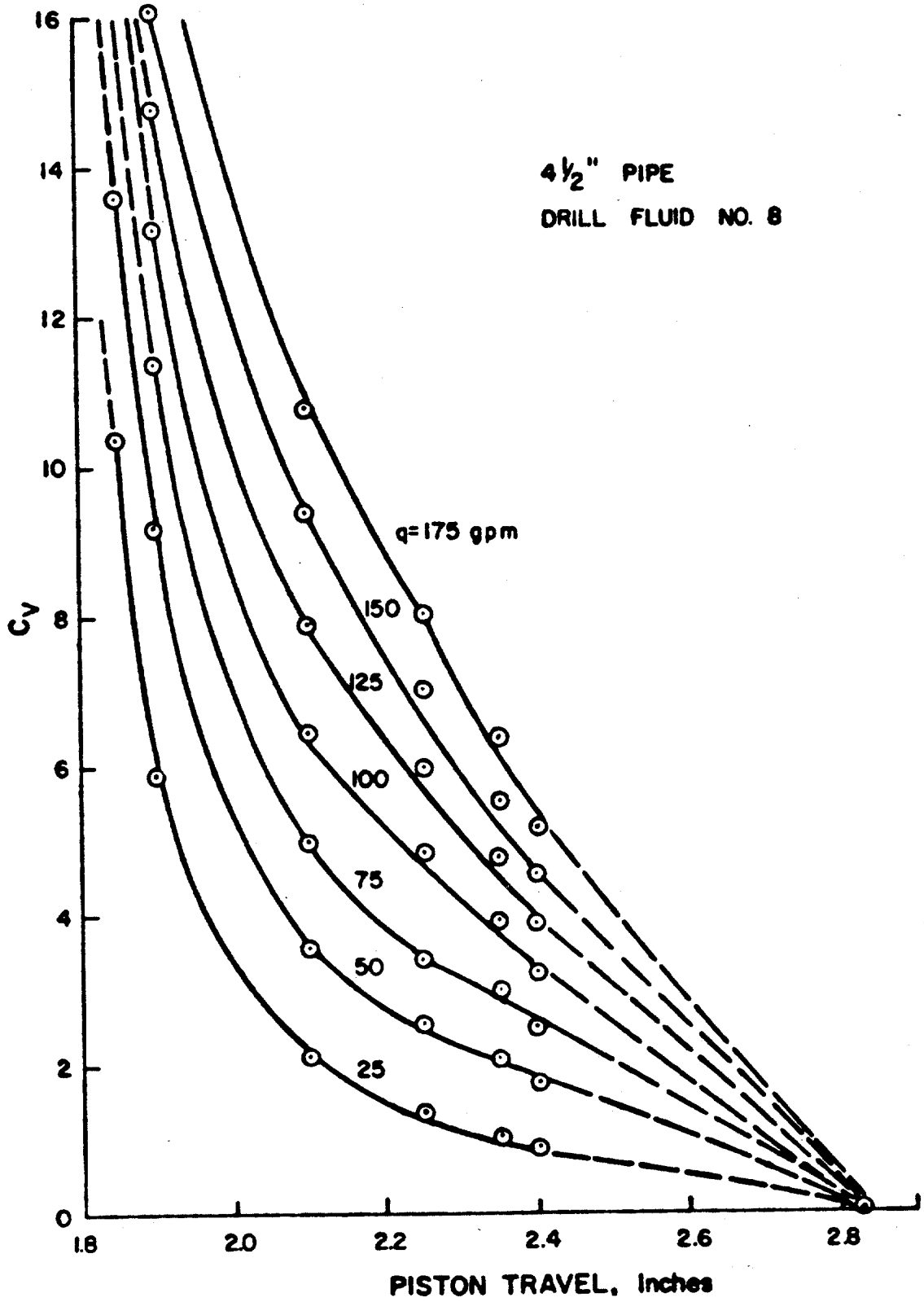

Figure 60 - Valve Coefficient For Spherical Preventer with Fluid 8 and Pipe Size 3

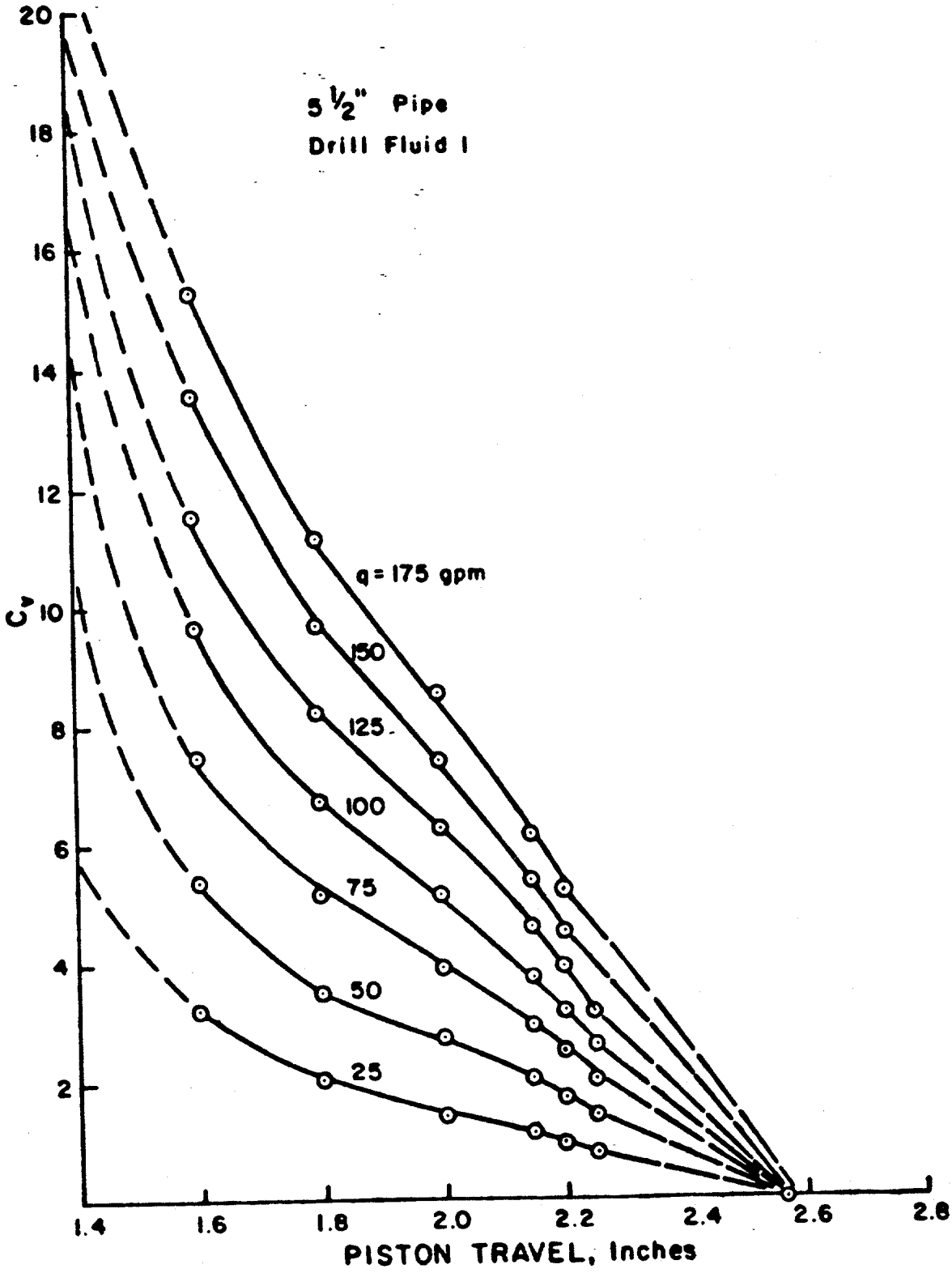

Figure 61 - Valve Coefficient For Spherical Preventer with Fluid 1 and Pipe Size 4

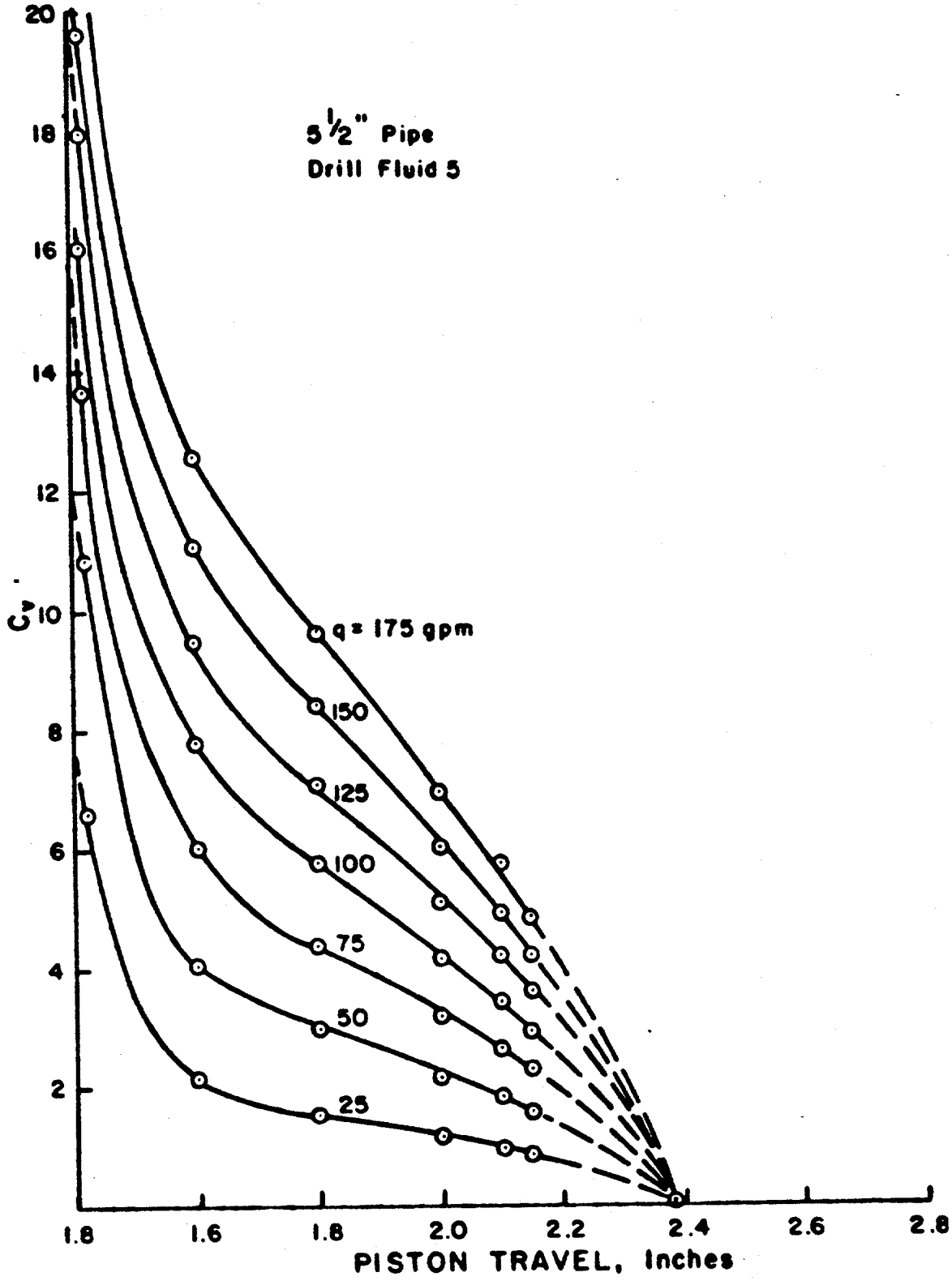

Figure 62 - Valve Coefficient For Spherical Preventer with Fluid 5 and Pipe Size 4

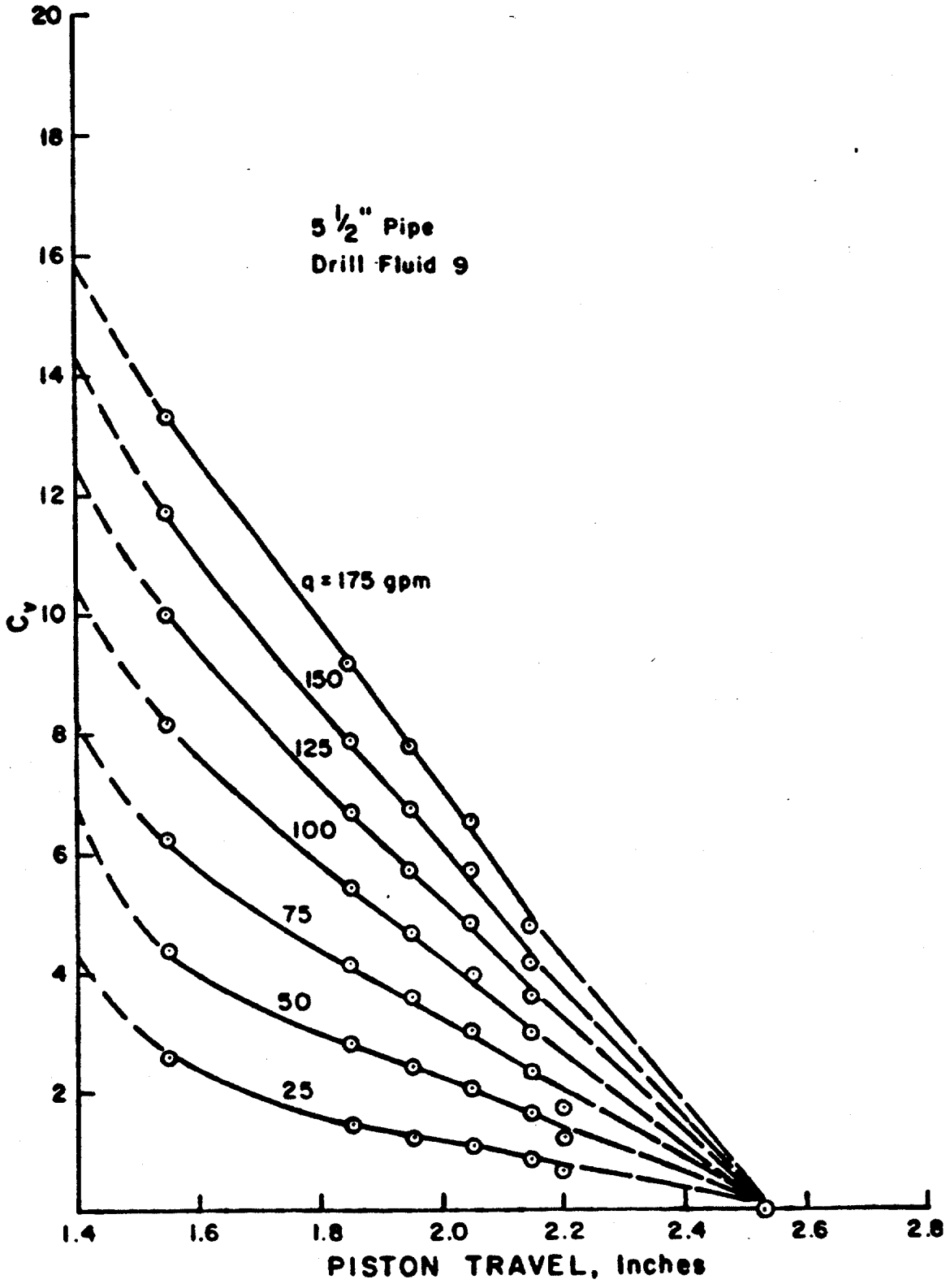

Figure 63 - Valve Coefficient For Spherical Preventer with Fluid 9 and Pipe Size 4

tion of the blowout preventer behavior during closure.

Some of the data obtained in this study seem to indicate that the viscosity of the fluid affects the pressure drop produced by a given flow rate through the blowout preventer. Figure 64 shows pressure drop data for flow through the annular preventer with 3-1/2 in. pipe in the hole. Three fluids of various viscosity are shown. The pressure drop is highest for the highest viscosity fluid and lowest for the lowest viscosity fluid. This seems to suggest that the pressure drop across the preventer is directly related to the viscosity of the fluid. Referring to Figure 65, however, which shows data for 2-3/8 in. pipe in the hole, no evidence is shown to indicate a relation between the fluid viscosity and the pressure drop characteristics of the blowout preventer. In fact pressure losses for the high viscosity mud (6) are lower than the low viscosity mud (2). Additional data for other geometries and viscosities shows similar results.

In light of the above evidence, the discrepancies between the results for various viscosity fluids can not be totally attributed to viscosity effects. Although viscosity may have a slight effect on the pressure drop characteristics it seems that the deformation and wear characteristics of the rubber element has a more dominant effect on the pressure drop across the blowout preventer. In other words, viscosity effects are relatively unimportant in comparison to the effects of the deformation behavior of the rubber element.

The effects of the annular geometry (pipe size in hole) on the closing characteristics of the blowout preventer are quite evident from Figure 66. The plot shows the piston travel required to achieve the initial restriction to flow and the total piston travel to complete closure around pipes ranging in diameter from 0 to 7 1/16 in., the bore diameter of the blowout preventer. Obviously the total travel of the piston to achieve full closure is less for the large diameter pipes. However, the plot also indicates that the intial pressure response occurs at a lower piston position for the larger diameter pipes than for the small diameter pipes. The initial response is produced sooner for larger pipe sizes, not only on the basis of actual piston travel, but also on the basis of the percentage of total piston travel. For instance, for closure on 3-3/8 in. pipe, the initial pressure response is

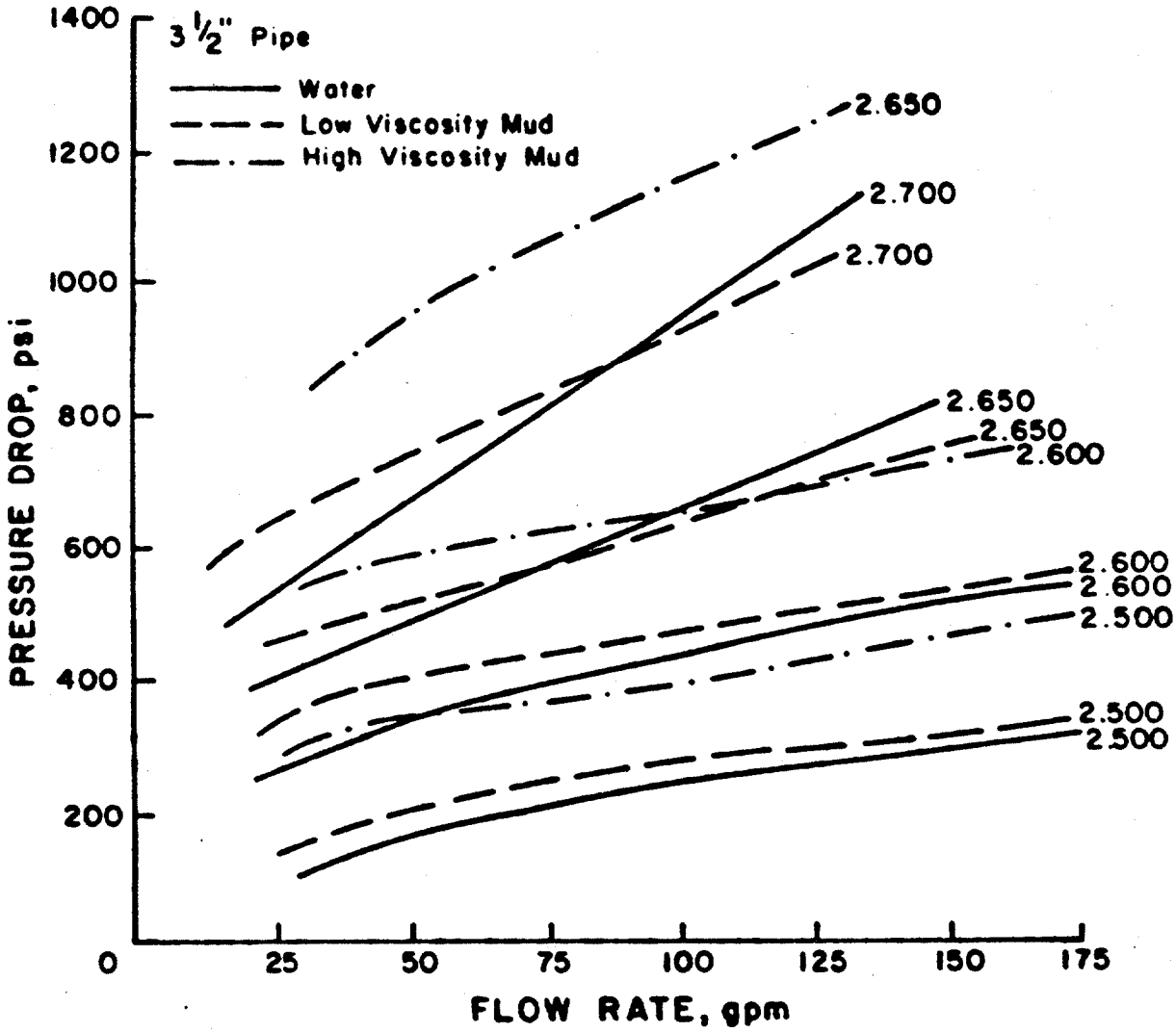

Figure 64 - Effect of Viscosity on Pressure Drop-Flow Rate Characteristics of Spherical Preventer for 3.5 in. Pipe

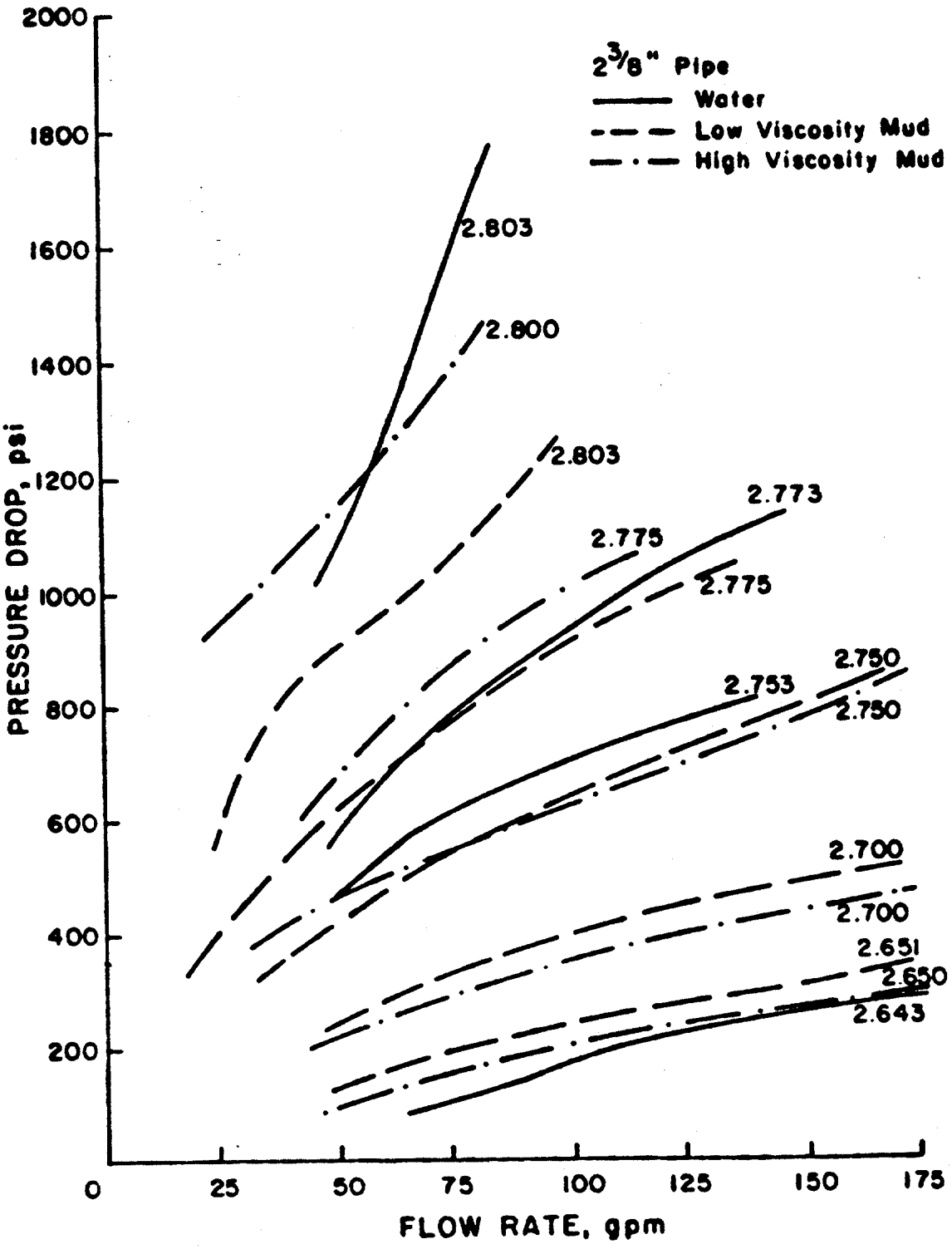

Figure 65 - Effect of Viscosity on Pressure Drop-Flow Rate Characteristics of Spherical Preventer for 2.375 in. Pipe

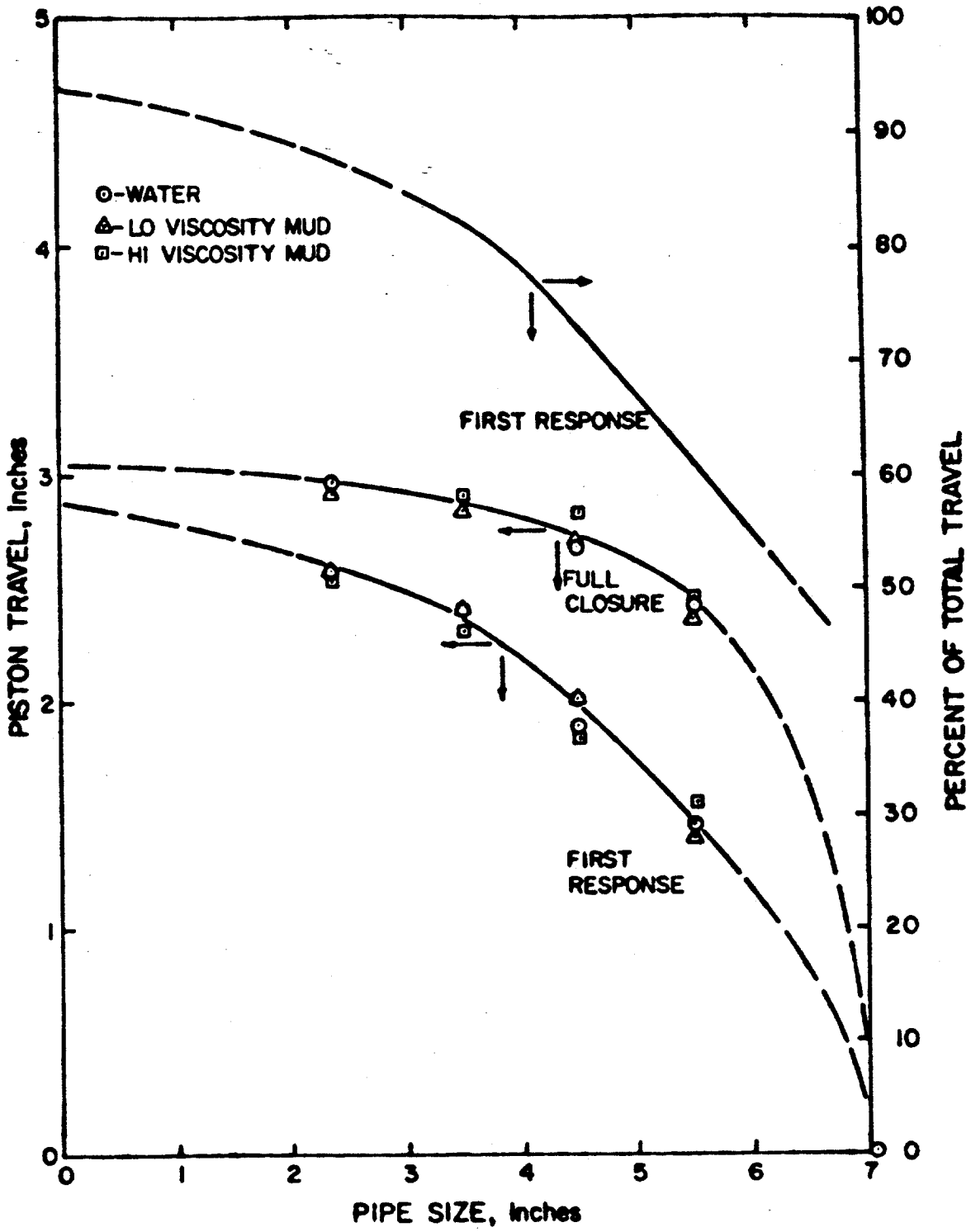

Figure 66 - Effect of Pipe Size on The Closing Characteristics of Spherical Preventer

shown at a piston position of 2.60 in. or 88% of the total piston travel from full open to full closed. For a 4-1/2 in. pipe the initial pressure response occurs at a piston position of 2.00 in., or 73% of the total piston travel.

Finally, the travel of the piston from the position where the initial pressure response occurs to the full closed position is, in general, longer for large diameters. For instance the "effective" travel is only 0.4 in. for 2-3/8 in. pipe while for a 4-1/2 in. pipe the "effective" travel is 0.8 in. This response suggests a more gradual closure is achieved with large diameter pipes in the hole than with small diameter pipes.

4.5 Experimental Study of Drilling Choke Flow Characteristics

An experimental study was also undertaken to determine the flow characteristics during closure of several drilling chokes of varying designs. These studies were needed to adequately define the boundary conditions for the pressure surge analysis for a soft shut-in procedure. Drilling chokes manufactured by Cameron, Swaco, NL Shaffer and Patterson were included in the study. These chokes were used because they were made available by the manufacturer for testing. The choking elements used in these chokes were felt to be representative of the designs that are currently available.

Pressure drop measurements were made for steady-state flow through each of the drilling chokes for varying flow rates, drilling fluids, and degrees of closure. The drilling fluid was allowed to circulate through the flow system for at least an hour prior to making any pressure measurements to allow the rheological properties of the drilling fluid to stabilize. During this time, pump factors were checked for a wide range of pump pressures by means of two 10 bbl metering tanks.

Experimental results for the drilling chokes studied are shown in Figures 67-72. In addition to conducting tests with water, several unweighted clay-water muds of varying viscosities, and two weighted clay-water muds were used. During the tests, choke position was measured mechanically at the choke and then converted to a fraction of full open as approximately shown by the choke position indicator in the remote control panel. The results indicated that the frictional area

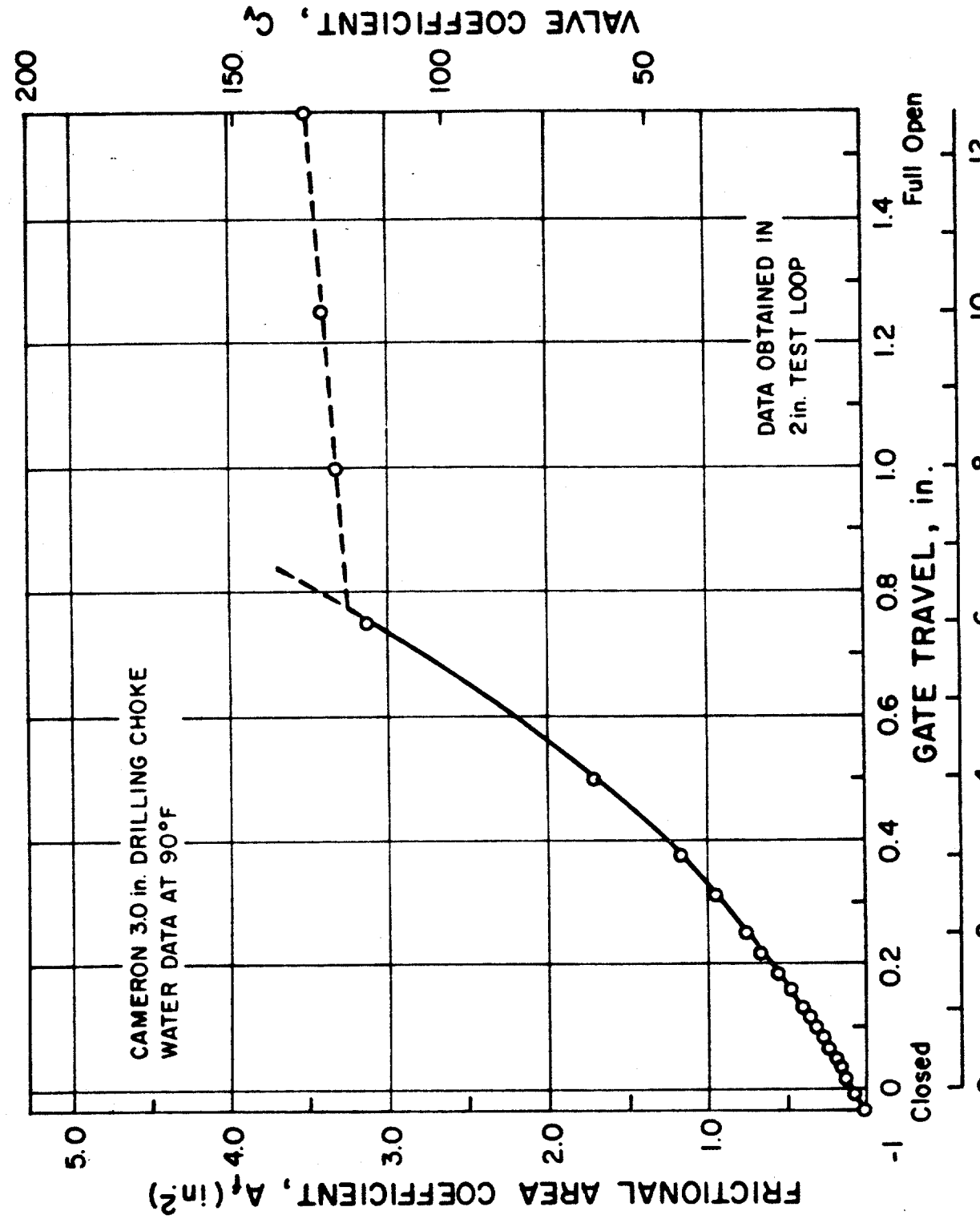

FIGURE 69. MEASUREMENT OF FRICTIONAL AREA COEFFICIENTS FOR 3.0 in. DRILLING CHOKE (Positive Shut-off Choke Element Design)

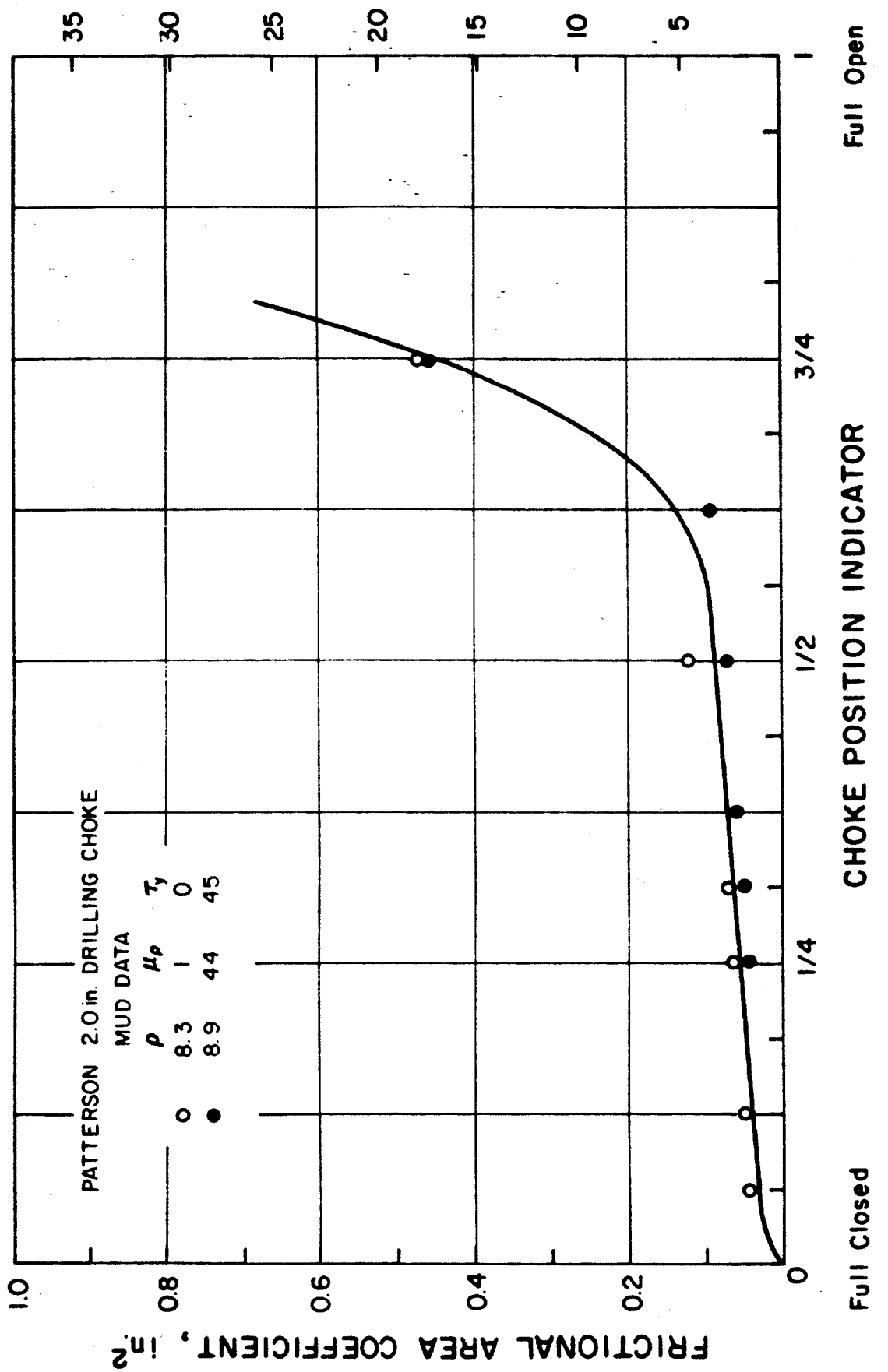

FIGURE 72. MEASURED FRICTIONAL AREA COEFFICIENTS FOR PATTERSON DRILLING CHOKE

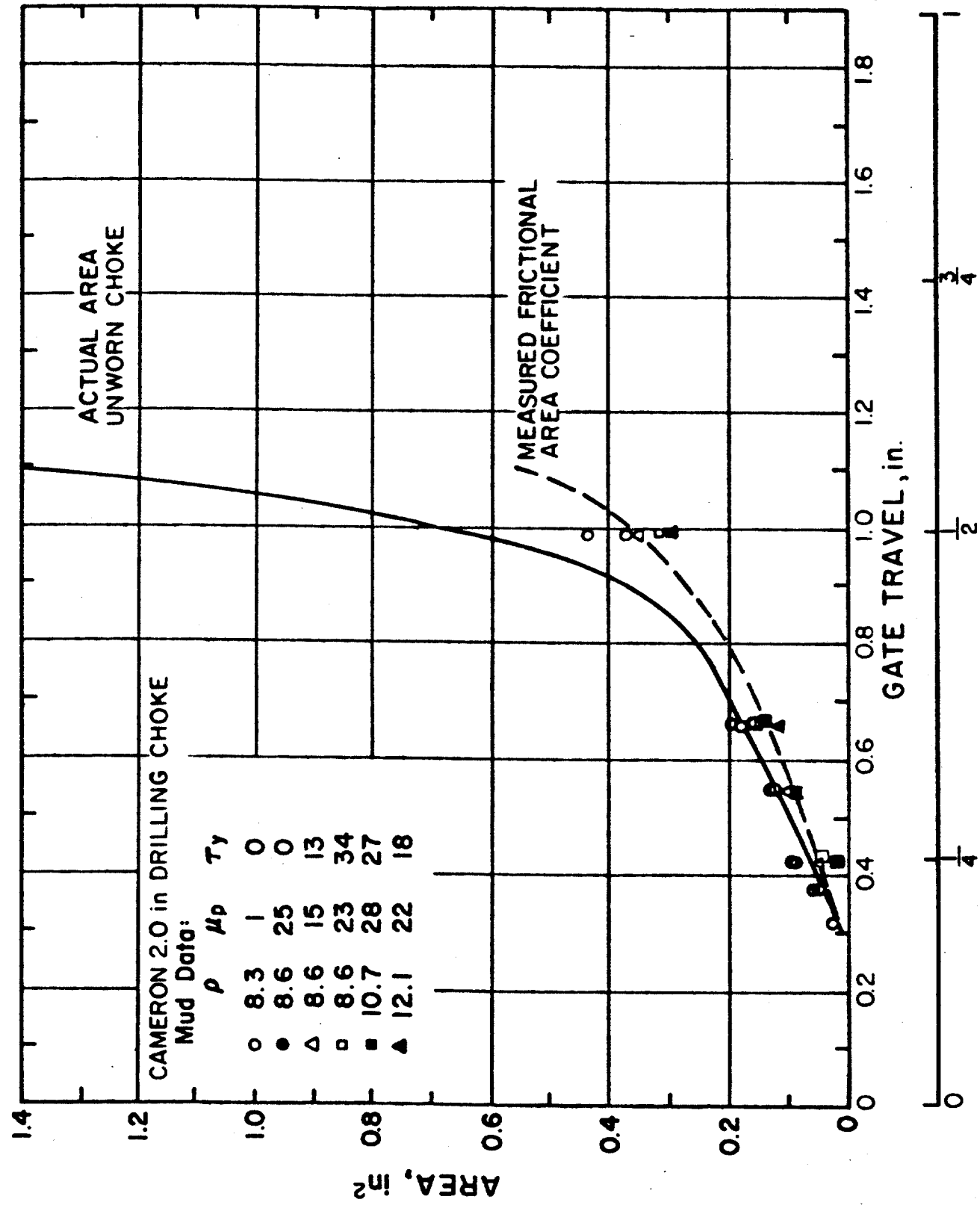

FIGURE 67. MEASURED FRICTIONAL AREA COEFFICIENTS FOR 2.0 in. CAMERON DRILLING CHOKE (Non-Positive Shut-off Choke Element Design)

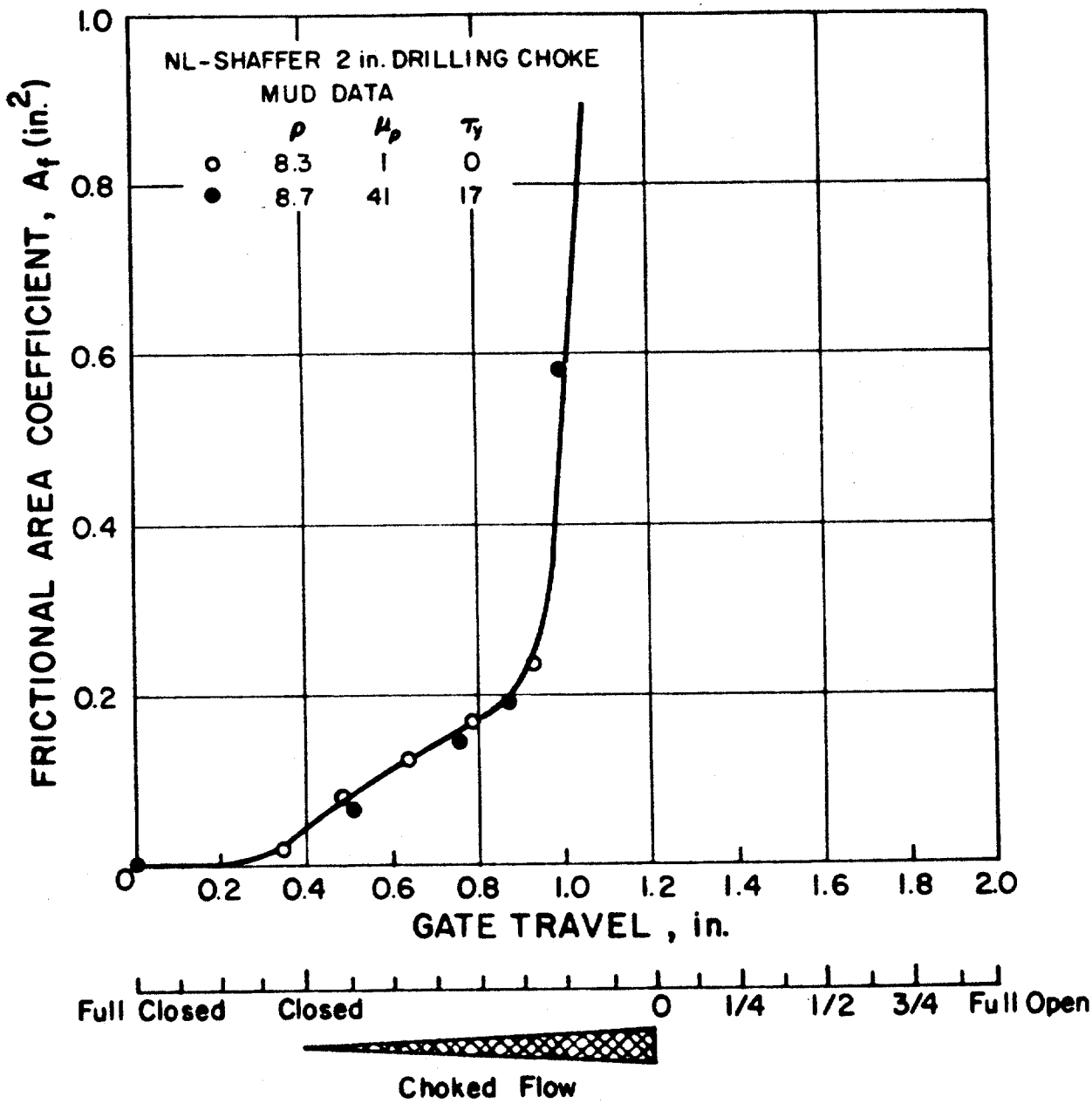

FIGURE 71. MEASURED FRICTIONAL AREA COEFFICIENTS FOR NL-SHAFFER DRILLING CHOKE

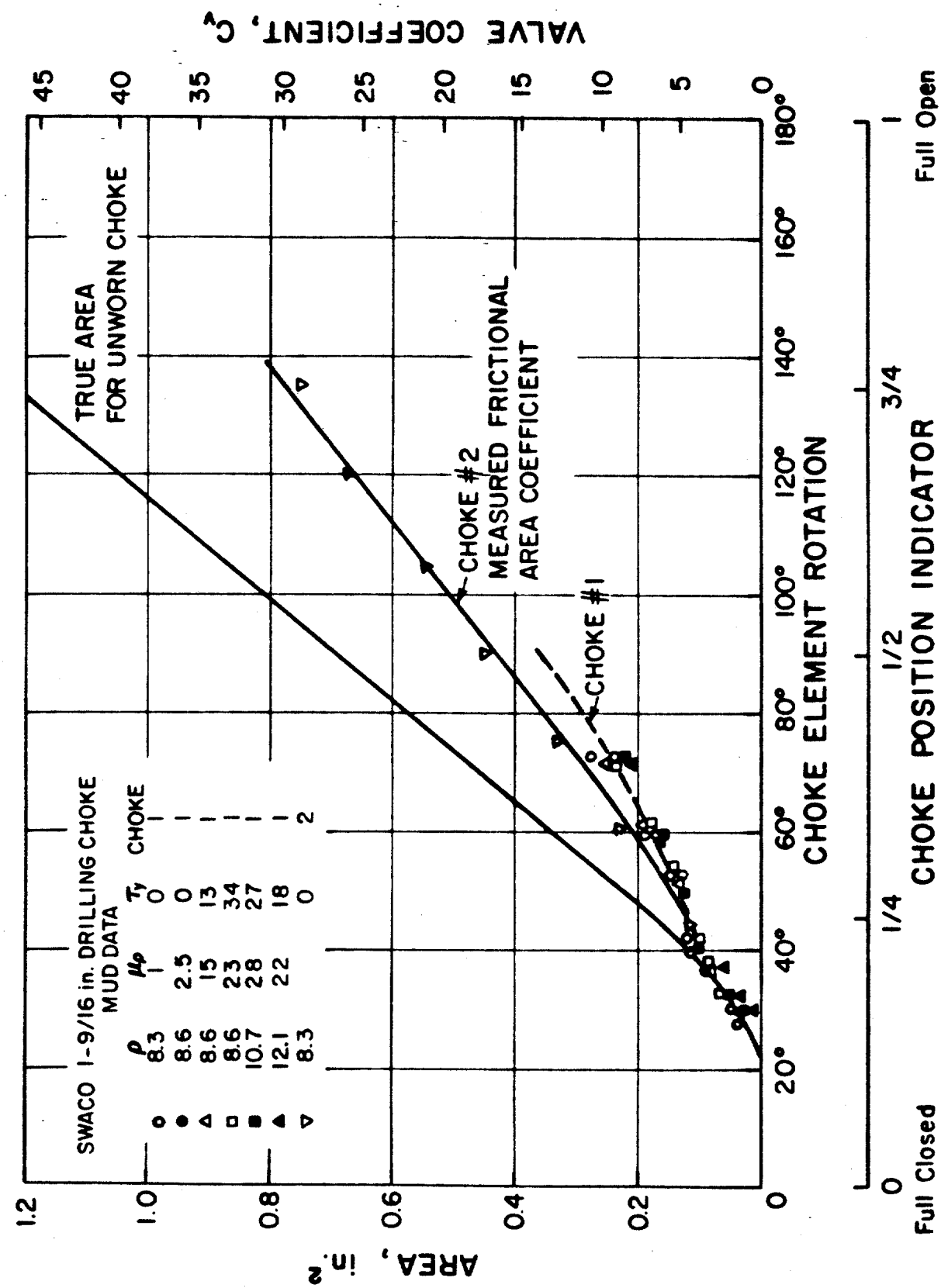

FIGURE 70. MEASURED FRICTIONAL AREA COEFFICIENTS FOR SWACO DRILLING CHOKE

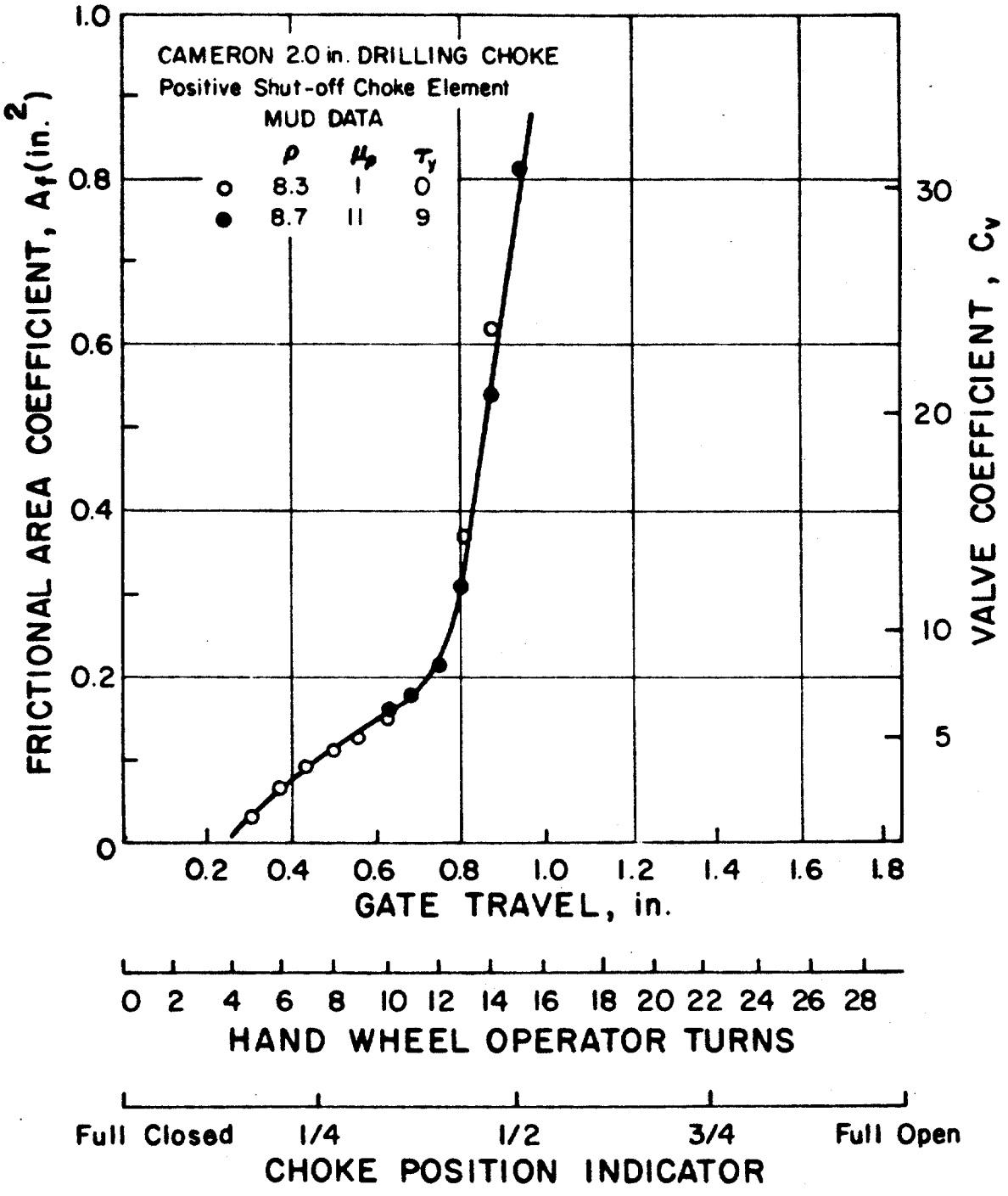

FIGURE 68. MEASUREMENT OF FRICTIONAL AREA COEFFICIENTS FOR 2.0 in. CAMERON DRILLING CHOKE (Positive Shut-off Choke Element Design)

coefficient for drilling chokes was relatively insensitive to mud viscosity over the usual range of field conditions. This was especially true for the sharp edge choke design used by Swaco. A single frictional area curve, which was independent of mud viscosity, was felt to be sufficient for computer simulation studies of well-control operations. As the choke elements wear, a shift to the left in the curve would be expected.

It was also noted that for the flow rate ranges commonly used in well control operations, only a very small portion of the total choke adjustment range is used. A large maximum choke opening is desirable due to concern about the ability to unplug a choke which has become blocked by cuttings in the mud. However, relatively small choke openings are required to impose a significant pressure on the well at typical kill speeds.

4.6 PRESSURE SURGES DURING SHUT-IN

A computer program for estimating pressure surges during shut-in was developed using the previously discussed method of characteristics. In order to adapt the technique to an annulus, it was necessary to develop an equation for the velocity of an annular pressure wave. The equations previously presented in this chapter were for a circular pipe. The impulse-momentum equation and the conservation of mass principle were employed to obtain the following equation:

$$a = \frac{24.886}{\sqrt{C_\ell P_{avg}\left(1 + \frac{C_1}{C_\ell E} A + (1-H_\ell)\frac{C_g}{C_\ell}\right)}} \qquad (4.26)$$

where

$$A = \frac{\frac{d_2^3}{t_2} + \frac{d_1^3}{t_1}}{\frac{d_2^2}{t_2} - \frac{d_1^2}{t_1}} \qquad (4.27)$$

d_2 = the diameter of the casing, in.

t_2 = the wall thickness of the casing, in.
d_1 = the diameter of the drill pipe, in.
t_1 = the wall thickness of the casing, in.
C = the compressibility of the mud, psi^{-1}
E = Young's modulus of elasticity, psi
P = the mud density, lb/gal
H_ℓ = the non-gaseous volume fraction of the mud or liquid holdup and where subscripts avg., ℓ., and g denote average, liquid, and gas respectively.

Turbulent viscous flow through the well annulus was determined using the Edebrook equation for computing fanning friction factors. A pipe roughness of zero was assumed and Reynolds numbers were computed using plastic viscosity. An equivalent diameter was chosen such that use of this equivalent diameter in a laminar pipe flow equation would given the same computed pressure gradient as the laminar slot flow approximation of laminar annular flow. For any coresistent set of metric or english units, these equations are defined by

$$\Delta p_f = \left(\frac{fL}{d_e}\right) \frac{2p\bar{u}^2}{gc} \tag{4.28}$$

$$\frac{1}{\sqrt{f}} = -4\log\left(\frac{1.255}{N_R \sqrt{f}}\right) \tag{4.29}$$

$$N_R = \left(\frac{p\bar{u}d}{\mu_p}\right) \tag{4.30}$$

$$d_e = 0.816\ (d_2 - d_1) \tag{4.31}$$

Pressure surges during well shut-in were calculated for various assumed deep water drilling situations. Typical results will be summarized for the case of the well conditions previously described in Figure 21 and Table 9 for the Discoverer Seven Seas drillship, and the Congo Well example.

The surge pressure which should be tolerated during shut-in should be of the order of magnitude of the pressure tolerance expected during the remainder of the well control operation. It has been found from other phases of this study that even an experienced choke operator cannot circulate a kick to the surface without allowing at least a 75 psi variation in bottom hole pressure above the desired bottom hole pressure. Thus it seems reasonable that if no more than a 75 psi pressure surge is allowed during shut-in, the shut-in procedure will not reduce the chance for a successful well control operation by increasing the chance for hydrofracture.

Some proponents of the soft shut-in procedure are concerned about pressure surge induced failure of surface equipment as well as causing hydrofracture. Stretched flange bolts on BOP stacks have been attributed to pressure surges during hard shut-ins by some field personnel attending the LSU BOP School. This of course would require surge pressures at least of the order of several thousand psi.

Shown in Figure 73 for the Congo Well Example are the effects of kick influx rate and effective closing time on the peak surge pressures produced above the initial static shut-in pressure. The top line shown is for instantaneous closure and was computed using the elastic model equations discussed in Section 4.1. The three lines below the top line were determined using the computer model for effective preventer closing times of 1, 3.5, and 7 seconds, respectively. Note that to obtain a 75 psi pressure surge above the static shut-in casing pressure, a kick influx rate above 10 bbl/min would be required for this example. Note also that to obtain surge pressures great enough to damage surface equipment, kick influx rates of the order of 1000 bbl/min would be required.

Shown in Figure 74 for the Congo Well Example are computer simulations of pressure surge with time caused by closing the BOP with a 10 bbl/min kick influx rate. The upper plot shows the pressure surge above the static shut-in pressure at the sea floor while the lower plot provides this same information at the casing seat. Zero time is when the annular BOP has closed to the point at which a significant flow restriction first occurs. The four curves shown correspond to effective closing times of 1 sec, 2 sec, 3.5 sec, and 7 sec, respectively. Note

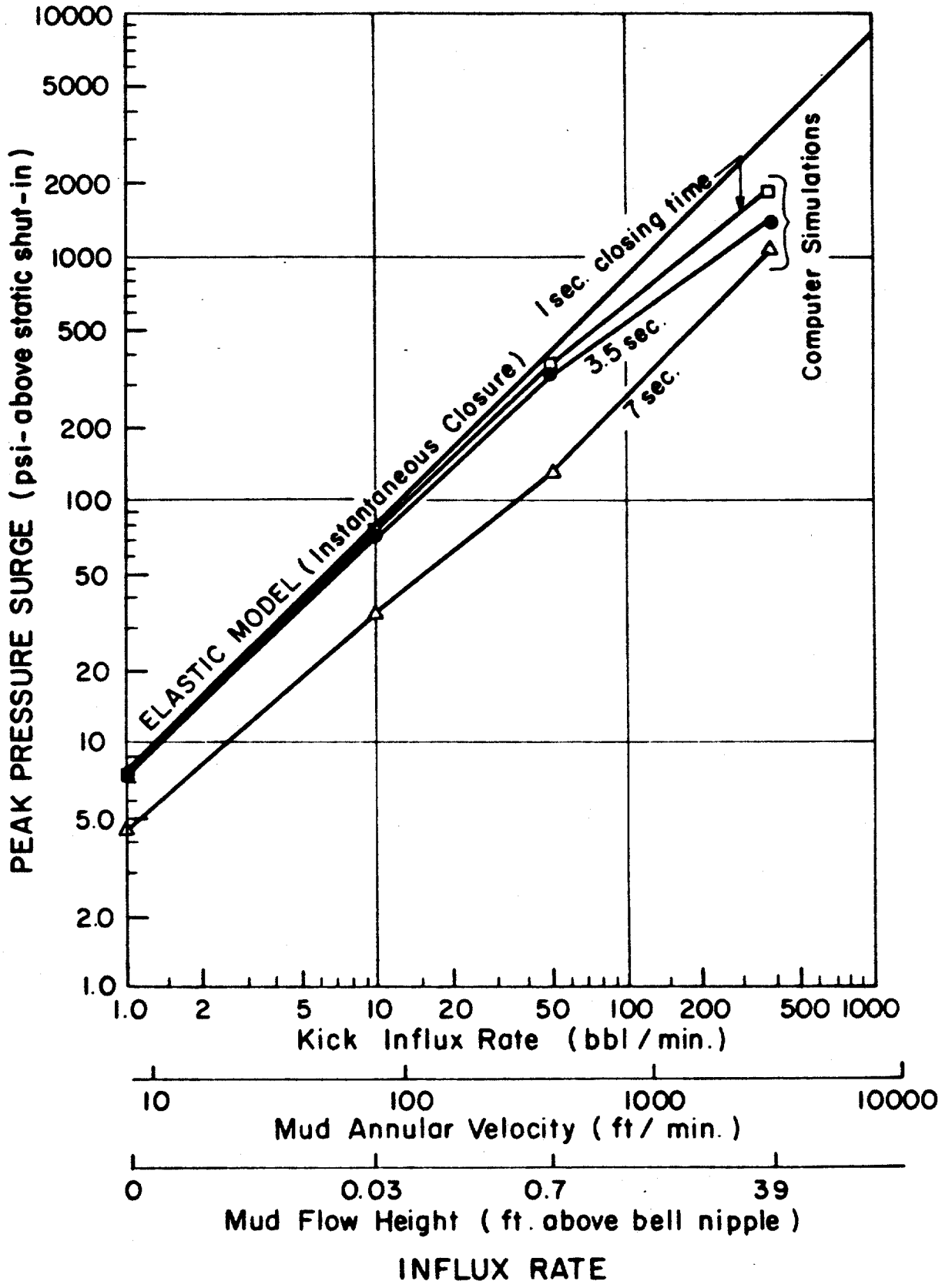

FIGURE 73. PEAK PRESSURE SURGES FOR CONGO WELL EXAMPLE

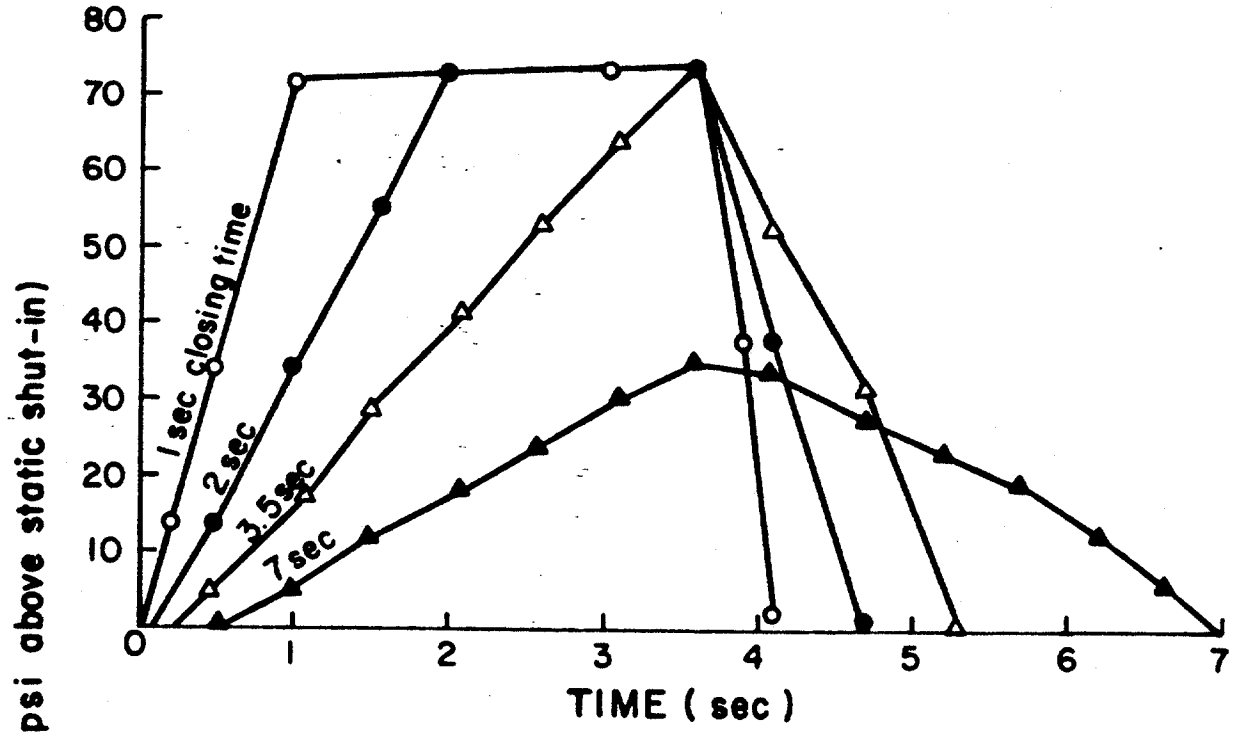

(a) At Sea Floor

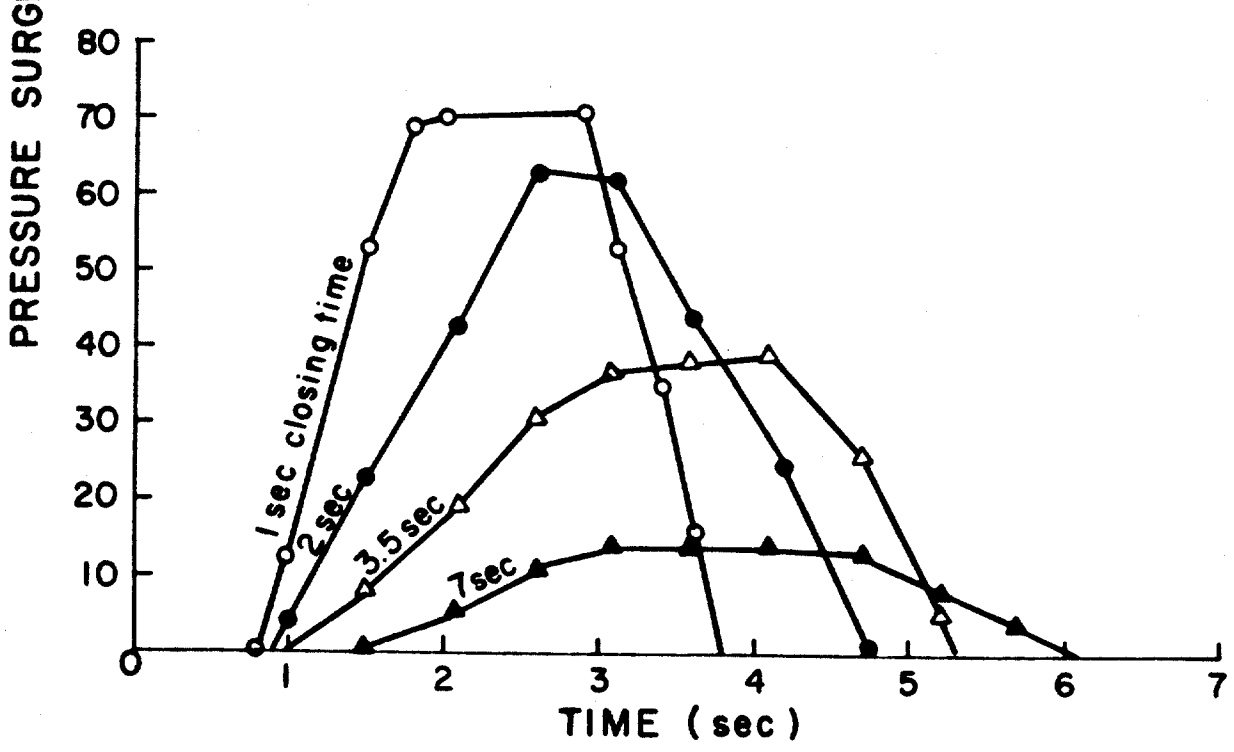

(a) At Casing Seat

FIGURE 74. COMPUTER SIMULATION OF PRESSURE SURGE WITH TIME USING 10bbl/min. INFLUX RATE FOR CONGO WELL EXAMPLE

that for this example, the time of druation of the excess pressure is on the order of a few seconds. Note, also, that for closing times of less than 2 seconds, the peak pressure increase experienced at the casing seat is near the peak pressure increase experienced at the sea floor.

Since the soft shut-in procedure takes longer to implement than the hard shut-in procedure, the size of the initial kick taken will be greater for the soft shut-in procedure. The relationship between kick influx rate and the additional shut-in casing pressure resulting from a soft shut-in procedure is shown in Figure 75 for various additional closing times needed to implement the soft shut-in procedure. As with Figures 73 and 74, this relationship was determined using the data for the Congo Well Example. Note that for a 10 bbl/min kick influx rate, the initial static casing pressure would be about 31 psi higher if an additional 60 sec were required to implement the soft shut-in procedure instead of the hard shut-in procedure. When the kick was pumped to the casing seat, this difference would be slightly greater due to the effect of gas expansion. However, the pressure surge on shut-in for the hard shut-in procedure would be more than twice as large as the pressure increase due to the resulting larger initial gain.

Proper implementation of a soft shut-in procedure requires an accurate knowledge of the BOP system response time after the "closing" button is pressed on the BOP control panel. This information is required to insure that the choke is not closed before the annular preventer achieves complete closure. The time required to close a completely open choke is often on the order of 30 sec-60 sec.

Proponents of the soft shut-in procedure have also expressed concern about pressure surges occurring in the choke line and choke manifold when the HCR value is opened after closing the BOP, especially if the choke line is only partially filled with liquid. Shown in Figure 76 are computed peak pressure surges in a single choke line for the Congo Well Example. Shown on this same graph is also a line representing frictional pressure loss in the choke line. The flow velocity of mud in a partially filled choke line will tend to be limited by choke line friction when the HCR valve is opened. Using this plot it can be shown that a shut-in casing pressure of 440 psi above hydrostatic (Congo Well Example) could cause a flow rate in the choke line of about 6.7 bbl/min.

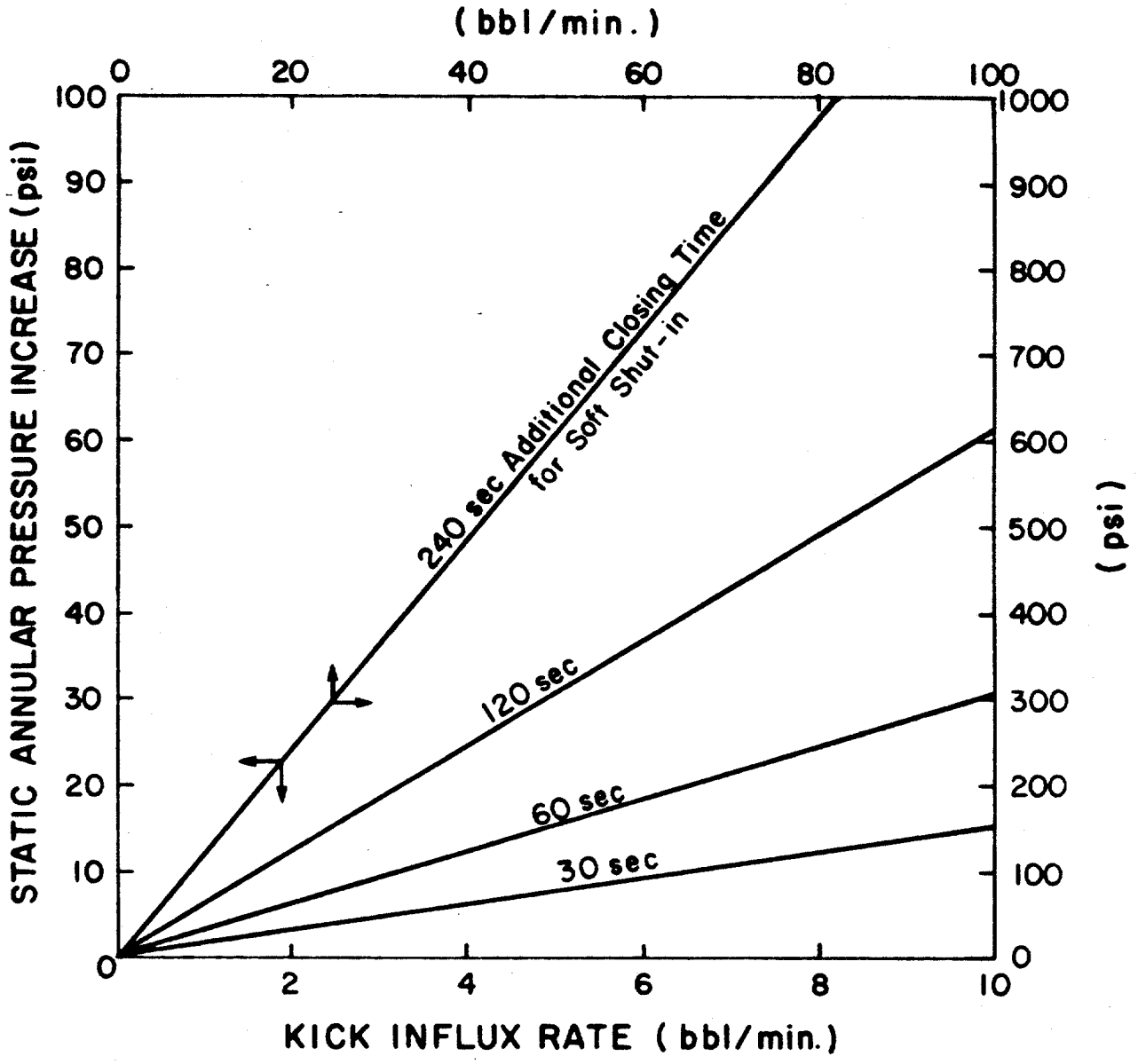

Figure 76. Static Annular Pressure Increase For Soft Shut-In over Hard Shut-In For Congo Well Example

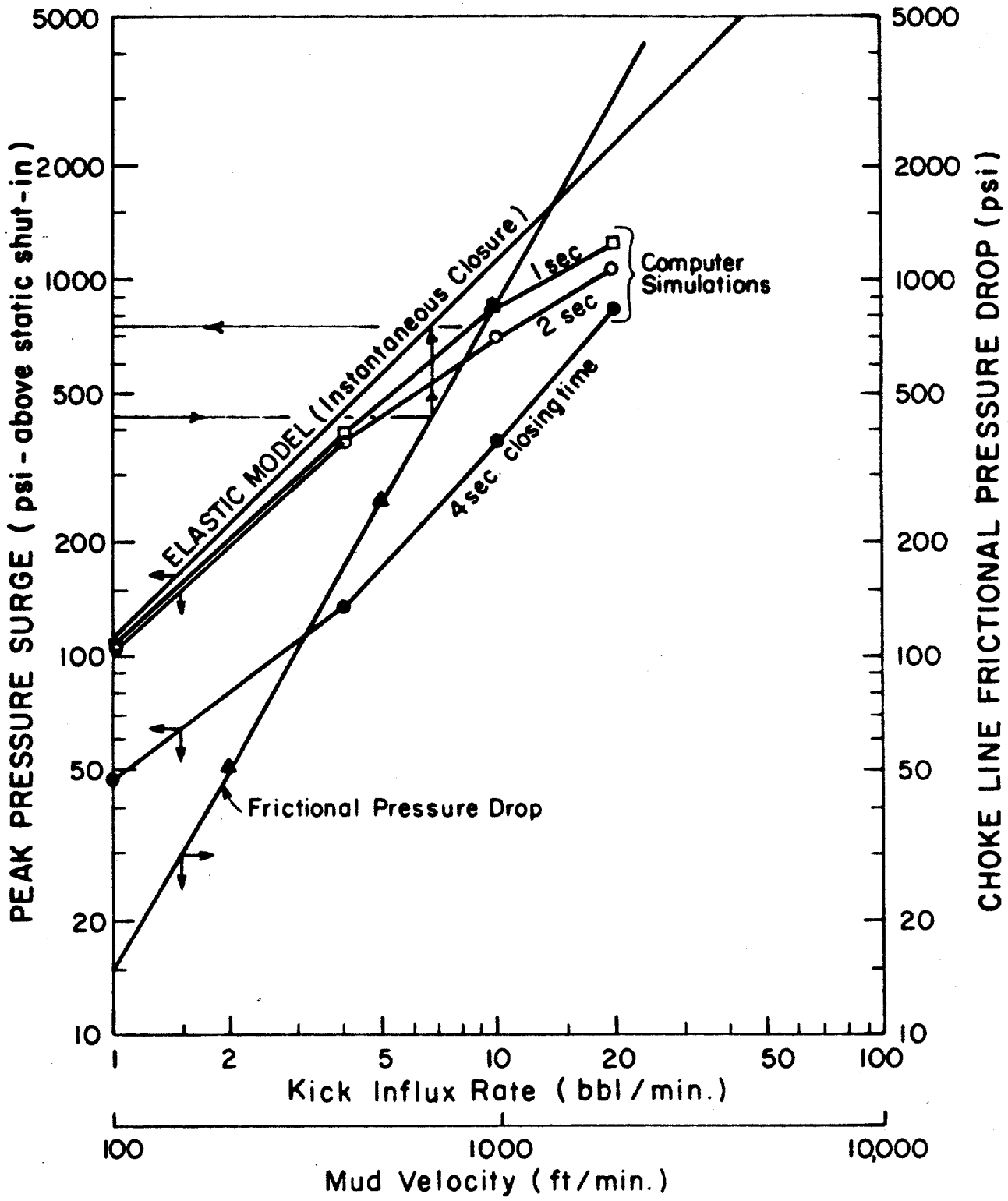

Figure 77. Peak Pressure Surve vs. Influx Rate In The Choke Line For the Congo Well Example

If this flow was then stopped instantaneously upon choke line fill-up, a surge pressure of 775 psi above the static shut-in pressure of 440 psi would be experienced in the choke manifold. Of course, the build-up of air pressure in the line would partially dampen this pressure surge.

For many of the chokes studied experimentally, the effective portion of the choke position was only a small part of the total choke position range. The effective closing time of these chokes if operated at maximum speed could be on the order of a few seconds. It can be seen from Figure 77 that larger pressure surges are possible in the small diameter choke line at low flow rates because of the greater velocity of the mud at lower diameters. However, in general these higher pressure surges will not be transmitted down the casing to the casing seat.

The results of this study indicate that the soft shut-in procedure does result in the lowest possible peak pressure at the casing seat. However, the advantages are slight for kick influx rates resulting in an annular mud velocity below 80 ft/min. For a typical deepwater drilling situation with 13 3/8 in. surface casing set, this would correspond to a kick influx rate of about 10 bbl/min.

CHAPTER 5

PROCEDURES FOR HANDLING UPWARD MIGRATION OF GAS KICKS

After a well has been shut-in due to the presence of a kick, there may be a considerable lapse of time before normal well control procedures can be implemented. These delays may be caused by (1) time to increase the mud density to the desired kill weight or (2) mechanical problems with drilling equipment or high pressure flow conduits. If the formation fluids are predominantly gas, the large density difference between the gas and the drilling fluid will cause the gas to migrate up the hole during this shut-in period. As the gas migrates upward, wellbore pressures continually increase until such time that the pressure opposite the weakest formation exceeds that formation's fracture pressure, resulting in the breakdown of that formation and possibly an underground blowout. If the formation fluid does not contain a gaseous phase, upward migration of the fluid is generally not significant and kick removal is relatively simple. This experimental study deals exclusively with gas kicks.

Under normal conditions, the excessive pressures resulting from upward gas migration in a shut-in well can be alleviated by allowing the gas to expand through periodic bleeding of mud at the surface. The expansion is best controlled by maintaining the drill pipe pressure at a value slightly in excess of its initial shut-in value through the use of an adjustable surface choke. This maintains the pressure held against the "kicking" formation above its pore pressure and additional fluids cannot enter the well. As the drill pipe pressure tends to increase due to the upward gas migration, mud is bled from the annulus using the surface choke, giving the kick room to expand in the annulus, and thereby reducing the kick's pressure.

However, certain situations arise when a meaningful drill pipe pressure is not available. These situations can arise if: (1) the drill bit is plugged, shutting off pressure communication between the drill pipe and formation; (2) the drill string has failed, allowing

communication between fluids in the drill string and annulus; and (3) the drill string is off-bottom, causing the drill pipe and casing pressures to read the same until the kick has migrated above the bit. In addition, the drill string could be out of the hole entirely. For kicks taken with the drill string off-bottom, the pipe could be stripped back to the bottom of the hole if proper precautions are taken, but this is time-consuming and significant gas migration will occur during the stripping operations.

To cope with the above situations where a meaningful drill pipe pressure is not available, volumetric methods of well control have been suggested by various authors[31, 32, 33] as an alternate method to handle upward gas migration. Volumetric methods are based on observed changes in casing pressure and metered volumes of drilling fluid bled from the well. The method is based primarily on theoretical considerations and largely without documented experimental verification. Simplifying assumptions generally made in developing the methods include: (1) the kick remains as a continuous slug occupying the entire annular cross-section, (2) the gas density is negligible, and (3) once gas reaches the surface, no gas is to be produced.

In this study, various proposed methods for safely handling the upward migration of gas kicks in a shut-in well were evaluated experimentally, using two 6000 ft. wells containing downhole pressure recording devices. One well was used to study the flow geometry present when a surface BOP stack is used and the second well was used to model the flow geometry present for a subsea BOP stack in 3000 ft. of water. To simulate shut-in conditions during a gas kick, nitrogen gas was used. The various techniques evaluated included methods involving the periodic release of mud from the annulus while monitoring changes in the surface drill pipe pressure, or changes in the casing pressure and volume of mud being released.

5.1 Methods For Handling Upward Gas Migration

The main requirement of any well-control technique is to maintain the bottom hole pressure constant and slightly above formation pore-pressure. This is most easily accomplished if the drill string is intact and near bottom, there are no obstructions in the drill string,

and, essentially, no kick fluids have displaced mud from inside the drill string. For this situation, bottom hole pressure differs from the observed shut-in drill pipe pressure primarily by the hydrostatic head of the mud in the drill string. Additional pressure gradients can be held as a result of the gel strength of the mud, but normally these can be neglected. Thus, if a reliable drill pipe pressure is available during the shut-in period after a kick has been taken, drill pipe pressure is allowed to increase only to a value slightly greater than its initial shut-in value. Then the drill pipe pressure is maintained at this value by bleeding small increments of mud from the well using a hand-adjustable surface choke (Fig. 77a). It is important to stress that only small volumes (e.g., about 0.5 bbl) should be bled rather than bleeding until the drill pipe pressure falls to the desired value. This is due to the amount of time required for pressure changes, due to choke manipulation, to be felt by the drill pipe pressure gauge. If excessive bleeding occurs, additional influx of formation fluid into the well may result.

5.1.1 Volumetric Methods

If a meaningful drill pipe pressure is not available, changes in bottom-hole pressure must be determined from observed changes in shut-in casing pressure and pit gain. The basis for this determination is illustrated in Fig. 78 and is discussed by Rehm[33]. Changes in bottom hole pressure $\Delta\rho_{bh}$, can result from both changes in surface casing pressure, ΔP_c, and/or changes in the hydrostatic pressure of the annular mud, Δp_h:

$$\Delta p_{bh} = \Delta p_c + \Delta p_h \tag{5.1}$$

Equation (5.1) assumes pressure variations due to the hydrostatic pressure of the gas phase, movement of the gas phase through the mud, and mud gellation are all negligible. Therefore, hydrostatic pressure changes on the annulus (Δp_h) are due only to the loss of mud from the annulus during gas expansion and are given by

$$\Delta\rho_h = 0.052\ \rho\ \Delta h_A$$

$$= 0.052\ \rho\ \frac{\Delta V}{C_A} \tag{5.2}$$

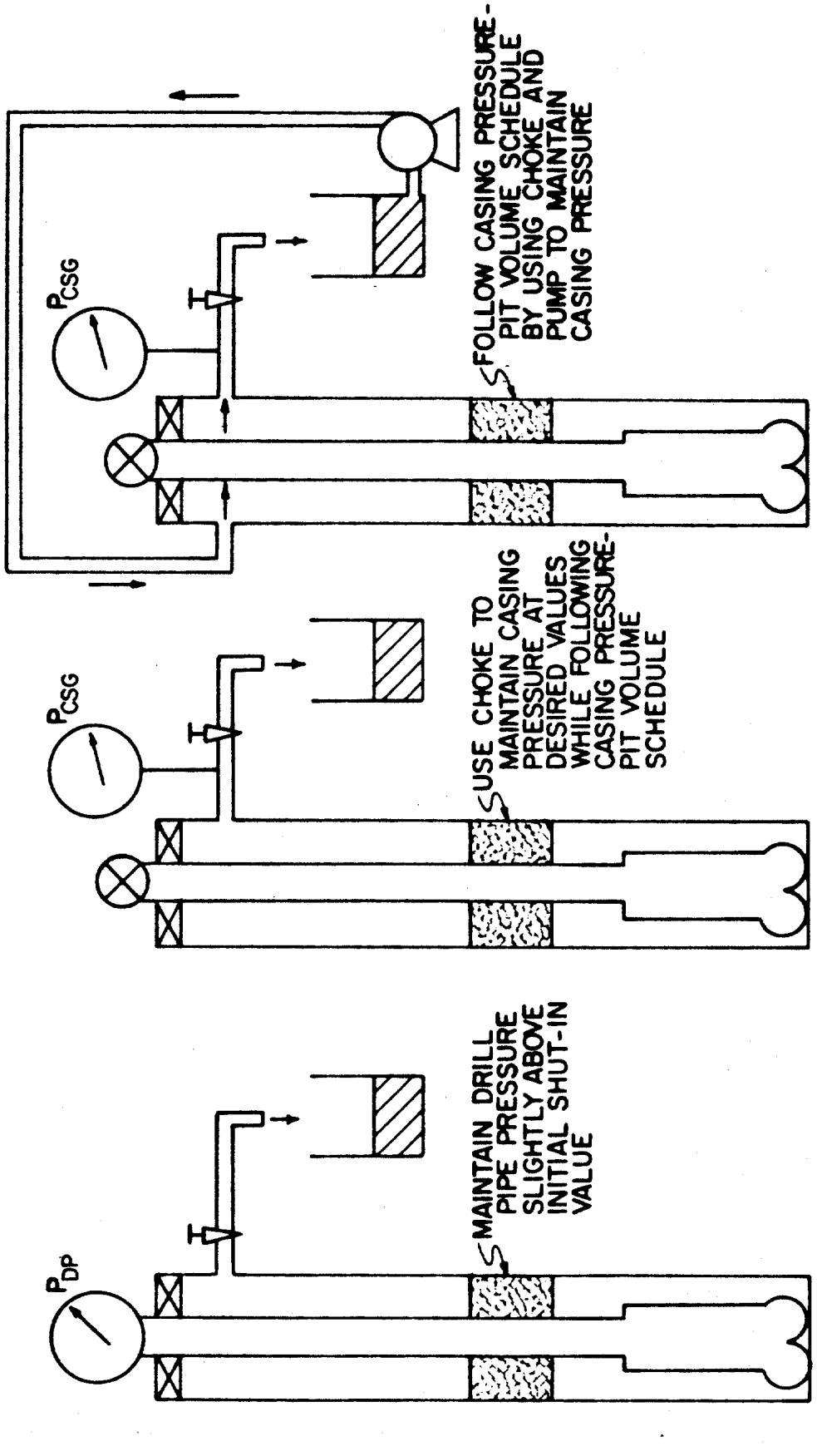

FIGURE 77. PROPOSED METHODS FOR SAFE HANDLING OF GAS KICK MIGRATION IN A SHUT-IN WELL

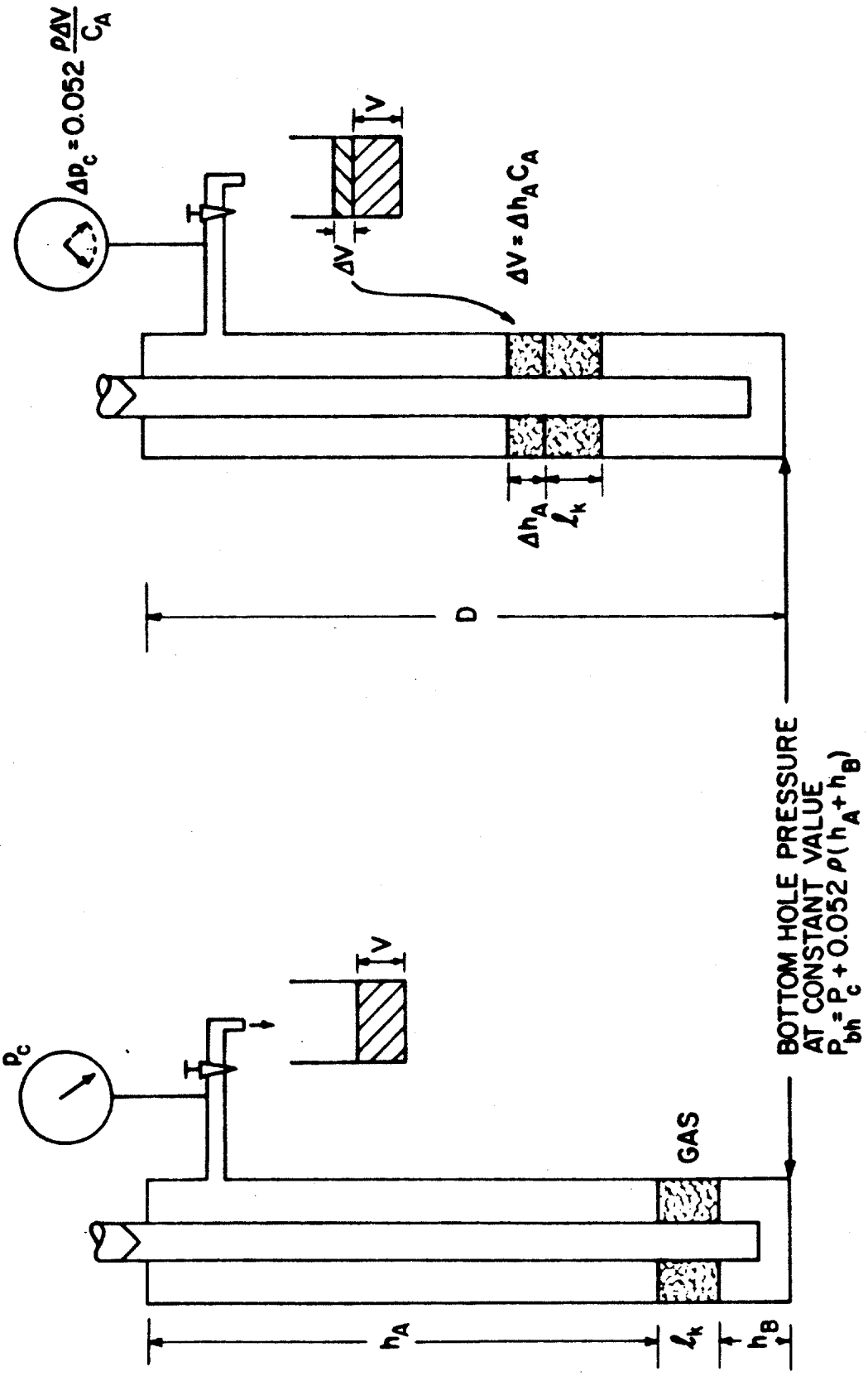

FIGURE 78. THEORETICAL BASIS FOR VOLUMETRIC METHODS

where ρ is the mud density in lb/gal, Δh_A is the change in height of the annular mud column, ΔV is the change in gas volume as determined by surface pit volume measurements in bbls, and C_A is the annular capacity in the vicinity of the gas kick in bbl/ft.

In the static volumetric methods, excessive well pressures are avoided by periodically bleeding mud from the surface choke (Figure 77b) in such a manner as to follow a predetermined schedule of casing pressure and pit gain. The first step is to allow the casing pressure to increase by a selected safety margin (e.g., 100 psi) above its initial shut-in value to allow a margin of error while manipulating the choke. Then casing pressure is allowed to increase by a convenient pressure increment and maintained at this value until a volume of mud, whose hydrostatic pressure in the annulus would equal the pressure increment, is bled from the well. For a pressure increment of 50 psi the mud volume, given by Equation (5.2), is

$$\Delta V = \frac{\Delta p_h C_A}{0.052\rho} = \frac{50\ C_A}{0.052\rho} = 962\ \frac{C_A}{\rho}$$

After this volume of mud is bled at constant casing pressure, the casing pressure is again allowed to increase by the selected pressure increment before bleeding any additional mud. By repeating this cycle as often as is necessary the gas can migrate to the surface as a nearly constant bottom hole pressure. An example schedule of casing pressure and pit gain illustrating this technique is shown in Figure 79.

After gas reaches the surface and the casing pressure stabilizes, an extension of the volumetric method, sometimes referred to as a "top kill" procedure, can be used to remove much of the gas kick from the upper portion of the well. With this technique a metered volume of mud is pumped into the casing until the casing pressure rises by a convenient pressure increment, e.g., 50 psi. After allowing some time for this mud to fall down the well annulus and clear of the choke line, gas is bled from the choke until the pressure falls by an amount equal to the selected pressure increment plus the hydrostatic pressure equivalent of the volume of mud injected (Eq. 5.2). This cycle can be repeated as often as desired to remove most of the gas from the well and reduce the

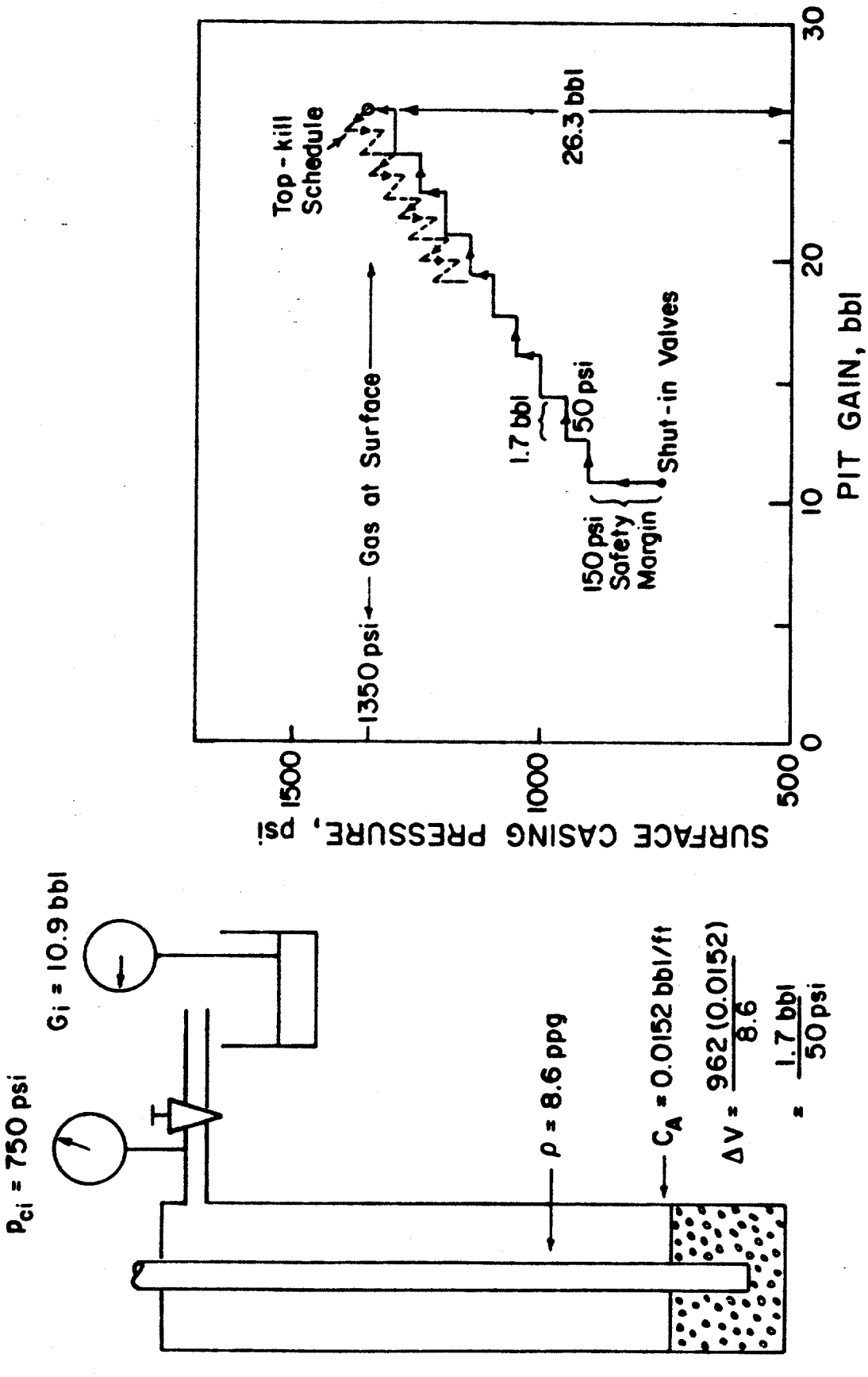

FIGURE 79. THEORETICAL CALCULATIONS FOR EXAMPLE OF STATIC VOLUMETRIC METHOD

shut-in casing pressure. Top kill procedures are sometimes employed to reduce well pressure prior to stripping or snubbing pipe into a shut-in well.

A significant limitation of the static volumetric method is that it can be easily applied only in a well having a relatively uniform annular capacity from the depth of the gas kick to the surface. Changes in annular capacity can cause changes in the effective length of the kick and thus, changes in the hydrostatic pressure of the annular mud. Two-phase mixing of the gas and mud, and the possibility that the gas can reside in several sections of different annular capacities, further complicates the situation. From a practical standpoint, an appropriate safety margin can be added initially to the casing pressure-pit gain schedule followed to account for minor variations in annular capacity. Also, it has been suggested that the entry of a gas kick into a section of different annular capacity can be detected by noting the rate of casing pressure increase with time due to upward gas migration.

For floating drilling operations in deep water, there is a very large decrease in cross-sectional area available to the gas which occurs at the subsea BOP stack. Above the subsea stack, the gas is forced to migrate the remaining distance to the surface in the subsea choke line which is attached to the outside of the marine riser. For this geometry, the static volumetric method is much more difficult to implement. One would have to be able to detect the entry of gas into the subsea choke line and have an accurate knowledge of the gas distribution and migration rate to be able to make appropriate changes in the casing pressure-pit gain schedule followed.

A second version of the volumetric method of well control is called the dynamic method. This method is similar in concept to the static method except that mud is pumped into the kill line, across the top of the annulus, and out the choke line through a choke (Fig. 77c). For a short length of kill line and choke line, frictional pressure losses in these lines can be neglected and either the pump speed or the choke setting is adjusted to control the casing pressure. In a sense, the well is being used as a mud-gas separator in that gas will exit the choke line preferentially to mud. By carefully monitoring the pit gain, an appropriate casing pressure can be selected to maintain a constant bottom hole pressure.

The example of Figure 79 has been reworked in Figure 80 for the dynamic method. To construct the base line, the initial shut-in casing pressure is plotted against the initial pit gain. A line is drawn through this point having a slope computed from Equation (5.2). The zero intercept of this line is the theoretical shut-in drill pipe pressure which would be observed if a meaningful drill pipe pressure were available. When it is desirable to add an appropriate safety margin, a line can be drawn above and parallel to the base line to provide the choke operator some margin for error.

In this work, an extension of the dynamic method is proposed for the case of a subsea BOP stack, in which mud is pumped down the kill line across the well head, and up the choke line. Since friction losses in the choke line are generally not negligible for this case, the pump must be operated at a constant speed and the choke line friction at that pump speed added to the surface pressures in the plot of Figure 80. The choke operator would then adjust the choke so that the pump pressure would follow the upper line on Figure 80. During the period when gas is migrating towards the surface, the pit gain and choke line pressure would tend to increase. After gas reaches the surface and is preferentially removed from the well, the pit gain and casing pressure would tend to decrease. As in the case of a surface BOP stack, the well is used as a mud-gas separator. Contrary to the static method, problems are not caused by the reduced area available in the choke line when implementing the dynamic method because pressure measurements made at the top of the kill line provide the criteria for choke operation and the kill line is maintained full of mud. This technique is a variation of the patented kick dispersion method of well control.[34, 35]

5.2 Experimental Well Facilities

In order to experimentally evaluate techniques for handling upward gas migration in a shut-in well equipped with a surface BOP stack, the LSU B-7 well was utilized. Figure 81 is a schematic of this training and research well. The casing is 5 1/2 inch, 17 lb/ft. J-55 pipe cemented at 6140 feet. The drill string is simulated using 6011 feet of 2 7/8 inch, 6.50 lb/ft, J-55 tubing. A 1.315 inch nitrogen injection line, run inside the 2 7/8 inch tubing to a depth of 6029 feet, is used

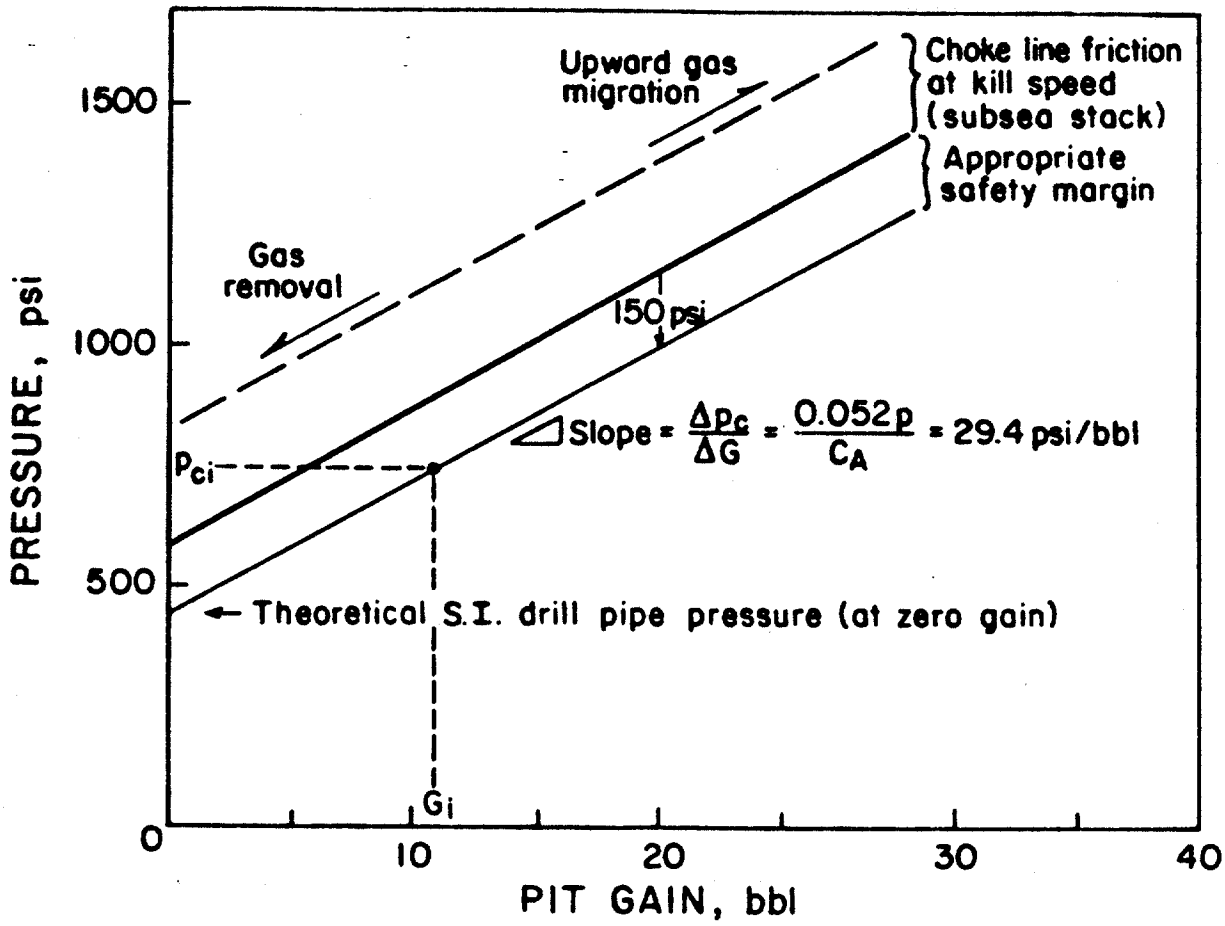

FIGURE 80. DYNAMIC VOLUMETRIC METHOD ILLUSTRATION

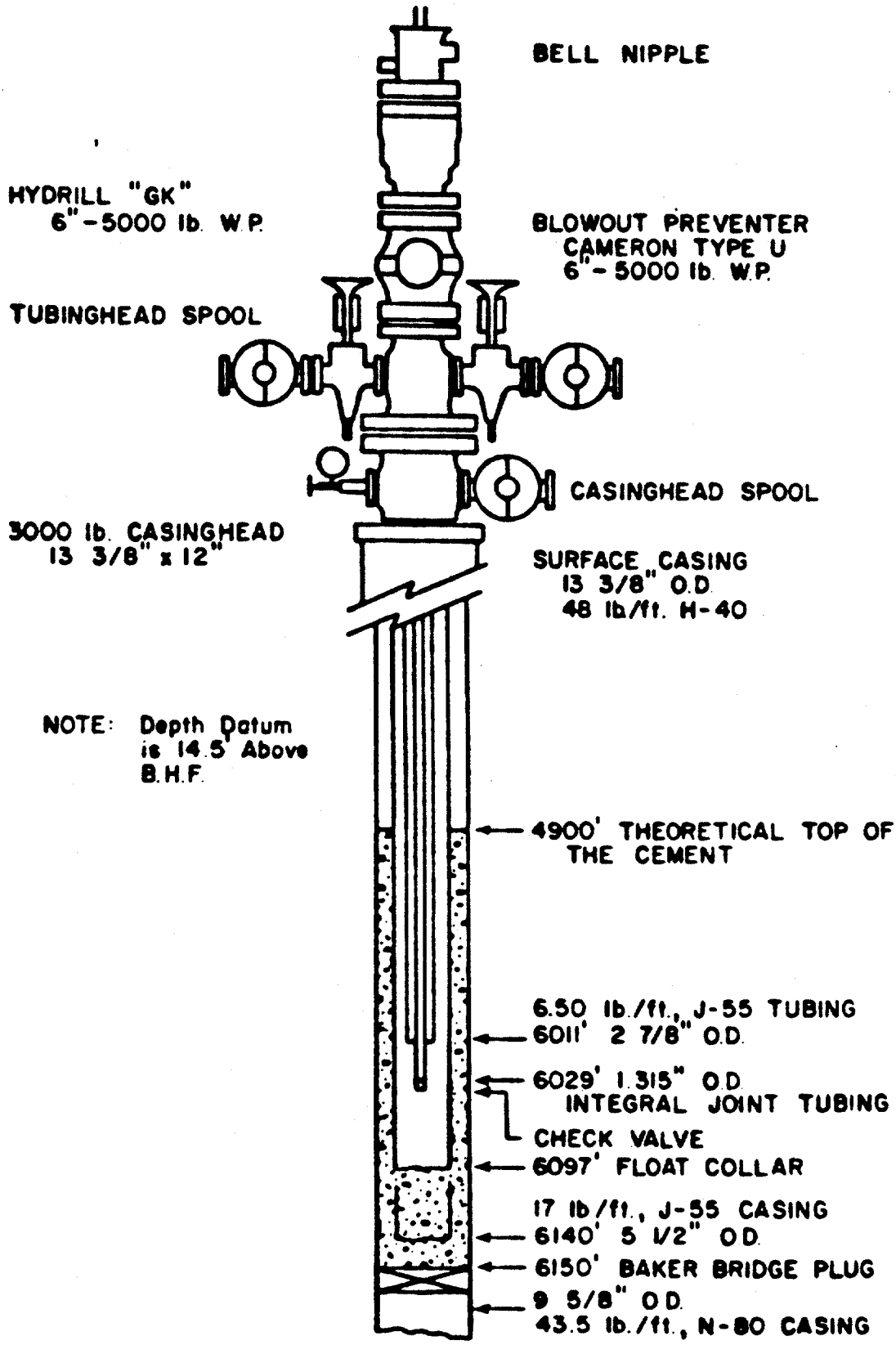

FIGURE 81. SCHEMATIC OF L.S.U. B-7 WELL

to inject nitrogen on bottom and thereby simulate a gas kick. A check valve, located at the bottom of the gas injection line, serves to hydraulically isolate this line from the well during the experimental runs.

The choke manifold contains one hand-adjustable choke and three remote-operated chokes of varying manufacturing designs. From the well, the mud flows through a choke, a mud-gas separator, and into one of two mud tanks. Mud conditioning equipment as well as a mixing pump are available if needed. The mud is circulated using a diesel-powered Halliburton Model T-10 pump. The 1 x 2 7/8-inch annulus at the wellhead, used to simulate the drill pipe, is connected to the pump discharge. An alternate path for the dynamic method is also provided to allow the mud to be pumped directly into a kill line, across the well head, and out the choke line.

In order to experimentally evaluate techniques for handling upward gas migration in a shut-in well equipped with a subsea BOP stack, the LSU-Goldking No. 1 research and training well facility described in Chapter 3 was utilized.

A lightly-treated fresh water-bentonite mud was used in both wells. Tables 12 and 13 list the mud properties for each experimental run. Plastic viscosity was varied from 1 to 57 cp and yield point from 0 to 59 lb/100 ft^2. This range of viscosities was accomplished by varying the bentonite clay content. Several experimental runs were conducted using water as the fluid medium.

For all experimental runs conducted with mud, the well fluid was circulated for several hours prior to gas injection to assure a reasonably uniform mud consistency. A fluid sample was taken at the flowline and fluid properties were measured just prior to gas injection. Nitrogen gas was injected into the well through the 1.315 inch line. Once the desired pit gain was achieved the well was shut-in. Nitrogen gas injection was continued for a short time period after shut-in until the casing (or choke line) pressure reached the desired value.

5.3 Results

Results are summarized for both surface and subsea well geometries for each method studied. The methods studied include: (1) conventional

RUN MUD NO.	DENSITY, lb/gal	PLASTIC VISCOSITY cp	YIELD POINT lb/100 ft^2	10 sec gel, lb/100 ft^2	10 min gel, lb/100 ft^2	METHOD USED	INITIAL GAIN(BBL)	GAS INJECTION (BBL/min)	INITIAL PRESSURES(psig) DRILL PIPE	INITIAL PRESSURES(psig) CASING	TOTAL BLED(BBL)
1s	8.5	4.0	1.0	--	--	Static	6.0	0.5	700	1000	2.2
2s	8.5	6.0	2.5	--	--	Static	10.3	0.5	530	830	3.3
3s	8.5	6.0	1.5	1.5	--	Conventional	17.5	1.2	280	620	0.8
5s	8.5	6.0	1.5	--	--	Dynamic	6.5	0.8	780	950	-6.5
6s	8.5	4.0	2.0	0.0	--	Dynamic	9.8	0.5	490	890	0.4
7s	8.5	26.0	23.0	7.0	29.0	Static	5.1	0.3	480	790	3.5
8s	8.5	21.5	12.0	2.0	14.5	Static	13.2	0.6	950	550	4.7
9s	8.5	15.0	6.0	3.0	4.0	Static	11.6	1.0	315	620	7.2
10s	8.8	57.0	59.0	31.0	48.5	Static	9.5	0.8	450	930	7.4
11s	8.6	33.0	24.0	24.0	--	Static	10.5	1.2	470	650	4.2
12s	8.7	26.0	16.0	12.0	15.0	Static	16.5	1.1	260	750	8.4
13s	8.8	48.0	44.0	31.0	45.0	Static	18.6	0.9	360	750	4.4
14s	8.6	9.0	4.0	1.5	1.5	Static	10.9	1.0	380	750	3.5
15s	8.6	11.0	4.0	2.0	1.0	Dynamic	10.9	0.9	340	755	4.9
16s	--	23.0	16.0	8.0	12.0	Static	18.5	1.3	200	760	5.7
17s	8.6	16.0	4.0	1.0	4.0	Dynamic	6.9	1.0	490	630	-3.3
18s	9.0	27.0	12.0	2.0	3.0	Dynamic	16.4	2.2	420	900	-0.7

* LSU B-7 Well

Table 12
Conditions Studied for Surface BOP Stack

RUN MUD NO.	DENSITY, lb/gal	PLASTIC VISCOSITY cp	YIELD POINT lb/100 ft^2	10 sec gel, lb/100 ft^2	10 min gel, lb/100 ft^2	METHOD USED	INITIAL GAIN(BBL)	GAS INJECTION RATE (BBL/min)	INITIAL PRESSURES(psig) DRILL PIPE	INITIAL PRESSURES(psig) CASING	TOTAL BLED(BBL)
1ss	8.3	1.0	0.0	0.0	0.0	Dynamic	15.3	1.1	540	640	-15.3
2ss	8.3	1.0	0.0	0.0	0.0	Static	13.1	0.8	740	900	8.3
3ss	8.9	17.0	9.0	--	--	Dynamic	17.0	1.4	635	775	-17.0
4ss	9.0	24.0	10.0	4.0	7.0	Dynamic	19.0	2.4	500	570	-17.0
5ss	8.6	16.0	5.5	8.0	2.0	Dynamic	12.9	1.7	1050	1175	-12.9
6ss	8.6	13.5	4.5	6.0	1.0	Static	11.8	1.6	1075	1180	2.3
7ss	8.5	18.0	5.0	4.0	2.0	Conventional	13.9	1.8	700	810	4.1

* LSU Goldking No. 1 Well

Table 13

Conditions Studied for Subsea BOP Stack

drill pipe pressure method; (2) static volumetric method; and (3) dynamic volumetric method.

5.3.1 Conventional Drill Pipe Pressure Method

Figure 82 is a pressure versus time plot for the conventional drill pipe pressure method for a surface BOP stack. The drill pipe pressure was held constant at 380 psi, 100 psi above its initial shut-in value of 280 psi, through manipulation of a hand-adjustable choke. By maintaining a constant drill pipe pressure, bottom hole pressure remained above formation pore pressure, thus maintaining well control. This method was relatively easy to execute. Changes in bottom-hole pressure were equal to changes in surface drill-pipe pressure.

An interesting feature of Figure 82 is that during the first two hours of maintaining constant drill pipe pressure, casing pressure continued to increase. This was due to the upward migration of the gas and required choke pressure compensation to offset the loss of hydrostatic head as mud was bled from the annulus. Once some of the gas reached the surface, changes in drill pipe pressure and casing pressure become essentially equal. This type of casing pressure profile is seen in normal well control operations, in that prior to gas reaching the surface, casing pressure builds although drill pipe pressure is held constant.

After approximately 8:30 in the experimental run, the fluid bled from the well was predominantly gas. Theoretical calculations, often used in practice, predict that well pressures would stabilize once gas reaches the surface. However, the gas did not reach the surface as a unit, but was apparently dispersed throughout a considerable volume of mud. Thus, well pressures continued to increase due to gas migration long after the leading edge of the gas reached the surface.

Results obtained using the conventional drill pipe pressure method for the subsea BOP stack well are shown in Figure 83. A 13.7 bbl kick was injected into the well in approximately 12 minutes, prior to closing the well. The drill pipe pressure was allowed to increase by approximately 200 psi prior to conducting the first mud bleed through a hand adjustable choke. It required approximately 84 minutes for this initial pressure increase to occur. For the first 50 minutes, the drill-pipe

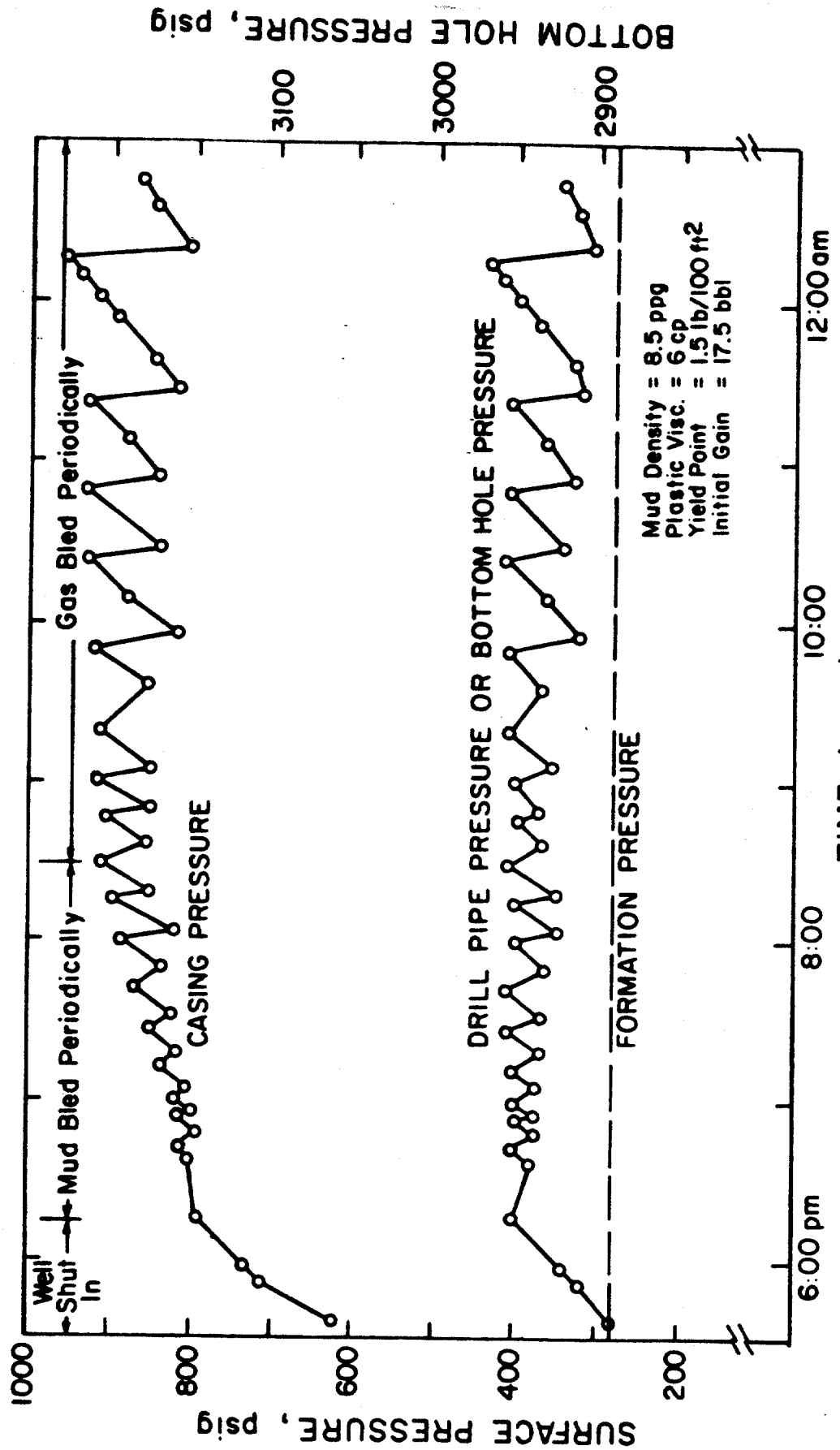

FIGURE 82. CONVENTIONAL DRILL PIPE PRESSURE METHOD FOR SURFACE BOP STACK (RUN NO. 3s)

pressure and casing pressure increased at the same rate, indicating that the gas kick had not yet reached the subsea choke line. After the leading edge of the gas progressed significantly into the choke line, casing pressure increased much faster than the drill-pipe pressure. The leading edge of gas reached the surface 270 minutes after the start of the experiment. Subsequent bleeding operations produced predominantly gas. After 320 minutes, the choke was closed for the last time and the drill-pipe pressure never built up sufficiently to warrent additional bleeding of well fluids. During the entire run, changes in bottom hole pressure were accurately reflected by changes in drill pipe pressure.

The experimental runs conducted for both the surface and subsea BOP stack well geometries indicated that the conventional drill-pipe pressure method was an excellent method for the safe handling of upward gas migration in a shut-in well. When the mud in the drill-pipe is not contaminated with gas, when there is not a severe mud gellation problem, and when the drill-string is near bottom, unobstructed, and without leaks, changes in bottom-hole pressure will be accurately reflected by changes in surface drill-pipe pressure.

5.3.2 Static Volumetric Method

When a meaningful drill pipe pressure is not available, the static volumetric method can be implemented by monitoring both casing (choke line) pressure and pit level changes. For experimental purposes, drill-pipe pressure and/or bottom-hole pressure was available to ascertain the success of the method's ability to maintain well control. This method was also modified in that bleeding of gas from the well was allowed, as long as well pressure continued to increase.

Figure 84 is a pressure-volume-time plot for one of the experimental runs for the surface BOP geometry. The well was shut-in with 750 psi casing and 380 psi drill pipe pressure. Casing pressure was allowed to increase 150 psi as a safety margin and then an additional 50 psi as the incremental pressure change. Then the static volumetric method was employed.

The important feature to note in Figure 84 is that at no time did drill pipe pressure come close to falling below its initial shut-in value. Reduction of drill pipe pressure during bleed cycles was due to

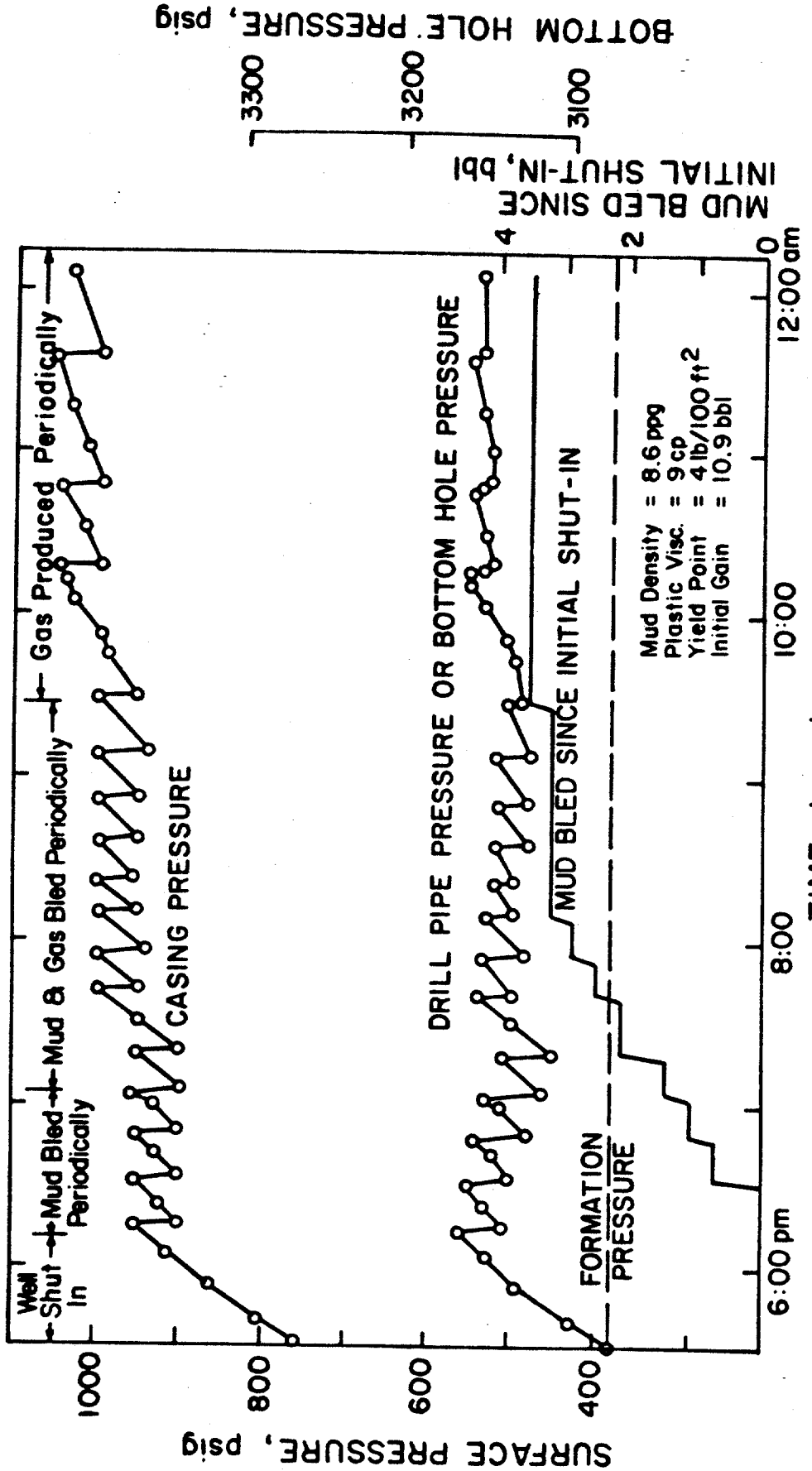

FIGURE 84. STATIC VOLUMETRIC METHOD FOR SURFACE BOP STACK (RUN NO. 14s)

loss of mud from the annulus. Once an incremental volume of mud of 1.7 bbls was bled, casing pressure was allowed to build an additional 50 psi, and drill pipe pressure came back up as well.

It should be pointed out that Figure 79 is the theoretical casing pressure pit gain schedule for Figure 84. Figure 79 is replotted in Figure 85 with well data included. Note that theoretical consideration of the gas law, treating the gas as a continuous slug, predicts a total of 15.4 bbls (26.3-10.9) to be bled from the well and a final casing pressure of about 1,350 psig. Actual well conditions followed the theoretical schedule during the first two steps only and a final pressure of 1050 psig was observed. Another observation is that gas was vented at the surface early in the experimental run. Subsequent bleeding of gas and mud, and finally only gas (pit volume did not change late in the run) did not cause drill-pipe pressure, and thus bottom-hole pressure, to decrease to a value below its initial shut-in value. Well control is once again maintained successfully and with relative ease.

When the static volumetric method is applied for a well with a non-uniform annular geometry, the choke pressure changes which will be caused by changes in the effective length of the gas kick in the different well sections must be estimated. For the case of the subsea well geometry, a gas kick having a volume of 12 bbl will have an effective length of approximately 3,000 ft. if contained in the choke line, but only approximately 300 ft. if contained in the annulus. Thus, the choke pressure should increase by about 1,200 psi when 8.6 lb/gal mud is replaced in the choke line with gas.

Shown in Figure 86 is an experimental run in which the static volumetric method was attempted for the subsea well geometry available. In order to provide a 100 psi safety margin, choke pressure was allowed to increase by 150 psi before bleeding any mud through the choke. This took approximately 80 minutes to occur. During the next hour, it was assumed that all of the gas remained in the well and mud was periodically bled from the choke, to maintain the casing pressure approximately constant. When all of the gas is contained in the well annulus, up to 4.2 bbl of mud could be safely bled before allowing the casing pressure to increase by another 50 psi increment. However, before this volume could be bled, the slope of the choke-pressure-time plot increased

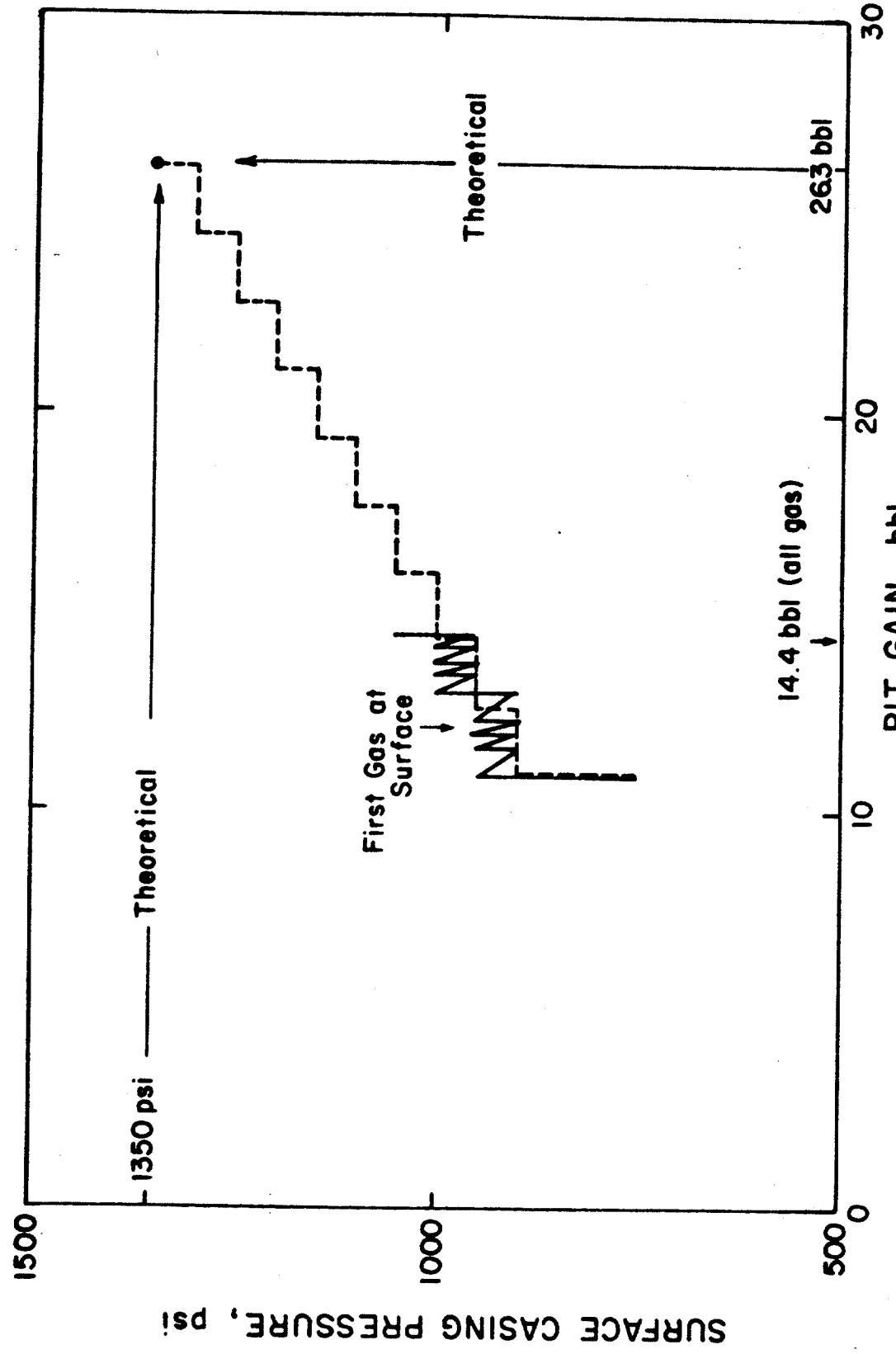

FIGURE 85 . COMPARISON OF THEORETICAL CASING-PRESSURE-PIT GAIN SCHEDULE TO ACTUAL WELL PERFORMANCE FOR RUN 14 s

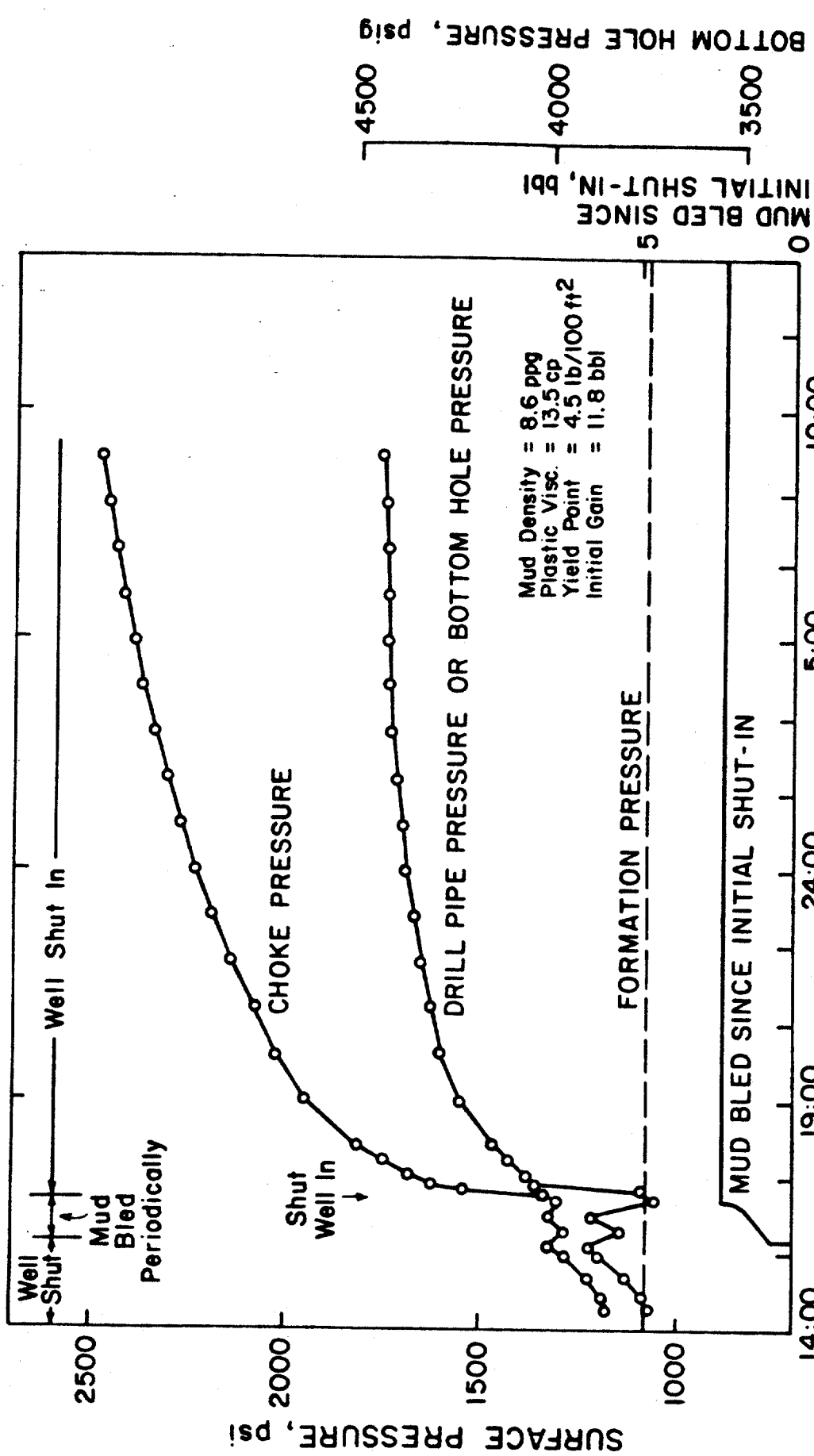

FIGURE 86. STATIC VOLUMETRIC METHOD FOR SUBSEA BOP STACK (RUN 6 ss)

greatly, indicating the entry of the leading edge of the gas in the subsea choke line. At this point, the well was closed and the choke pressure allowed to increase by 1,200 psi to 2,500 psig to account for the maximum pressure increase required by gas elongation as the gas left the well and replaced the mud in the vertical subsea choke line. After approximately 16 hours, well pressures stabilized just prior to the choke pressure reaching 2,500 psig. If the choke pressure had continued to increase while the gas was in the choke line, a mud volume of 0.42 bbl of mud could be bled for each 50 psi increased noted.

Figure 86 shows unacceptable large increases in bottom-hole pressure can occur when the static volumetric method is applied for a subsea BOP stack in deep water. Also, in other similar runs conducted, unacceptable large decreases in bottom-hole pressure resulted when gas entry into the choke line was not detected soon enough. An example of this behavior is shown in Figure 87 for the experimental data of Run 2ss. In this run, water was used as the drilling fluid and the gas was dispersed in a greater volume of liquid. The lower gas concentration makes the change in slope of casing pressure versus time (which occurs when gas enters the choke line) more difficult to detect.

5.3.3 Dynamic Volumetric Method

Typical results obtained using the dynamic volumetric method with a surface BOP stack are shown in Figures 88-89. Figure 88 illustrates the desired casing pressure as a function of pit gain for a 200 psi excess bottom-hole pressure. Also, shown in this figure is a comparison between the desired and observed casing pressures and bottom hole pressures. Figure 89 gives these same results plotted as a function of time. In general, no difficulty was experienced in employing this method and the bottom-hole pressure was held near the desired value.

For the case of the subsea BOP geometry, initial implementation of the dynamic method is more complex. A choke line frictional pressure at a given pump rate must be known. This value of pressure is then added to the base line of the casing pressure-pit gain schedule as in Figure 80, in addition to any safety margin which may be applied. The uppermost line of Figure 80 would then be the guide to follow. In addition, a pump start-up procedure often used during normal kill opera-

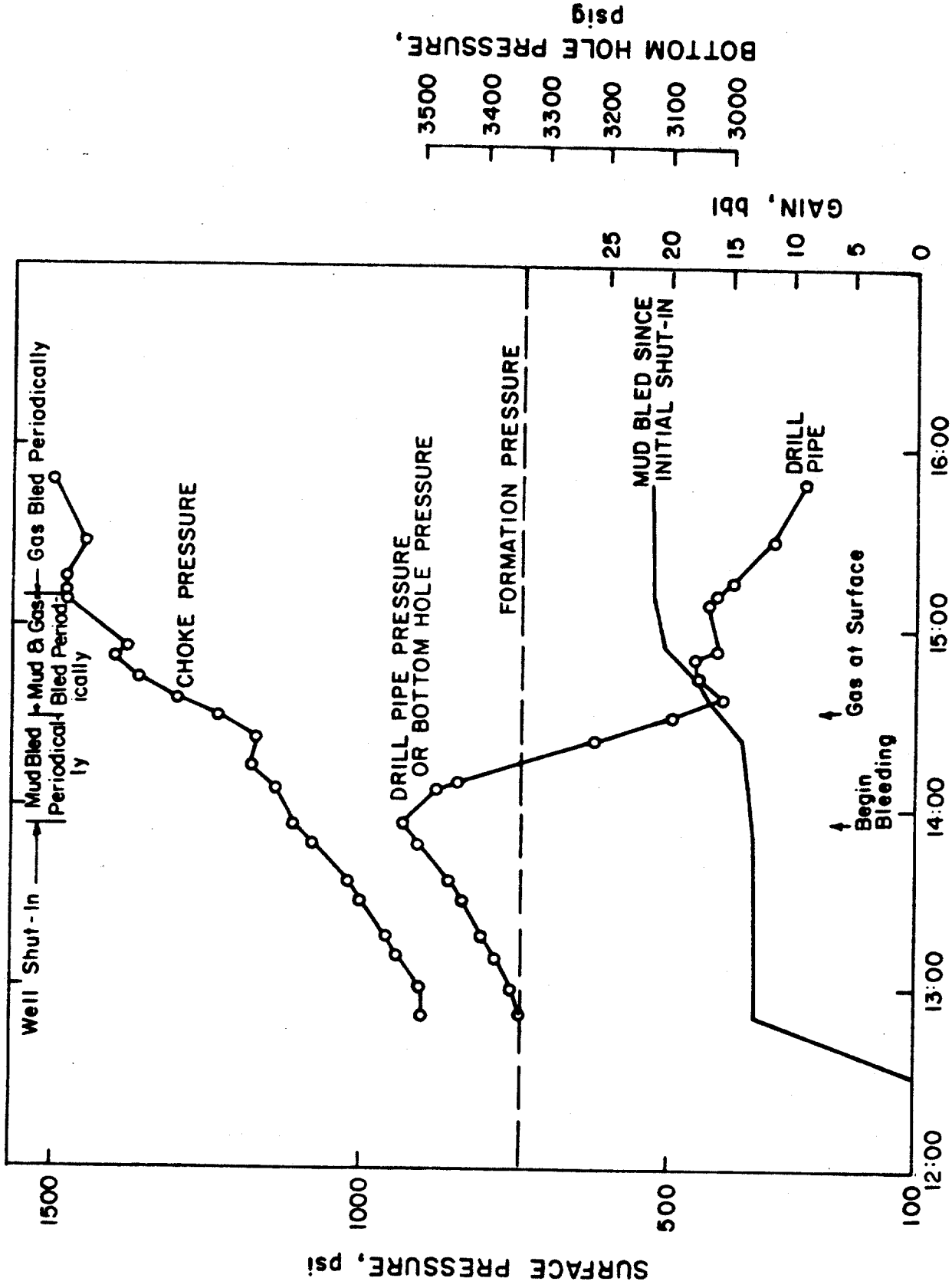

FIGURE 87. STATIC VOLUMETRIC METHOD FOR SUBSEA BOP STACK (RUN 2ss)

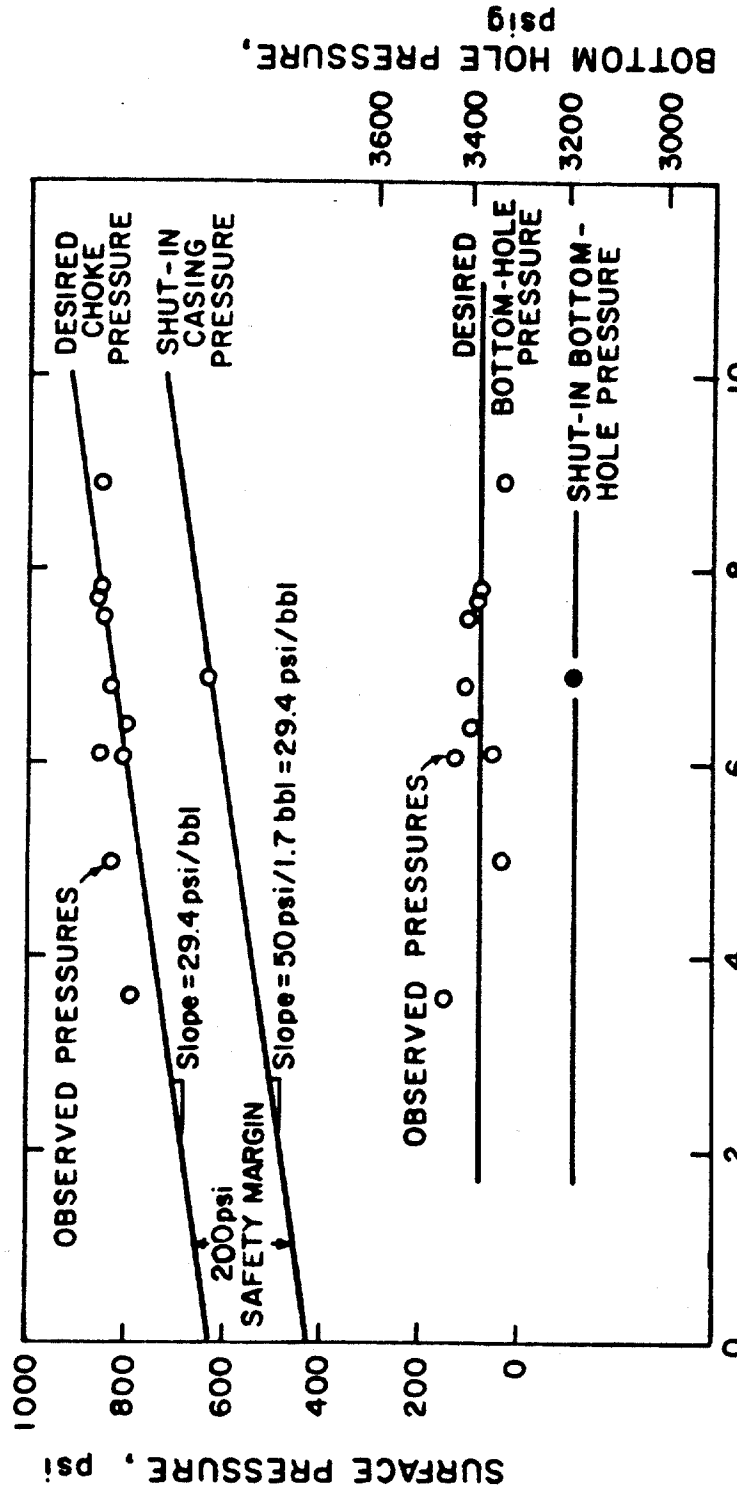

FIGURE 88. DESIRED AND OBSERVED CHOKE PRESSURES AS A FUNCTION OF PIT GAIN FOR RUN 17

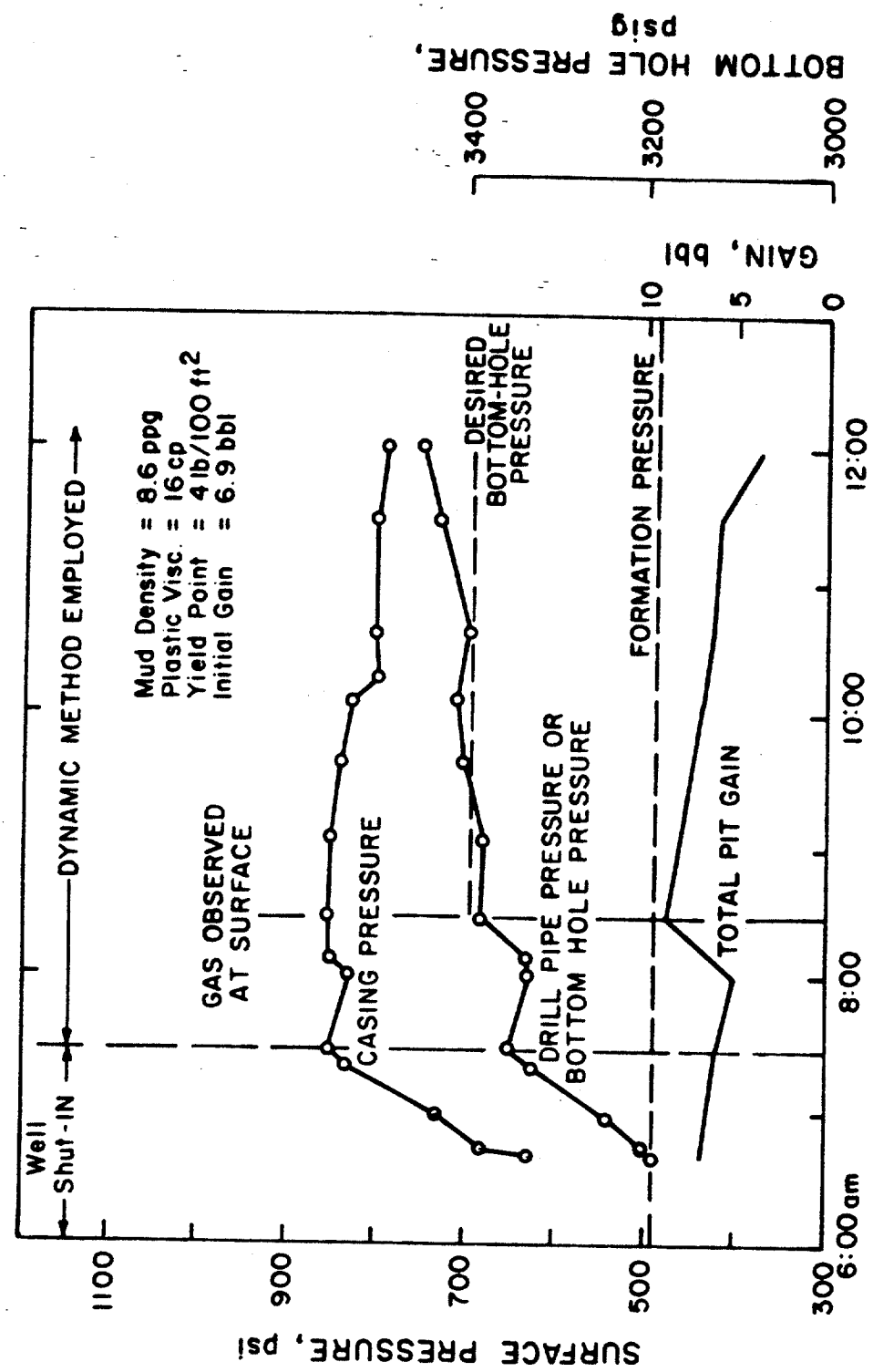

FIGURE 89. DYNAMIC VOLUMETRIC METHOD FOR SURFACE BOP STACK (RUN 17 a)

tions for a subsea stack should be implemented. The pump start-up procedure calls for slowly increasing pump rate while allowing choke line pressure to be reduced by an amount equal to choke line friction. Once the pump is brought up to speed, the kill line pressure (pump pressure) is monitored instead of choke line pressure and is adjusted according to changes in pit level (Fig. 80).

Typical results obtained using the dynamic volumetric method with the subsea stack well are shown in Figures 90-91. These data were obtained in experimental run 5ss. Figure 90 shows how closely the circulating kill line pressures could be maintained to the desired circulating pressures. By also maintaining the pump speed constant (71 strokes/min), the bottom-hole pressure was maintained slightly above the formation pressure during the entire run. This can be seen from the bottom curve of Figure 90. Shown in Figure 91 are the same data plotted versus time. The shut-in conditions were a 12.9 bbl gain with 1175 psi choke line and 1050 psi drill pipe pressures. The choke line pressure was allowed to build by slightly over 100 psi as a safety margin. Prior choke line friction measurements gave a 350 psi friction loss at 71 spm. The pump was brought up to speed slowly, allowing choke line pressure to fall to a final value of 975 psi at 71 spm, or 350 psi less than its initial value. Pump speed was maintained at 71 spm and kill line pressure was monitored and adjusted with the choke according to the pressure-pit level schedule shown in Figure 15 (uppermost line).

Referring to Figure 91, it can be seen that once the pump start-up procedure was completed, drill pipe pressure remained virtually constant for the rest of the run at a value approximately 80 psi above the initial shut-in value. Kill line pressure was reduced as time progressed due to removal of gas from the well. The leading edge of gas reached the surface 2 hours after initiation of the experimental run. After an additional 3 hours, the well was completely cleaned of all gas. The method was very simple to run and choke adjustments required were quite infrequent.

Another important feature of Figure 91 is the choke line pressure plot. There were no significant increases in choke pressure, due to the dispersion of the gas into the mud as the mud was pumped down the kill line, across the top of the annulus, and back up the choke line. This

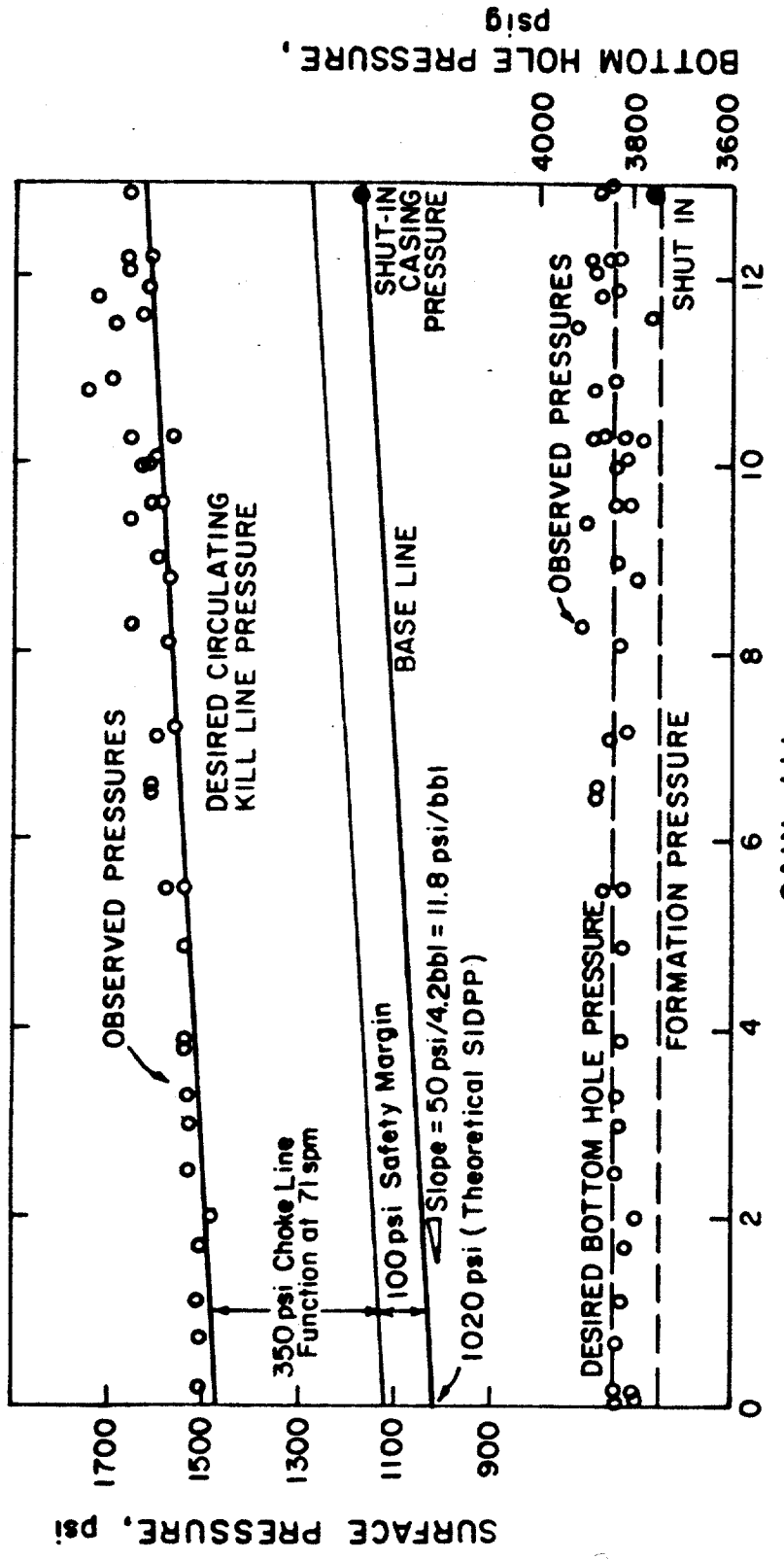

FIGURE 90. DESIRED AND OBSERVED KILL LINE PRESSURES AS A FUNCTION OF PIT GAIN FOR RUN 5 ss

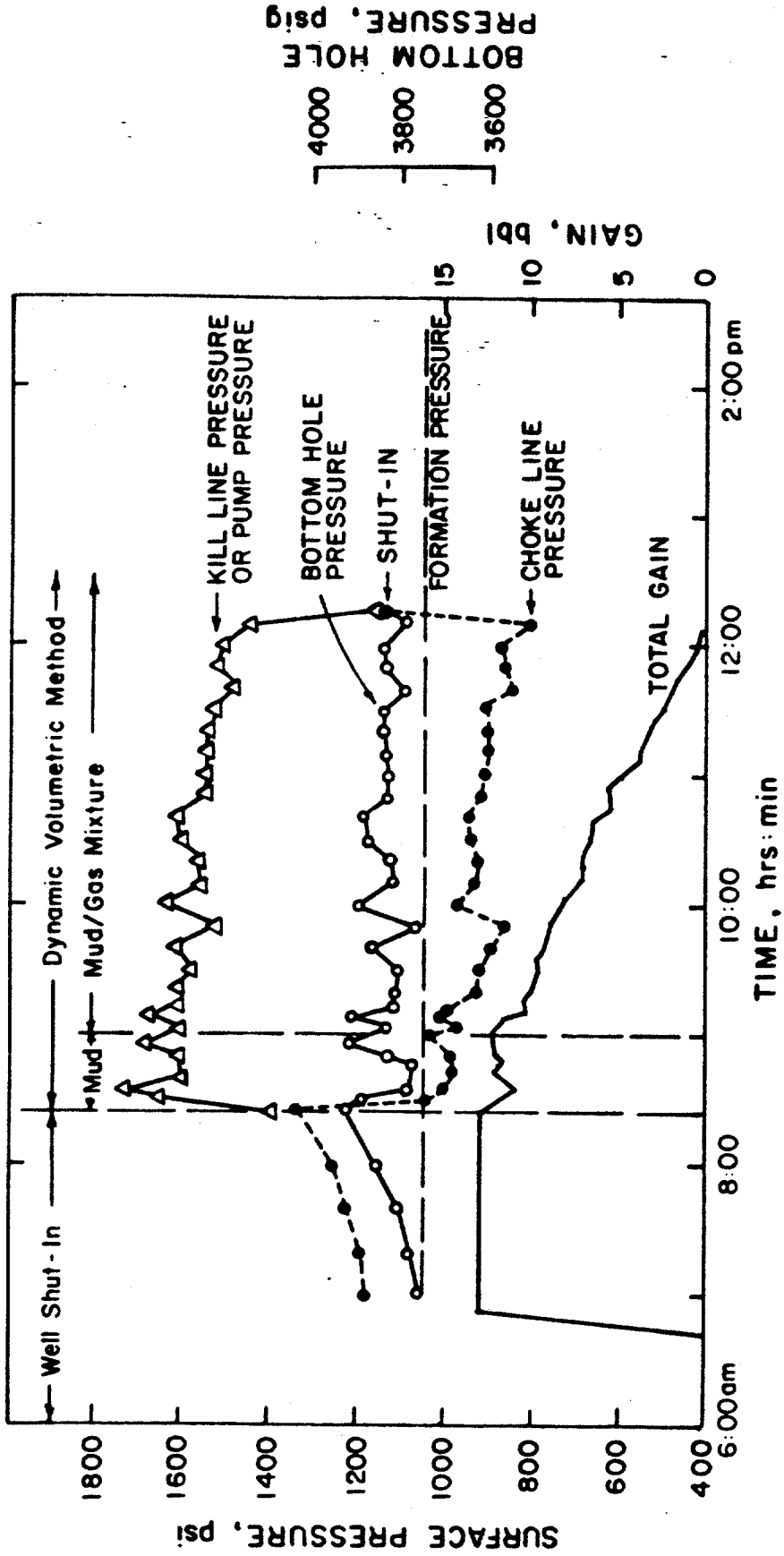

FIGURE 91. DYNAMIC VOLUMETRIC METHOD FOR SUBSEA BOP STACK (RUN 5ss)

dispersion reduced the severity of choke line pressure variations to such a degree that no major choke adjustments were required.

The dynamic volumetric method for subsea stacks is a variation of the kick dispersion method of well control.[34] Peak pressures are greatly reduced using this method because the gas region is broken up and brought to the surface in smaller increments. Thus, some gas is removed before the remaining gas is brought to the surface. In this way, gas expansion within the well is minimized. A new device[35] called "the bubble chopper" is being developed which will allow use of this technique on any well. The use of an MWD device which could provide a surface readout of bottom hole pressure would greatly simplify use of the kick dispersion method of well control.

CHAPTER 6

PUMP START UP-PROCEDURES

Starting the pump, like well closure, is a critical part of the overall well control procedure. Many underground blowouts are thought to occur during pump start-up. Problems occur at this time because in modern well control procedures, operation of the adjustable choke is based primarily on drill pipe pressure observations made while the pump is running at a constant speed, called the kill speed. Unfortunately, before the pump speed is brought to and stabilized at this kill speed, the transient well conditions are more difficult to describe and control.

The basic intent during pump start-up, as in all phases of well control operations is to keep the bottom hole pressure at a value equal to or slightly above the formation pressure. Usually, the bottom hole pressure is allowed to increase during pump start-up by an amount equal to the frictional pressure loss in the well annulus at the selected kill speed. A small pressure increase is desirable because it provides some margin for error on the part of the choke operator. Annular frictional pressure loss is a good means of providing this safety margin because the portion of the frictional pressure loss in the annulus which occurs below the casing seat does not add to the pressure at the casing seat.

The control of bottom hole pressure during pump start-up must be accomplished using the well pressure information routinely available at the surface. Techniques have been developed for using either the surface drill pipe pressure or casing pressure for ascertaining changes in bottom hole pressure.

6.1 Conventional Drill Pipe Pressure Controlled Start-up

Under shut-in conditions, the relation between bottomhole pressure and drill pipe pressure is given by:

$$P_{bhs} = P_{dps} + 0.052\ \rho_1\ D \qquad (6.1)$$

where: P_{bhs} = static bottom hole pressure after shut-in, psig
P_{dps} = static drill pipe pressure after shut-in, psig
ρ_1 = mud density in well system when kick was taken, lb/gal
D = vertical depth of well, ft

After well circulation is initiated, if the bottom hole pressure is allowed to increase by an amount equal to the frictional pressure loss in the annulus, the relation becomes:

$$P_{bhs} + \Delta P_{fa} = P_{dpc} + 0.052\rho_1 D - 0.052(\rho_2 - \rho_1)L_2 - \Delta P_{fp} - \Delta P_b \quad (6.2)$$

where ΔP_{fa} = total frictional pressure loss in annulus, psig
P_{dpc} = circulating drill pipe pressure after initiation of well control operations, psig
ρ_2 = kill mud density, lb/gal
L_2 = vertical length of kill mud in the drill string after initiation of well control operations, ft
ΔP_{fp} = total frictional pressure loss in drill string, psig
ΔP_b = circulating pressure drop across jet bit nozzles, psig

The sum of the flowing pressure losses in the drill string, across the bit, and in the annulus at any given reduced pump rate is generally called the reduced pump pressure.

$$P_r = \Delta P_{fp} + \Delta P_b + \Delta P_{fa} \quad (6.3)$$

The reduced pump pressure at several pump rates is routinely measured and recorded at least twice a day so that in the event a kick is taken, its value would be accurately known. Combining Equations (6.2) and (6.3) and then equating the resulting expression for static bottom hole pressure with that of Equation (6.2) yields:

$$P_{dpc} = P_{dps} + P_r - 0.052\ (\rho_2 - \rho_1)\ L_2 \quad (6.4)$$

During the relatively short time period of pump start-up, the last term of Equation (6.4) is small and can be neglected. Thus, the correct circulating drill pipe pressure, P_{dpc}, during pump start-up is approximately equal to the shut-in drill pipe pressure, P_{dps}, plus the reduced pump pressure at the given pump rate.

The choke operator must manipulate the choke as the pump speed is increased to maintain the correct drill pipe pressure for the current pump speed. A plot of reduced pump pressure versus pump rate can be used to conveniently establish the proper value of P_r for any pump rate up to the kill speed. This is best accomplished by plotting the reduced pump pressure data previously recorded by the driller on a log-log graph as shown for an example by the lower line in Figure 92. For those who prefer not to use a graphical approach, the following approximate relationship can be used:

(1) At a pump speed of one-half of the kill speed, P_r is one-fourth of the reduced pressure at the kill speed.

(2) At a pump speed of three-fourths of the kill speed, P_r is one-half of the reduced pressure at the kill speed.

(3) At a pump speed of seven-eighths of the kill speed, P_r is three-fourths of the reduced pressure at the kill speed.

Conventional Casing Pressure Controlled Start-up

Under shut-in conditions, the relation between bottom hole pressure and casing pressure is given by:

$$P_{bhs} = P_{cs} + 0.052\rho_1(D - L_{ks}) + 0.052\rho_{ks}L_{ks} \qquad (6.5)$$

where: P_{cs} = static casing pressure after shut-in, psig

L_{ks} = length of kick fluids for shut-in conditions, ft

ρ_{ks} = density of kick fluid during shut-in period, lb/gal

After well circulation is initiated, but before kill mud reaches the bit, if the bottom hole pressure is allowed to increase by an amount equal to the frictional pressure loss in the annulus, the relation becomes:

$$P_{bhs} + \Delta P_{fa} = P_{cc} + 0.052\rho_1(D-L_k) + 0.052\rho_k L_k + \Delta P_{fa} \qquad (6.6)$$

where: P_{cc} = circulating casing pressure after initiation of well control operation, psig

ρ_k = density of kick fluids after initiation of well control operations, lb/gal

L_k = effective length of kick fluids after initiation of well control operations, ft

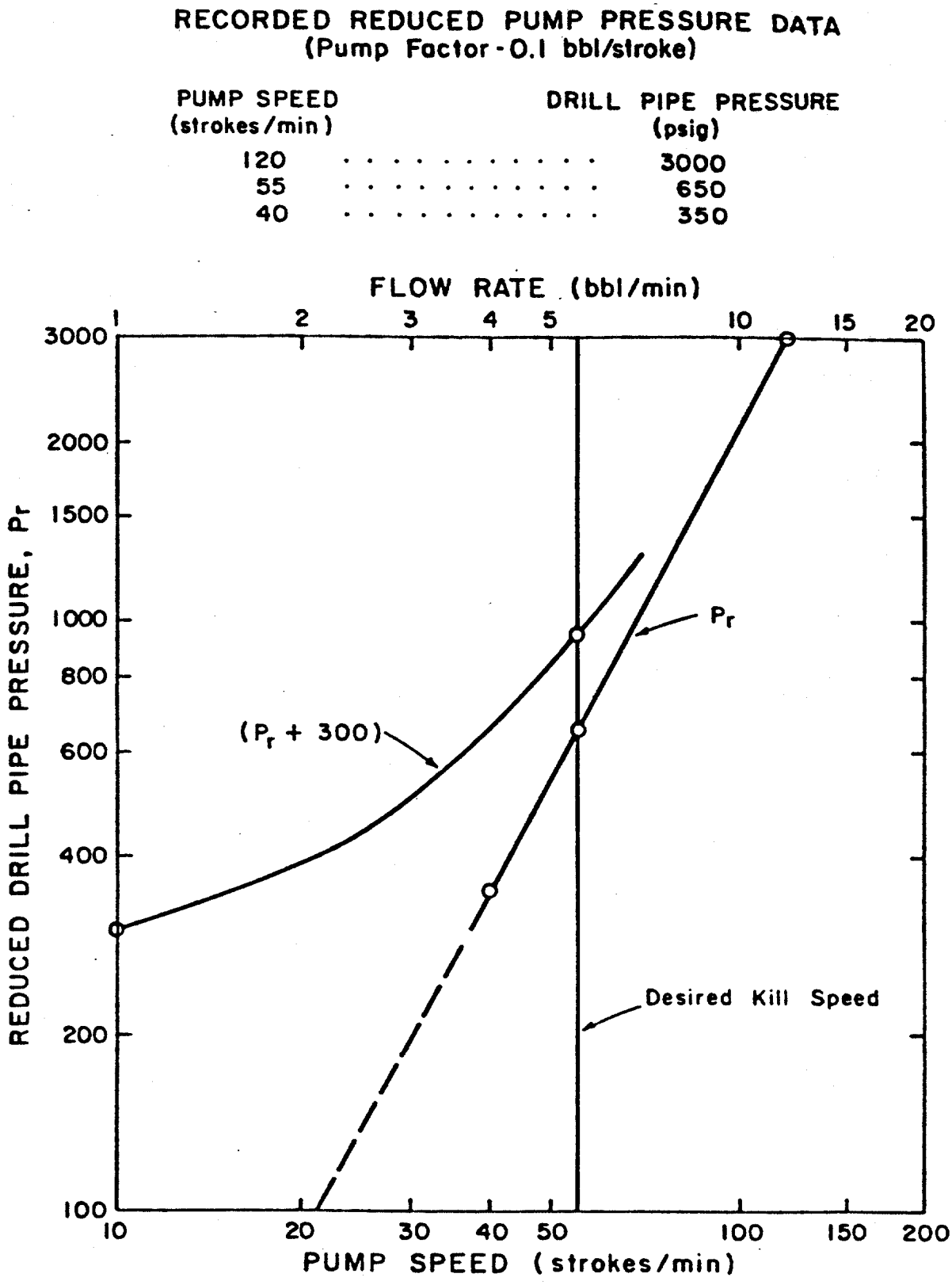

Figure 92. Example Reduced Pump Pressure Plot

Equating the two expressions for static bottom hole pressure defined by these equations yields:

$$P_{cc} = P_{cs} + 0.052\rho_1(L_k - L_{ks}) + 0.052(\rho_{ks}L_{ks} - \rho_k L_k) \qquad (6.7)$$

During the relatively short time period of pump start-up, the second and third terms of Equation (6.7) are small and can be neglected. Thus, the correct circulating casing pressure during pump start-up is approximately equal to the shut-in casing pressure. The choke operator simply manipulates the choke to maintain the casing pressure constant at the shut-in value until the pump is running smoothly at the kill speed.

A conventional pump start-up is illustrated in Figure 93 for a land drilling example. When circulating the well at the kill speed during normal drilling operations prior to taking the kick (Figure 93a), a reduced pump pressure of 650 psig was noted. The annular frictional pressure loss for the well conditions given, accounts for only 70 psig of this total pressure required to circulate the well at the kill speed under normal conditions. Approximately 35 psig of the annular frictional pressure loss occurred in the casing and surface choke line with the remaining 35 psig pressure loss occuring below the casing seat. After taking a kick and implementing the shut-in procedure (Figure 93b), the drill pipe pressure stabilized at 300 psig and the casing pressure stabilized at 455 psig. This resulted from the bottom hole pressure of 3744 psig and a casing seat pressure of 1900 psig. When initiating well circulation (Figure 93c), the bottom hole pressure was allowed to increase by an amount equal to the annular friction, thus going from 3744 to 3814 psig as the pump speed was increased from zero to the selected kill speed of 55 strokes/min. This could be accomplished either by adjusting the choke to obtain a drill pipe pressure of 950 psig (300 psig shut-in pressure plus 650 psig reduced cicrulating pressure) or a casing pressure of 455 psig (same as shut-in value). Note that the resulting annular pressure at the casing seat increased only half as much as bottom hole pressure during pump start-up.

The well pressure behavior during pump start-up for this example at intermediate pump speeds is further illustrated in Figure 94. The approximate relationship was used to compute the drill pipe pressure

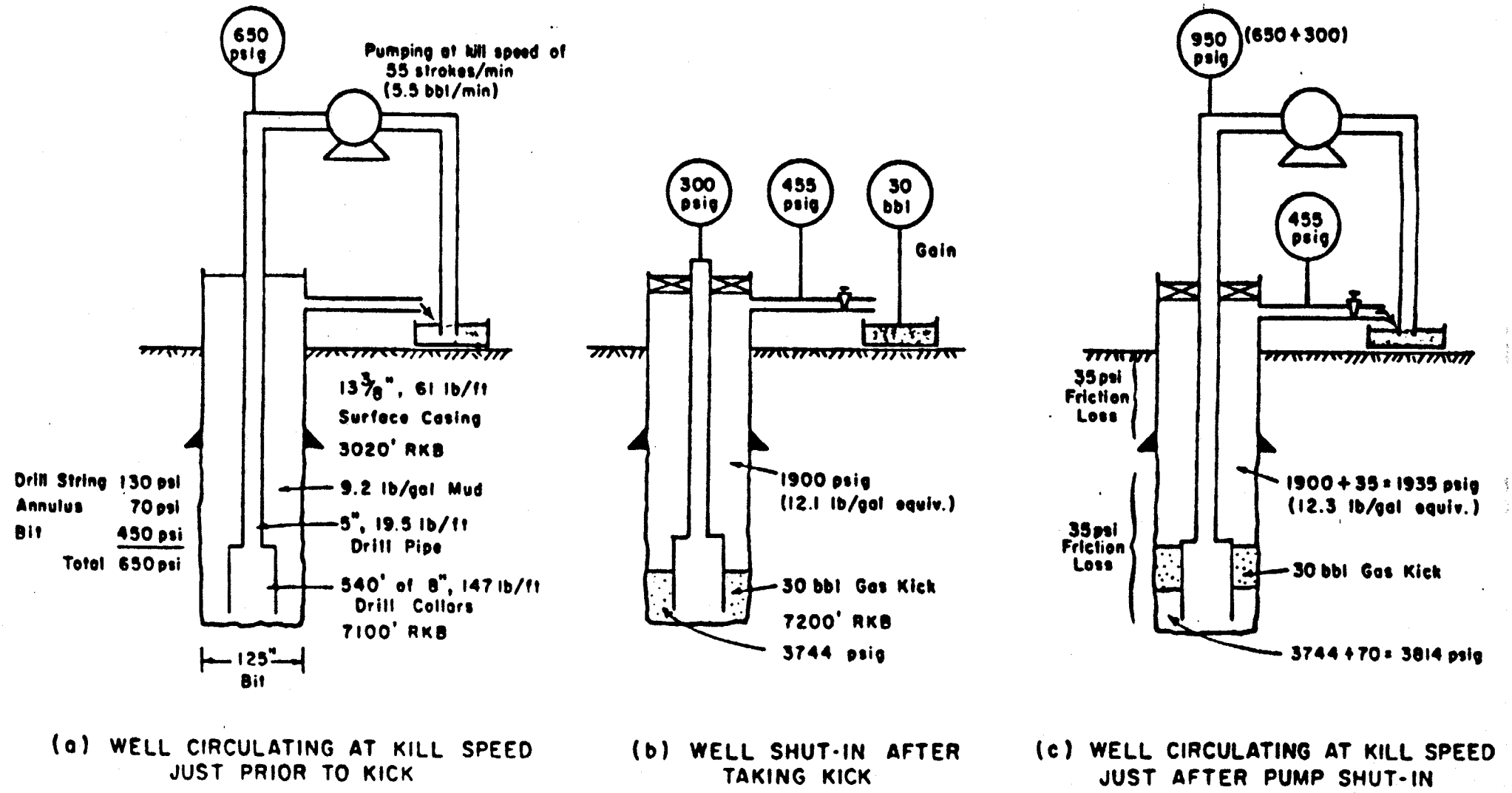

Figure 93: Schematic Diagram and Well Data For an Example Kick Taken During Land Drilling Operation

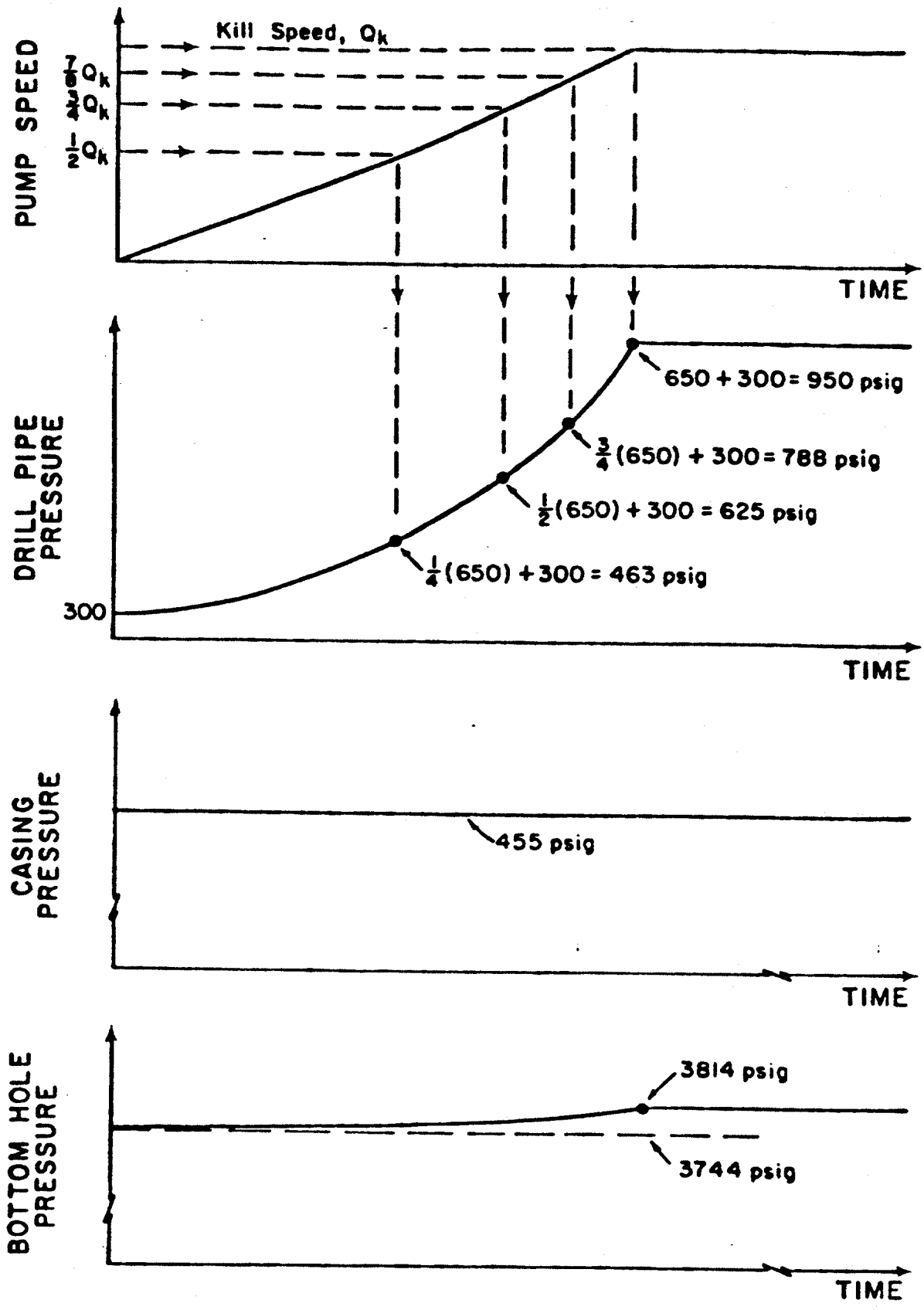

Figure 94: Ideal Well Pressure Behavior During Pump Start-up for Land Drilling Example

behavior. The circulating drill pipe pressure behavior obtained graphically by adding the shut-in drill pipe pressure of 300 psig to the reduced pump pressure line is also shown in Figure 92 for comparison.

In recent time, the conventional casing pressure controlled pump start-up procedure has gained the most wide-spread acceptance because of its greater simplicity. Advocates of this method also point out that it does not depend upon a predetermined reduced pump pressure which could have changed in value since being recorded. Instead, a current value of the reduced pump pressure can be obtained as the difference between circulating drill pipe pressure, just after pump start-up, and the shut-in drill pipe pressure. However, important assumptions implied in the use of the conventional casing pressure controlled pump start-up method are:

1. The frictional pressure loss in the choke lines and well annulus for flow rates up to the kill speed are small.
2. The liquid column in the annulus and choke line is of uniform density.
3. Any gaseous regions in the well are sufficiently deep such that the percentage change in mud hydrostatic pressure above the gaseous regions will be small during pump start-up.
4. The length of any gas zone in the well will not change significantly during pump start-up, as when a gaseous zone moves into an annular region having a significant change in cross-sectional area.

For land or shallow water marine drilling operations, these assumptions are usually sufficiently valid to allow a safe pump start-up. However, the first two assumptions tend to become less valid as drilling operations extend to greater water depths.

6.3 Choke-Line Frictional Pressure Loss

Annular friction in subsea choke lines has been studied emperically by Goins.[39] Shown in Figure 95 are frictional pressure losses for a 9.2 lb/gal mud in a 2.62 in. I.D. subsea choke line based on rig site measurements. As shown in this figure, choke line friction increases greatly with increasing water depth or pump rate. As discussed in Chapter 2, efforts made to reduce the magnitude of choke line friction in deep water include:

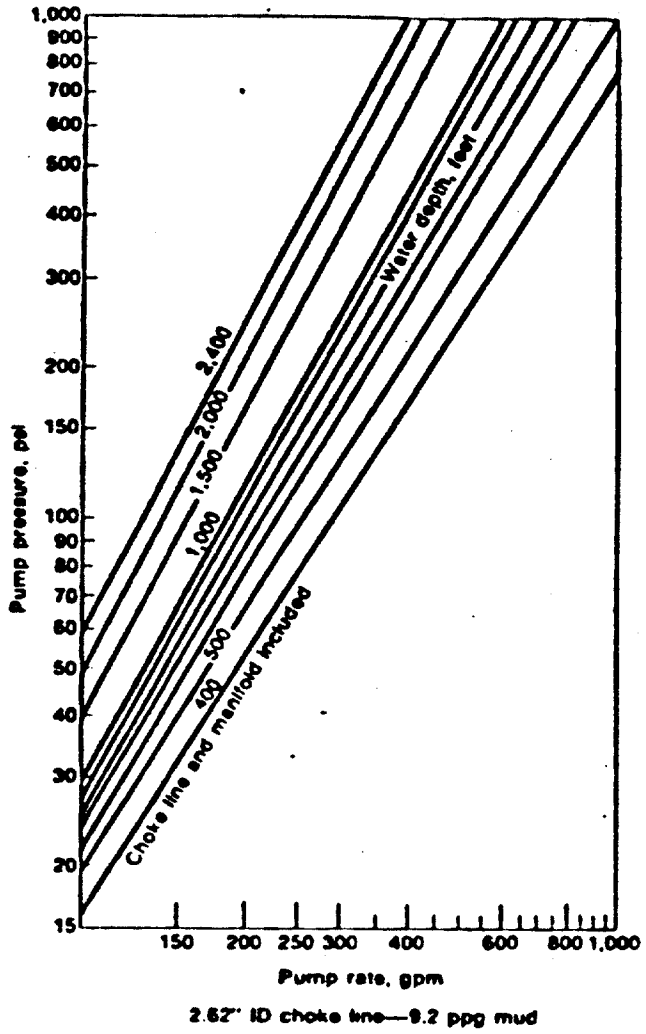

Figure 95: Effect of Pump Rate and Water Depth on Frictional Pressure Loss in Subsea Choke Lines (After Goins[1])

1. Use of larger diameter choke lines (up to 3.15 in. I.D.).
2. Use of slower kill speeds.
3. Use of both subsea kill line and subsea choke line in parallel for well circulation.

However, many operators working in deep water have found it also necessary to modify the conventional start-up procedure.

Figure 96 illustrates the importance of frictional pressure losses in the subsea choke line when circulation of a kick is initiated in deep water using the conventional casing pressure controlled method. For this example, the equivalent density at the casing seat for shut-in conditions is 10.3 lb/gal equivalent. After increasing the circulation rate to a speed of 5.5 bbl/min, the frictional pressure loss in the 3.15 in. choke line would be approximately 300 psi. This additional pressure increases the equivalent circulating density at the casing seat to 11.1 lb/gal equivalent, which is well above the 10.6 lb/gal equivalent fracture gradient for the conditions given. Thus, fracturing of a formation exposed below the casing seat would occur, possibly resulting in an underground blowout.

The subsea choke and kill lines are often filled with water during routine drilling operations, especially when a weighted mud system is in use, in order to prevent plugging of these lines. Unfortunately, this practice can lead to an additional complication during pump start-up because the rapid displacement of water from the choke line by higher density drilling fluid can cause a significant change in the hydrostatic pressure as well as a change in frictional pressure loss in the choke lines. A 15 ppg mud displacing 8.3 ppg water from a 2.5 in. I.D. choke line causes a 57 psi reduction in annular hydrostatic pressure for every barrel of mud pumped until the choke line is completely displaced. The total loss in hydrostatic pressure in 3000 feet of water would be 1045 psi. Use of the conventional casing pressure controlled start-up method under these conditions would cause an unacceptable large increase in bottom hole pressure and casing seat pressure.

6.4 Modified Pump Start-up Procedures

When the choke line frictional pressure loss or the change in choke line hydrostatic pressure becomes significant, a more complex pump start-up procedure is justified. Reliance should be placed on actual

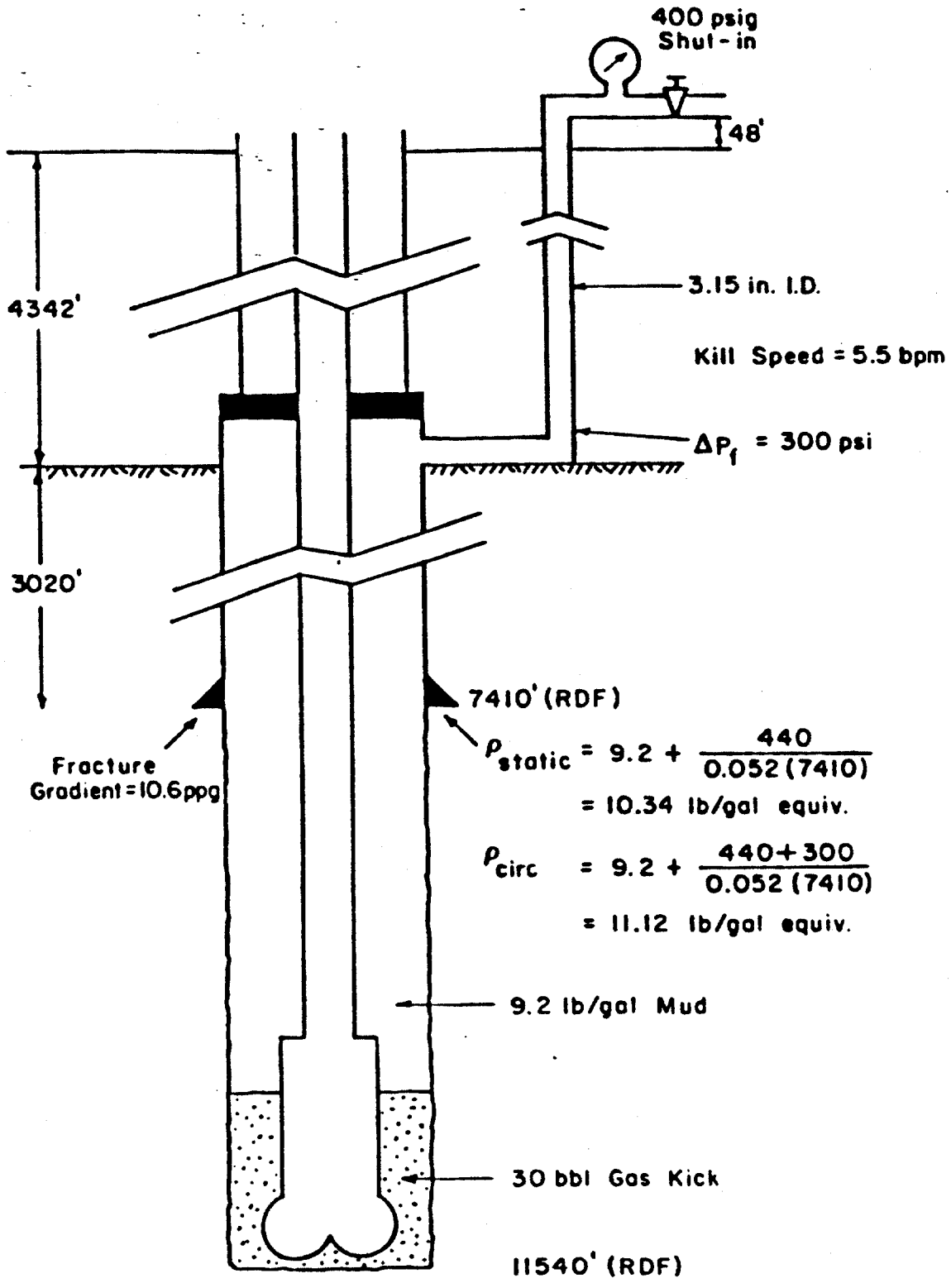

Figure 96: Example Illustrating Effect of Chokeline Frictional Pressure Loss on Equivalent Mud Density at Casing Seat

pressure measurements whenever possible. Goins[1] recommends determining the choke line frictional pressure loss at three or more flow rates and plotting the results on log-log graph paper as shown in Figure 95.

Several techniques that have been proposed for routine measurement of choke line friction are shown in Figure 97. The first method involves taking the difference between the drill pipe pressure required to circulate the well through the choke line with the BOP closed and the drill pipe pressure required to circulate the well through the marine riser with the BOP open. Care must be taken to insure that the same pump rate is used in both measurements and that the mud properties in the well are not changing significantly between measurements. Ilfrey, et al.[40] recommends adjusting the choke when using this technique until a mid-range choke pressure is also observed while flowing through the choke line. In this case, the circulating frictional pressure loss in the choke line is the drill pipe pressure, observed when circulating through the choke line, minus choke pressure, minus the drill pipe pressure observed when circulating through the marine riser.

The second technique, shown in Figure 97, involves circulating the well through the choke line with the BOP closed and noting the pressure observed on a static kill line. If care is taken to insure that the same fluid is in both the choke line and the kill line, the kill line pressure will be equal to the circulating frictional pressure loss in the choke line at the given pump speed. Again, Ilfrey et al.[40] recommends adjusting the choke so that a midrange choke pressure is observed. If this is done, the circulating frictional pressure loss in the choke line is equal to the kill line pressure minus the choke pressure.

The third technique, illustrated in Figure 97, involves pumping down the choke line and up the marine riser with the BOP open. In this case, the pump pressure required for circulation, which is equal to the surface pressure on the choke line, is also equal to the circulating frictional pressure loss in the choke line.

A distinct disadvantage of the first two techniques is that while measuring the choke line friction, the well bore is subjected to a total pressure in excess of that imposed while drilling. The excess pressure is the frictional pressure loss in the choke line. The third technique has the advantage of not placing any additional back-pressure on the

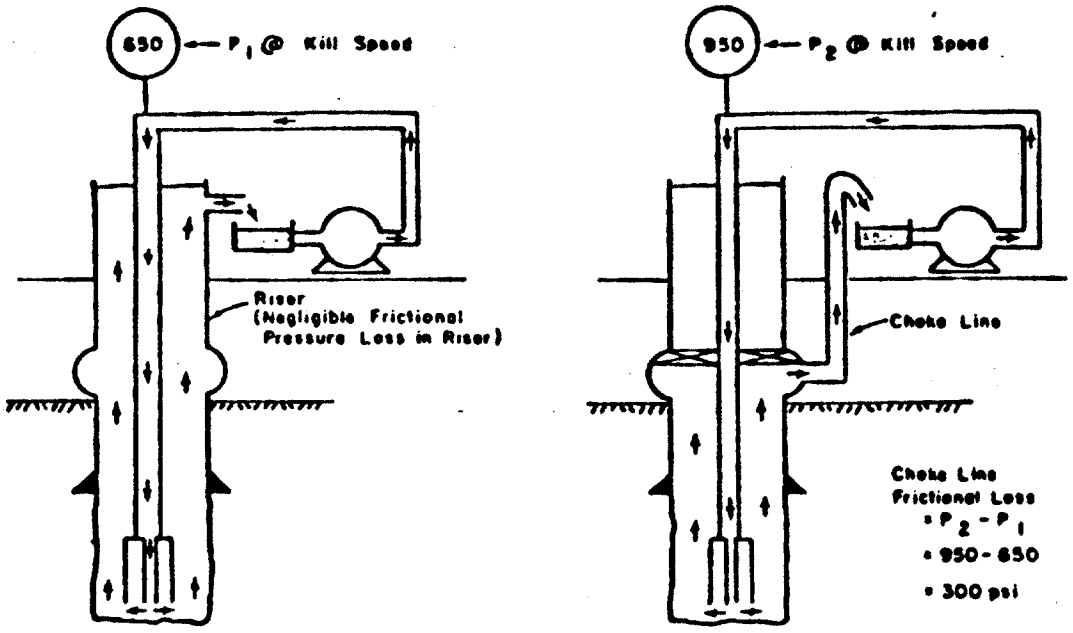

(a) MEASUREMENT OF REDUCED PUMP PRESSURE THROUGH MARINE RISER AND THROUGH CHOKE LINE

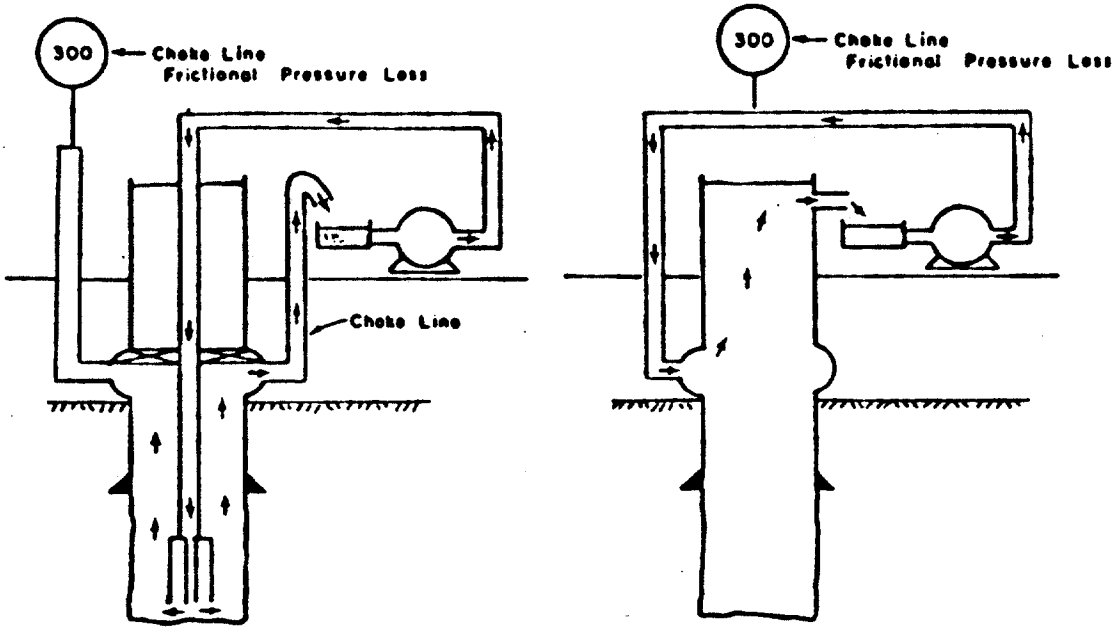

(b) Use of kill line as monitor line

(c) Reverse circulation down choke line

Figure 97: Techniques for Measurement of Frictional Pressure Loss in Choke Line

well. Thus, choke line friction can be measured without any fear of hydrofracture in the uncased portion of the well bore. As a consequence, more frequent measurements of friction could be made, say, twice a day. Then upon taking a kick, the most recent measurement of choke line friction would be more representative of the flow behavior of the mud currently in the well.

Circulation frictional pressure losses measured in the choke line of the experimental well are shown in Figure 98 for one mud. Pressures were measured using a 0-5000 psi Bourns model 520 transducer. The mud properties were measured in a standard rotational viscometer at 600 and 300 rpm, with samples taken from the return flow line at the surface. The solid line indicates values computed using the Fanning equation, the Colebrook function with absolute pipe roughness, ε, of 0.00095 in. and the use of plastic viscosity in the calculation of Reynolds numbers. For any consistent set of metric or english units, these equations are given by:

$$\Delta p_f = \left(\frac{fL}{d}\right) \frac{2\rho v^{-2}}{g_c} \tag{6.8}$$

where

$$\frac{1}{\sqrt{f}} = -4 \log\left(\frac{\varepsilon}{3.72d} + \frac{1.255}{N_R \sqrt{f}}\right) \tag{6.9}$$

$$N_R = \frac{d\bar{v}\rho}{\mu_p} \tag{7.0}$$

Note that there is good agreement between the measured and computed values.

6.5 EXPERIMENTAL RESULTS

Alternative pump start-up procedures that have been experimentally studied for the case of a floating vessel in deep water include the use of (1) a computed choke pressure schedule, (2) a casing pressure monitor, (3) multiple choke lines, and (4) a computed drill pipe pressure schedule. The first two alternatives, as illustrated in Figure 99, attempt to keep the pressure on the subsea wellhead constant by dropping

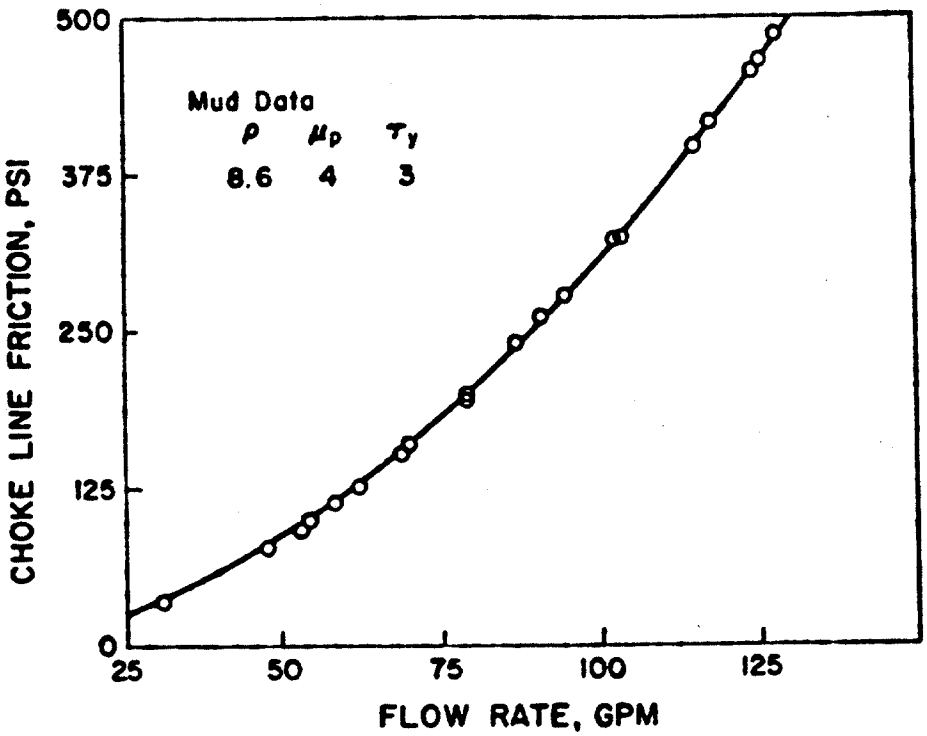

Figure 98: Comparison of Measured and Calculated Frictional Pressure Losses in a 1.995 in. I.D. Choke Line

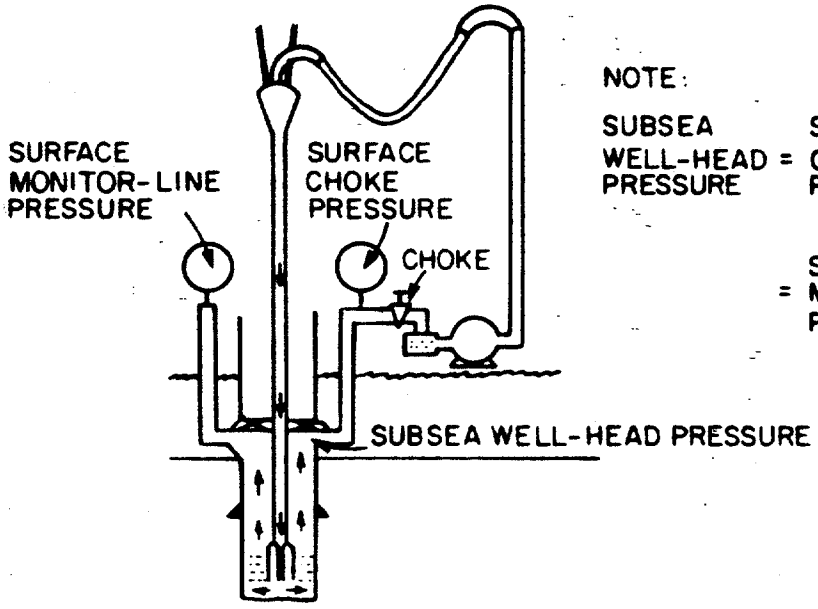

NOTE:

SUBSEA WELL-HEAD PRESSURE = SURFACE CHOKE PRESSURE + CHOKE-LINE HYDROSTATIC PRESSURE + CHOKE-LINE FRICTIONAL PRESSURE LOSS

= SURFACE MONITOR-LINE PRESSURE + MONITOR-LINE HYDROSTATIC PRESSURE

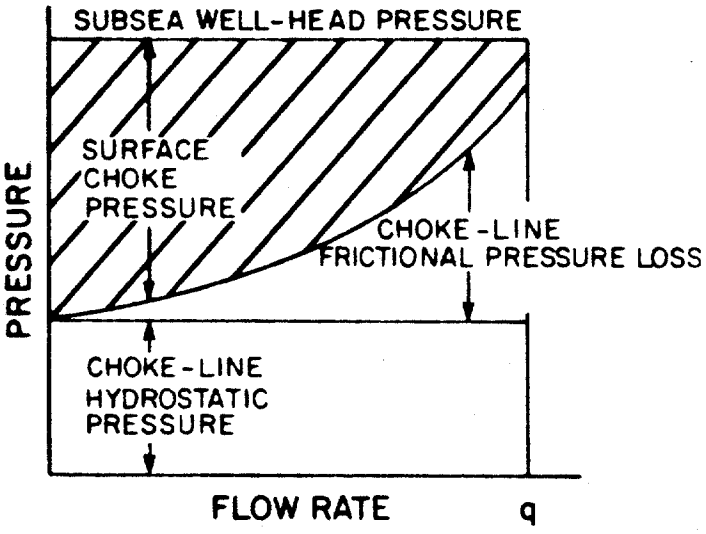

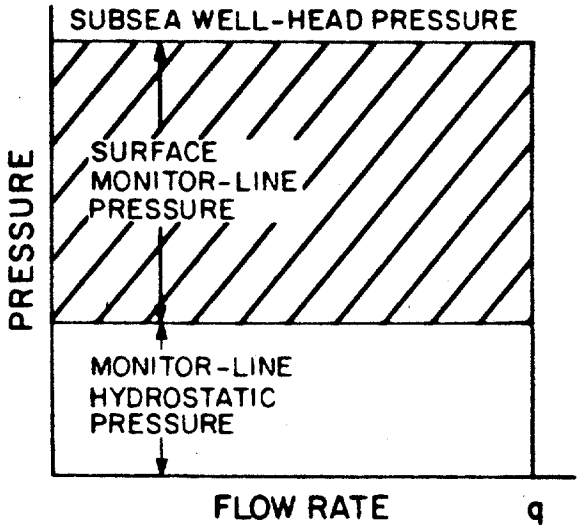

(a) Adjust Choke so that Surface Choke Pressure Decreases by an Amount Equal to the Choke Line Frictional Pressure Loss

(b) Adjust Choke so that Surface Monitor-Line Pressure Remains Constant at Shut-in Value

FIGURE 99. PROPOSED TECHNIQUES FOR PUMP START-UP

the choke pressure by an amount equal to the frictional loss in the choke line at the given intermediate pump rate. In the first case, the choke operator accomplishes this by adjusting the choke so that the choke pressure will follow the computed pressure schedule. In the second case, the choke operator adjusts the choke to maintain the static kill line pressure constant. Both of these techniques are completely applicable only for pump rates at which the circulating frictional pressure loss in the choke line is less than the shut-in choke pressure. If the choke and kill lines contain a fluid of different density than the current drilling mud, then application of the first technique is not practical, but the second technique can still be applied.

The third alternative procedure is based on greatly reducing the frictional pressure loss held against the well through use of multiple choke lines. For example, by taking half of the mud returns through each of two choke lines, the frictional pressure would be reduced to about one-fourth of the value observed using a single line. In most cases, the reduction is sufficient to allow the conventional constant-choke-pressure pump start-up procedure to be safely employed. A disadvantage of using this approach is that a redundant system is no longer on stand-by in the event the choke lines become plugged.

The fourth alternative is much the same as that sometimes used for a surface BOP stack. Since this technique makes use of the drill pipe pressure rather than the annular pressure, it is extremely important for the pump rate to be increased in a slow but steady manner.

Simulated well control exercises conducted using the research well facility indicate that the first three alternative procedures evaluated were all feasible. However, they all require considerable practice to master with a high degree of accuracy. The procedure which requires the least practice to master is the use of a computed pump start-up choke pressure schedule. This technique appears to be easier because changes in pressure caused by choke manipulation appear first in the choke pressure. Shown in Figure 100 are typical results obtained during training exercises. Pressure variations of the order of 150 psi above or below the target pressure are common. With considerable practice, these variations can be reduced to about 50 psi.

EXAMPLE 1 - Novice

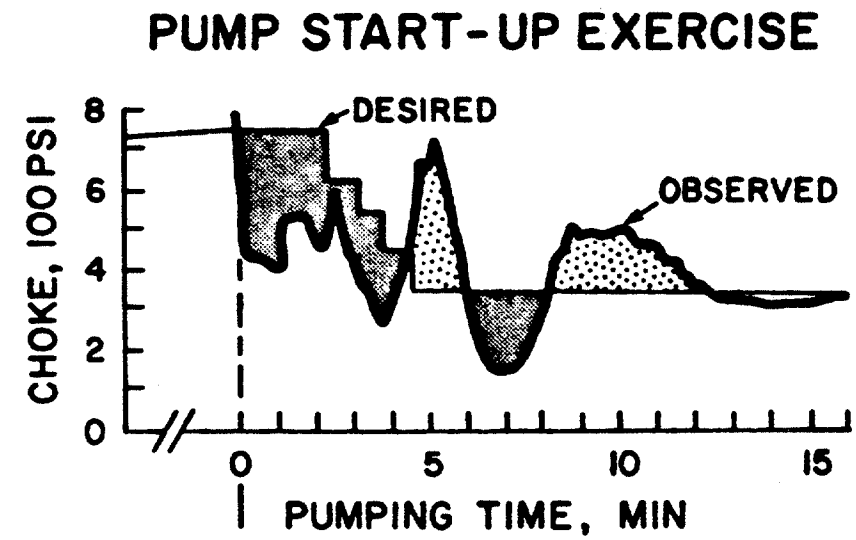

EXAMPLE 2 - Intermediate Experience

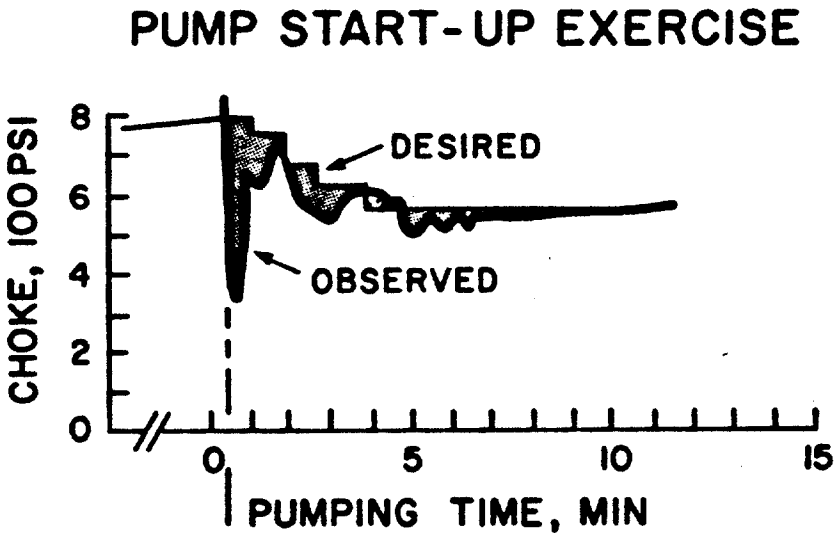

Figure 100: Typical Choke-Pressure Error Observed During Pump Start-up

CHAPTER 7

KICK PUMP-OUT PROCEDURES

7.1 Problem Description

One of the most significant problems encountered during the circulation of a gas kick on a deep water floating drilling vessel begins when the gaseous kick fluids reach the sea floor and begin rapidly displacing mud from the choke line. As discussed in Chapter 3, one of the main design features of the new research well facility was the ability to accurately model this phenomenon. Besides the pressures developed across the surface choke and the flow friction in the subsea choke line, it is the hydrostatic pressure of the long mud column in this same line which makes the largest contribution to the total back-pressure imposed on the well, below the closed BOP's. When circulating out a gas kick, this hydrostatic pressure will rapidly decrease when the gas reaches the sea floor, exits the large casing annulus and proceeds up the small subsea choke line. Coupled with a simultaneous loss of mud-flow frictional pressure in the line, the back pressure at the BOP's will be drastically reduced unless there is a corresponding increase in surface choke pressure to offset these losses. As rapid changes in choke pressure are required, choke operation can become much more difficult during this critical period. A slow response on the part of the operator or the control equipment will result in a (temporary) loss in BHP and the influx of a second kick into the well.

The reverse situation awaits the operator once the gas kick has been circulated to the surface. For when the choke line begins to refill with mud, the additional hydrostatic pressure of the rising mud column adds to the pressure at the well head. Now the operator must be prepared to reduce the pressure across the choke if he hopes to maintain the BHP constant. Failure to react quickly to this new situation will result in excess pressure at the well head to be followed by hydro-fracture of the bore hole.

Until the construction of the new well facility, anticipated well control problems for deepwater operations could only be studied using computer simulations to predict the pressure response of the well to various control procedures being evaluated. Reliable simulations, however, require both an accurate mathematical description of fluid flow behavior in the well and a detailed knowledge of equipment response. Considerable difficulty is associated with accurately modeling the flow behavior of mixtures of formation gas and drilling fluid in the complex geometry of a subsea well system.

Computer simulations of well-control operations for floating drilling vessels in deep water, such as the examples shown in Chapter 3, have indicated that very rapid changes in choke pressure are required when the gas reaches and exits the BOP stack at the seafloor. A major question to which this study was directed is whether a choke operator can react in step with rapidly changing conditions. Suggested solutions to this anticipated problem include:

1. Use of greatly reduced pump rates, perhaps just before the gas reaches the seafloor.
2. Use of multiple choke lines.
3. Use of larger diameter choke lines.
4. Development of a subsea choke

All of these suggested solutions attempt to give the choke operator additional reaction time by slowing the average upward fluid velocity in the choke line.

7.2 Experimental Results

Simulated well control exercises conducted in the experimental well have indicated that the demands placed on the choke operator are not as severe as previously anticipated. What is observed when the gas kick reaches the sea floor and begins entering the choke line is a natural tendency for the casing pressure to increase with time. Although some choke adjustments are required to maintain the desired drill pipe pressure, they are much less severe and frequent than expected, and can be handled by an experienced operator. Shown in Figure 101 are the results of a simulated well-control exercise in which a 20 bbl gas kick was pumped out at a kill speed of 2.5 bbl/min using a single choke line. In

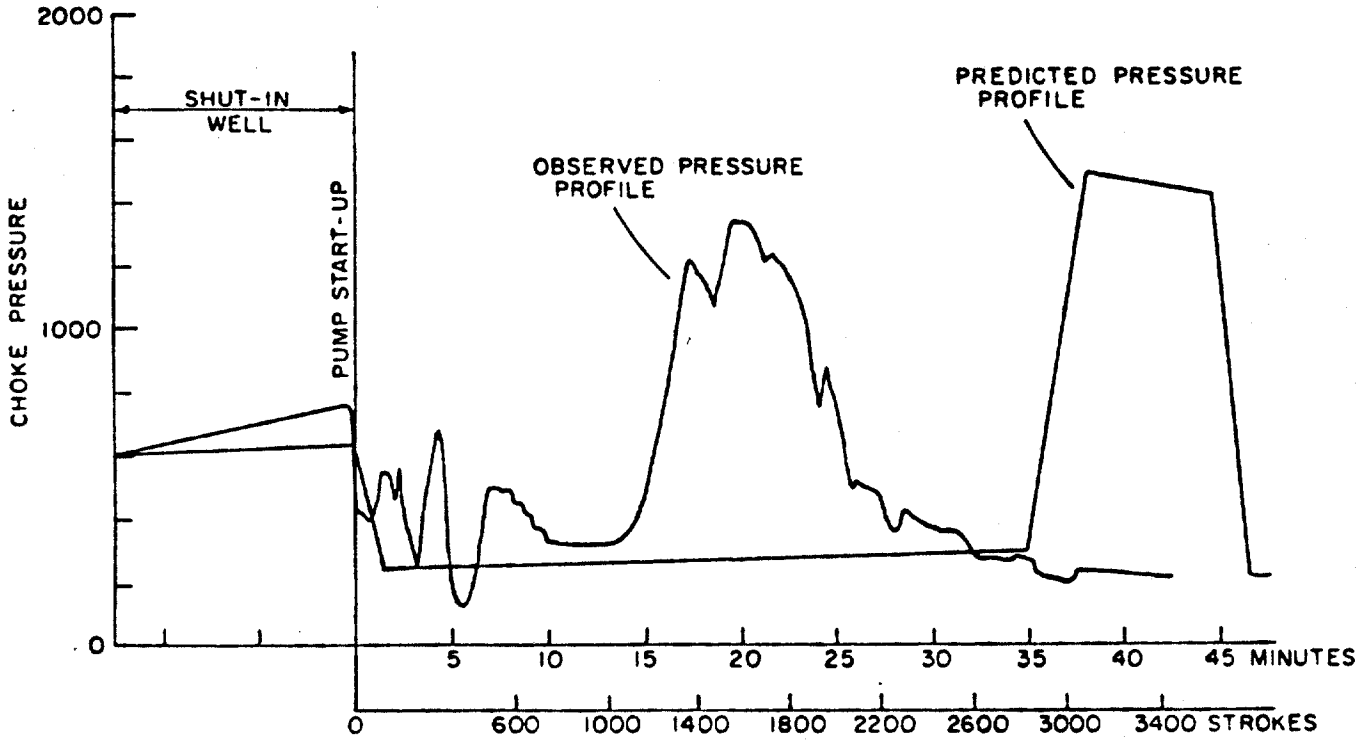

Figure 101: Comparison of Observed and Predicted Choke Pressure Profile for 20 BBL Gas Kick

this example the choke was operated by Mr. Robert Duhon of Chevron, USA. The exercise was handled with minor difficulties encountered when the trailing edge of the gas zone was displaced up the choke line. The choke adjustment was varied in this exercise between a maximum setting of 0.25 and a minimum setting of 0.10.

Although the problems encountered when a gas kick reaches the seafloor appear to be less severe than originally anticipated, they should not be taken too lightly. For many individuals, considerable practice is required to maintain the bottom hole pressure constant during the period that gas is being produced. Maximum difficulty tends to occur when the trailing edge of the gas region is being displaced up the choke line. Shown in Figure 102 are the results of a well control exercise conducted with a less experienced choke operator.

The results of conventional computer simulations of expected choke pressures for a perfect choke operator are also shown in Figures 101-10 for comparison to the observed behavior. Recall that the computer model ignores the effect of upward gas slippage with respect to the mud and the effect of gas-mud mixing. Note that the effect of gas-mud mixing is also significant, as observed peak pressures are lower than predicted because the displacement of mud from the choke line is not complete. Peak pressures observed were found to be strongly influenced by the gas influx rate at the time the kick is taken.

Shown in Figure 103 and 104 are additional examples of well control exercises, with additional parameters, such as monitor line pressure, pump speed, drill pipe pressure, and gas flow rate from the well, plotted for comparison. These results were obtained by experienced choke operators. Figure 103 gives results for an 18 bbl kick and a single choke line at a pump speed of 50 spm, which resulted in a choke line mud velocity of about 400 ft/min. Note that the maximum choke operator error is about 75 psi in this run. Luke Eaton and J. W. Goodwin of Shell Oil conducted this well control operation. Figure 104 is a run for similar conditions except that two choke lines were used when circulating the kick, thus reducing the mud velocity in the choke lines to about 200 ft/min. Note that the maximum choke operator error is about 40 psi. J. A. Grant and J. W. Goodwin of Shell Oil conducted this run.

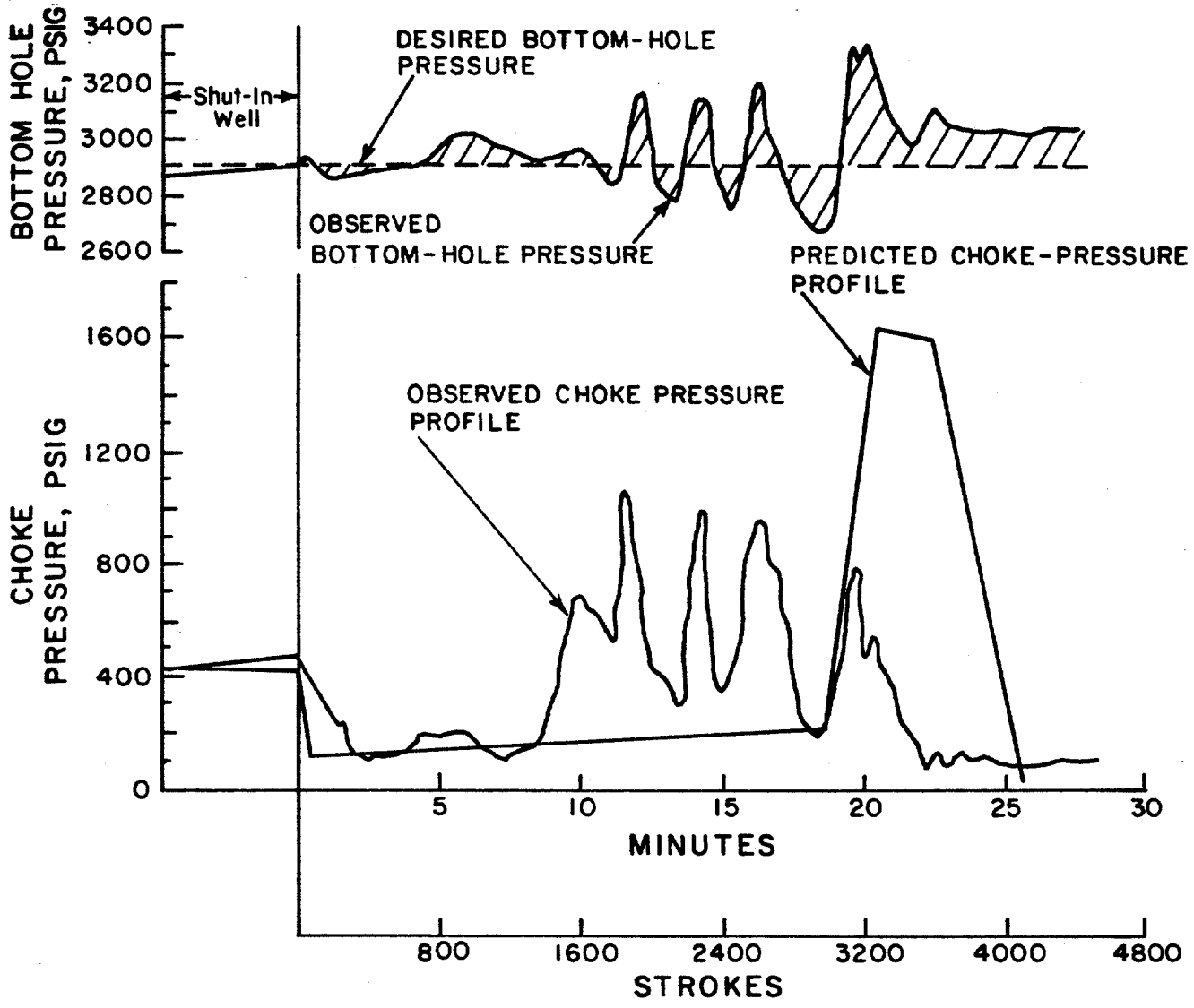

FIGURE 102. COMPARISON OF OBSERVED AND PREDICTED CHOKE PRESSURE PROFILES FOR 15 BBL GAS KICK

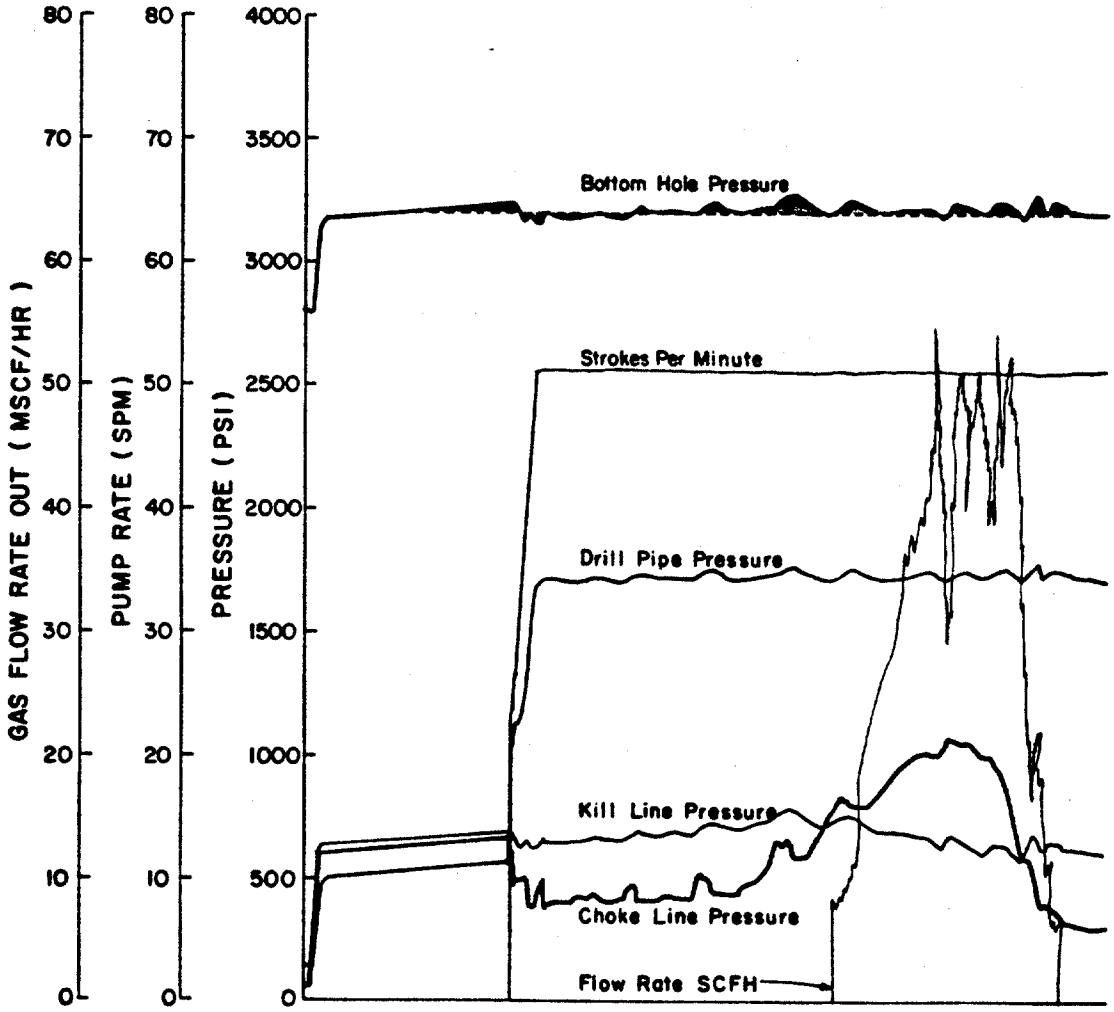

Figure 103: Well Control Operation for 18 bbl Kick Using Single Choke Line and an Experienced Choke Operator

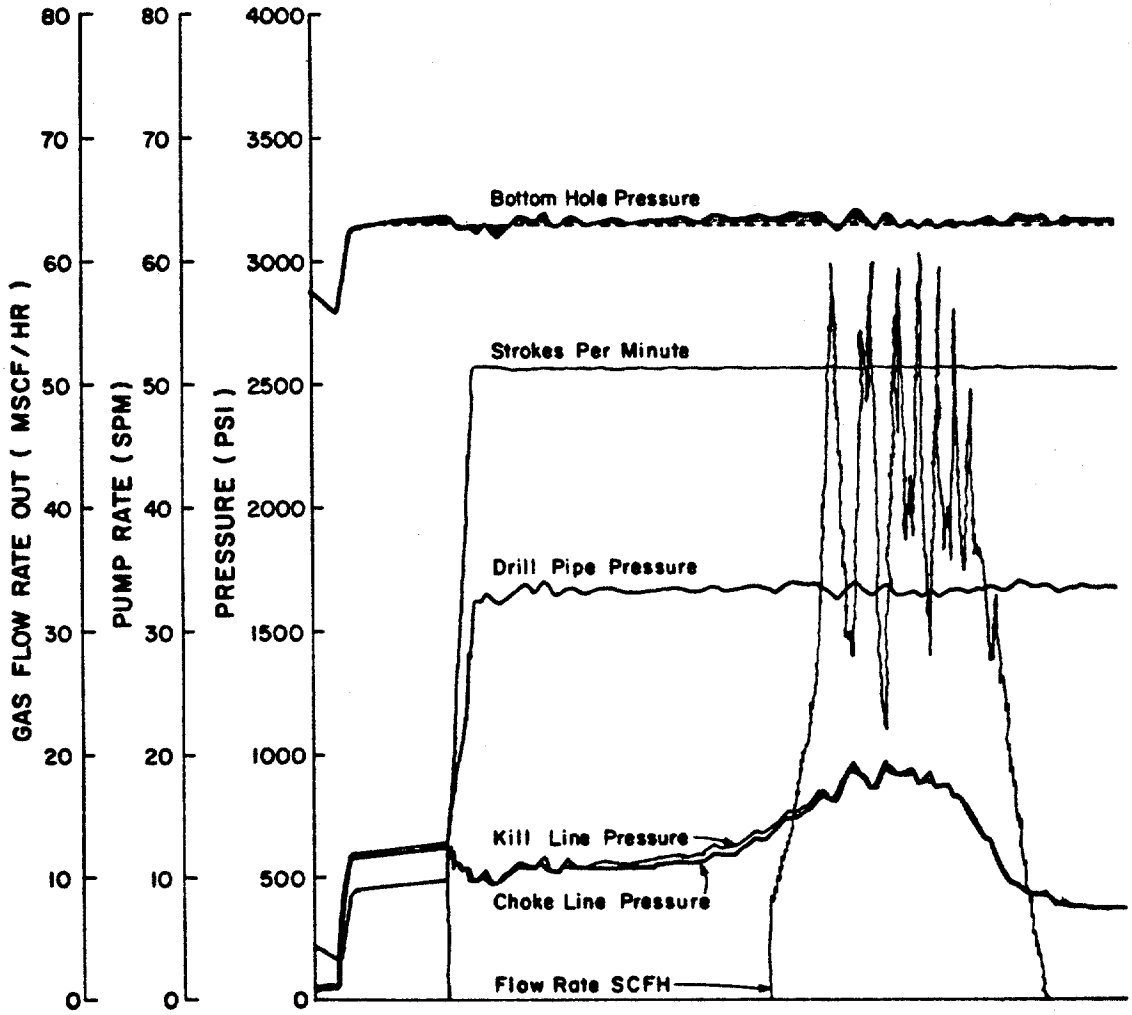

Figure 104: Well Control Operation for 18 bbl Kick Using Two Choke Lines and an Experienced Choke Operator.

Shown in Figure 105 is an experimental run similar to the one shown in Figure 103, except that a less experienced choke operator conducted the well control operations. Note that the maximum choke operator error is about 250 psi.

In general it was found that acceptable results could be achieved (with practice) if the pumping velocity in the choke line was less than about 500 ft./min. The most difficult portion of the kick circulation to control occurs when mud displaces the bottom of the gas kick region from the choke line. Improvement in the overall accuracy can be achieved through use of two choke lines, but one choke line appears adequate.

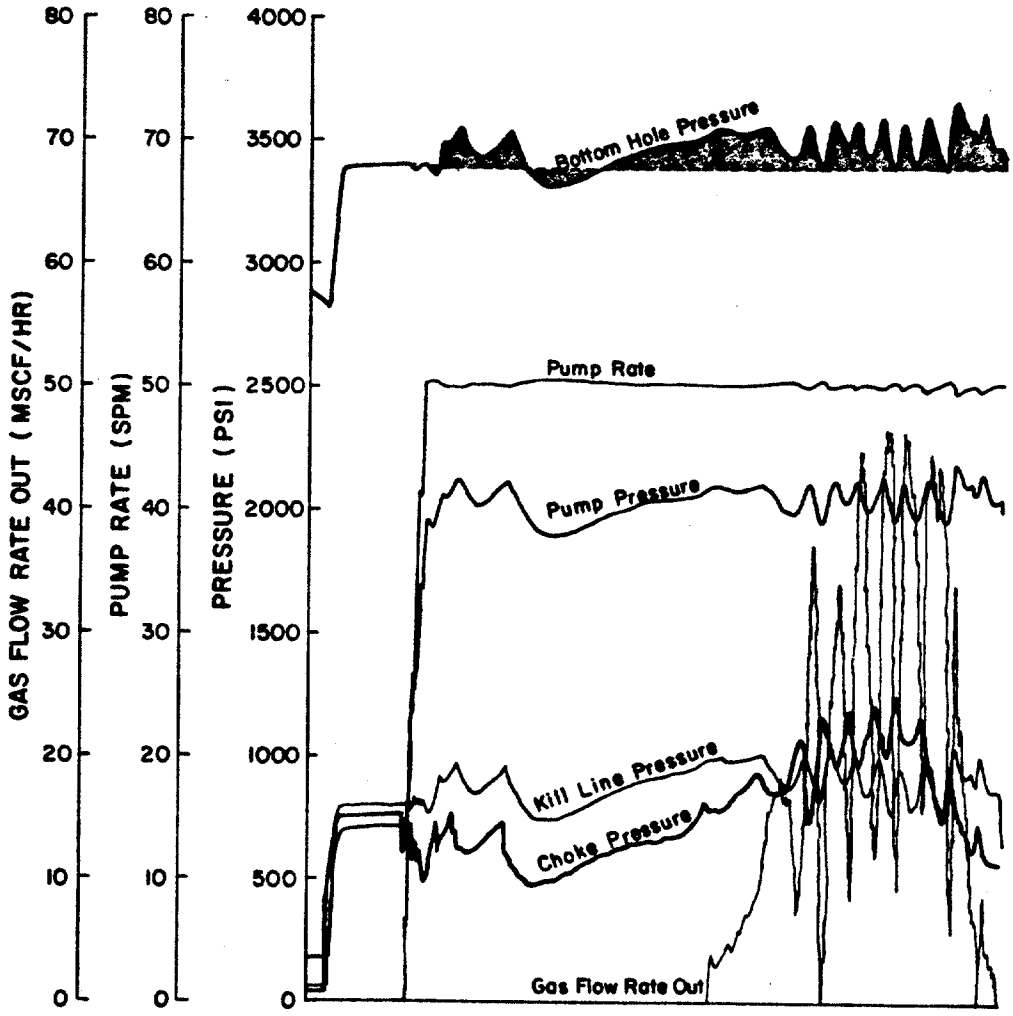

Figure 105: Well Control Operation for 18 bbl Kick Using Single Choke Line and Inexperienced Choke Operator

CHAPTER 8

IMPROVED MATHEMATICAL MODEL

Most modern pressure control procedures are evaluated at least in part by computer studies predicting the pressure response of the well during various phases of the pressure control operations. Computer simulations of pressure control operations are also carried out on a real time, interactive basis to train field personnel in those pressure control procedures selected for routine applications. Several pressure control simulators are manufactured specifically for such training exercises. The M.M.S. accepts training achieved on these simulators as partial fulfillment of the requirements for certification in pressure control operations.

Accurate computer simulation of pressure control operations require an accurate knowledge of fluid behavior in the well. The results shown in the previous chapter indicates that the assumptions used at present in blowout control simulations do not always predict actual well behavior when gas is present. Two assumptions found to be at fault are (1) that gas influx enters the wellbore as a continuous slug which occupies the entire annular cross section of the well and remains in this configuration during subsequent pressure control operations, and (2) that the gas zone does not migrate upward through the column of drilling fluid, but moves instead at the same velocity as the circulating drilling fluid.

The primary objectives of this phase of the research was to experimentally determine for gaseous formation fluids and the flow geometry present on a floating drilling vessel:

(1) the bubble rise velocity of the gas contaminated zone
(2) the two phase flow patterns occuring during pressure control operations
(3) the gas concentration in the gas contaminated zone
(4) the two phase frictional pressure gradients occuring during pressure control operations, particularly in the subsea choke

lines where these gradients tend to be quite significant and

(5) the development of an improved computer model for accurately predicting well behavior during well control operations on a floating drilling vessel in deep water.

Both circulating and noncirculating well conditions were included in the study. The flow geometry effect was considered by using segments of annuli and tubes. The combined effect of different sizes of annuli and tubes connected in series could not be studied because of size limitations of the experimental apparatus.

An extensive literature search was made in each of the fluid mechanics areas addressed. Considerable information was obtained on bubble rise velocity, on flow patterns, and on liquid hold-up and two phase flowing gradients. This material was too extensive for detailed coverage in this report, but can be found in the Master's Thesis of Vicente Casariego[41].

8.1 Experimental Study of Gas Slip and Flow Patterns

8.1.1 Apparatus and Procedure

After completing a review of the previous investigations related to the determination of flow patterns, gas slip velocity, and gas concentrations in a well during pressure control operations, it was felt that considerable additional experimental work would be required before any major improvements in the accuracy of computer simulations of pressure control operations could be achieved. As was noted in the previous chapter, most of the previous work was done in tubes or extended liquids rather than in an annulus. Also, essentially all of the flow pattern work was done for steady state conditions involving the continuous injection of gas and liquid into the bottom of the tubular section. This previous flow pattern work was directed towards an understanding of producing wells, especially those producing by means of artificial gas injection using gas lift valves. Almost no previous work towards an improved understanding of two-phase flow patterns occuring during pressure control operations was found. Thus, the next phase of this study involved the design and construction of an experimental apparatus for modeling an annular well geometry. After construction of the model was completed, several types of experiments were conducted.

A diagram of the model constructed is shown in Figure 106. the main feature of the model is the 32 ft vertical tube having an internal diameter of 6.375 and an external diameter of 6.625. This tube stimulates the casing or bore hole of a well. The casing consists of four sections of transparent, PVC pipe joined by flanges. The lower end of the casing is attached to a pressure vessel by means of a ball valve. This vessel has a pressure relief valve to prevent the pressures in excess of 80 psig, the working pressure of the PVC tube. The upper end of the casing is connected to a gas/liquid separator vessel by means of a tube having the same diameter as the casing.

In order to simulate drill pipe within the casing a 2 inch diameter tube of PVC with a check valve attached to its lower extreme could be placed in the casing.

Liquid could be circulated down the drill string and up the annulus by means of a centrifugal pump. Gas could be injected into the bottom of the model either from the pressure vessel by means of a quick open ball valve or in a continuous manner by means of a pressure regulated gas supply.

Mixtures of water and glycerine were used to investigate the effect of the viscosity of the flow patterns. The range of liquid viscosities was from 1 to 146 cp, and the range of liquid densities was from 1 to 1.231 gr/cc, measured at 29°C, respectively. The liquid phase was colored with green food dye to obtain contrast in the photographs of the bubbles. A 35 mm camera loaded with Kodak Tri-X pan film was used. Two neon-tubes and two flooding lamps were used to light the casing section of interest. A mirror was arranged near a section of the vertical column to allow opposite sides of the column to be simultaneously photographed. The negatives were anlayzed in an enlarger. Finally, to analyze whether the small gas bubbles are incorporated to the main initial bubble, a movie camera was used.

The initial experimental procedures used in the new apparatus were designed to test the Bourgoyne-Rader gas slip velocity correlation that had been developed in a prior LSU study based on data collected by Rader[42], by Ward[43], and by Koederitz[44]. The experimental apparatus used in these previous studies were inferior to the new apparatus in that (1) circulation was possible only in very small, 0.58 in diameter models

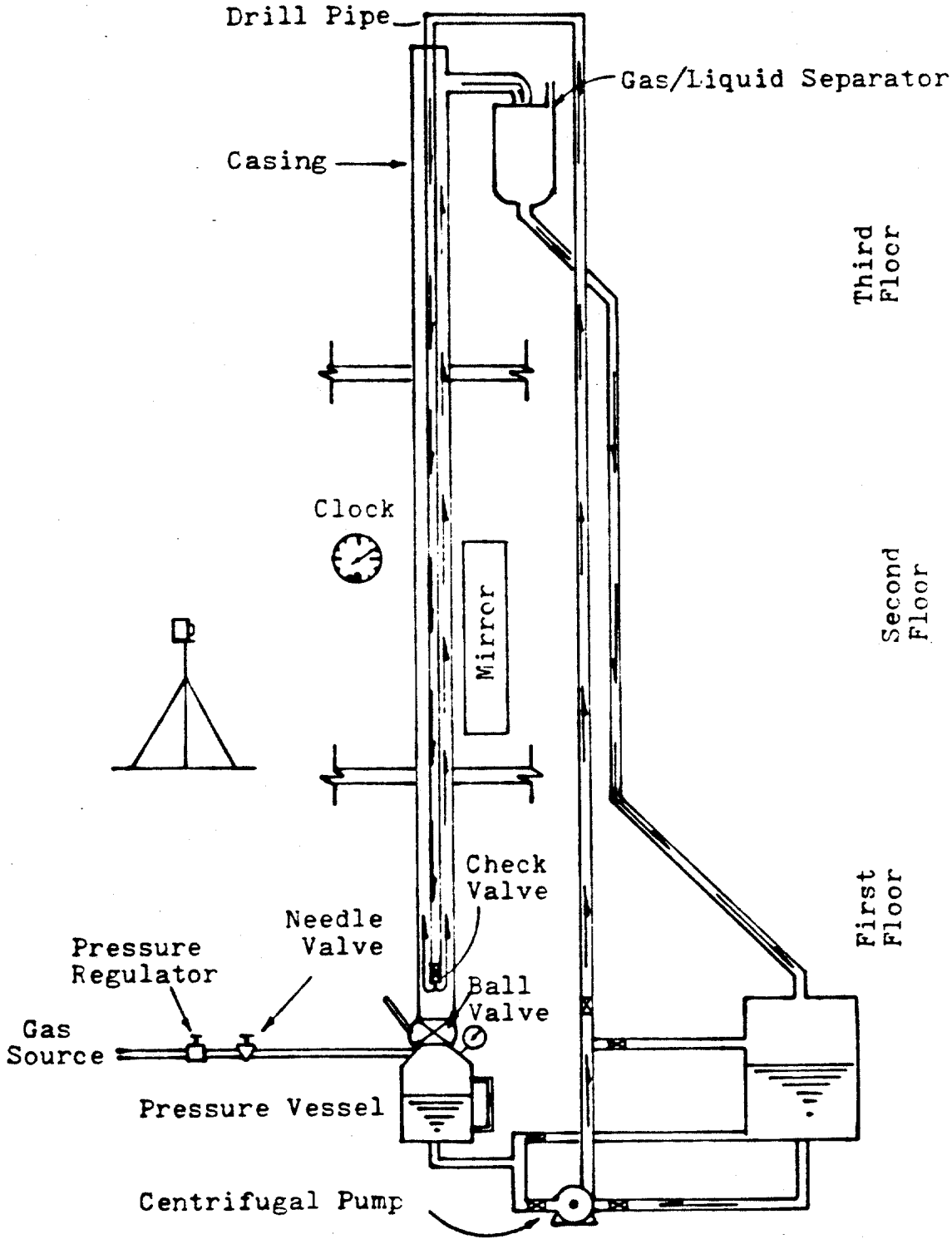

Figure 106: Diagram of the Model

and (2) the large diameter models were relatively short, having a maximum length of 12 ft. Also, the previous studies included only a fully developed slug flow pattern which occurs for very high gas injection rates.

Application of the Bourgoyne-Rader correlation to tests conducted in a 6000 ft. well by Mathews,[38] indicated that real well behavior could not be adequately described using this correlation. Mathews concluded that the difference in predicted and observed well behavior was probably due to the presence of smaller gas bubbles in the 6000 ft. well during simulated pressure control operations. The observed pressure behavior of the well indicated a lower gas migration velocity than obtained through use of the Bourgoyne-Rader correlation.

The first set of experiments were conducted to measure the slip velocity of a wide range of gas bubble sizes for several different liquid flow rates and liquid viscosities. The experimental procedure followed is illustrated in Figure 107.

The desired liquid was placed in the holding tank (1). The liquid was pumped into the wellbore (2) using the centrifugal pump (3). A throttle valve (4) was fixed at the desired setting during model fill-up and the effective pump characteristics were defined during fill-up by plotting the change in fluid height in the model wellbore with time versus the bottom-hole pressure (5). After fill-up, the ball valve (6) was closed and the desired gas volume was placed in the pressure chamber (7) by pressuring the upper portion of the chamber using a pressure regulated gas supply (8) and draining liquid from the lower portion of the chamber through the drain valve (9). Gas injection was accomplished by rapidly opening the ball valve (6). The velocity of the gas slug or bubble was obtained by noting the elapsed time (10) for the top of the slug to pass between two markers (11) at the second floor level. The gaseous region was photographed using both a 35 mm camera and a 16 mm movie camera. Slug length was estimated from the photographs.

The second set of experiments were conducted to determine the effect of constant flow rate on the flow pattern of a gas kick, and particularly, on the initial gas distribution. These experiments were made for different fluid rates and liquid viscosities. The experimental procedure followed is illustrated in Figure 108.

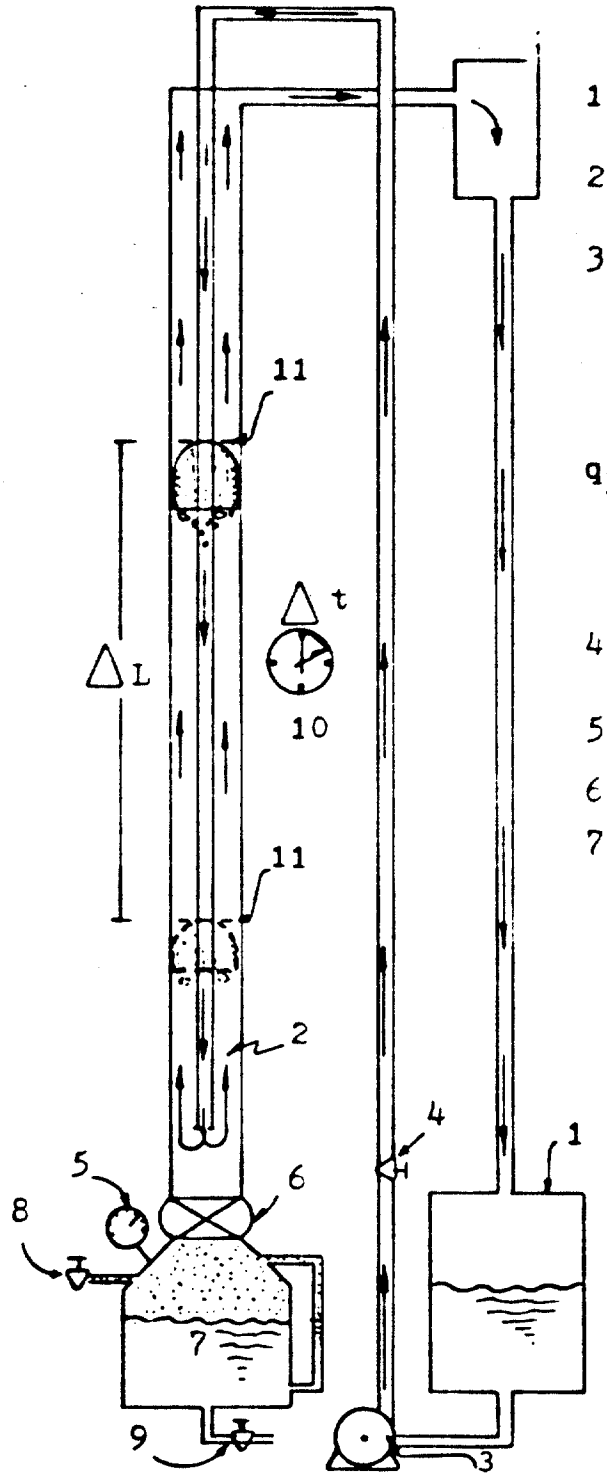

1. Store desired gas volume in pressure vessel (7).
2. Set pump throttle valve (4).
3. Note fill-up time to various heights and plot pump flow rate, q_L, versus bottom hole pressure.

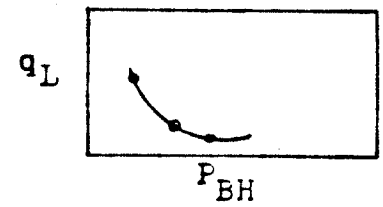

4. Estimate final flow rate at P_{BH}.
5. Open ball valve (6).
6. Measure ΔL and Δt.
7. Photograph the gas bubble.

Figure 107: Experimental Procedure Followed in Bubble Rise Velocity Measurements

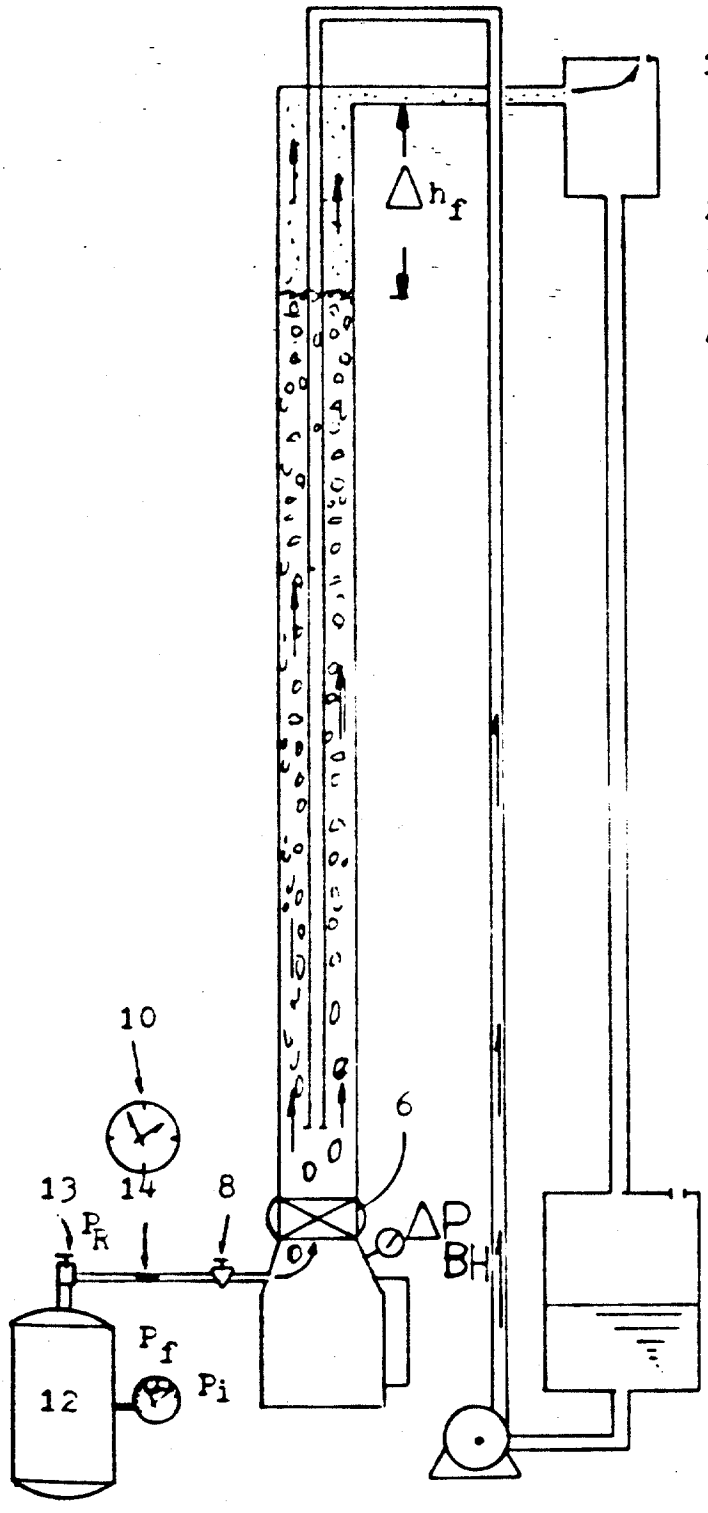

1. Fill column with liquid and adjust liquid flow rate as described previously.
2. Fill gas tank to P_i.
3. Set regulator (13) to P_R.
4. Set needle valve (8) and open ball valve (6).
5. Photograph the initial slug formed (leading edge) and state flow pattern achieved
6. Note time for tank to fall to Pressure P_f.
7. Close valve and record ΔP_{BH} and/or Δh_f .

Figure 108: Flow Pattern Observations

The model fill-up was made as it was described above. The ball valve (6) remained open. The gas tank (12) was filled to a pressure P_i and the regulator (13) was set to obtain a reduced pressure P_R. The gas flow rate was controlled by setting the needle valve (8) at a desired opening. The quick opening valve (14) was opened suddenly and simultaneously the time counter (10) was turned on. Both the leading edge of the gas and the developed flow pattern were photographed. The time elapsed for the tank pressure (12) to fall from P_i to P_f was noted. The ball valve (14) was closed. The final static bottom hole pressure was recorded to obtain the change in bottom-hole pressure and/or the change on the liquid level was recorded.

8.1.2 Experimental Results For Gas Slip

Before the results, it is convenient to describe the relations between the parameters used in developing the present work. Figure 109 illustrates the nomenclature and describes the velocities and their relationships. The velocities are presented by vectors and are scaled to show their relationship. The definition of the terms is as follows:

A is the fixed observation point or reference point.

v_{L-} is the average velocity of the liquid flowing behind the gas contaminated region.

v_{L+} is the average velocity of the liquid flowing ahead of the gas contaminated region.

v_b is the measured velocity of the leading edge of the gas contaminated region.

v_E is the component of the gas velocity caused by gas expansion.

$v_b - v_{L-}$ is the slip velocity of the leading edge of the gaseous region with respect to the liquid below.

$v_b - v_{L+}$ is the slip velocity of the leading edge of the gaseous region with respect to the liquid above. When slug flow develops at the top of the gaseous region and v_{L-} is zero, this relative velocity is equal to the limiting gas slug velocity v_{bo} as it is defined by Dumitrescu's equation, or as it is measured in a closed end tube.

8.1.2.1 Gas Slip in a Tube

The first runs were performed in the 6.375 in internal diameter

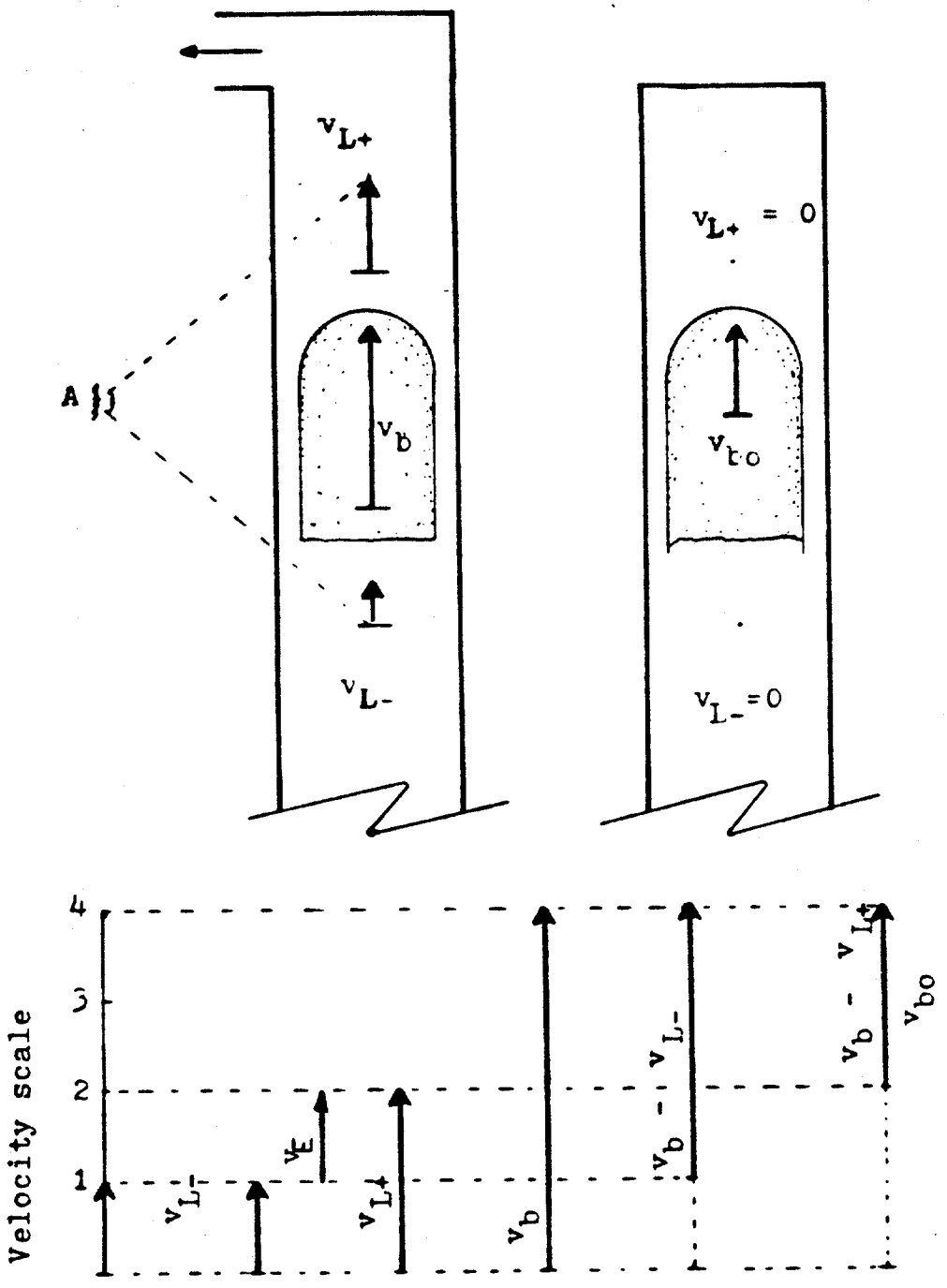

Figure 109: Definition of Velocities and Its Relationships

Figure 109: Definition of Velocities and Its Relationships

tube. These runs were aimed at determining the effect of the liquid viscosity on the limiting velocity of gas bubbles in a large vertical tube. Previous experimental data were not available for tube diameters greater than about 2 in. Tap water and a 146 cp solution of glycerine were used as liquid phases. All measurements were obtained in static liquids, i.e., with v_{L-} equal to zero. The obtained data are presented in Table 14 and were plotted in Figure 110 after correcting for gas expansion effects. The cylindrical bubble velocities, corrected by gas expansion effect were in good agreement with the velocity predicted by Dumitrescu's theory.[45]

8.1.2.1 Gas Slip in an Annulus

The velocities of both lenticular bubbles and large slugs in quiescent fluids were determined in a 6.375 in by 2.375 in annulus. The obtained data for water, 80 cp glycerine solution and 146 cp glycerine solution are presented in Table 15a to Table 15c. Shown in Figure 111 are the measured velocities as a function of the equivalent diameter of the bubbles. The actual velocities of the bubbles were in agreement with theoretical values up to an equivalent diameter of around 1.8 inches. From 1.8 to 3 inches of equivalent diameter the bubble velocity for lenticular bubbles. The boundary effects caused by the annular walls became more pronounced as the bubble size was increased.

From around 3.5 to 9 inches of equivalent diameter the bubbles appeared to reach a limiting slug velocity of about 1.55 ft/sec. However, the gas slugs were not well defined. Fully developed slugs (d_e > 9 in) increased their velocities up to 2 ft/sec. The phenomenon was believed to be due to the expansion of the bubble as it rose in the open tube. The more pronounced effect in the high viscosity fluid is explained by the closer agreement between the theoretical slug length and observed slug length. The injected gas was indeed traveling as a single cylindrical bubble and gas expansion occurred at a higher rate. However, in water, bubble fragmentation was observed to occur due to turbulence, and only a fraction of the injected gas traveled in the main gas body. Unfortunately, the pictures of gas bubbles in water lack good definition and no actual slug length was reported.

The measured velocity of the gas slugs was corrected for expansion effects by computing bubble expansion using the theoretical slug length. The corrected bubble velocity is plotted in Figure 112. The limiting

FLUID	Measured Velocity v_b (ft/sec)	Bubble Length Theoretical[1] (ft)	Bubble Length Actual[2] (ft)	Non-Expanding Bubble Velocity $v_b - K_{Lv} v_{L+}$ (ft/sec)	Non-Expanding Bubble Velocity Eq.4.1 (ft/sec)
Water	1.475	1.18	-	1.427	1.44
= 1.0 cp	1.519	1.76	-	1.445	1.44
= 1.0	1.506	1.50	1.08	1.444	1.45
	1.521	2.00	1.33	1.437	1.44
	1.567	2.50	1.69	1.458	1.46
	1.580	3.12	1.94	1.445	1.45
	1.740	6.17	-	1.442	1.52
Glycerine	1.553	1.67	-	1.449	1.467
= 146 cp	1.565	1.43	1.50	1.475	1.493
= 1.231	1.583	1.91	1.97	1.462	1.48
	1.614	2.38	2.38	1.460	1.49
	1.613	2.96	-	1.422	1.47
	1.983	5.86	-	1.517	1.73

[1] Gas volume injected, corrected for average gas pressure during the velocity determination, divided by the cross sectional area of the tube.

[2] The overall length of the leading slug determined photographically.

Table 14: Velocity of Cylindrical Bubbles in A 6.375 in. Tube

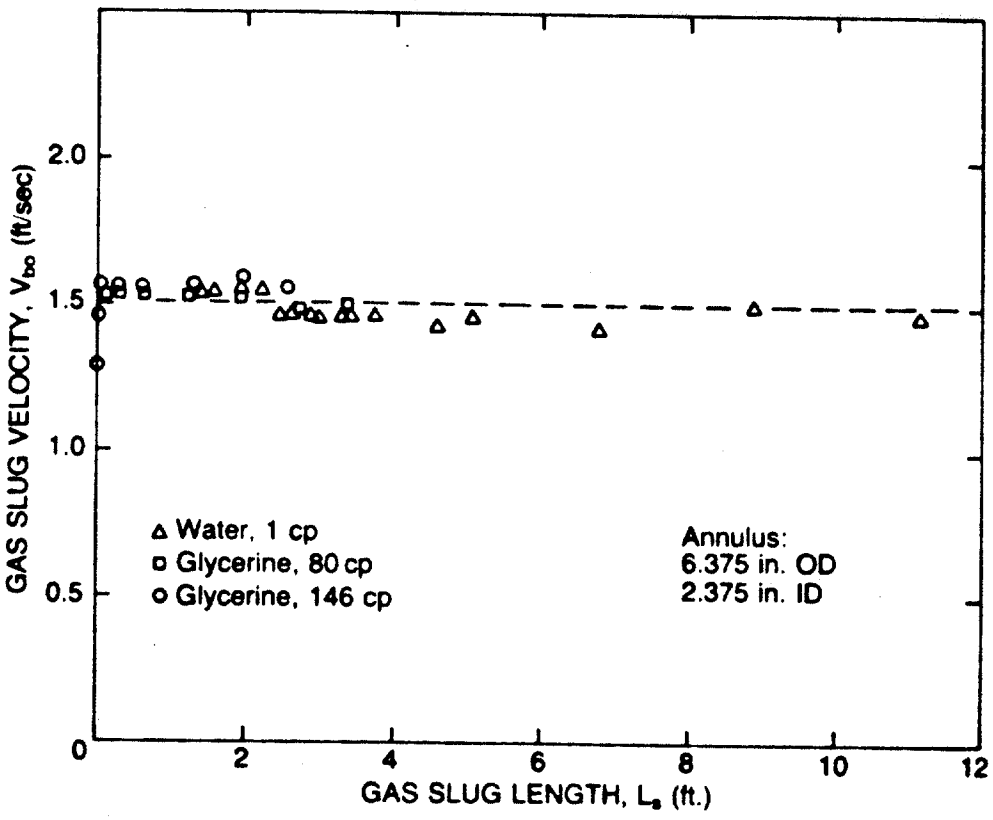

Figure 110: Velocity of Cylindrical Bubbles Versus Slug Length for Low and High Viscosity Liquids. Tube Diameter 6.375 in.

Equivalent Diameter[1], d_e (inches)	Measured Velocity, v_b (ft/sec)	Non-Expanding Bubble Velocity Eq. 2.63 (ft/sec)	$v_b - K_{Lv} v_{L+}$ (ft/sec)	Eq. 4.2 (ft/sec)	Bubble Length[2] Theoretical (ft)
1.66	1.28	1.771	-	-	.007
2.01	1.41	1.771	-	-	.013
2.15	1.41	1.771	-	-	.015
2.45	1.42	1.771	-	-	.023
2.61	1.47	1.771	-	-	.028
2.95	1.45	1.771	-	-	.041
9.70	1.55	1.771	1.471	-	1.450
10.01	1.56	1.771	1.477	-	1.590
10.51	1.57	1.771	1.472	1.41	1.850
10.85	1.57	1.771	1.463	1.40	2.020
11.22	1.56	1.771	1.468	1.39	2.240
11.57	1.57	1.771	1.465	1.40	2.460
11.84	1.58	1.771	1.466	1.40	2.640
12.22	1.59	1.771	1.468	1.41	2.890
12.41	1.58	1.771	1.450	1.40	3.030
12.80	1.61	1.771	1.464	1.42	3.330
12.92	1.61	1.771	1.460	1.42	3.430
13.33	1.62	1.771	1.455	1.42	3.760
14.27	1.63	1.771	1.425	1.42	4.610
14.72	1.69	1.771	1.457	1.47	5.070
16.24	1.74	1.771	1.410	1.50	6.800

[1] Gas volume injected, corrected for average gas pressure during the velocity determination, expressed as the diameter of sphere which would contain this volume.

[2] Gas volume injected, corrected for average gas pressure during the velocity determination, expressed as the length of annulus which would contain this volume.

Table 15a: Velocity of Air Bubbles in an 6.375 in. By 2.375 in. Annulus through Quiescent Water

Equivalent[1] Diameter, d_e (inches)	Measured Velocity, v_b (ft/sec)	Non-Expanding Bubble Velocity Eq. 2.63 (ft/sec)	$v_b - K_{Lv} v_{L+}$ (ft/sec)	Eq. 4.2 (ft/sec)	Bubble Length[2] Theoretical (ft)
0.75	1.27	1.235	-	-	-
0.74	1.03	1.235	-	-	-
0.77	1.15	1.235	-	-	-
0.91	1.12	1.235	-	-	-
0.97	1.20	1.235	-	-	-
1.29	1.32	1.235	-	-	-
1.60	1.38	1.235	-	-	-
1.71	1.37	1.235	-	-	-
2.19	1.44	1.235	-	-	-
2.77	1.49	1.235	-	-	.033
3.45	1.53	1.235	1.52	1.51	.065
4.68	1.54	1.235	1.49	1.49	.163
5.82	1.56	1.235	1.53	1.47	.326
7.44	1.57	1.235	1.53	1.45	.652
9.30	1.61	1.235	1.53	1.46	1.275
10.79	1.65	1.235	1.52	1.42	1.993
12.00	1.67	1.235	1.49	1.47	2.742
12.85	1.73	1.235	1.50	1.51	3.365

[1] Gas volume injected, corrected for average gas pressure during the velocity determination, expressed as the diameter of sphere which would contain this volume.

[2] Gas volume injected, corrected for average gas pressure during the velocity determination, expressed as the length of annulus which would contain this volume.

Table 15b: Velocity of Air Bubbles in an 6.375 in. By 2.375 in. Annulus through a Quiescent 80 cp Glycerine Solution

Equivalent[1] Diameter, d_e (inches)	Measured Velocity, v_b (ft/sec)	Non-Expanding Bubble Velocity Eq. 2.63 (ft/sec)	$v_b - K_{Lv} v_{L+}$ (ft/sec)	Eq. 4.2 (ft/sec)	Bubble Length Actual[3] (ft)	Theoretical[2] (ft)
1.28	1.26	1.157	-	-	-	-
1.74	1.34	1.157	-	-	-	-
2.16	1.47	1.157	-	-	-	-
2.73	1.60	1.157	-	-	-	-
3.45	1.57	1.157	-	-	-	-
4.66	1.68	1.157	1.67	1.61	0.23	0.16
5.86	1.59	1.157	1.57	1.48	0.50	0.32
7.39	1.59	1.157	1.55	1.45	0.88	0.64
9.44	1.65	1.157	1.57	1.48	1.63	1.33
10.71	1.73	1.157	1.60	1.53	2.41	1.94
10.69	1.73	1.157	1.60	1.53	2.46	1.94
11.77	1.75	1.157	1.57	1.54	2.67	2.59

[1] Gas volume injected, corrected for average gas pressure during the velocity determination, expressed as the diameter of sphere which would contain this volume.

[2] Gas volume injected, corrected for average gas pressure during the velocity determination, expressed as the length of annulus which would contain this volume.

[3] Slug length determined from photographs.

Table 15c: Velocity of Air Bubbles in an 6.375 in. By 2.375 in. Annulus through a Quiescent 146 cp Glycerine Solution

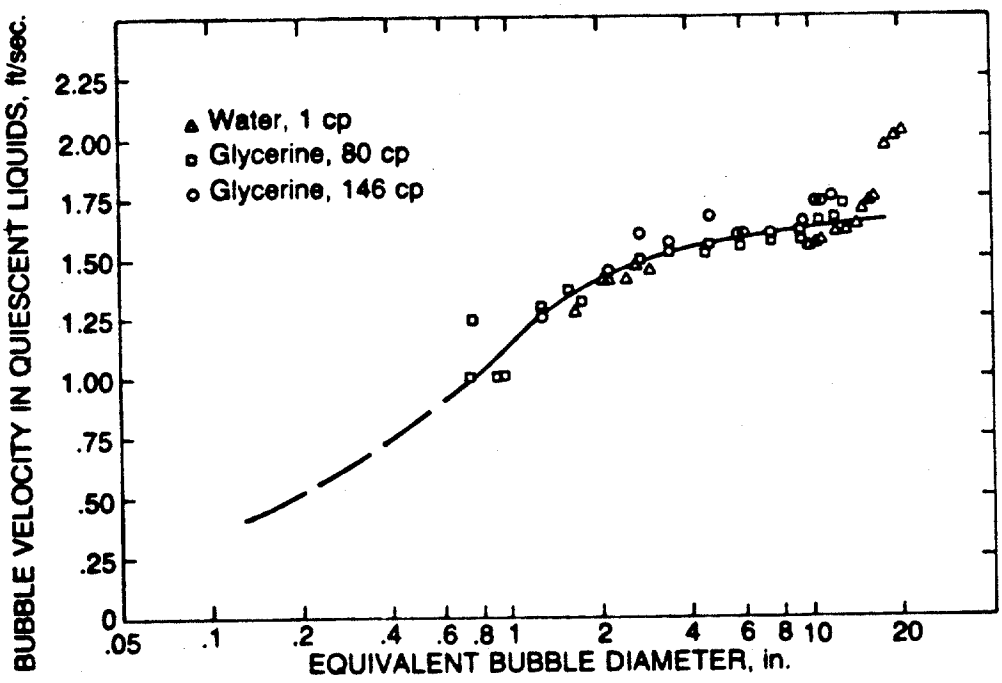

Figure 111: Measured Bubble Velocity Versus Equivalent Diameter of the Bubbles in A 6.375 in by 2.375 in Annulus (Zero Liquid Velocity)

velocity appeared to be 1.51 ft/sec which is in good agreement with the value predicted by theory for a non-expanding bubble.

Also shown in Tables 15a-c are values of bubble rise velocity computed using equations developed by Rader, Bourgoyne and Ward. Note that values predicted tended to be in agreement with the values obtained for fully developed gas slugs in water (Table 15a), however, this equation predicted velocities around 33% lower for the fully developed gas slugs flowing in high viscosity fluids (Tables 15b and 15c).

8.1.3 Flow Pattern Observations

In the former section, it was shown that the basic velocity of gas slugs or limiting velocity of cylindrical bubbles is around 1.5 ft/sec for the tubes and annulus dimensions of actual wells. On the other hand, Rehm[46] states that it is generally accepted that gas in annulus will rise at about 0.28 ft/sec. Such a velocity would require a very small equivalent bubble diameter of around .026 inches, rising in water, and further indicate a gas migration in bubble flow pattern.

In an attempt to determine what flow pattern will rule the migration of a given gas kick, a qualitative series of tests were run in the laboratory equipment previously described. Constant gas flow rates ranging from a fraction of barrel per minute to around 4 barrels per minute were fed to the annulus limited by a 6.375 in casing and a 2.375 in drill pipe. The results are presented in Tables 16-17.

The high viscosity liquids showed a tendency to facilitate the generation of initial slugs; for the range of flow rates studied, the initial slug length was almost proportional to the increase of flow rate. Practically, there was no difference in the observed behavior of the 80 cp fluid and the 146 cp fluid. A single curve describes the trend of both fluids. The low viscosity fluid (water) showed a different profile. Even when there is an increase in initial slug size with increase in gas velocity, the change is a gradual one. The gas slug increases slowly with the gas flow rate up to around 1.2 ft/sec superficial gas velocity. Further increment in gas flow rate, resulted in a sharp increase of flowing gas fraction of 0.36. The flow patterns were observed to be related to the initial slug sizes as follows:

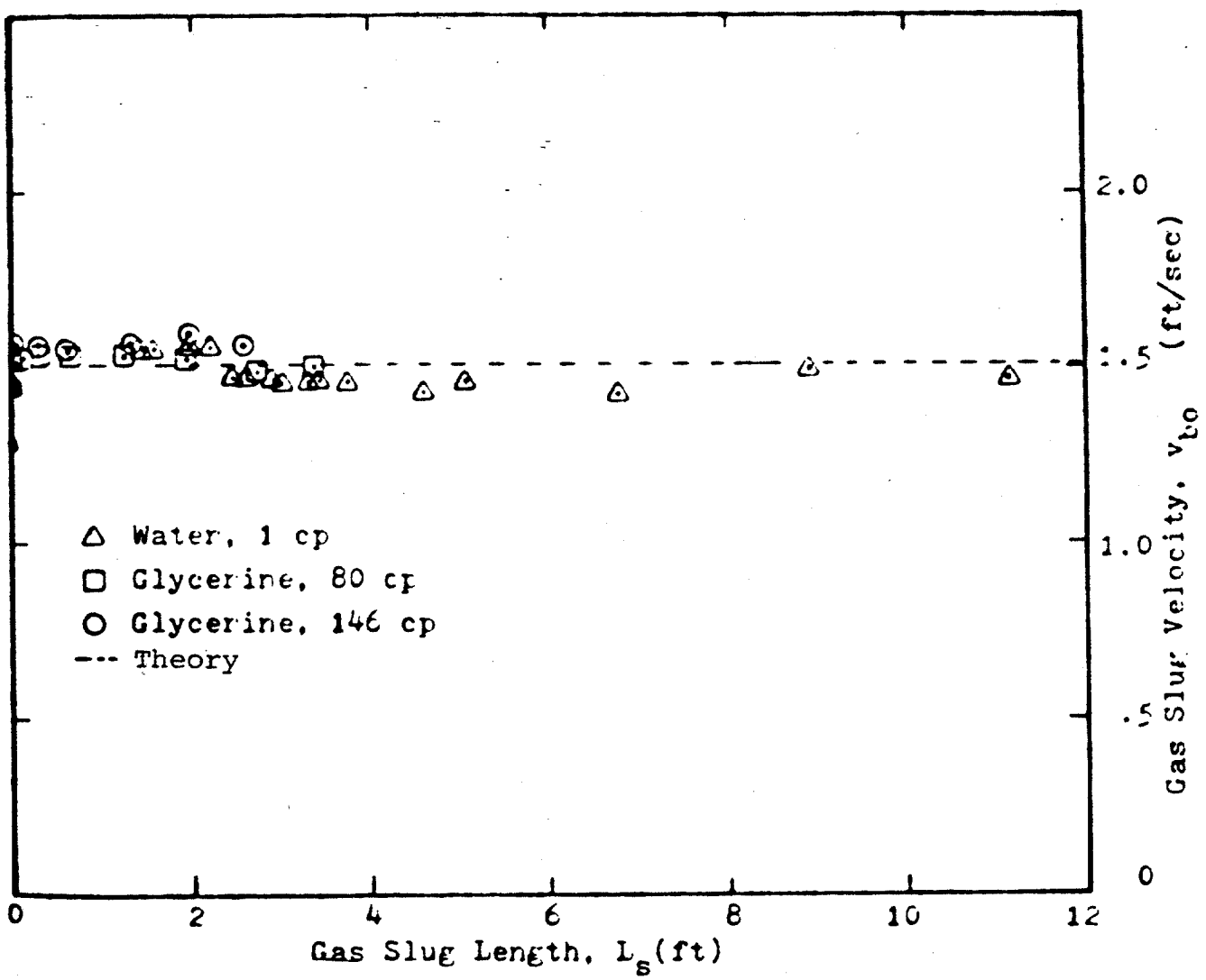

Figure 112: Velocity of Large Bubbles Through a Static Liquid in a 6.375 in by 2.375 in annulus

Gas Feed Rate, v_{sg} (ft/sec)	Initial Bubble Length, L_{si} (ft)	Average Gas Fraction	Average[1] Bubble Velocity, v_b (ft/sec)	Equivalent[2] Bubble Diameter (inches)	Comments
.293	.26	.119	2.462	3.257	Bubble flow.
.440	.36	.170	2.588	3.104	Bubble flow.
.548	.43	.195	2.810	3.388	Bubble flow.
.795	.54	.252	3.155	3.542	Bubble flow.
.895	.60	.275	3.255	3.477	Ibid. Occasional slugs.
.972	.63	.292	3.329	3.419	Agitated bubble flow.
1.230	.69	.370	3.324	2.498	Ibid.
1.597	.89	.446	3.581	2.026	Resembles churn flow.
1.520	1.50	.453	3.355	1.715	Ibid.
1.780	1.50	.480	3.708	1.808	Ibid.

[1] Average bubble velocity computed from gas friction

[2] Computed using $v_b = 1.01\ (g\ r_e)^{0.5} + K_{Lv}\ \bar{v}_{L+}$

Table 16a: Initial Slug Length and Gas Fractions For Constant Gas Flow Rates in Static Column of Water (6.375 in by 2.375 in Annulus)

Gas Feed Rate, v_{sg} (ft/sec)	Initial Bubble Length, L_{si} (ft)	Average Gas Fraction	Average[1] Bubble Velocity, v_b (ft/sec)	Equivalent[2] Bubble Diameter (inches)	Comments
.014	.08	.011	1.273	1.46	Lenticular bubbles.
.049	.38	.023	2.130	3.097	Ibid.
.072	.08	.034	2.118	2.958	Ibid.
.111	.46	.034	3.265	7.03	Ibid.
.197	.92	.045	4.378	12.210	Larger bubbles than the former ones.
.281	1.17	.073	3.849	8.621	Ibid.
.560	1.83	.152	3.684	5.963	Apparently churn flow.

[1] Average bubble velocity computed from gas fraction

[2] Computed using $v_b = 1.01\ (g\ r_e)^{0.5} + K_{Lv}\ \bar{v}_{L+}$

Table 16b: Initial Slug Length and Gas Fractions For Constant Gas Flow Rates in Static Column of 80 cp Glycerine (6.375 in by 2.375 in Annulus)

Gas Feed Rate, v_{sg} (ft/sec)	Initial Bubble Length, L_{si} (ft)	Average Gas Fraction	Average[1] Bubble Velocity, v_b (ft/sec)	Equivalent[2] Bubble Diameter (inches)	Comments
.028	0.17	.017	1.647	1.885	Large lenticular bubbles. Occasional larger bubbles.
.087	0.48	.027	3.222	6.998	Ibid. Lenticular bubbles.
.192	0.88	.039	4.923	15.737	Ibid. Turbulence and stream lined slugs.
.313	1.29	.081	3.864	8.459	Developed slug flow.
.453	1.79	.120	3.775	7.049	Ibid.
.538	2.25	.139	3.871	6.912	Wavey slug. Slug or churn flow.

[1] Average bubble velocity computed from gas fraction

[2] Computed using $v_b = 1.01\ (g\ r_e)^{0.5} + K_{Lv}\ \bar{v}_{L+}$

Table 16c: Initial Slug Length and Gas Fraction For Constant Gas Flow Rates in Static Column of 146 cp Glycerine (6.375 in by 2.375 in Annulus)

Gas Feed Rate, v_{sg} (ft/sec)	Initial Bubble Length, L_{si} (ft)	Average Gas Fraction	Average[1] Bubble Velocity, v_b (ft/sec)	Equivalent[2] Bubble Diameter (inches)
.101	0.42	.025	4.040	10.243
.262	0.88	.036	7.278	33.241
.415	1.29	.072	5.764	18.295
.453	1.42	.072	6.292	21.907
.582	1.71	.122	4.771	10.345

[1] Average bubble velocity computed from gas fraction

[2] Computed using $v_b = 1.01\ (g\ r_e)^{0.5} + K_{Lv}\ \bar{v}_{L+}$

Table 17: Initial Slug Length and Gas Fraction For Constant Gas Flow Rates in a Flowing Column of 146 cp Glycerine (6.375 in by 2.375 in Annulus with v_{sL} = .10 ft/sec)

1. Bubble flow occurred with vanishing sizes of initial slug or lenticular bubbles.
2. Slug flow occurred with fully developed initial cylindrical bubbles which filled most of the available cross sectional area.
3. Churn flow occurred with large initial cylindrical bubbles having a length of at least two outer tube diameters.

These relationships are based on observations in the laboratory model and are not necessarily valid for field conditions. A small initial slug could become a very large slug in a well high above the injection point. Gas availability and gas expansion would increase the size of the gas slug if bubble fragmentation does not occur. Similarly, the steady flow of gas in liquid for long time intervals may not accurately model the condition under which gas kicks are generated and the two-phase flow pattern could change as the gas contaminated region propagates to the surface. Under rather short times, the formation gas flows into the wellbore and then normally the gas flow is controlled by closing the well. From this instant the gas will travel upward as a disturbance through a continuous body of liquid.

Finally, a test was run to simulate a gas kick entering the annulus while the fluid is circulating through the hydraulic system of the well. A moderate liquid velocity, 0.1 ft/sec, was used to allow time for observation of the leading edge of the gas. For these conditions, the relationship between gas flow rate and initial slug length becomes a linear one. The sizes of the generated slugs were slightly lower than those obtained with static liquid for the same gas flow rates. This was to be expected since the effect of the liquid flow rate is to diminish the flowing gas fraction. Under these curcumstances a decrease in the coalescence of the bubbles was indicated.

8.2 Experimental Study of Flowing Pressure Gradients

The vertical flow of mud and gas-mud mixtures in long pipes is of interest in the design and operation of subsea well control equipment where long choke lines are required. Heretofore, the question of two-phase flow of non-Newtonian drilling muds has not been investigated experimentally in full scale well systems.

Frictional pressure losses were measured in a 2 3/8", 3000 ft. long vertical tubing when flowing drilling mud alone, and flowing mud-gas mixtures. The single phase data was compared to values predicted by both the Bingham Plastic and Power Law Rheological Models, which are commonly used to describe non-Newtonian fluids. The multiphase pressure loss data were used to evaluate various published correlation techniques.

The two-phase flow work is to simulate the effects of a gas kick being circulated with subsea well control equipment. When a gas kick enters the wellbore and is circulated out, the gas mixes and gravity segregates with the mud in the hole. This mixture has little noticeable effect on pressure losses while it is in the open hole or casing annulus. However, when the gas-mud mixture enters the choke line, a rapid loss of hydrostatic pressure is experienced. Simultaneously, frictional pressure losses increase as flow in the choke line changes to two-phase flow.

8.2.1 Single-Phase Flow

Both the Bingham Plastic Model and the Power Law Model were used to predict the observed frictional pressure losses for single-phase flow. The Bingham Model requires a determination of plastic viscosity and yield strength which are obtained by the use of a Model 35 Fann Viscometer. For laminar flow, the frictional pressure loss predicted by the Bingham Model is given by

$$\frac{\Delta P}{\Delta L} = \frac{\mu_p \bar{v}}{1500 d^2} + \frac{\tau_y}{225 d} \qquad (8.1)$$

For turbulent flow, pressure loss is given by

$$\frac{\Delta P}{\Delta L} = \frac{f \rho \bar{v}^2}{25.8 d} \qquad (8.2)$$

where the friction factor, f, is given by the Colebrook function as

$$\frac{1}{\sqrt{f}} = -4 \, \mathrm{Log}\left[\frac{1}{3.72}\frac{\varepsilon}{d} + \frac{1.225}{N_R\sqrt{f}}\right] \qquad (8.3)$$

and the Reynolds Number, N_R, is defined as

$$N_R = \frac{928\rho d\bar{v}}{\mu_p} \tag{8.4}$$

The Power Law Model is characterized by the flow behavior index, n, and the consistency index, k, determined from a Model 35 Fann Viscometer as

$$n = 3.32\ \mathrm{Log}\left(\frac{\theta_{600}}{\theta_{300}}\right) \tag{8.5}$$

$$k = \frac{510(\theta_{300})}{(511)^n} \tag{8.6}$$

For laminar flow, the frictional pressure loss predicted by the Power Law Model, as presented by Metzner and Reed, is given by

$$\frac{\Delta P}{\Delta L} = \frac{k\bar{v}^n}{144{,}000d^{n+1}}\left[\frac{3 + \frac{1}{n}}{0.0416}\right]^n \tag{8.7}$$

Equation (8.2) above is also used to describe turbulent flow pressure losses with the Power Law Model, with a modified friction factor, as given by Dodge and Metzner

$$\frac{1}{\sqrt{f}} = \frac{4}{n^{.75}}\ \mathrm{Log}\left[N_{Re} f^{1-\frac{n}{2}}\right] - \frac{0.4}{n^{1.2}} \tag{8.8}$$

where N_{Re} is the generalized Reynolds number defined by Metzner and Reed

$$N_{Re} = \frac{89088\rho\bar{v}^{(2-n)}}{k}\left[\frac{0.0416d}{3 + \frac{1}{n}}\right] \tag{8.9}$$

The Reynolds Number criteria used to predict the transition from laminar to turbulent flow is defined for the Bingham Model by

$$N_R = \frac{928\rho d\bar{v}}{\mu_e}$$

where

$$\mu_e = \mu_p + \frac{6.65\tau_y d}{\bar{v}}$$

and by Equation (8.9) above for the Power Law Model. In each case, the transition point was expected in the vicinity of a Reynolds Number of 2000. Rather than depend solely on a Reynolds Number criteria, frictional pressure losses were calculated for both laminar and turbulent flow. The larger value is then assumed to be the correct regime and the intersection of the two calculations predicts the transition point.

For single-phase flow, mud was pumped down the drill pipe, up the casing x drill pipe annulus, and then up the choke line. The surface choke was manipulated to obtain various surface pressures. Pressure at the 3000 foot level was monitored with the capillary tube as well as surface pressure on the closed kill line. The frictional pressure losses of the mud flowing up the casing x drill pipe annulus was determined to be negligible, so changes from the initial reading on the capillary tube, less the surface choke line pressure, represented the frictional pressure losses in the choke line. The closed kill line was used in the same fashion to obtain a verification. Flow rates were obtained from pump calibrations and then counting strokes.

8.2.2 Single-Phase Flow Pressure Gradient Measurements

Three different clay-water, unweighted muds were used in this study, with properties as shown in Table 18. These properties were measured at surface flowing temperatures. A calculation of circulating mud temperatures as a function of depth was obtained by the method suggested by Holmes and Swift,[47] indicating that the temperature variation with depth was insignificant and would have negligible effect on mud properties.

A relatively low plastic viscosity and yield point characterized mud No. 1. A graph of flow rate vs. frictional pressure loss is shown

Mud Property	Mud No. 1	Mud No. 2	Mud No. 3
Density, ppg	8.6	8.8	8.8
Plastic Viscosity, cp	4	20	38
Yield Point, lb/100 ft^2	3	8	27
Flow Behavior Index, n	0.65	0.78	0.66
Consistency Index, eq. cp	61	112	527
Bentonite Content, % by volume	2	3	3
Average Flowing Temperature, °F	79	84	82
Gas Injection Rate, SCF/min	650	625	650

Table 18. Properties of Clay-Water Muds

in Figure 114. Since Reynolds numbers are relatively high, the mud is certainly in turbulent flow. The Power Law Model, as applied in this paper, is independent of pipe roughness; however, the Bingham Model is dependent on pipe roughness. Pipe roughness is of significance when calculating a turbulent flow friction factor at high Reynolds numbers. This is evident by comparing Figure 114 where pipe roughness is 0.0 and Figure 115 where pipe roughness is 0.00065 as suggested by Cullender and Smith.[48] At these high Reynolds numbers and low plastic viscosity, the Bingham Plastic Model more accurately predicts frictional pressure losses, particularly if a pipe roughness of 0.00065 is used.

Mud No. 2 is characterized by a plastic viscosity of 20 cp and a yield point of 8 lb/200 ft^2. However, surface horsepower limitations restricted flow rates to a relatively intermediate range of Reynolds numbers. The turbulent flow friction factor is practically independent of pipe roughness in this range of Reynolds numbers. This can be seen by comparing Figures 116 and 117, which represent pipe roughness of 0.0 and 0.00065, respectively. Note, however, that the Power Law Model better predicts pressure losses in this case. This is attributable to the fact that this mud with a higher plastic viscosity than mud No. 1 is a more non-Newtonian fluid; whereas mud No. 1 was a Newtonian-like fluid and better described by the Bingham Plastic Model.

Mud No. 3 had a plastic viscosity of 38 cp and a yield point of 27 lb/100 ft^2. The range of Reynolds numbers obtained with the available pump horsepower indicates both laminar and turbulent flow (see Figure 118). In fact, the high flow rates were probably in transition flow and had not achieved fully turbulent flow. The experimental data indicates the onset of turbulent flow, i.e., the deviation from the straight line of laminar flow, at approximately point A. The Bingham Model predicts this point very well.

8.3.2 Two-Phase Flow

The frictional pressure losses associated with the flow of a gas-mud mixture in relatively small, vertical flowlines was of particular interest to the authors in order to model well control operations with subsea blowout preventers. In this situation, a gas kick being circulated from a well will cause a sudden reduction in hydrostatic pressure

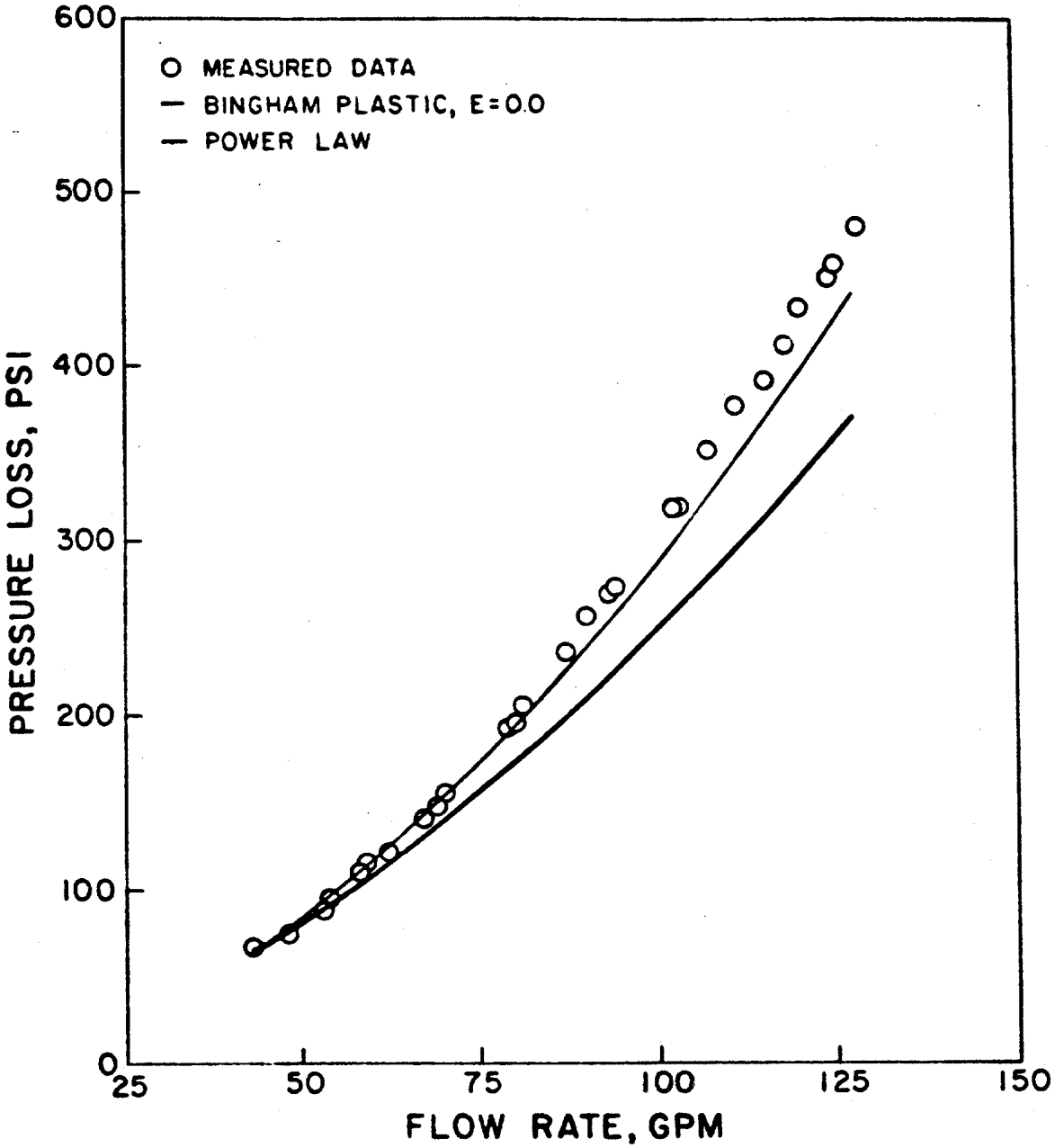

Figure 114: Calculated and Observed Single Phase Flowing Gradients for Mud No. 1 and Zero Pipe Toughness

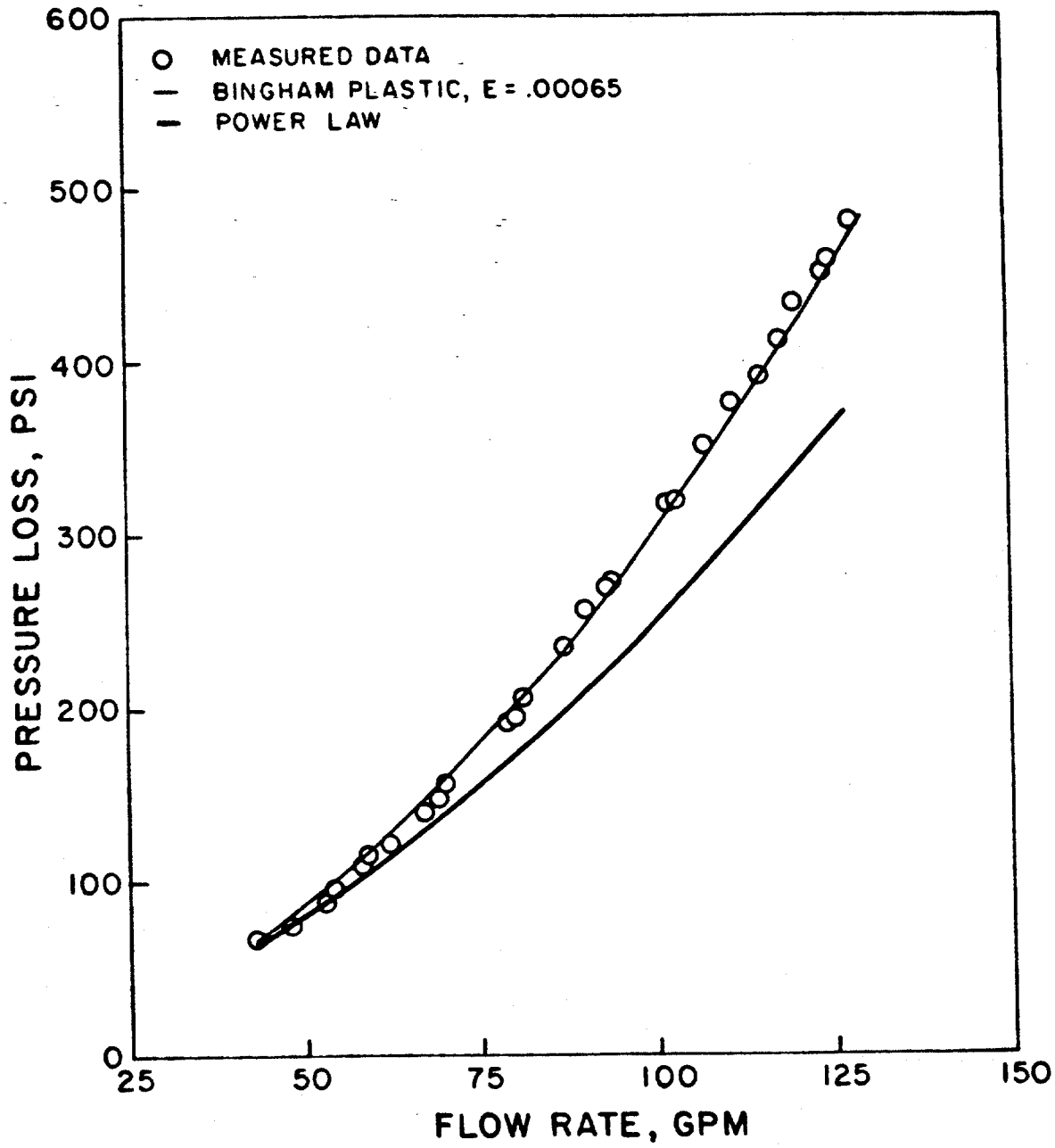

Figure 115: Calculated and Observed Single Phase Flowing Gradients for Mud No. 1 and 0.00065 Pipe Roughness

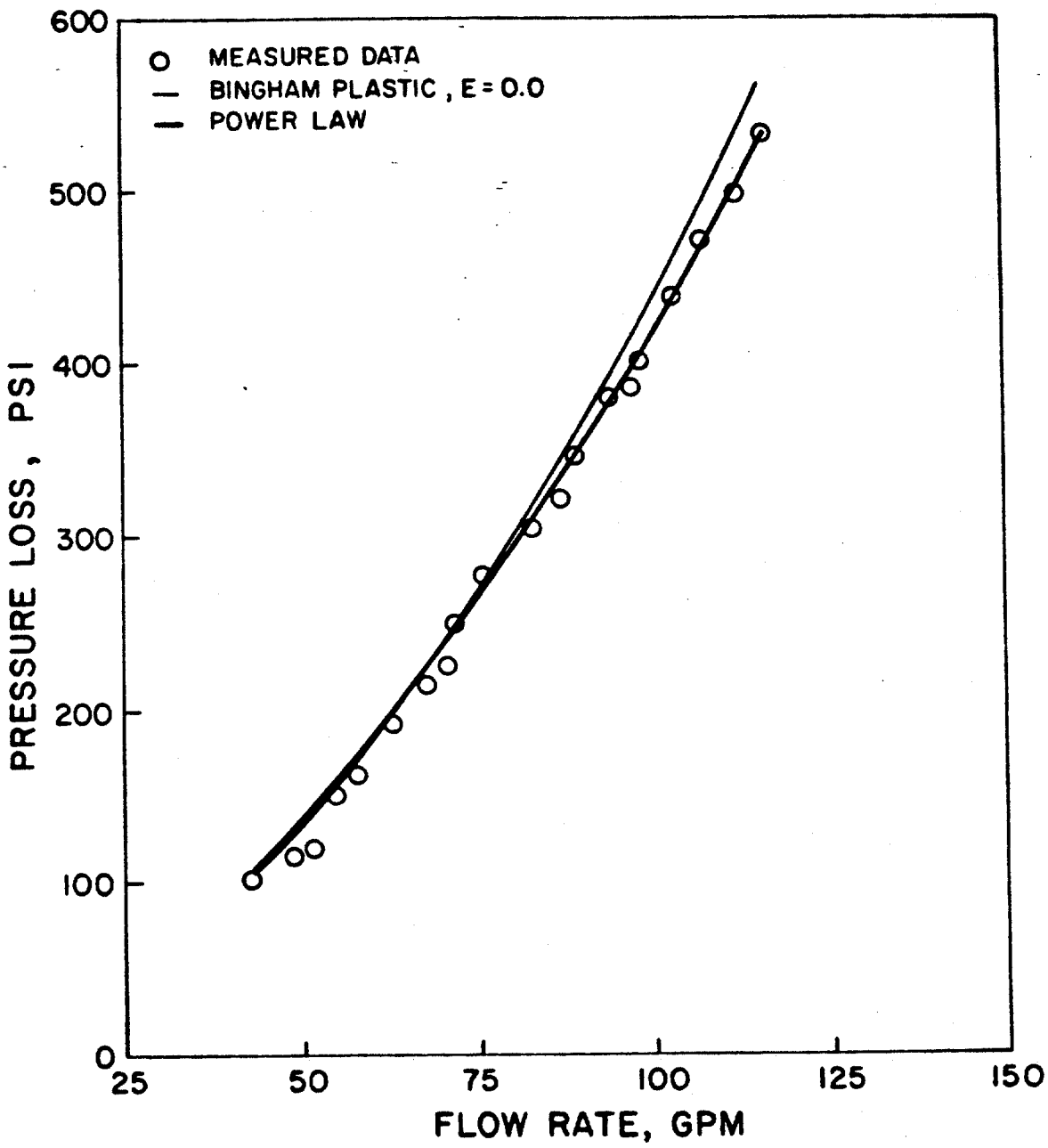

Figure 116: Calculated and Observed Single Phase Flowing Gradients for Mud No. 2 and Zero Pipe Roughness

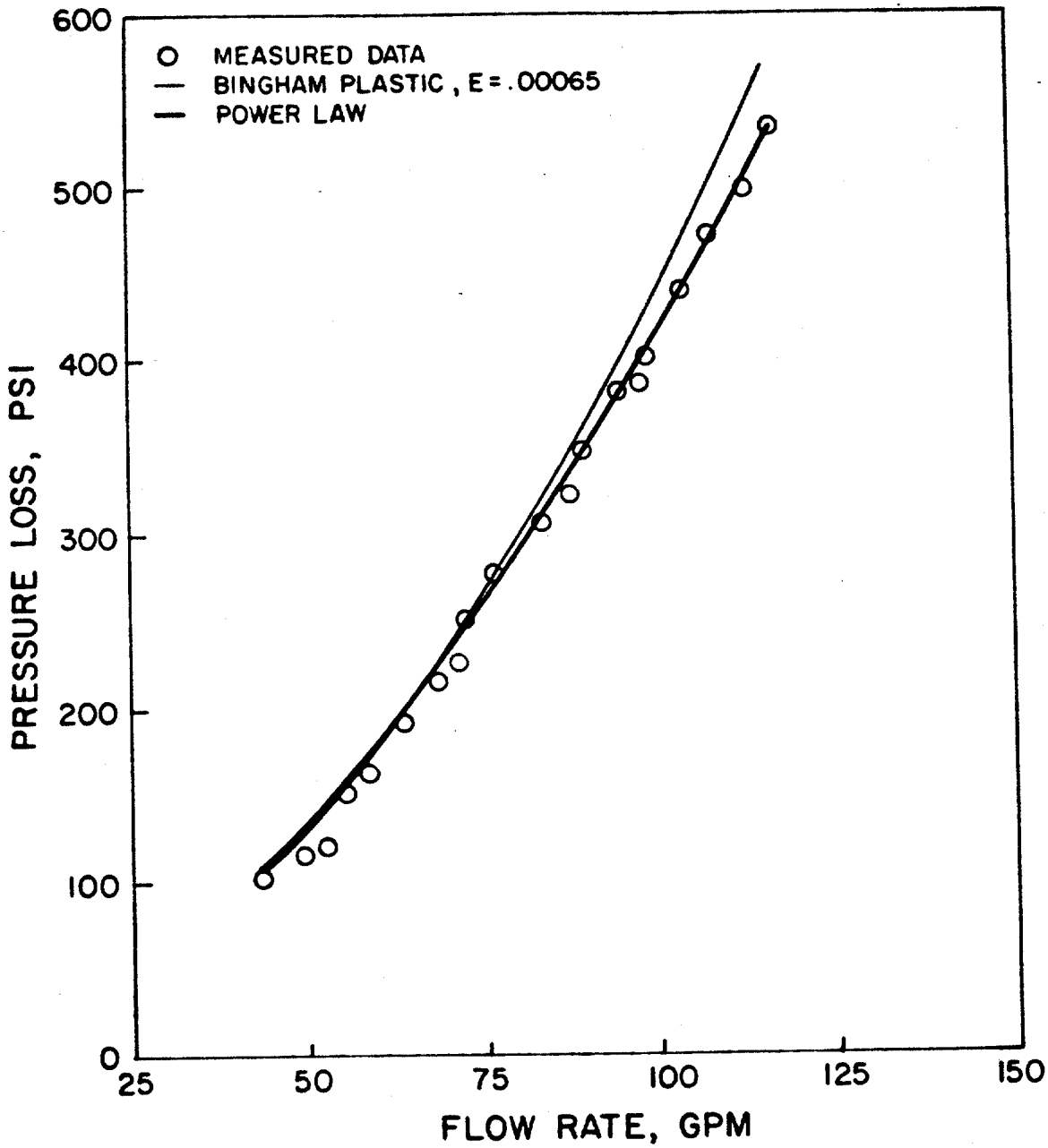

Figure 117: Calculated and Observed Single Phase Flowing Gradients for Mud No. 2 and 0.00065 Pipe Roughness

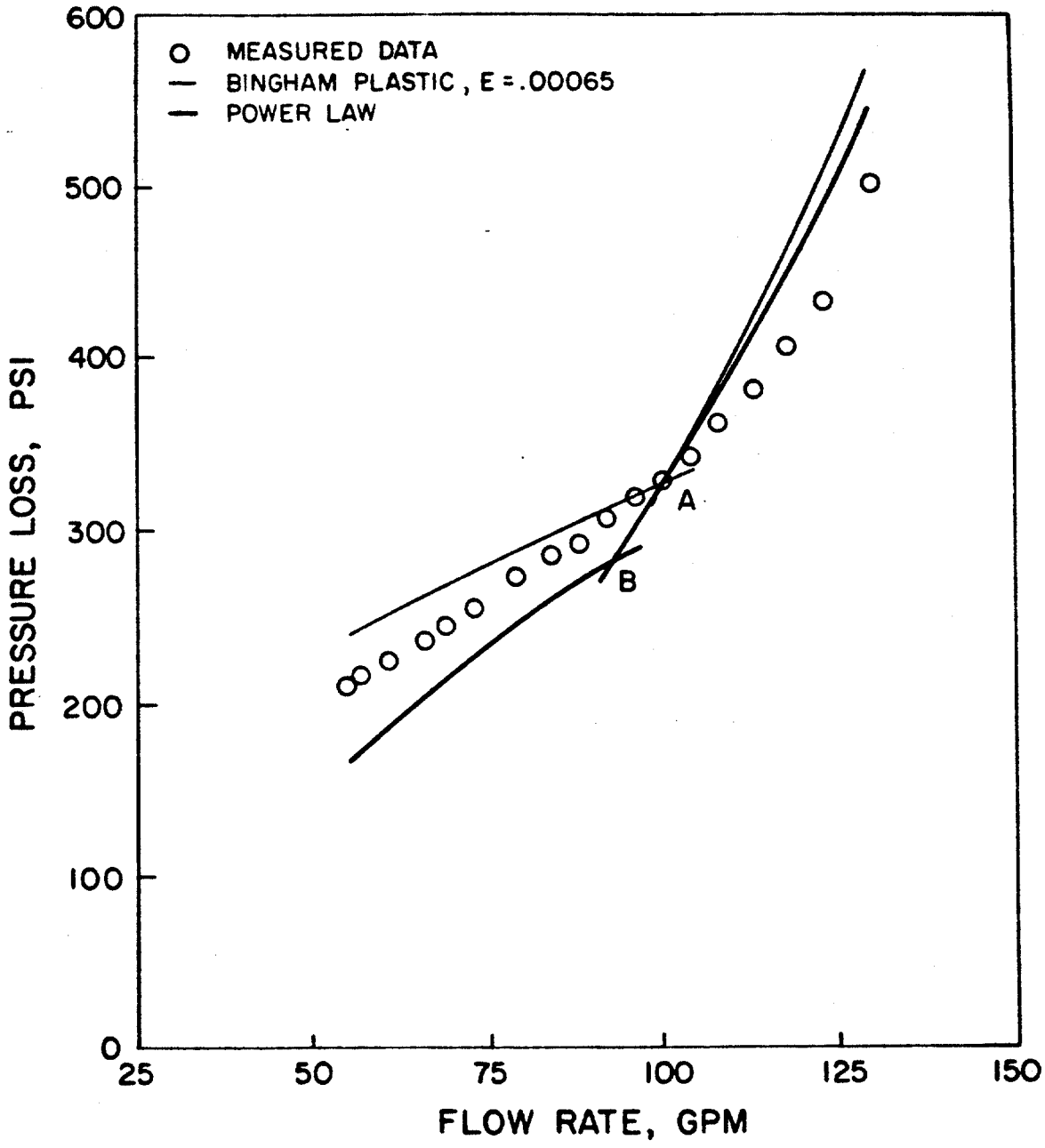

Figure 118: Single Phase Flowing Gradients for Mud No. 3

when the gas enters the smaller choke line. However, the high velocities achieved in the choke line with two-phase flow will cause significant frictional pressure losses. Consequently, a full scale simulation was designed, again using the research and training well at LSU, to measure pressure drops in a 3000 foot vertical flowline of 2 3/8" tubing.

Both the Bingham Plastic Model and the Power Law Model were used to describe the mud rheological properties. This was then combined with the two-phase flow correlations of Poettmann and Carpenter,[49] Hagedorn and Brown,[50] Orkiszewski,[51] and Beggs and Brill.[52] These correlations were modified to reflect nitrogen and mud properties as well as introducing a modified viscosity into the calculations.

The plastic viscosity, defined using a Model 35 viscometer as

$$\mu_p = \theta_{600} - \theta_{300} \tag{8.10}$$

was used with the Bingham Plastic Model calculations. With the Power Law Model, the Dodge and Metzner[46] friction factor equation (Equation 8.8, Part I) was used, where the equivalent viscosity is defined as

$$\mu_e = \frac{kd^{1-n}}{96(\bar{v}_m)^{1-n}}\left(\frac{3 + \frac{1}{n}}{0.0416}\right)^n \tag{8.11}$$

Note that this expression requires a velocity, for which a two-phase superficial velocity defined as[53]

$$\bar{v}_m = \frac{q_g + q_m}{A} \tag{8.12}$$

was used.

In the case of two phase flow studies, mud was pumped down the drill pipe and up the casing annulus to the 3000 foot level. Here, nitrogen gas was introduced by injecting the gas down the kill line using a commercial liquid nitrogen supplier. The gas-mud mixture then flowed up the 2 3/8" choke line to the surface.

Downstream pressure was varied by manipulation of the well control choke. Gas-liquid ratio was varied with the mud pump while keeping the

gas rate constant. Upstream and downstream pressures were obtained from the capillary tube and pressure monitors on the choke manifold. Data was taken with downstream pressures as low as 200 psi and as high as 1800 psi. See Table 19 for mud and gas properties for each experimental run made.

8.3.2 Two-Phase Flow Pressure Gradient Measurements

Since the frictional and potential pressure losses are inseparable in two-phase flow observed data, the sum of these two components are compared with predicted values as shown in Figures 119 through 122. Perfect agreement would yield points on the 45° line. A ± 10% band is shown for comparative purposes. The absolute pipe roughness was taken to be 0.00065 with the Bingham Plastic Model as suggested in Part I. The Power Law Model does not consider roughness. Figure 119 represents the observed data plotted against the pressure drop calculated by the Poettman and Carpenter correlation. Poettman and Carpenter did not consider liquid viscosity, liquid hold-up or flow regime. Hence, this correlation had the highest deviation, consistently predicting values lower than observed data.

The correlation by Beggs and Brill is compared to the measured data in Figure 120. This correlation was originally obtained with laboratory work using air and water flowing in a 90 foot section of 1" and 1½" pipes. In fact, excellent performance of this correlation was noted for the low viscosity mud, which was most like the air and water used in the laboratory experiments. However, the higher viscosity muds showed significant deviation from the ± 10% band.

Next, the Orkiszewski correlation is compared with measured data and is shown in Figure 121. the comparison is good, but the correlation of Hagedorn and Brown (Figure 122) was the best of the four. The work of Hagedorn and Brown was conducted in a 1500 foot well using water and oil of different viscosities in 1", 1¼" and ½" tubing. This would explain the excellent agreement obtained using Hagedorn and Brown correlations.

A statistical comparison is shown in Table 19. As can be seen, the Hagedorn and Brown correlation gives the best results. Also, the Orkiszewski correlation is within acceptable limits. The Beggs and

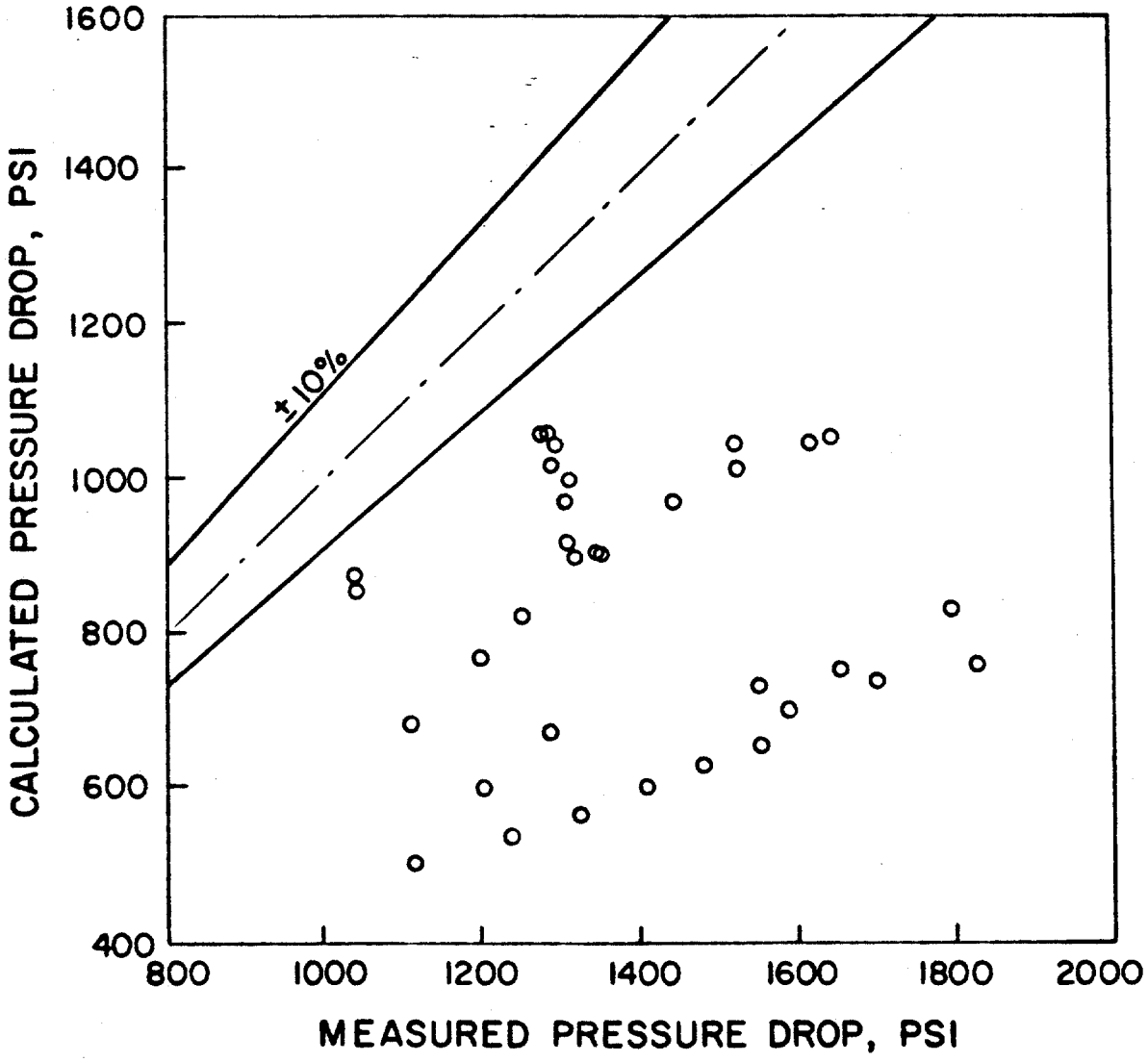

Figure 119: Comparison of the Gas-Mud Mixtures Pressure Drop Data, Poettmann and Carpenter Correlation

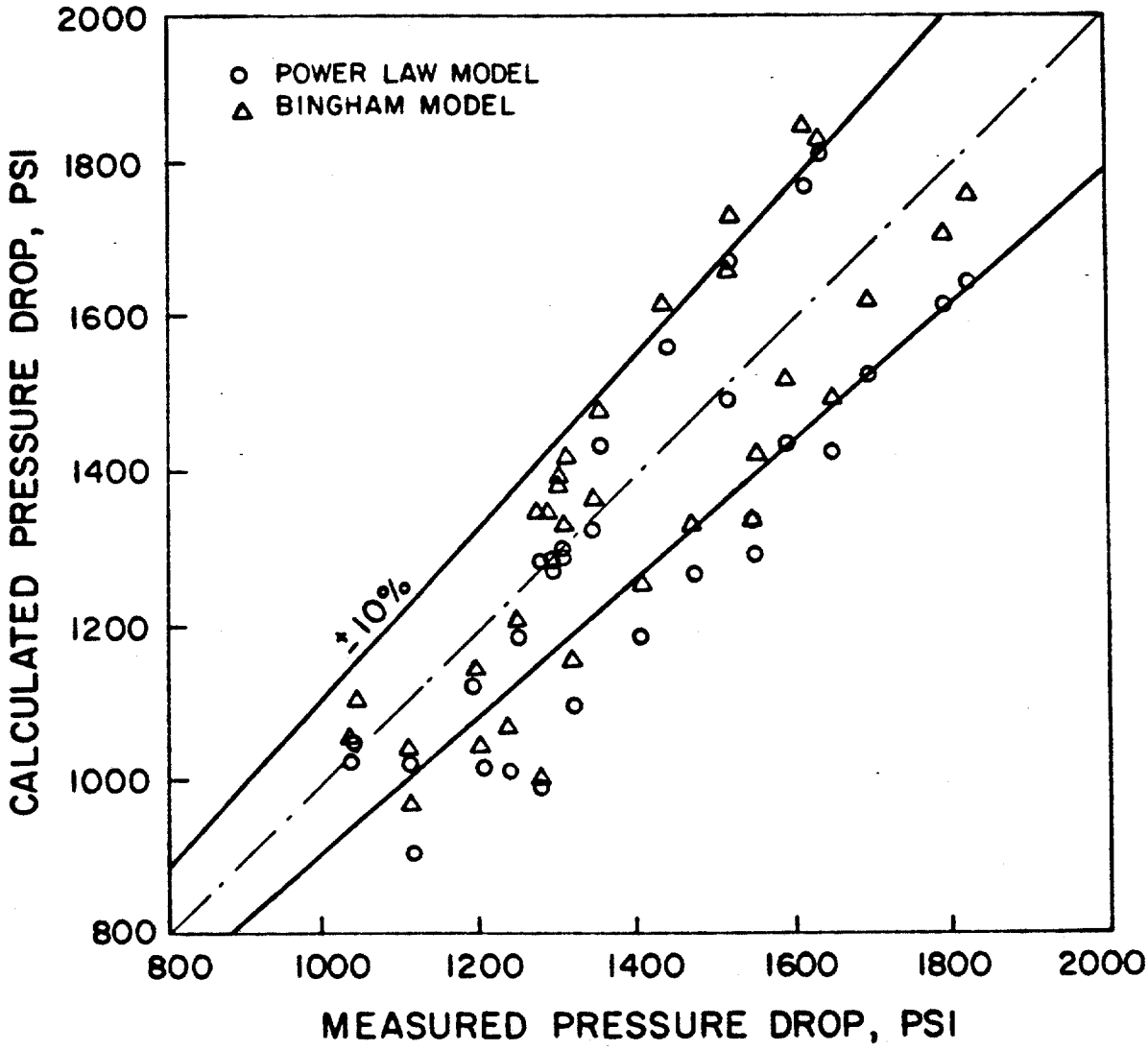

Figure 120: Comparison of the Gas-Mud Mixtures Pressure Drop Data, Beggs and Brill Correlation

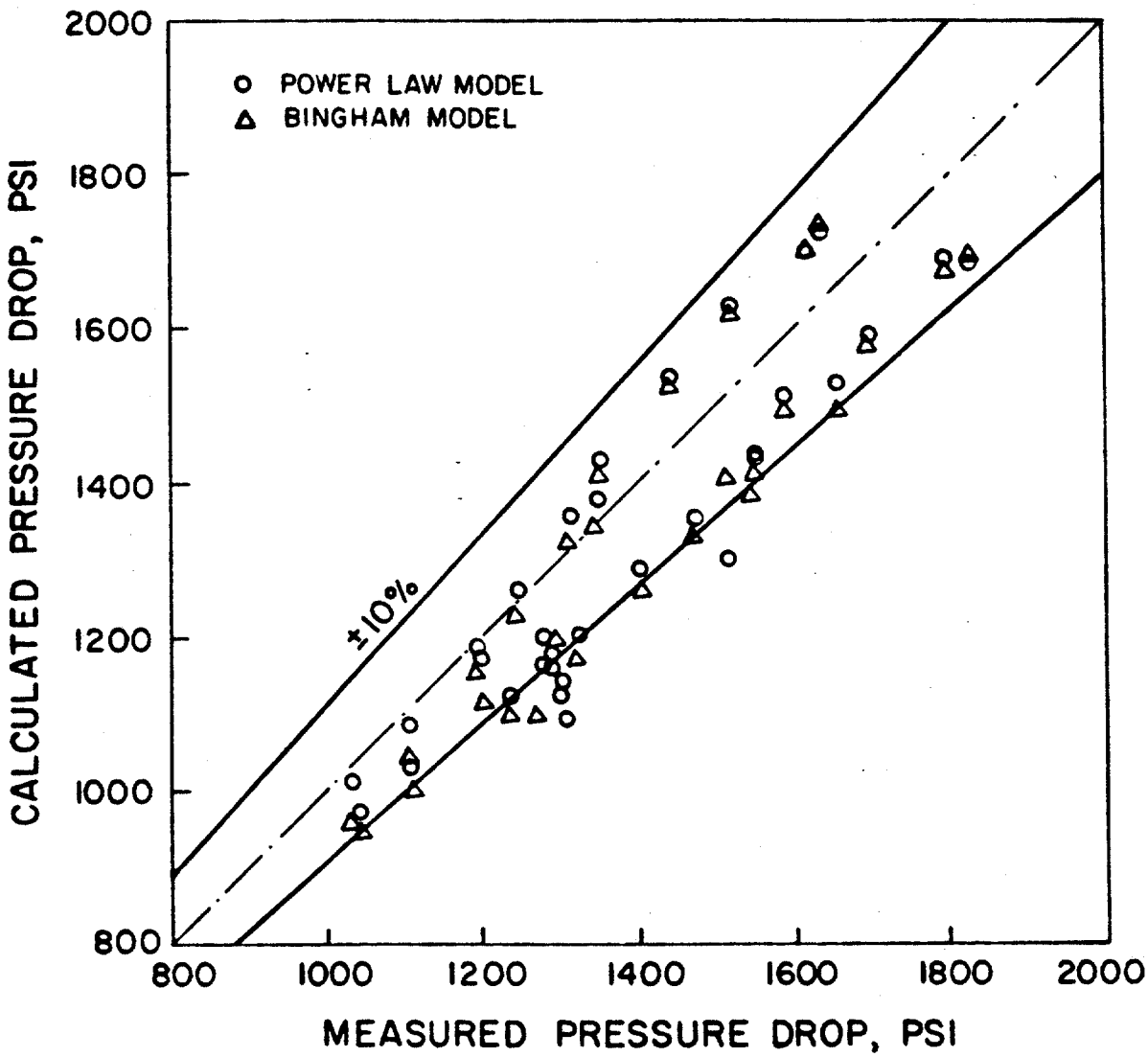

Figure 121: Comparison of the Gas-Mud Mixtures Pressure Drop Data, Orkiszewski Correlation

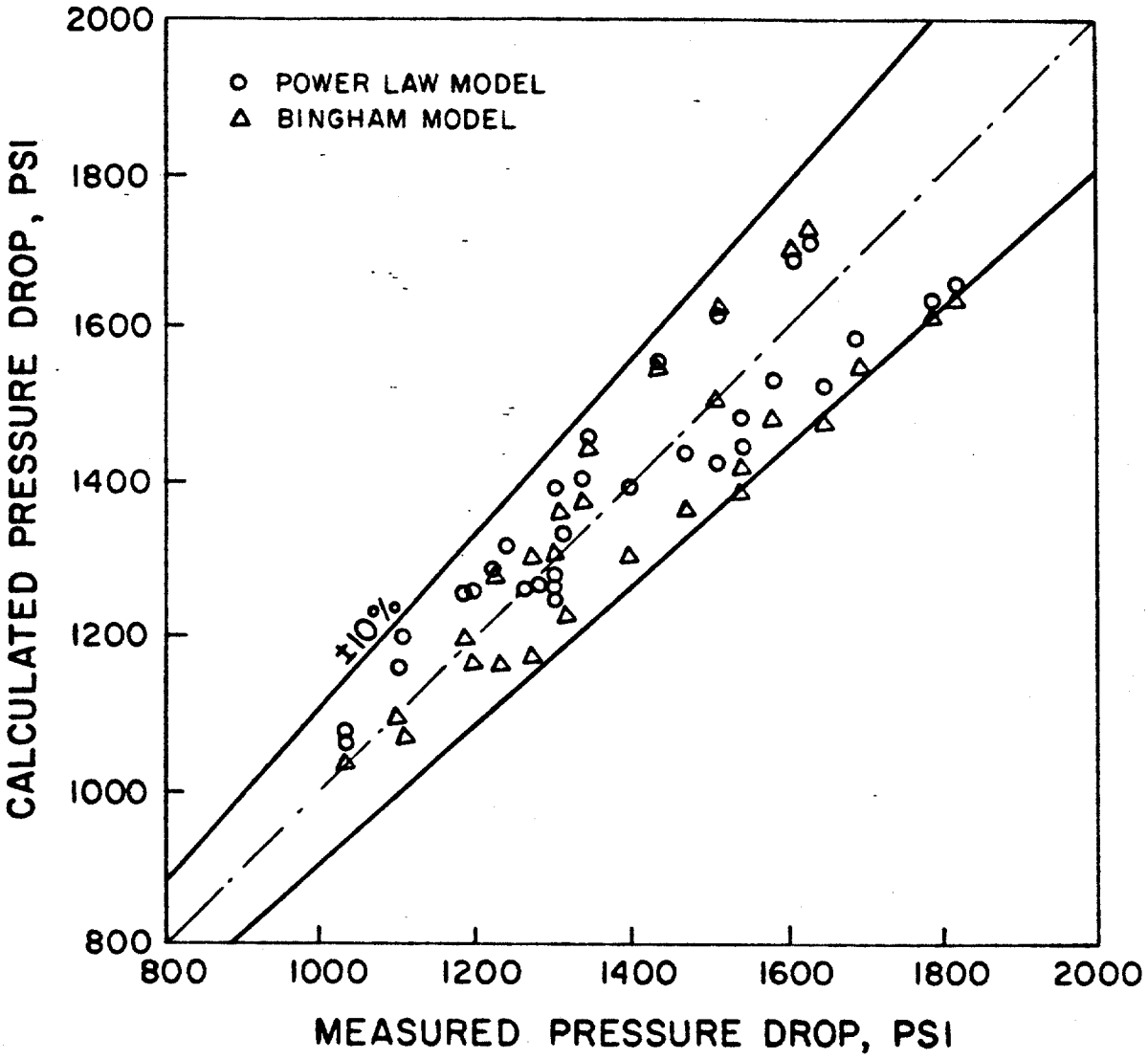

Figure 122: Comparison of the Gas-Mud Mixtures Pressure Drop Data, Hagedorn and Brown Correlation

Table 19

Summary of Statistical Analysis for the Gas-Mud Mixtures
The Bingham Plastic Model (Power Law Model)

Correlation	Run No. 1 (10 data points)	Run No. 2 (10 data points)	Run No. 3 (14 data points)	Overall (34 data points)
		Average Absolute Percent Deviation		
Poettmann and Carpenter	21.6 (21.6)	34.0 (34.0)	54.8 (54.8)	38.9 (38.9)
Hagedorn and Brown	0.9 (2.4)	3.9 (5.6)	7.9 (4.8)	4.7 (4.3)
Orkiszewski	8.3 (9.6)	4.0 (4.0)	9.4 (7.2)	7.5 (6.9)
Beggs and Brill	5.8 (1.0)	7.8 (6.5)	10.11 (14.5)	8.2 (8.2)
		Estimated Standard Deviation		
Poettmann and Carpenter	5.5 (5.5)	2.1 (2.1)	3.1 (3.1)	14.8 (14.8)
Hagedorn and Brown	1.2 (2.9)	3.0 (1.4)	2.3 (5.2)	5.6 (5.1)
Orkiszewski	1.4 (4.5)	4.4 (3.2)	2.3 (1.8)	5.7 (6.3)
Beggs and Brill	2.1 (1.0)	8.1 (7.3)	5.0 (3.9)	9.5 (9.0)

Brill correlation shows good agreement at low viscosity, but has poor agreement at high viscosity.

8.3 Improved Well Control Simulation Computer Program

Information gained concerning the behavior of a gaseous region in pipes and annuli was used to modify an existing well control simulation computer program at LSU. The basic approach used in the program was to break the drill pipe and annulus into small cells of constant mud volume, but variable total volume, which moved at the velocity of the mud contained in the cell. When gas was present in a cell, it was assumed to be uniformly distributed. Material balance, PVT properties, and flowing gradients are computed for each cell for each time step. Gas migration from cell to cell is determined using gas slip velocity determinations and material balance concepts.

Currently, the simulation program assumes an infallible choke operator which maintains a constant bottom-hole pressure throughout the well control operation. Future plans include the development of a system for allowing choke operation to be simulated on a real time basis. Sufficient experimental data are presented in Chapter 4 to now make this programming work feasible.

A typical comparison of observed well behavior and computed well behavior (using the modified computer program) is shown in Figure 123. Note that the accuracy of the modified computer program has been greatly improved over the results previously achieved and discussed in Chapter 7.

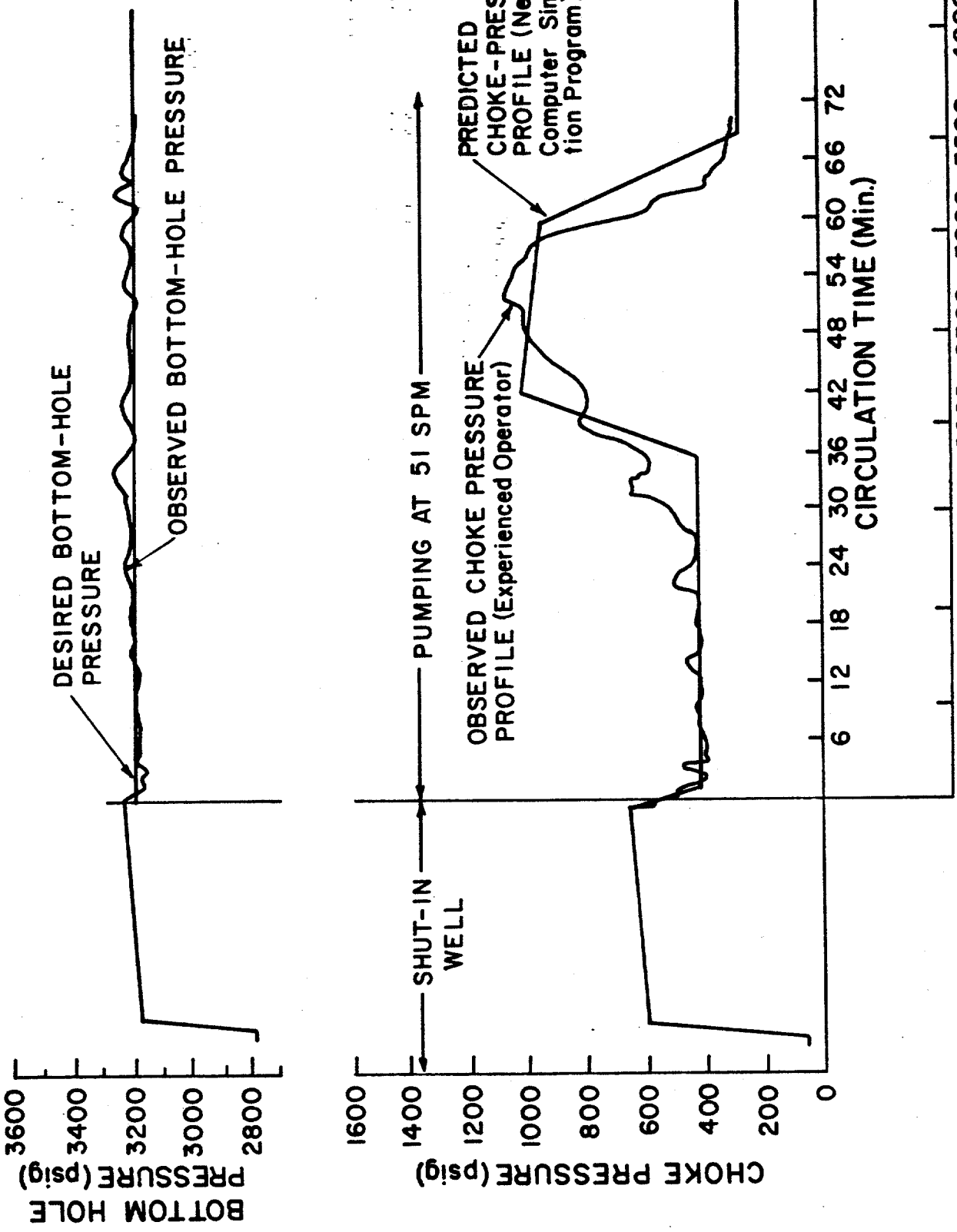

FIGURE 123. COMPARISON OF OBSERVED AND PREDICTED CHOKE PRESSURE PROFILE FOR 18 bbl GASKICK USING NEW COMPUTER MODEL

CHAPTER 9

CONCLUSIONS

Based on the results obtained in the various phases of this study, the following conclusions can be drawn:

1. The drilling industry has steadily extended exploratory drilling to increasing water depths. The record water depth is now in excess of 5600 ft.
2. There are only about 12 floating vessels currently available which have drilled in water depths in excess of 2000 ft. Over half of the wells drilled in water depths in excess of 2000 ft have been drilled by only four vessels.
3. No major modifications have been made to the subsea equipment used to drill in deep water. The wells drilled in deep water have all used a 16 3/4 in. BOP stack rated at 10,000 psi, using Cameron ram-type preventers and Hydril or Shaffer annular type preventers.
4. No special procedures or special training are required by MMS for drilling in deep water. The MMS training requirements only address surface and subsea BOP stack arrangements, regardless of water depth.
5. An experimental well facility has been used successfully to model the well-control flow geometry present on a floating drilling vessel operating in 3000 feet of water.
6. The model provides realistic conditions with respect to circulating frictional pressure losses in the choke line and with respect to rapid changes in choke pressure when a gas kick is circulated through the choke line.
7. The model is reasonably economical to operate, requiring relatively small gas volumes, pump horsepower, and circulating times to complete a kick simulation.

8. The conventional drill pipe pressure method (maintaining a drill pipe pressure slightly above initial shut-in pressure) provides good well control for both surface and subsea BOP systems.
9. The static volumetric method works well for surface BOP systems with a uniform annular capacity.
10. The static volumetric method cannot always be safely executed in a deep-water subsea BOP system due to the large change in capacity or cross-sectional area from the well to the subsea choke line. Schemes for taking the capacity change into account do not always work because gas may be dispersed over a considerable portion of the well.
11. The dynamic volumetric method is a viable alternative for removing gas kicks from both surface and subsea BOP systems. For deep-water subsea BOP systems, the peak pressure seen during executing the dynamic method is not as severe as for other methods, including a conventional kick circulation.
12. The assumption often made in practice that the gas kick remains as a continuous slug during upward gas migration was found to be invalid.
13. In spite of a portion of the gas reaching the surface prematurely due to fragmentation, the modified volumetric methods of handling upward gas migration are valid and practical techniques.
14. Contrary to previously accepted practices, the venting of the initial gas that reaches the surface does not cause any problems in maintaining well control, as long as a portion of the gas is still rising in the well. Continuing upward gas migration is indicated by a continuing increase in the shut-in casing pressure.
15. The restriction of flow through a spherical-type annular blowout preventer during closure is negligible until the preventer is very near to being fully closed.
16. The rubber sealing element in the spherical blowout preventer cannot be treated as a rigid orifice for pressure drop - flow rate calculations. For a given piston position, the element deforms to assume the least restrictive configuration for any given flow rate.
17. The rubber sealing element deforms slightly differently each time the element is exercised by opening or closing the blowout preventer.

18. The effect of fluid viscosity on the pressure drop - flow rate characterisitcs of the blowout preventer is negligible compared to the effects of the deformation characteristics of the rubber element.
19. The "effective" piston travel for the spherical blowout preventer (over which flow is actually restricted) is very short. It is on the order of 1/10 ths of an inch of pison travel.
20. The "effective" piston travel is a function of the size (O.D.) of pipe in the hole. Large diameter pipes show a longer effective piston travel (both in terms of actual inches of travel and in terms of percentage of total piston travel) than small diameter pipes.
21. The valve coefficient, C_v, is not constant for a given partial closure of the blowout preventer (piston position). The valve coefficient, C_v, is also a function of the flow rate.
22. Flow of mud through several commercially available drilling chokes can be modeled using frictional area coefficient correlations.
23. Frictional area coefficients for drilling chokes are only slightly influenced by mud viscosity for the range of viscosities commonly used in field practice.
24. Pressure surges during shut-in can be conveniently estimated using conventional elastic theory equations for instantaneous valve closure.
25. For typical deep-water well conditions, the theoretical peak pressure experienced at the casing seat will be less for the soft shut-in procedure than for the hard shut-in procedure. (Pressure surge effects are greater than increased bulk volume effects)
26. The beneficial effects of the soft shut-in procedure are slight for gas influx rates which produce annular velocities less than about 80 ft/min.
27. Frictional pressure losses in choke lines for unweighted clay-water muds were accurately predicted by flow equations based on a Bingham Plastic Model.
28. Several alternative procedures can be successfully used to cancel the detrimental effect of choke-line frictional pressure losses during pump start-up. However, all of these procedures require considerable practice to master.

29. The demands placed on a choke operator when gas is circulated through a subsea choke line in deep water were not as great as predicted by computer simulations of well-control operations.
30. Well-control operations on floating vessels in deep water can be safely managed with existing equipment. However, proper choice of choke line diameter for the water depth range of the vessel is of critical importance. In addition, considerable hands-on practice may be required for the operator to master the needed special procedures.
31. The velocity of large gas slugs relative to the liquid above the slug is not significantly influenced by viscosity for tubes and annuli in the size range present in well control operations.
32. The predominant flow patterns present during well control operations is bubble flow, especially in low viscosity fluids.
33. For a bubble flow pattern, gas slip velocity is controlled primarily by bubble size.
34. Gas slip velocities of the order of 10-35 ft/min were observed for the well geometry, mud properties, and gas influx rates used in the experimental well facility.
25. The Bingham Plastic Model accurately predicts frictional pressure losses in subsea choke lines for low viscosity muds in turbulent flow, when using the plastic viscosity defined by a viscometer operated at 600 and 300 rpm.
36. The Power Law Model accurately predicts frictional pressure losses in subsea choke lines for high viscosity muds in turbulent flow, when viscosity is defined as above.
37. The modifications of the two-phase correlations by introducing either a plastic viscosity or equivalent viscosity to represent the non-Newtonian liquid phase yielded acceptable accuracy in calculating total pressure drop in vertical pipes by the Orkiszewski and the Hagedorn and Brown correlations. Hagedorn and Brown seem to be marginally better for the data analyzed.
38. The inclusion of accurate correlations for determining two-phase flowing gradients and gas slip velocity in well control simulations are needed for an acceptable estimation of well pressures during well control operations on a floating drilling vessel.

REFERENCES

1. Maddox, Pat; "Deep Water Report", Offshore, Vol. 37, No. 6, (June, 1977), p. 44.

2. Leonhardt, G. W., "Drilling in record water depth was an operational success", World Oil, (February, 1980), p. 57-60.

3. "Deep Water Report", Offshore, Vol. 41, No. 7, (June, 1981) p. 72-84.

4. "1978-1979 Directory of Marine Drilling Rigs", Ocean Industry, Gulf Publishing Co., (1978), p. 46-100.

5. Robertson, Rob; "Pelerin Drills in 3,046 Feet of Water", Offshore, Vol. 37, No. 5, (May, 1977), p. 121.

6. Gulf of Mexico Outer Continental Shelf Orders Governing Oil and Gas Lease Operations", (January, 1980) p. 2-16.

7. "Ocean Margin Drilling Program", Vol. III-Final Report for December, 1980, prepared by Santa Fe Engineering Services Company for the National Science Foundation under Contract No. ODP79-26019 (1980), p. 9-29 & 9-30.

8. Guidelineless Deepwater Drilling System", Technical Bulletin VTB1-10 (1977), p. 5.

9. "API Recommended Practices for Blowout Prevention Equipment Systems", API R P 53, (February, 1976).

10. "Land and Marine Drilling", Cameron Iron Works Catalog. (1980-1981), p. 1436-1437.

11. "Shaffer Pressure Control", NL Rig Equipment, p. 5220-5221.

12. "Blowout Preventers", Hydril Catalog 802, (1980), p. 30-31.

13. "Control Systems", Cameron Iron Works Catalog, (1980-1981), p. 1620-1629.

14. "Outer Continental Lands Act Amendments of 1978", Public Law 95-372, (September, 1978).

15. "Outer Continental Shelf Standard Training and Qualifications of Personnel in Well-Control Equipment and Techniques for Drilling on Offshore Locations", GSS-OCS - T 1 First Edition, (December, 1977).

16. "API Recommended Practice for Training and Qualification of Personnel in Well Control Equipment and Techniques for Drilling on Offshore Locations", API R P T-3, (July, 1976).

17. "Ocean Margin Drilling Program: Final Report, Vol. III", National Science Foudnation, 1980.

18. McKenzie, M. F.: "Factors Affecting Surface Casing Pressures During Well Control Operations," M.S. Thesis, Louisiana State University, Baton Rouge (1974).

19. Daugherty, R. L. and Ingersoll, A. C.: Fluid Mechanics with Engineering Applications, McGraw - Hill Book Company, Inc., New York (1954).

20. Joukovsky, N.: "Water Hammer," translated by O. Simin, Proceedings of American Water Works Association, Vol. 24 (1904) 341-424.

21. Parmakien, J.: Waterhammer Analysis, Prentice - Hall, Inc., New York (1955).

22. Rich, G. R.: Hydraulic Transients, McGraw - Hill Book Company, Inc., New York (1951).

23. Streeter, V. L.: Fluid Mechanics, 2nd ed., McGraw - Hill Book Company, Inc., New York (1958).

24. Streeter, V. L. and Wiley, E. B.: Fluid Mechanics, 6th ed., McGraw - Hill Book Company, Inc., New York (1975).

25. Streeter, V. L. and Wiley, E. B.: Hydraulic Transients, McGraw - Hill Book Company, Inc., New York (1967).

26. Allievi, L.: Theory of Water-Hammer, translated by E. E. Halmos, Printed by Riccardo Garoni, Rome, Italy (1925).

27. Moody, L. F.: "Simplified Derivation of Water-Hammer Formula," Symposium on Waterhammer, ASME - ASCE (1933) 25-28.

28. Glover, R. E.: "Computation of Water-Hammer in Compound Pipes," Symposium on Waterhammer, ASME - ASCE (1933) 64-71.

29. Watters, G. Z.: "Modern Analysis and Control of Unsteady Flow in Pipelines," Ann Arbor Science Publishers, Inc., Ann Arbor, Michigan, 1980.

30. Tullis, J. P., V. L., Streeter, and Wylie, E. B.: "Waterhammer Analysis with Air Release," Second International Conference on Pressure Surges, City University, London (1976).

31. Hawthorne, J. W., "Hole Conditions Govern Gas Kick Circulating Method," World Oil (September 1978) 67.

32. Hise, Bill R., ed., Blowout Prevention, Louisiana State University Petroleum Engineering Department (October 1978).

33. Rehm, B., Pressure Control in Drilling, Tulsa, Oklahoma: The Petroleum Publishing Company (1970).

34. Bourgoyne, A. T.: "Well Drilling Method" U.S. Patent 4,310,058 (January 12, 1982).

35. Bourgoyne, A. T.: "Well Drilling Apparatus" U.S. Patent 4,310,050 (January 12, 1982).

36. Holden, W. R. and Bourgoyne, A. T.: "An Experimental Study of Well Control Procedures for Deep Water Drilling Operations", OCT 4353, Proceedings of the 14th Annual OTC, Houston, Texas (May 3-6, 1982).

37. Bourgoyne, Adam T., Jr., "University Uses On-Campus Abandoned Well to Simulate Deepwater Well-Control Operations," Oil and Gas Journal (May 31, 1982).

38. Mathews, J. L.: "Upward Migration of Gas Kicks in a Shut-in Well", M.S. Thesis, Louisiana State University, Baton Rouge, La. (1980).

39. Goins, W. C.: "Kick Control on Floaters Presents Unique Problems", World Oil (Oct., 1977) 47.

40. Ilfrey, W. T., Alexander, C. H., Neath, R. A., Tannich, J. D. and Eckel, J. R.: "Circulating Out Gas Kicks in Deepwater Floating Drilling Operations," paper SPE 6834 presented at 52nd Tech. Conf. of SPE, Denver, Oct. 9-12, 1977.

41. Casariego, V. G.: "Experimental Study of Two Phase Flow Patterns Occurring in a Well During Pressure Control Operations," M.S. Thesis, Louisiana State University (May, 1981).

42. Rader, D. W.: "Movement of Gas Slugs Through Newtonian and Non-Newtonian Liquids in Vertical Annuli", M.S. Thesis, Louisiana State University, Baton Rouge, LA. (May, 1973).

43. Ward, R. H.: "Movement of Gas Slugs Through Static Liquids in Large Diameter Annuli", M.S. Thesis, Louisiana State University, Baton Rouge, LA. (August, 1974).

44. Koederitz, W. L.: "The Mechanics of Large Bubble Rising in an Annulus", M.S. Thesis, Louisiana State University, Baton Rouge, LA. (May, 1976).

45. Dumitrescu, D. T., "Stromungan einer Luftblase imsenkrechten Rohr". Z. Angew, Math. Mech. (June 1943) V. 23, 139-149.

46. Rehm, B.: Pressure Control in Drilling". Petroleum Publishing Co., Tulsa, Oklahoma (1970).

47. Holmes, C. S. and Swift, S. C., "Calculation of Circulating Mud Temperatures," Journal of Petroleum Technology (June, 1970).

48. Cullender, M. H. and Smith, R. V., "Practical Solution of Gas-Flow Equations for Wells and Pipelines with Large Temperature Gradients," Trans. AIME, Vol. 207 (1956).

49. Poettmann, F. H. and Carpenter, P. G., "The Multiphase Flow of Gas, Oil, and Water through Vertical Flow Strings with Application to the Design of Gas Lift Installation," Drilling and Production Practices (1952).

50. Hagedorn, A. R. and Brown, K. E., "Experimental Study of Pressure Gradients Occurring During Continuous Two-Phase Flow in Small Diameter Vertical Conduits," Journal of Petroleum Technology (April, 1965).

51. Orkiszewski, J., "Predicting Two-Phase Pressure Drop in Vertical Pipe," Journal of Petroleum Technology (June, 1967).

52. Beggs, H. D. and Brill, J. P., "A Study of Two-Phase Flow in Inclined Pipes," Journal of Petroleum Technology (May, 1973).

53. Brill, J. P. and Beggs, H. D., Two-Phase Flow in Pipes, the University of Tulsa (1968).